50 ปีความสัมพันธ์ทางการทูตไทย - จีน
中泰建交50周年

STT51

The 51st International Congress on Science, Technology, and Technology-based Innovation

Collaboration Across Frontiers

From Quantum and Cosmos to Global Biodiversity

Abstract Book

TABLE OF CONTENTS

A: PHYSICS/APPLIED PHYSICS

B: BIOLOGICAL SCIENCES

C: ANALYTICAL CHEMISTRY

C: INORGANIC CHEMISTRY

C: ORGANIC & MEDICINAL CHEMISTRY

C: PHYSICAL & THEORETICAL CHEMISTRY

D: MATHEMATICS / STATISTICS / COMPUTER SCIENCE / DATA SCIENCE / AI

E: ENERGY / ENVIRONMENTAL & EARTH SCIENCE / MATERIALS SCIENCE / CHEMICAL TECHNOLOGY

F: FOOD SCIENCE AND TECHNOLOGY/AGRICULTURAL SCIENCE

SP3: NEXGEN ENERGY: STORAGE AND CONVERSION FOR SUSTAINABILITY

SP7: COLOUR SCIENCE/TECHNOLOGY, LIGHT AND APPLICATIONS

SP8: CULTURAL HERITAGE: TRADITIONAL/DIGITAL COLOR

SP9: EXPLORING THE COSMOS: ADVANCES IN OBSERVATIONAL AND THEORETICAL ASTROPHYSICS

SP10: X-RAY CRYSTALLOGRAPHY

SP11: RADIOECOLOGY AND ENVIRONMENTAL RADIOACTIVITY

SP12: THE 2ND INTERNATIONAL SYMPOSIUM OF SCIENCE COMMUNICATION AND PUBLIC SCIENCE LITERACY

SP14: VALORIZATION OF BIOMASS-RELATED WASTES

A: PHYSICS/APPLIED PHYSICS

A COMPARATIVE STUDY OF LINEAR EXPANSION COEFFICIENTS OF DIFFERENT METALS USING AN INDUCTION HEATING SYSTEM

Kitisak Boonkham, Thanyanan Somnam*
Department of Physics, Mahidol Wittayanusorn School, Nakhon Pathom, Thailand
*e-mail: thanyanan.phu@mwit.ac.th

Abstract:
The study of thermal linear expansion is a fundamental topic in high school physics. However, effective demonstration tools for classroom use are often lacking. This study addresses this gap by investigating and comparing the linear expansion coefficients of two metals, copper and aluminum, using a custom-designed experimental setup based on an induction heating system. Each metal sample, machined to identical dimensions (8 mm in diameter and 100 mm in length), was fixed at one end, while the other end was placed in contact with a dial gauge to measure the change in length as the temperature increased. Heat was applied using a commercial induction coil wrapped around the sample, with thermal energy controlled by adjusting the input voltage. A digital thermometer positioned at the free end of the sample monitored temperature changes in real time. As the input voltage increased, the sample's temperature rose, resulting in measurable linear expansion. For each material, the data were plotted as temperature change (ΔT) versus change in length (ΔL), and the slope of the graph was used to calculate the linear expansion coefficient. The experimentally determined coefficients of copper and aluminum were 1.57×10^{-5} °C^{-1} and 2.52×10^{-5} °C^{-1}, respectively. The results showed a deviation of less than 8% compared to the corresponding theoretical values, demonstrating the accuracy and reliability of the proposed setup. The study not only highlights the differences in thermal expansion behavior among materials but also presents an efficient and practical alternative to conventional heating methods such as water baths and circulating pumps. The apparatus, constructed using modular and commercially available components, provides an accessible and cost-effective tool (under 30 USD) for enhancing the teaching and learning of fundamental physics concepts.

A PRELIMINARY STUDY OF 3D FACIAL RECONSTRUCTION IMAGE FOR FORENSIC SCIENCE APPLICATIONS

Settawut Boonsuk[1], Kittichai Wantanajittikul[2], Uten Yarach[2], Atita Suwannasak[2], Komsanti Chokethawai[3*]
[1]Multidisciplinary and Interdisciplinary School, Chiang Mai University, Chiang Mai 50200, Thailand
[2]Department of Radiologic Technology, Faculty of Associated Medical Sciences, Chiang Mai University, Chiangmai 50200, Thailand
[3]Department of Physics and Materials Science, Faculty of Science, Chiang Mai University, Chiang Mai 50200, Thailand
*e-mail: komsanti.chokethawai@cmu.ac.th

Abstract:
Facial reconstruction from skulls is a significant approach in forensic science, serving as an alternative when biological evidence is unavailable. This study employed a U-Net deep learning model to reconstruct 3D facial images from skull data obtained from 1,080 Pseudo-CT scans. The model was trained to generate reconstructed images that closely resembled reference MRI scans, with qualitative and quantitative analyses conducted to assess its accuracy. The findings revealed that the reconstructed facial images demonstrated high similarity to the reference data, especially in preserving anatomical features and facial skin continuity. The results suggest that U-Net-based reconstruction can enhance the reliability of forensic identification and provide practical applications in cases with limited biological evidence.

An Analytical Framework for Processing and Interpreting Experimental Data from Thailand Tokamak-1 (TT-1)

Kasidit PIEKBUT,[1] Pasit Wonghabut,[2] Nopporn POOLYARAT,[2] Jiraporn PROMPING,[2] Arlee TAMMAN,[2] Apisit DANG-IAD,[2] Rattacha BOONCHOO,[2] Suebsak SUKSAENGPANOMRUNG,[2] Apiwat WISITSORASAK,[3] and Boonyarit CHATTHONG[1]*
[1] Division of physical science, Faculty of Science, Prince of Songkla University, Songkla, Thailand
[2] Thailand Institute of Nuclear Technology(Public Organization), Nakhon Nayok, Thailand
[3] Department of Physics, Faculty of Science, King Mongkut's University of Technology Thonburi, Bangkok, Thailand
*e-mail: boonyarit.ch@psu.ac.th

Abstract:
This study presents a MATLAB-based framework for analyzing experimental data from the Thailand Tokamak-1 (TT-1). The framework is designed to automatically convert raw diagnostic signals into plasma parameters that describe the behavior of discharges, reducing the need for manual calculation and providing a more systematic workflow for experimental studies. Input signals include plasma current (I_p) from Rogowski coils, loop voltage (U_{loop}), and other standard diagnostics. Using calibration relations and simple plasma models, the framework calculates key quantities such as toroidal magnetic field (B_{tor}), electron density (n_e), electron temperature (T_e), and plasma heating power (P_{heat}), which are important information to analyse plasma insight and capable to use as initiative database for development some other advanced diagnostic tools in the future, using combination of fundamental and approximate plasma models. The toroidal field and electron density are computed using calibration equations from TINT and ASIPP. Temperature is estimated by combining current data with resistivity models and polynomial fitting, and heating power is calculated from the Ohmic heating equation. Applied to more than 80 TT-1 discharges, the framework has shown consistent and reproducible results, capturing important plasma trends under different conditions. The main contribution is the integration of multiple diagnostics into a single tool, reducing manual effort and errors while supporting efficient comparison between experiments. This provides researchers with a reliable method for interpreting TT-1 performance and a flexible foundation for future upgrades in plasma analysis. This work is partially supported by Thailand Science Research and Innovation (TSRI) Fundamental Fund project number 204521.

Analysis of Error in the Photoelectric Experiment Using a Light Filter: A Case Study

Pinthudit Klinkajorn[1],Nimit Kimpraphan [2], Dusit Ngamrungroj[1], PrajyaTangjitsomboon[3],

Rattachat Mongkolnavin[4]

[1]King Mongkut's University of Technology North Bangkok, Bangkok 10800, Thailand
[2]Program of Physics, Faculty of Science, Chandrakasem Rajabhat University, Bangkok, Thailand
[3]Department of General Education, Faculty of Science and Health Technology, Navamindradhiraj University, Bangkok, 10300, Thailand
[4]Department of Physics, Faculty of Science, Chulalongkorn University, Bangkok 10330, Thailand
*e-mail: Pinthudit.k@cit.kmutnb.ac.th

Abstract:

Studying of photoelectric effect is important for understanding wave-particle duality, and this subject is still being taught to first-year students at the College of Industrial Technology, King Mongkut's University of Technology North Bangkok. The principle of this phenomenon has diverse applications, such as in solar cells, smoke detectors, night vision devices, and remote controls. The experiment, which was conducted in two steps use five colored light filters to filter the light from the source. Firstly, the relationship between light intensity and the number of photoelectrons was investigated. Secondly, the effect of the stopping potential on the photocurrent was studied to calculate Planck's constant. Based on the students' experimental results, it was found that a decrease in the number of photoelectrons was caused by a decrease in the light intensity. Furthermore, it was found that the stopping potential measured for the yellow and blue filters were similar. However, the analysis of the light spectrum using a spectrometer showed that the light passing through the filters was not monochromatic. The minimum wavelength value from both filters were nearly identical. Therefore, the experimental results obtained under these conditions were not totally accurate.

Keywords: Photoelectric effect, Discrepancy of photoelectric, Photoelectric

APPLICATION OF MACHINE LEARNING TECHNIQUES FOR IMPROVING CENTROIDING ACCURACY OF CHARGE CLOUD FOOTPRINTS AT THE EDGES OF PIXELATED DETECTORS

Thawatchai Sudjai*, Nitat Sripongpun
Department of Physics, Mahidol wittayanusorn School, Nakhon Pathom, Thailand
*e-mail: thawatchai.sdi@mwit.ac.th

Abstract:
Centroiding charge cloud footprints at the edges of pixelated detectors is challenging due to the distorted shape of the footprints in these regions. When a charge cloud impacts near the boundary of a pixelated pad, the resulting footprint becomes asymmetric because the collected charge is distributed unevenly across adjacent pixels. This asymmetry limits the accuracy of conventional centroiding techniques, such as Gaussian fitting, which rely on symmetric distributions. Therefore, machine learning techniques are proposed as an alternative approach for accurately estimating the centroid positions under such conditions. In this study, charge cloud footprints generated from microchannel plate (MCP) detectors are analyzed and compared using both traditional Gaussian fitting and machine learning-based methods. The results demonstrate that machine learning techniques provide more accurate centroiding near the detector edges, more closely matching the true signal positions.

COLOR IDENTIFICATION OF LIGHT AND PIGMENT BY USING OPTICAL SPECTROSCOPY

Apisara Harinthachart,[1,*] Apichart Limpichaipanit,[1] Athipong Ngamjarurojana [1]
[1] Department of Physics and Materials Science, Faculty of Science, Chiang Mai University, Chiang Mai, 50200, Thailand
*e-mail: apisara.harin@gmail.com

Abstract:

Optical spectroscopy analyzes the interaction of light with a material to determine its color. By measuring how light is absorbed and reflected across a spectrum of wavelengths, it provides detailed information about chemical composition, structure, and physical properties, allowing for its identification, characterization, and analysis without direct contact with the sample. CIE Color refers to using spectral data from an optical measurement to determine a color's coordinates within the International Commission on Illumination (CIE) color system, such as CIE 1931 XYZ , CIE 1976 Lab*. This process involves integrating the spectrum measured spectral power distribution (SPD) with the tristimulus values of a standard observer to calculate colorimetric values (x, y, Y or L*, a*, b*) that represent the color objectively. In this study, color identification of light such as incandescent lamp, fluorescent lamp, LED (warm white, neutral white, cool white, light color temperature and RGB) and pigment (fluorescent pigment, thermochromic pigment: color change with temperature) were investigated by using optical spectrometer in combination colorimeter (CIE 1931 XYZ color space, CIE 1976 Lab* color space) that is essential tool for color identification.

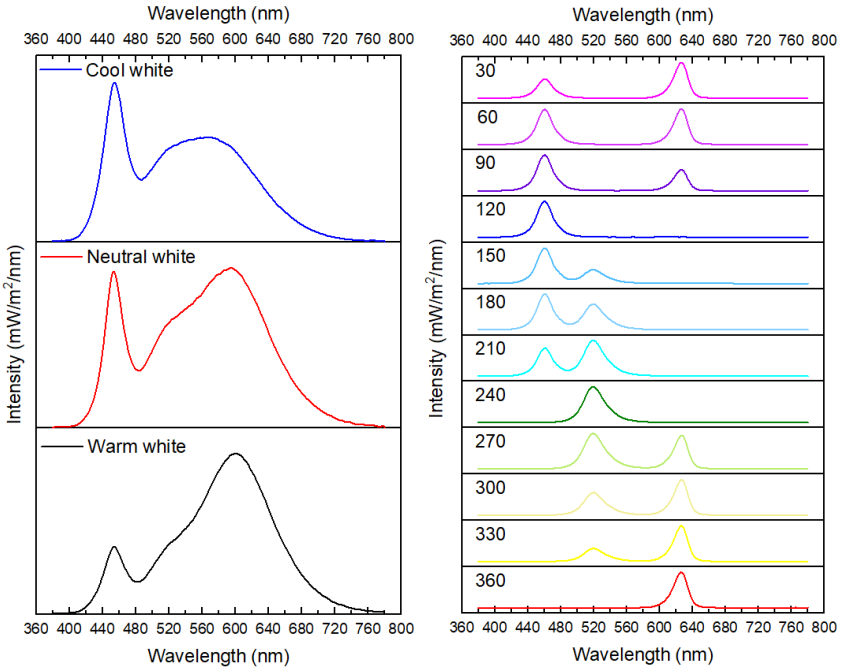

(a) (b)

Figure 1. Optical spectrum of
(a) warm white LED, neutral white LED and cool white LED (b) RGB LED

DEUTERIUM LABELING OF AMINES USING A PROTON-CONDUCTIVE GRAPHENE OXIDE MEMBRANE REACTOR

Ami Takase,[1] Imam Sahroni,[2] Ahmad Sohail,[2] Yusuke Inomata,[3] Tetsuya Kida,[2]*
[1] Graduate School of Science and Technology, Kumamoto University, Japan
[2] Graduate School of Institute of Industrial Nanomaterials, Kumamoto University, Japan
[3] Faculty of Advanced Science and Technology, Kumamoto University, Japan
*e-mail: 242d8814@st.kumamoto-u.ac.jp tetsuya@kumamoto-u.ac.jp

Abstract:

Deuterium-labeled compounds, where hydrogen is replaced by deuterium (D), have attracted attention for pharmaceutical and tracer applications due to their enhanced metabolic stability and detectability. However, conventional deuteration methods often require high temperatures and pressures, leading to high costs.

To address this, we developed a graphene oxide (GO)-based solid electrolyte membrane doped with Ce^{4+} and 2-hydroxyethanesulfonic acid (sGO–Ce^{4+}), aiming for low-temperature, electrochemical deuteration. GO is a low-cost, carbon-based material known for proton conductivity, and previous reports have shown that it can transport D^+ at room temperature.

The sGO–Ce^{4+} membrane was prepared by oxidizing graphite via the Tours' method, followed by the addition of $Ce(SO_4)_2 \cdot 4H_2O$ and 2-hydroxyethanesulfonic acid to the GO dispersion. After 2 hours of stirring, the membrane was obtained via vacuum filtration.
XRD and FT-IR measurements confirmed the successful synthesis of the GO membrane and interlayer expansion due to Ce^{4+} and sulfonic acid insertion. Proton transport number was close to 1, indicating proton-dominant conduction. Conductivity measurements showed significant enhancement upon Ce^{4+} doping.

An electrochemical membrane reactor using the sGO–Ce^{4+} membrane was constructed (Fig.1 (a)). Using D_2O as the deuterium source, deuteration of aniline and benzylamine was carried out at room temperature and atmospheric pressure under a constant voltage of 3 V for 24 h. ^1H NMR and ^2H NMR analyses revealed selective deuterium incorporation at the amino group of aniline(Fig.1 (b)) and benzylamine. The D incorporation rates were 70 % (FE : 15.6 %, TON : 114) and 89 % (FE : 19.9 %, TON :145), respectively. These results demonstrate the potential of functionalized GO membranes for efficient, low-temperature electrochemical deuteration.

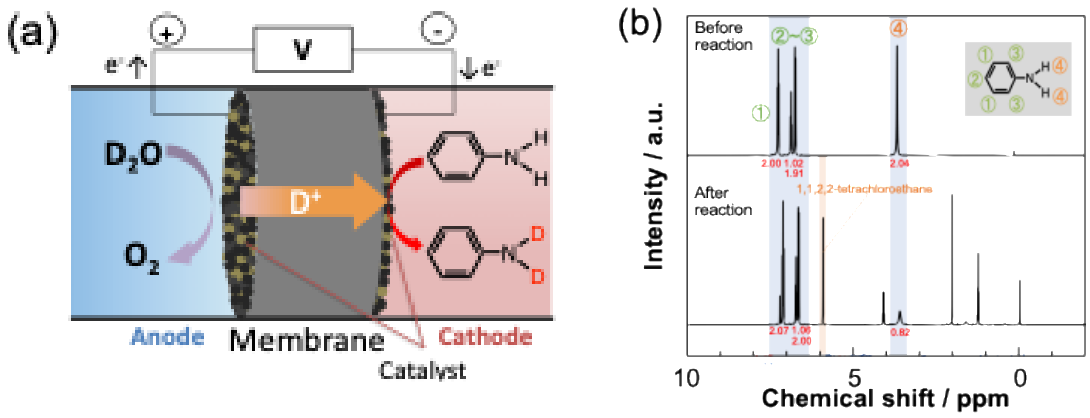

Figure 1. (a) Deuteration process using the GO membrane as a proton conductor. (b) ^1H NMR spectrum of aniline before and after the reaction.

EFFECT OF PM2.5 AIR POLLUTION ON COSMIC RAY DETECTION AT PRINCESS SIRINDHORN NEUTRON MONITOR STATION, CHIANG MAI, THAILAND

Nattnaphak Dararak, Suttiwat Madlee*
Department of Physics, Faculty of Science, Ramkhamhaeng University, Bangkok 10240, Thailand
*e-mail: suttiwat.m@rumail.ru.ac.th

Abstract:
Cosmic rays (CRs), high-energy particles originating from space, continuously bombard Earth's atmosphere, creating cascades of secondary particles including neutrons. Neutron monitors (NMs) have been the standard for ground-based CR detection, utilizing BF_3-filled proportional counters surrounded by polyethylene moderators to detect CR-induced neutrons, while bare counters (BC) detector operate without lead producers, providing enhanced sensitivity to lower-energy neutrons. The Princess Sirindhorn Neutron Monitor station (PSNM) in Chiang Mai, Thailand, operates at a vertical cutoff rigidity of ~16.8 GV, positioning it uniquely for studying CR variations in the equatorial region and features both an 18-tube NM and a BC detector. This study investigates the impact of PM2.5 atmospheric pollution on the counting rates of both NM and BC detectors at PSNM station using Monte Carlo simulations using FLUKA program based on actual PM2.5 concentration data from Chiang Mai Province during 2024. Atmospheric particulate matter, particularly PM2.5 (particles with aerodynamic diameter ≤ 2.5 μm) as a mixture of carbon, oxygen, and nitrogen compounds typical of biomass burning aerosols, with density calculations based on observed concentration levels, can significantly affect CR propagation through the atmosphere by providing additional interaction sites for neutron absorption and scattering processes. The results showed that during peak pollution periods in April with a concentration of 78.6 $\mu g/m^3$, the NM counting rate decreased by 0.92%, while the BC detector showed a reduction of 1.09% compared to clean atmospheric conditions. These findings provide quantitative evidence of PM2.5 impacts on CR measurements at high cutoff rigidity locations and are crucial for accurate data interpretation in polluted environments and space weather monitoring applications.

ENTROPY AND LEARNING EFFICIENCY IN SPECIAL RELATIVITY: AN INFORMATION-THEORETIC LENS ON ASSESSMENT DESIGN

Jatuporn Puntree,* Kamolporn Kantawong, Rungroj Tuayjaroen, Pornmongkol Jimlim

Mahidol Wittayanusorn School, Salaya, Phutthanmonthon, Nakhon Pathom, Thailand

*e-mail: jatuporn.ptr@mwit.ac.th

Abstract:
Special Relativity is a threshold concept in physics, often associated with persistent misconceptions despite extensive instruction. Traditional exam analyses, based on item difficulty and discrimination, provide limited insights into why students succeed or fail. This study introduces an integrative framework that combines psychometrics with principles from information theory and thermodynamics of learning. Using exam data from 232 students, we computed not only difficulty and discrimination but also entropy as a measure of cognitive variability and the Learning Efficiency Index (LEI) as a proxy for diagnostic information gained per unit of cognitive effort. Findings highlight that those conceptual foundations of relativity (Q1) exhibited high entropy, with students scattering across misconceptions of simultaneity, inertial frames, and relativity principles. The invariance of light speed (Q2.2) showed Newtonian reasoning persisting across ability groups. By contrast, muon velocity addition and energy-momentum tasks (Q4) yielded high discrimination and efficiency, effectively separating mastery levels. Entropy thus functions as a misconception detector, while LEI identifies efficient diagnostic tasks versus low-yield items. This framework offers actionable tools for redesigning physics assessments and scaffolding fragile concepts, while also pointing toward applications in AI-driven adaptive learning systems.

REAGENTLESS AND LABEL-FREE ELECTROCHEMICAL APTASENSOR USING POLYANILINE INCORPORATED WITH BATTERY-FREE NFC POTENTIOSTAT FOR ONE-STEP DETECTION OF SALIVARY CORTISOL

Chawin Srisomwat,[1,*] Supada Khonyoung,[1] Nuttanan Thanedsed,[1] Warawut Tiyapongpattana,[1] Sopon Butcha,[1] Orawon Chailapakul,[2]
[1] Department of Chemistry, Faculty of Science and Technology, Thammasat University, Pathumthani, 12121, Thailand
[2] Department of Chemistry, Chulalongkorn University, Pathumwan, Bangkok, 10330, Thailand
*e-mail: chawinsr@tu.ac.th

Abstract:
Cortisol serves as a vital biomarker for stress levels, but current evaluation methods are complex and resource intensive. Traditional detection approaches require elaborate procedures and sophisticated equipment, limiting their accessibility and practical application. There is a pressing need for user-friendly, cost-effective, and portable technologies that can efficiently monitor cortisol levels in real-world settings. We developed a reagentless and label-free electrochemical aptasensor for one-step detection of salivary cortisol, utilizing polyaniline (PANI) as an active conductive polymer and integrating it with a battery-free NFC potentiostat. The PANI-modified screen-printed electrode exhibited excellent conductivity and surface-enhancing properties, facilitating efficient aptamer immobilization and enabling reagentless electrochemical detection of cortisol without the need for additional redox reagents. The battery-free NFC integration enables seamless data transfer to mobile devices, providing real-time analysis capabilities. The proposed sensor achieved the linear range between 0.1 to 10 nM with a low detection limit of 27 pM or 33 minutes of analysis time and exhibited high selectivity for cortisol, which makes it suitable for patients with Addison's disease. Moreover, the good reproducibility of the five different devices (%RSD = 4.3) was accomplished. Also, the matrices in artificial saliva were not affected for cortisol detection. A performance comparison between commercial EmStat4s and our NFC-based potentiostat, in artificial saliva, validated the accuracy of the system with acceptable range (% recovery = 95 – 97; NFC, 91 – 107; EmStat4s). This innovative platform represents a significant advancement in point-of-care diagnostics by combining advanced conductive materials with modern electronics. The system's portability, cost-effectiveness, and user-friendly design make it particularly valuable for non-invasive stress monitoring through salivary analysis, opening new possibilities for accessible bioanalysis and personalized health monitoring.

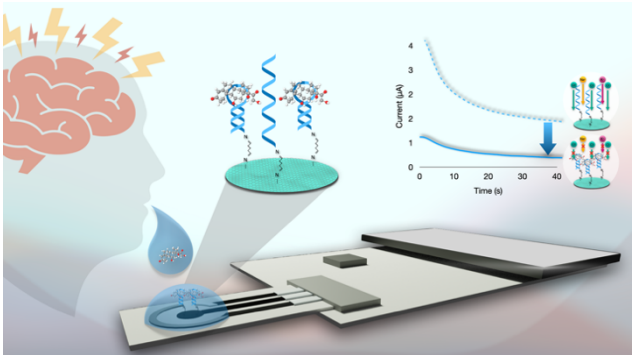

Figure 1. The proposed electrochemical aptasensor for salivary cortisol detection
(Leave a blank line before and after Figures.)

FAST SIMULATION OF ATMOSPHERIC MUON AT SURFACE WITH CORSIKA USING GENERATIVE MODEL

Tananan Anansubying
Department of Physics, Faculty of Science, Chulalongkorn University, Bangkok, Thailand.

Email: 6434226323@student.chula.ac.th

Abstract: Neutrino observatories in deep ice or water, such as IceCube and KM3NeT, require accurate modeling of atmospheric muons because these particles can closely mimic neutrino signals. Simulations at the Earth's surface are therefore crucial for detector calibration, veto system design, and background estimation. CORSIKA, a Monte Carlo simulation of cosmic ray air showers, provides detailed and reliable predictions by modeling the cascade from the primary collision to particles arriving at the surface. While accurate, CORSIKA becomes prohibitively slow and computationally expensive when millions of events are needed. We present a generative approach using normalizing flows to accelerate surface muon simulations. The model is trained on CORSIKA data to learn the joint distribution of muon features conditioned on primary cosmic ray properties. It generates muon events that maintain event-level correlations. Validation against independent test samples shows that the method reproduces key observables, including flux spectra, multiplicity distributions, energy and zenith relations, and the lateral spread of muon bundles. Initial results demonstrate that the model reduces the computational cost of atmospheric muon simulations by nearly two orders of magnitude while preserving high accuracy. This improvement enables faster calibration studies, large systematic scans, and flexible integration into existing workflows for current and future neutrino observatories.

INVESTIGATION OF CORRELATION BETWEEN GEOMAGNETIC-AND-SOLAR INDICES AND GROUND-BASED NEUTRON MONITOR COUNT RATE

Kledsai Poopakun*, Natdaporn Thongphan, Kamolporn Kanthawong, Pranee Disrattakit
Mahidol Wittayanusorn School, Salaya, Nakhon Pathom, Thailand 73170
*e-mail: Kledsai.poo@mwit.ac.th

Abstract:
Galactic cosmic rays (GCRs) are highly energetic particles originating outside our solar system. As they travel through the heliosphere, their intensity and energy are modulated by the solar activity, a phenomenon known as solar modulation. This modulation can be monitored via the neutron count rate (NCR) measured by ground-based neutron monitors. In this study, we examine the relationship between NCR and several indicators of solar and geomagnetic activity, including sunspot number (SSN), F10.7 solar radio flux, planetary Kp index, and auroral electrojet (AE) index. To investigate these relationships, we collected, visualized, and analyzed data using Python with correlation and time series comparisons. Our results reveal a negative correlation between NCR and both AE and Kp, suggesting that as auroral activity increases, cosmic ray levels decrease. Thus, geomagnetic storms, reflected in these parameters, play an important role in cosmic ray modulation. Because geomagnetic storms can disturb radio communication, satellite operations, and GPS accuracy on Earth, identifying the best predictive measures is important. Ultimately, understanding which parameters most closely align with cosmic ray behavior may enhance the accuracy of space weather forecasting.

INVESTIGATION OF VIBRATION EFFECTS ON FRICTION COEFFICIENTS BETWEEN SURFACES: EXPERIMENTAL MEASUREMENT AND ANALYSIS

Punphum Jarunyakorn,[1] Mathus Manedam,[1] Kriangkamon Sawangsri[1,*]

Kamnoetvidya Science Academy, Pa Yup Nai, Wangchan District, Rayong 21210, Thailand

e-mail: kriangkamon.s@kvis.ac.th

Abstract:

Friction between material surfaces is a key factor influencing the performance, durability, and stability of engineering devices, machines, and everyday applications. Although the interaction between material friction has been extensively studied in both static and dynamic conditions, the presence of external vibrations creates complex and unpredictable behaviors that can significantly alter the coefficient of friction in many real-world situations, such as rotating machinery, transportation systems, or structural components. Repetitive motion, environmental disturbances, or mechanical actions are the most common factors to cause vibrations. These vibrations can both increase and decrease friction, depending on the situation. This necessitates a more profound understanding of the interplay between vibration and friction.

The objective of this research was to systematically study the influence of vibration parameters, particularly frequency and amplitude, on the coefficient of friction between a brass sheet and a medical latex glove. Although much research measures both variables by using sensors to detect the value of amplitude, our group uses a microscope to detect the small value of amplitude to make it the most accurate. The team developed a controlled experimental setup that included a vibration generator, force sensor, and platform. This setup allowed for independent control of vibration frequency and amplitude, and friction values were recorded via force sensors connected to data acquisition and analysis software. In addition to vibration conditions, this study also examined other important variables affecting friction behavior, such as the type of contacting material surface and the speed at which the workpiece was pulled.

The results indicate that vibration can reduce the coefficient of friction by approximately 16.49% depending on amplitude and frequency. This study shows that vibration affects friction behavior and shows the importance of considering vibration in friction studies. Moreover, this result supports the development of strategies to control or mitigate the effects of vibration in engineering applications.

OFFICE SYNDROME THERAPY KIT WITH PORTABLE AUTOMATED ELECTRICAL STIMULATION

Paphangkorn Phetrak,[1] Thunhirun Thongkundam,[1] Nurulhuda Doloh,[1] Sinchai Jandang,[2,*] Patipat Kamdenlek,[2,*] Supachai Kaewpoung[3,*]
[1]Thaksin University Demonstration Secondary School, Phatthalung, Thailand
[2]Department of Biomedical Engineering, Faculty of Engineering, Thaksin University Phatthalung Campus, Phatthalung, Thailand
[3]Department of Electrical Engineering, Faculty of Engineering, Thaksin University Phatthalung Campus, Phatthalung, Thailand
[*]email: sinchai.j@tsu.ac.th, patipat.k@tsu.ac.th, supachai.ka@tsu.ac.th

Abstract: In the context of technological development in Thailand, a considerable portion of the workforce spends prolonged hours working on computers while maintaining repetitive postures in suboptimal working environments. This behavior has led to a high prevalence of musculoskeletal disorders, particularly office syndrome, among working-age individuals. To address this issue, a portable automated electrical stimulation device has been developed as a therapeutic intervention for office syndrome. Unlike commercially available stimulators, the proposed device is lightweight, battery-operated, and designed for user-friendly operation, with adjustable electrical current in the range of 10–70 mA and additional programmable parameters tailored to individual user needs. Moreover, it is safe to use when operated according to the recommended guidelines, as it has undergone thorough inspection and testing. The objective is to design a safe, effective, and practical device capable of alleviating pain, enhancing muscular function, and reducing symptoms associated with office syndrome.The system utilizes an automated neuromuscular electrical stimulation (NMES) mechanism with adjustable parameters, including frequency, current intensity, and duty cycle. Optimal stimulation settings were determined to be a contraction time (Ton) of 10 seconds and a relaxation time (Toff) of 50 seconds, with a total treatment duration of 1,800 seconds at 65 mA. The developed therapeutic kit measures pain levels before and after treatment to compare outcomes, adopting a within-subject pre–post design without a separate control group, as the purpose was to establish feasibility and preliminary effectiveness prior to larger controlled trials. These parameters demonstrated effective symptom relief in preliminary evaluations. The case study indicates that the proposed portable NMES device may serve as a practical, safe, and non-invasive preliminary treatment option to reduce musculoskeletal discomfort related to office syndrome.

Plasma Temperatures and Density Profiles Simulations of Thailand Tokamak 1 using CRONOS code

Faneel Nontree,[1] Nopporn Poolyarat,[2] Jiraporn Promping,[2] Arlee Tamman,[2] Apiwat Wisitsorasak, [3] Boonyarit Chatthong[1,*]
[1]Division of Physical Science, Faculty of Science, Prince of Songkla University, Songkhla, Thailand
[2]Thailand Institute of Nuclear Technology (Public Organization), Nakhon Nayok, Thailand
[3]Department of Physics, Faculty of Science, King Mongkut's University of Technology Thonburi, Bangkok, Thailand
*e-mail: boonyarit.ch@psu.ac.th

Abstract:
The simulations of the plasma profiles in the tokamak device are essential in current plasma fusion research. To better understand and optimize the experiments, planning and analyzing simulation results are necessary. The main goal of this work is to study plasma performance in the Thailand Tokamak 1 (TT-1) device using the 1.5D CRONOS integrated predictive simulation code. This study predicts the time evolution profiles of the ion and electron temperatures and electron density (Figure 1) in TT-1 by adjusting various parameters and models. The transports used are combination of neoclassical effect via NCLASS model and anomalous effect via Mixed Bohm/gyro-Bohm and the Mixed 97 models with set parameters for external sources, neutrals, and edges modules, used to calculate the electron source at the plasma edge. It was found that in the range of toroidal magnetic fields from 0.7 to 1.9 Tesla with plasma current of 50 kA, the electron density at plasma center is found to be around 1.5-2.3 x 10^{19} m^{-3}. This work is partially supported by Thailand Science Research and Innovation (TSRI) Fundamental Fund project number 204519.

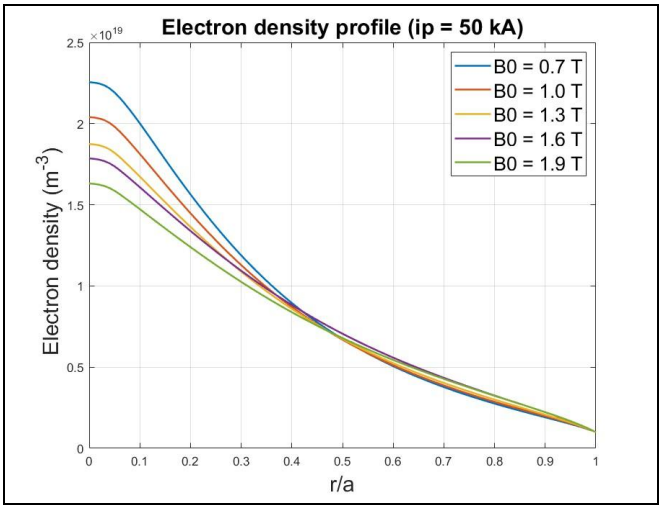

Figure 1. Electron density profiles as a function of normalized radius with various toroidal magnetic fields.

SEARCHING FOR NEUTRINO BY EVENT SELECTION WITH NEURAL NETWORK AT SCATTERING NEUTRINO DETECTOR AT THE LHC

Sirawarit Chuethamchan
Department of Physics, Faculty of Science, Chulalongkorn University, Bangkok, Thailand.

Email: 6434254923@student.chula.ac.th

Abstract: The Scattering Neutrino Detector at the LHC (SND@LHC) is positioned 480 m downstream of the ATLAS interaction point in the TI18 tunnel, providing coverage in the forward pseudo-rapidity interval $7.2 < \eta < 8.4$. In this kinematic regime, the flux of neutrinos is substantial. Yet, their feeble, weak-interaction cross-section renders direct observation challenging and vulnerable to contamination from neutral hadrons that produce similar detector signatures. Conventional cut-based selections achieve excellent background rejection but at the cost of severely reduced signal efficiency. We therefore explore a supervised neural-network classifier trained on simulated SND@LHC data to discriminate neutrino-induced events from neutral-hadron backgrounds. Compared with the optimized cut-based strategy, the neural network preserves high accuracy, approximately greater than 80%, while maintaining high signal efficiency, without compromising background suppression. These results demonstrate the potential of machine-learning techniques to maximize the yield of observable neutrino events from SND@LHC data. This further helps achieve the goal of the SND@LHC being more reachable.

STUDY OF HORIZONTAL MOVEMENT IN *Periplaneta americana* TO DEVELOP A BIO-INSPIRED ROBOT

Sirawut Kulareerat, Suphitchaya Krachangmon, Theparak V Palma, Tanawan Leeboonngam*
Kamnoetvidya Science Academy, Rayong, Thailand
*e-mail: tanawan.l@kvis.ac.th

Abstract:

The American cockroach (*Periplaneta americana*) showed special ability in both horizontal and inclined climbing due to adhesion forces made by its tarsal pads under its feet. This study focuses on mimicking the horizontal movement of the American cockroach by observing leg morphology under a microscope and walking behavior specialized in tarsal pad structure. From observing leg morphology, the data show that the longest parts of the legs are the tibia (0.87±0.15 cm). The video analysis indicates that the cockroach exhibits a hexapod gait pattern, with span angles of 80±5.77° between the coxa and femur, 76.67±26.67° between the femur and tibia, and 90±0° between the tibia and tarsus. The stereomicroscope result showed the four lobes of tarsal pads at the base of the tarsus and one lobe at the tip in every leg. We try to mimic the structure of tarsal pads by using different shores of silicone. The silicone samples (0, 10, 20, and 30 shore) were tested for friction to find the appropriate shore that suits the robot. The results showed that the softest one (0 shore) showed the highest resistance to motion (9.30±0.37 N), making it the most effective in mimicking cockroach-like adhesion. These results illustrate that adhesion and friction are important for effective locomotion. These findings can assist engineers in designing cockroach-inspired robots in the future.

TEMPERATURE-DEPENDENT ANNEALING STUDY OF PROTON-IRRADIATED APTS SENSORS FOR RADIATION-HARD APPLICATIONS

Jetnipit Kaewjai,[1] Natthawut Laojamnongwong,[1] Abdul Rahman Alfarasyi,[1] Chinorat Kobdaj, [1] Kritsada Kittimanapun [2,*]
[1]School of Physics, Institute of Science, Suranaree University of Technology, Nakhon Ratchasima, 30000, Thailand
[2]Synchrotron Light Research Institute (SLRI), Nakhon Ratchasima, 30000, Thailand
*e-mail: kritsadak@slri.or.th

Abstract:
Silicon pixel sensors are critical components in high-radiation environments such as space missions and high-energy physics experiments. To evaluate the radiation tolerance and post-irradiation recovery of the APTS sensor, we conducted a systematic irradiation and annealing study at King Chulalongkorn Memorial Hospital (KCMH) using a 70 MeV proton beam. The total ionizing dose (TID) applied to the sensors ranged from 600 krad to 9 Mrad. Post-irradiation, the sensors were subjected to controlled annealing at temperatures T=50 °C in an incubator setup. Performance characterization was performed before and after annealing using pulsing tests, threshold scans, and Fe-55 source scans. Particular attention was given to the evolution of mean cluster size as a function of bias voltage (VBB), comparing non-irradiated sensors to those subjected to different annealing durations from one to four weeks. The results demonstrate that irradiation induces a reduction in mean cluster size compared to the non-irradiated baseline, indicative of increased charge trapping and defect formation. However, systematic annealing at elevated temperatures results in a progressive recovery of cluster size with increasing annealing time, approaching the performance of non-irradiated sensors after several weeks. This time-dependent annealing effect underscores the efficiency of defect healing in the silicon lattice and highlights the importance of optimizing both annealing temperature and duration for sensor longevity.

THE ONE-DIMENSIONAL MODEL OF STATE TRANSITION IN MAGNETIZED PLASMA BASED ON BIFURCATION ANALYSIS

Thiti Aungcharoen,[1] Nopporn Poolyarat,[2] Jiraporn Promping,[2] Arlee Tamman,[2] Apiwat Wisitsorasak,[3] Boonyarit Chatthong[1,*]
[1]Division of Physical Science, Faculty of Science, Prince of Songkla University, Songkhla, Thailand
[2]Thailand Institute of Nuclear Technology, Nakhon Nayok, Thailand
[3]Department of Physics, Faculty of Science, King Mongkut's University of Technology Thonburi, Bangkok, Thailand
*e-mail: boonyarit.ch@psu.ac.th

Abstract:
In this work, we carried out the bifurcation analysis of the zero-dimensional primitive multi-predator one-prey model to describe the complex interaction among plasma turbulence, turbulence-driven zonal flow, and externally driven mean flow shear. Numerically, it was found that two distinct critical external power thresholds exist to access the limit-cycle oscillation (LCO) phase and high-performance (H) mode, respectively. Surpassing the former gives rise to the Hopf bifurcation of the intermediate fixed point. As a result, the turbulence and zonal flow perform the feedback loop, hence the LCO behavior. On the other hand, surpassing the latter gives rise to the transcritical bifurcation. The H-mode fixed point becomes stable, attracting the trajectory from the limit-cycle orbit to such a fixed point. This results in the transition to the H-mode state, where the strong mean flow shear suppresses plasma turbulence and zonal flow. Significantly, we also extend the zero-dimensional primitive model to the one-dimensional in radius by introducing the Spatio-temporal energy transport equation along with the turbulence spreading effect. Numerically, we found that the extended model exhibits qualitatively similar dynamics of the model's fixed point to the primitive model. However, we also found that with the inclusion of the spatial effect, the LCO originates at the plasma edge due to the plasma pressure-driven turbulence linear instability. Such behavior also propagates into the core region due to the turbulence spreading effect. Moreover, we also observed the formation of an edge transport barrier in the plasma pressure profile once the external power surpasses the second critical power threshold. This work is partially supported by Thailand Science Research and Innovation (TSRI) Fundamental Fund project number 197257.

B: BIOLOGICAL SCIENCES

ADAPTIVE RESPONSE OF NATIVE *Geranium nepalense* TO INVASIVE *Ageratina adenophora* IN NEPAL

Gyanu Thapa Magar[1,2], Krittika Kaewchumnong[3], Lal B Thapa[1]*, Mohan Siwakoti[1]
[1]*Central Department of Botany, Tribhuvan university, Kathmandu, Nepal*
[2]*Department of Botany, Amrit Campus, Tribhuvan university, Kathmandu, Nepal*
[3] *Division of Biological Science, Faculty of Science, Prince of Songkhla University, Songkhla, Thailand*
*e-mail: lal.thapa@cdb.tu.edu.np

Abstract
Crofton weed (*Ageratina adenophora*), which is widely invading different ecosystems across subtropical to the lower temperate region in Nepal, has caused threat to native biodiversity. Studies have shown that several native plant species are replaced by its invasion. However, some of the native species show co-existence with this weed. *Geranium nepalense* is one of the herbaceous species, which co-exist frequently with *A. adenophora*. Out of invasion this plant grows well along road sides, fallow areas and forest margins. We collected clones of this native herbs from single population of two sets of individuals: one with a prior history of growing in invaded sites i.e., they were co-existed with *A. adenophora* (experienced), and another that had previously grown in uninvaded sites (unexperienced). Clones were allowed to grow alongside *A. adenophora* in pot (sized 22 cm diameter and 15 cm height, six replication) and then morphological traits were measured after two months. Results showed that the experienced clones of *G. nepalense* developed significantly longer roots (1.27 times) and internodes (1.57 times) than the previously unexperienced clones. Further the clones which were experienced had significantly higher biomass allocation to root and leaves 1.16 and 2.12 times respectively compared to the unexperienced ones. We conclude that *G. nepalense* clones with prior exposure to *A. adenophora* invasion can exhibit fitness under invasion. It further highlights the role of prior exposure to invasion in adaptive performance of native plants and may indicate towards potential transgenerational plasticity, that further needs intergenerational trait analysis for confirmation. In addition, there should be further experiment and genetic barcoding to confirm whether the change is genetic or environmentally induced. It shows how some native plant species can co-exist with invasive plants and may have potential to outcompete invasive species.

AN IN VITRO ANTI-HYPERTROPHIC EFFECT OF *Calotropis* spp. LATEX EXTRACT ON ISOPROTERENOL-INDUCED HUMAN CARDIOMYOCYTES HYPERTROPHY

Worachit Suwannoppadol[1,2,3], Onnicha Srisopar[2,3], Thanyanan Wannathong Brocklehurst[4], Sarawut Kumphune[2,3], Wattanased Jarisarapurin[2,3,5,*]

[1]Ekamai International School 57 Ekamai 12 (Soi Charoenjai), Sukhumvit 63, Klongton Nua, Vadhana, Bangkok 10110, Thailand

[2]Biomedical Engineering and Innovation Research Centre, Biopolis building, Chiang Mai University, Mae-Hia, Mueang, Chiang Mai, 50100 Thailand

[3]Biomedical Engineering Institute, Biopolis building, Chiang Mai University, Mae-Hia, Mueang, Chiang Mai, 50100 Thailand

[4]Department of Biology, Faculty of Science, Silpakorn University, Nakhonpathom 73000, Thailand

[5]Office of Research Administration, Chiang Mai University, Chiang Mai 50200, Thailand

*e-mail: wattanased.j@cmu.ac.th

Abstract:

Cardiac hypertrophy (CH) after myocardial infarction increases the risk of heart failure (HF). Current treatments, such as beta blockers, have possible side effects such as bradycardia. Alternatively, a cardiac glycoside-derived compound, such as Digoxin, serves as treatment for HF. However, other natural compounds are still being investigated as alternatives. *Calotropis* spp. is a plant found throughout Thailand used to treat diseases. *Calotropis* spp. latex extract (CLE) contains cardiac glycosides and therapeutic compounds, but its ability to treat myocardial hypertrophy has not been investigated. The cytotoxicity of CLE in heart, kidney, neuron, liver, and lung cell lines was measured by the MTT assay. The results demonstrated a safe dosage of 1 µg/ml in AC16, HEK293T, and SH-SY5Y cells, and 0.1 µg/ml in HEPG2 and A549 cells. The anti-hypertrophic effect was evaluated in isoproterenol-induced human cardiomyocytes (AC16) and analyzed through actin cytoskeleton staining for cell surface area measurement. The results demonstrated that 20 µM isoproterenol (ISO) treatment induced cardiac hypertrophy, characterized by increased cell surface area. Pretreatment with 1 µg/ml CLE prior to ISO treatment significantly reduced hypertrophy. Our findings suggest CLE may be a viable option for the treatment of CH. This research promotes the advancement of plant-based pharmaceuticals to reduce import reliance and improve Thailand's healthcare sector.

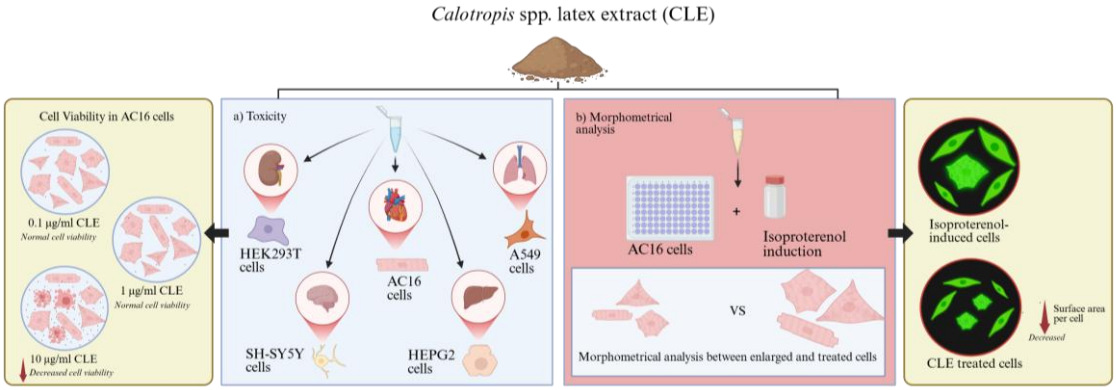

Figure 1. The diagram illustrates an in vitro anti-hypertrophic effect and safety of CLE.

Antimicrobial Efficacy and Compositional Analysis of Three Thai Salts against *Pseudomonas aeruginosa*

Nattha Khamchatturat[1], Nanthanit Jaruseranee[1,2], Somboon Kamtaeja[3]

[1] School of Science Mae Fah Luang University, Muang Chiang Rai, Thailand; [2] Microbial Products and Innovation Research Group, Mae Fah Luang University, Muang Chiang Rai, Thailand; 3 Faculty of Education, Chiang Rai Rajabhat University, Muang Chiang Rai, Thailand.

* Corresponding author. Nattha Khamchatturat Division of Bioscience, School of science, Mae Fah Luang University, Thailand, 0828046842.

E-mail address: 6531105029@lamduan.mfu.ac.th (Nattha Khamchatturat).

Abstract

This study investigated the antimicrobial properties of three unique rock salt sources (Salt A, B, and C) from Thailand against the opportunistic pathogen Pseudomonas aeruginosa, with a comparison to the conventional antibiotic, ampicillin. These salts, historically sourced from ancient rock salt wells in the mountains of Nan and Phitsanulok provinces, are believed to contain a distinct mineral composition due to their unique geological origin. Elemental analysis by X-Ray Diffraction (XRD) and Micro X-Ray Fluorescence (MicroXRF) revealed that while the salts are predominantly sodium chloride (NaCl), they also contain varying amounts of trace elements such as magnesium and sulfur. These minor components, potentially present as chlorides or sulfates, may contribute to the overall biological effect through mechanisms beyond simple osmotic stress.

Our results showed a clear dose-dependent inhibitory effect from all three salts, with the Minimum Inhibitory Concentration (MIC) conservatively observed around 5 g/L. However, the rock salts did not achieve complete growth inhibition, even at the highest concentration of 20 g/L, with absorbance values remaining above zero (Salt A: 0.699, Salt B: 0.699, and Salt C: 0.704). In comparison, ampicillin demonstrated a much more potent inhibitory effect at lower concentrations, achieving near-complete growth cessation (absorbance of 0.056 at 0.78 mg/mL). While ampicillin was more effective at low doses, the Thai rock salts proved to have a sustained inhibitory effect across a broader concentration range. This research confirms the intrinsic antimicrobial potential of these indigenous Thai rock salts, suggesting that future application should focus on testing the combination effect of these salts with conventional antibiotics to potentially enhance efficacy and overcome resistance challenges.

BIOCONTROL POTENTIAL OF CHITINASE-PRODUCING ACTINOMYCETES FROM GIANT MUD CRAB (*Scylla serrata*) ON EGG HATCHING AND JUVENILE MORTALITY OF THE ROOT-KNOT NEMATODE (*Meloidogyne enterolobii*)

Kittipong Chanworawit,[1] Paphitchaya Chokruai,[1] Chirath Pitakkhuamdee,[1] Anongnuch Sasnarukkit,[2] Pinsurang Deevong[1,*]
[1]Department of Microbiology, Faculty of Science, Kasetsart University, 10900, Bangkok, Thailand
[2]Department of Plant Pathology, Faculty of Agriculture, Kasetsart University, 10900, Bangkok, Thailand
*e-mail: fsciprd@ku.ac.th

Abstract:
Root-knot nematodes in the genus *Meloidogyne* cause substantial damage to plants by infecting their roots, leading to gall formation and impairing the plants' ability to absorb water and nutrients. Chitinase, an enzyme that hydrolyzes chitin, offers potential as a biocontrol agent against the root-knot nematodes by targeting their eggshell masses, which are primarily composed of chitin. The objectives of this study were to isolate and characterize chitinolytic actinomycetes from the giant mud crab for biological control against the root-knot nematode, *Meloidogyne enterolobii*. Eighteen chitinolytic actinomycetes were isolated using humic acid vitamin agar and then classified into six bacterial groups based on their morphological characteristics. Molecular identification based on the sequence analysis of 16S rRNA gene revealed that the representative isolates were closely related to *Cellulosimicrobium funkei*, *Streptomyces althioticus*, *Streptomyces griseoincarnatus*, *Streptomyces ardesiacus*, and *Streptomyces thermocarboxydus*. Among them, crude chitinase and spore suspensions of *C. funkei* C01 exhibited the strongest inhibition of egg hatching (64.28 ± 4.30% and 85.60 ± 4.93%, respectively) and the highest induction of juvenile mortality (90.13 ± 6.01% and 87.70 ± 6.77%, respectively) against *M. enterolobii*. Furthermore, the 64-kDa chitinase of *C. funkei* C01 displayed the highest enzymatic activity (0.28 ± 0.07 U/mL) at 96 h of cultivation. These findings provide valuable insights that could contribute to the development of sustainable and environmentally friendly strategies for future agricultural applications.

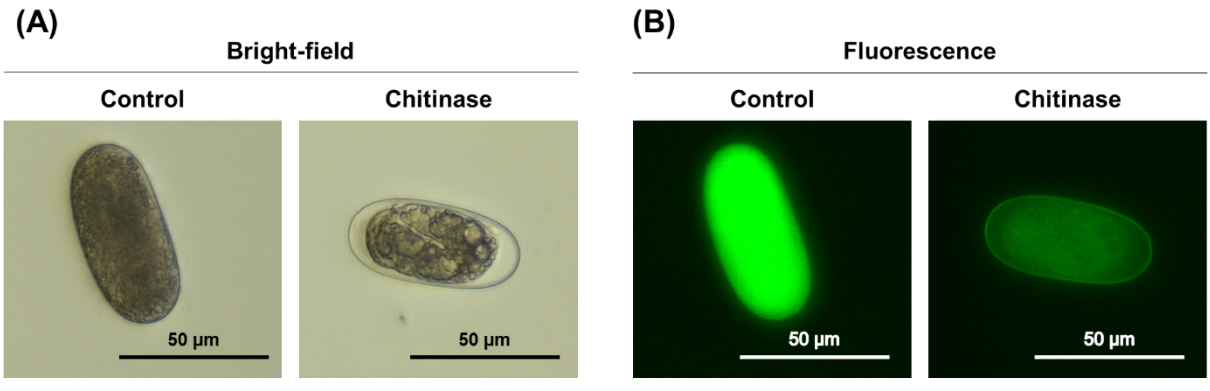

Figure 1. Imaging of *Meloidogyne enterolobii* eggs treated with chitinase from *Cellulosimicrobium funkei* C01 under (A) bright-field and (B) fluorescence microscopes.

COMMUNITY STRUCTURE AND ABUNDANCE OF BENTHIC INVERTEBRATES ON CORAL REEFS AND AN UNDERWATER PINNACLES AT KO KUT, THAILAND

Thamasak Yeemin*Laongdow Jungrak, Wiphawan Aunkhongthong, Charernmee Chamchoy, Sittiporn Pengsakun, Wanlaya Klinthong, Maneerat Sukkeaw, Makamas Sutthacheep
Marine Biodiversity Research Group, Department of Biology, Faculty of Science, Ramkhamhaeng University, Huamark, Bangkapi, Bangkok, Thailand
*e-mail: thamasakyeemin@hotmail.com

Abstract:
Benthic invertebrates play a crucial role in coral reef ecosystems by contributing to overall biodiversity and maintaining ecological balance. Their diversity and abundance are widely recognized as sensitive indicators of reef health, as many groups respond rapidly to environmental changes such as habitat degradation, overfishing, and climate-driven disturbances. This study focuses on comparing the composition and density of benthic invertebrates from a coral reef and an underwater pinnacle at Ko Kut, the Eastern Gulf of Thailand. Benthic invertebrates were surveyed using SCUBA diving along permanent belt transects, with three replicates set at each site. Composition and density were recorded following standard belt transect procedures, and species were identified directly in the field. The results showed that the density of benthic invertebrates differed statistically significantly between sites (ANOVA, p=0.000), with the highest density observed at Hin Bang Bao (24.76 ± 1.96 individuals/m²) and the lowest at Ko Maisi (4.28 ± 0.87 individuals/m²). The diversity of benthic invertebrates varied among sites, with Hin Ao Chak exhibiting the highest diversity, while Hin Ao Yai, Ao Phak Waeng, and Ao Supparot showed the lowest. The dominant species were *Diadema setosum*, *Pedum spondyloidium*, and *Lamarcka ventricosa*. A cluster dendrogram from Bay-Curtis Similarity provided similarity of benthic invertebrate community among the study sites, showing five groups: Group 1: Hin Bang Bao, Group 2: Hin Ao Chak, Group 3: Ko Maisi, Group 4: Hin Ao Yai, and Group 5: Ao Phak Waeng and Ao Sapparot. These findings demonstrate clear spatial variation in benthic invertebrate communities between the study sites, reflecting localized environmental conditions and anthropogenic influences, and provide essential baseline knowledge for monitoring reef health, guiding conservation measures, and informing sustainable management strategies in the Eastern Gulf of Thailand.

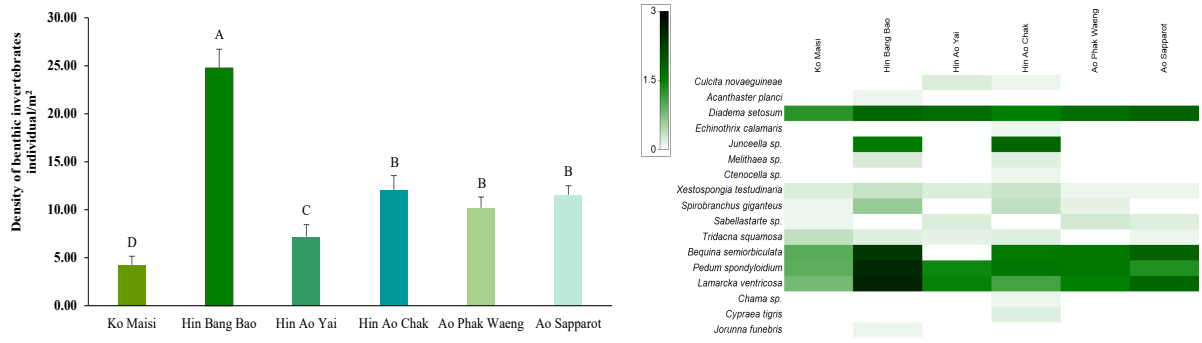

Figure 1.
Density of benthic invertebrates at the study sites (left)
and composition of benthic invertebrates at the study sites (right)

COMPARATIVE SKIN HISTOLOGY OF FARMED FROG SPECIES IN THAILAND

Junpanin Ratanachokthorani[1], Wichase Khonsue[2], Jirarach Kitana[2], Noppadon Kitana[2], Khattapan Jantawongsri[2,*]
[1]Bachelor of Science Program in Biology, Department of Biology, Faculty of Science, Chulalongkorn University, Bangkok 10330, Thailand
[2]BioSentinel Research Group (Special Task Force for Activating Research), Department of Biology, Faculty of Science, Chulalongkorn University, Bangkok 10330, Thailand
*e-mail: khattapan.j@chula.ac.th

Abstract:
Amphibian skin is a complex organ that serves essential functions in osmoregulation, respiration, immunity, and ecological adaptation. Histologically, amphibian skin exhibits species-specific variation in epidermal structure, dermal thickness, gland distribution, and collagen composition. Comparative histological analysis provides insights into structural variation across habitats and informs potential applications for amphibian skin, particularly as a sustainable source of collagen. This study aims to conduct a comparative histological assessment of three economically farmed frog species in Thailand: rice field frog (*Hoplobatrachus rugulosus*), American bullfrog (*Lithobates catesbeianus*), and blunt-headed burrowing frog (*Glyphoglossus molossus*). These species represent distinct ecological habitats—semi-aquatic and fossorial. Skin samples from dorsal and ventral regions were collected from frogs reared at the Huai Hong Khrai Royal Development Study Centre, Chiang Mai province. Samples were fixed in 10% neutral buffered formalin, processed using a standard paraffin-embedding technique, sectioned at 4 µm, and stained with haematoxylin and eosin (H&E). Microscopic analysis focused on epidermal and dermal organisation, glandular composition, and collagen layer thickness, with morphometric quantification using ImageJ. Preliminary results show that fossorial species (*G. molossus*) has a thinner epidermis and fewer dermal glands than semi-aquatic species (*H. rugulosus* and *L. catesbeianus*) The results are expected to demonstrate interspecific differences in integumentary architecture. These may reflect habitat-specific adaptations and influence collagen yield. Findings will enhance understanding of amphibian skin microanatomy, support frog skin valorisation in sustainable farming, and inform potential applications for amphibian skin.

COW URINE ENHANCES GROWTH AND MYCORRHIZAE COLONIZATION IN TOMATO UNDER WATER-STRESSED CONDITION

Rita Timilsina[1], Bimala Gharti Magar[2], Hari Prasad Aryal[1], Lal Bahadur Thapa[1,*]
[1]Central Department of Botany, Institute of Science and Technology, Tribhuvan University, Kathmandu, Nepal
[2]Central Department of Anthropology, Faculty of Arts and Humanities, Tribhuvan University, Kathmandu, Nepal
*Corresponding author: lal.thapa@cdb.tu.edu.np

Abstract:
Tomato (*Solanum lycopersicum* L.) is an important, popular and nutritious vegetable crop. Water scarcity severely affects tomato cultivation, which reduces growth, fruit quality and overall productivity. In this context, mycorrhizal colonization is a particular importance, as the mycorrhizae forms symbiotic associations with roots, which enhance water and nutrient uptake under drought condition. Inclusion of mycorrhizae as study factor is crucial because it offers eco-friendly strategy to minimize adverse effect of water stress on tomato as well as it provides valuable insight into the plant adaptation mechanisms. In addition to mycorrhizae, alternative approaches should be explored to improve plant resilience that can enhance mycorrhizal activity and promote plant growth. In this study, cow urine was applied to tomato (Sirjana variety) in Nepal to evaluate its effects on growth, development, and mycorrhizal colonization under water stress conditions. For this, tomato seedlings were grown under regular watering (control), intermittent watering (drought), regular watering with cow urine, and intermittent watering with plant growth stimulant (Figo). Growth parameters like plant height, root length, plant biomass and mycorrhizal association were measured in each treatment. Water stress decreased plant height and shoot length but increased root length. Application of cow urine enhanced the growth and development of seedlings in both control and under water stress comparing to Figo. Similarly, mycorrhizal colonization was increased under water stress and showed an additional increase with application of cow urine. Hence, cow urine can be applied for growth and development and mycorrhizal colonization under water stress condition in tomato. This result indicates that cow urine is effective for growth and development of seedling and mycorrhizal colonization of in tomato than that of commercially available plant growth promotors.

CRUDE EXTRACT FROM BACTERIA FROM RHIZOSPHERE SOIL OF BANANA FOR INHIBITING *Colletotrichum gloeosporioides* CAUSED OF ANTHRACNOSE IN CHILLI

Panrape Teawsakul,[1,*] Thanakorn Poompothingam,[1] Orawan Piyaboon [1]
[1] Mahidol Wittayanusorn School, Phutthamonthon, Nakhon Pathom, Thailand
*e-mail: panrape.tea_g33@mwit.ac.th

Abstract:

Anthracnose disease in chilli, caused by *Colletotrichum gloeosporioides*, is a significant issue for important economic crops. The chemical treatments like benomyl are commonly used, but they pose harm to both the environment and human health. In recent years, biological control treatments, particularly the use of bacteria from rhizospheres soils, are interested for alternative plant diseases controlling method. These bacteria have been reported to act as potential antagonists against various plant pathogens and to produce secondary metabolites against plant pathogens. This research aimed to develop the crude extract from bacteria from the rhizosphere soil of banana, which could effectively inhibit *C. gloeosporioides*, caused of anthracnose in chilli. Rhizosphere soil samples were collected from Nan province, Thailand. Ten bacterial isolates from the rhizosphere soil samples were identified based on their morphological characteristics and confirmed as Gram-positive bacteria. The inhibitory effect of each isolates on *C. gloeosporioides* growth was assessed using the dual culture test. Disease control percentages were calculated and used to determine mean value, standard deviation and statistically significant differences between groups. Subsequently, bacterial isolate 7-1 was extracted using ethyl acetate as a solvent. 42.5 mg/ml of crude extract was tested for the efficiency in controlling *C. gloeosporioides* using the dual culture test. The result demonstrated that the 42.5 mg/ml of crude extract of rhizosphere bacteria significantly inhibited the growth of *C. gloeosporioides,* with a statistically significantly different from 0.75 mg/ml of benomyl (P<0.05). In conclusion, this research identified rhizosphere bacteria and their crude extract, which can act as an agent against *C. gloeosporioides*, the cause of anthracnose in chili. These findings suggest the potential of developing the crude extract into a bioproduct for agricultural use.

DEVELOPMENT OF A PH AND THERMO-RESPONSIVE INJECTABLE HYDROGELS FOR CANCER THERAPY

Meghamouli Rana[1], Kanlaya Katewongsa[1, 2,*]
[1] School of Materials Science and Innovation, Faculty of Science, Mahidol University, Thailand
[2] Department of Biochemistry, Faculty of Science, Mahidol University, Thailand
*e-mail: kanlaya.pra@mahidol.ac.th

Abstract:
Stimuli-responsive hydrogels have emerged as promising platforms for localized and controlled drug delivery in cancer therapy. Given the slightly acidic nature of the tumor microenvironment, pH-sensitive hydrogels can enhance site-specific drug release at tumor sites while minimizing systemic toxicity. In this study, an injectable dual-responsive hydrogel was developed using dialdehyde carboxymethyl cellulose (DA-CMC) and chitosan, designed to respond to both pH and temperature stimuli. The optimized hydrogel formulation exhibited rapid gelation within 2 minutes, forming a stable and non-flowing gel. Under mildly acidic conditions (pH 6.8), the hydrogel demonstrated an 18% increase in swelling compared to physiological pH (7.4), enabling enhanced pH-triggered drug release. The incorporation of Pluronic introduced thermo-responsive properties, resulting in a sol-gel transition where the system remained in a liquid form at temperatures ranging from 0 °C to 25 °C and instantly gelled within approximately 1 minute at body temperature (37 °C). Overall, this dual-responsive hydrogel provides a versatile, biocompatible, and minimally invasive approach for cancer drug delivery, with the potential to enhance treatment precision and minimize side effects.

DISTINGUISHING SPOTTED BABYLON (*Babylonia areolata*) FROM SPIRAL BABYLON (*Babylonia spirata*) USING VGG16 TRANSFER LEARNING

Worraprot Theerachaisupakit[1,*]
[1]Bangkok Christian College, Thailand
*e-mail: woraprotbcc@gmail.com

Abstract:
The spotted babylon (*Babylonia areolata*) is a premium seafood species in Thailand, valued nearly five times higher than the spiral babylon (*Babylonia spirata*). Despite their economic differences, the two species share highly similar shell morphology and coloration, often causing consumer confusion and fraudulent trade practices. To address this issue, this project developed an automated classification system using deep learning techniques, designed for deployment through smartphones. A dataset of 145 publicly available images of whole snail with shells was divided into training, validation, and testing sets. Data augmentation (rotation, shifting, zooming, and flipping) was applied to increase diversity and reduce overfitting. Transfer learning with a pre-trained VGG16 model was used, where convolutional layers were frozen and new dense layers were added for binary classification. The model was trained for 30 epochs using the Adam optimizer and categorical cross-entropy loss. Performance was monitored with accuracy and loss curves, and further evaluated using a confusion matrix to ensure classification reliability. The proposed system achieved a training accuracy of over 95% with stable convergence across 30 epochs. On an independent test set, the model reached 92% accuracy, with the confusion matrix confirming reliable classification: 18 out of 20 *Babylonia areolata* and 19 out of 20 *Babylonia spirata* were correctly identified. However, the potential overfitting needs to be further addressed through expanding the dataset with additional images using a mix of natural and laboratory lighting conditions. To ensure practical usability, the system will be adapted for smartphone-based deployment via a web link, allowing users to upload snail images to receive instant classification result without the need for additional hardware. This innovation can potentially reduce misclassification, prevent consumer fraud, and enhance transparency in seafood trading. By empowering aquaculture farmers and consumers, it has the potential to reduce economic losses, support AI adoption at the community level, and strengthen the seafood supply chain while promoting sustainability.

Figure 1.
Training and validation accuracy (left), snail images (middle) and confusion matrix (right)

LEACHATE EFFECT OF *Chromolaena odorata* ON SEEDLING GROWTH OF *Aegle marmelos* UNDER SHADE AND DROUGHT

Sunita Poudel,[1] Ramesh Raj Pant,[2] Mukesh Kumar Chettri,[3] Lal Bahadur Thapa,[1]*
[1]Central Department of Botany, Institute of Science and Technology, Tribhuvan University, Kathmandu, Nepal
[2]Central Department of Environmental Science, Institute of Science and Technology, Tribhuvan University, Kathmandu, Nepal
[3]Department of Botany, Amrit Campus, Tribhuvan University, Kathmandu, Nepal
*e-mail: lal.thapa@cdb.tu.edu.np

Abstract:
Chromolaena odorata, a rapidly spreading invasive weed, has been successfully colonized even in dry environments. This species outcompetes native plants by using available resources like water, light and nutrients which limit the survival of native species. In this study, *Aegle marmelos* seedlings were grown in pot to examine the effects of the weed's leachate on their growth and development under shade and drought condition. One set of pots were exposed to full light condition (5000 to 6000 lux) and another was kept under artificial shade (50 to 60 lux). Each group was further divided into treatment with leaf leachate and normal water. Secondly, the seedlings were also grown in pots which were treated with normal water and leaf leachate under control and dry environment (watered after plant began to wilt). Morphological traits as root length, shoot length, seedling biomass, specific leaf area (SLA), number of leaves were measured. Biomass and root length of the seedlings were suppressed by combined effect of shade and leaf leachate by around 63.9% and 65.9%, respectively. In contrast, shoot length and number of leaves showed its resilience, showing no difference across any treatments. However, specific leaf area (SLA) elevated under shaded conditions by 40 to 50%, showing its plasticity. Furthermore, SLA was unaffected by water stress in the presence of leachate of C. odorata but was reduced under the treatment of water by nearly 33%. These results indicate that seedlings of Aegle marmelos undergo morphological changes mostly due to drought and shade. The study indicates response of this native tree seedlings to several stressors and offers quantitative information that is crucial for predicting the impacts of invasion and climate change.

Effects of Nitrogen Sources on The Growth of *Lentinus polychrous* Lev.

Patbawaon Nauldua[1] and Thanyaporn Tangjaroenchai [1,2*]
[1]Demonstration School, University of Phayao, Phayao 56000, Thailand
[2]Division of Biology, School of Science, University of Phayao, Phayao 56000, Thailand
*e-mail: thanyaporn.bo@up.ac.th

Abstract:

Lentinus polychrous Lev. is a popular mushroom used in cooking due to its high nutritional value, especially in terms of protein, carbohydrates and various minerals. Nitrogen, a key component of amino acids, is an essential nutrient for the growth of mushroom mycelium. This study aims to investigate the effects of 6 different media on the growth of mycelium by measuring the radial of mycelial. The characteristics of mycelia density was also identified by visual observation as described by Guadarrame – Mendoza et al., (2014). The result showed that, the 6 different media was significantly affecting the mycelia growth. The most favourable culture media was PDA supplemented with ammonium chloride (9.10±0.10 cm) and malt extract (9.10±0.19 cm) for *Lentinus polychrous* Lev. ($p < 0.05$). The mycelia density of *Lentinus polychrous* Lev. showed that PDA supplemented with yeast extract, ammonium sulfate, ammonium chloride and malt extract were compact.

Efficacy of endophytic fungi against disease in Lettuce leaf spot

Priyakorn Rabaebloed,[1,*] Suwaree Nithichotnuwat,[1]Jaraslak Pechwang,[2] Wanlee Phatthanathalang[2]
[1]PSU Wittayanusorn Suratthani School, Thailand
[2]Prince of Songkla University, Surat Thani Campus, Thailand
*e-mail: kanpriyakorn@gmail.com

Abstract:

Leaf spot disease caused by *Alternaria* sp. is a common disease in lettuce. Disease outbreaks can significantly damage to the crops and negatively impacting farmers. Currently, chemical fungicides are commonly employed to manage leaf spot disease. However, prolonged or excessive use of chemical agents may pose risks to consumers health and the environment. In response to these issues, this study investigates the biological control of leaf spot disease by using endophytic fungi. The application of these fungi in agriculture could reduce the reliance on chemical fungicides, minimize crop losses, mitigate environmental impacts, and improve food safety for consumers. Then, this research focuses on isolating endophytic fungi from Green oak lettuce leaves and evaluating their anti-fungal activity against *Alternaria* sp. A total of seven endophytic fungal isolates: GL01, GL02, GL03, GL08, GL09, GL11, and GL12 were obtained from Green oak lettuce leaves. The results revealed that GL01 cultured on Potato Dextrose Agar (PDA) had the highest inhibitory activity against *Alternaria* sp. using dual culture technique at 60.87% and possessed the largest zone of inhibition (Table 1.) Therefore, GL01 was selected for future culture in Potato Dextrose Broth for 21 Days. The culture filtrate was extracted using ethyl acetate to obtain a viscous brown crude extract. The minimum inhibitory concentration of the crude extract was determined at 100 mg/mL using agar well diffusion method. The results demonstrated that ethyl acetate crude extracts of GL01 suppressed growth of *Alternaria* sp. in vitro. Base on morphological structure and spore of the fungus indicated that GL01 belongs to *Curvularia* sp.

Isolate	Inhibition percentage (%) Type of Culture Media			Fungal inhibition characteristics
	PDA	MEA	YESA	
GL01	60.87 ± 2.17^{a}	35.77 ± 5.07^{d}	58.87 ± 2.45^{ab}	antibiosis
GL02	55.8 ± 1.25^{ab}	52.03 ± 1.41^{b}	58.16 ± 1.22^{ab}	competition
GL03	52.17 ± 2.17^{bc}	53.00 ± 3.05^{bc}	51.06 ± 2.12^{bc}	grow cover pathogen
GL08	58.7 ± 2.18^{a}	54.75 ± 3.06^{b}	59.57 ± 2.13^{a}	grow cover pathogen
GL09	45.65 ± 2.17^{c}	37.39 ± 5.07^{d}	43.26 ± 1.23^{c}	antibiosis
GL11	26.81 ± 2.18^{e}	34.96 ± 1.41^{d}	37.59 ± 1.23^{d}	competition
GL12	52.17 ± 2.17^{bc}	54.75 ± 3.06^{b}	54.61 ± 3.25^{b}	antibiosis

Table 1.
Anti-fungal activities of endophytic fungi against *Alternaria* sp.

ENCAPSULATED FERRITIN FOR CANCER THERAPY

Phatcharinthon Phimsr, Kingsak Mahingsadet, Rung-Yi Lai*
School of Chemistry, Institute of Science, Suranaree University of Technology, Nakhon Ratchasima, 30000, Thailand
*e-mail: rylai@sut.ac.th

Abstract:
Photodynamic therapy (PDT) has become a topic of intense research in cancer treatment due to its reduced side effects compared to traditional therapies. This therapeutic approach employs photosensitizers, such as aza-boron-dipyrromethene (Aza-BODIPY) derivatives, which generate singlet oxygen ($^1O_2$) upon irradiation with a specific wavelength of light, ultimately leading to cell death. However, the poor aqueous solubility of Aza-BODIPY derivatives limits their biological applications. To overcome this limitation, human ferritin (HFn) was utilized as a nanocarrier in this work because HFn has been known to self-assemble into a spherical structure with a hollow interior cavity and can specifically target cancer cells by recognizing transferrin receptor 1 (TfR1), which is highly expressed on the surface of many cancer cell types. The encapsulated HFn nanoparticles, HFn@AZB-OMe-I, were prepared using a pH-dependent loading method at a 1:10 molar ratio of AZB-OMe-I to HFn monomer. The loading numbers of AZB-OMe-I per ferritin nanoparticle was quantified using UV-Vis spectroscopy shows an average loading of 168.68 molecules per nanoparticle. Dynamic Light Scattering (DLS) analysis showed a significant increase in particle size from 10.43 ± 0.37 nm (apo form of HFn) to 87.30 ± 4.61 nm after loading, indicating successful encapsulation and potential structural changes in the nanocage. The PDT capability of HFn@AZB-OMe-I was evaluated under 660 nm light irradiation using 9,10-anthracenediyl-bis(methylene)dimalonic acid (ABDA) as a singlet oxygen probe. A time-dependent decrease in ABDA absorbance confirmed the generation of singlet oxygen, highlighting the potential of HFn@AZB-OMe-I for photodynamic cancer therapy. Subsequent studies will involve in vitro assays aimed at assessing both the cytotoxic effects and cellular uptake efficiency of HFn@AZB-OMe-I nanoparticles.

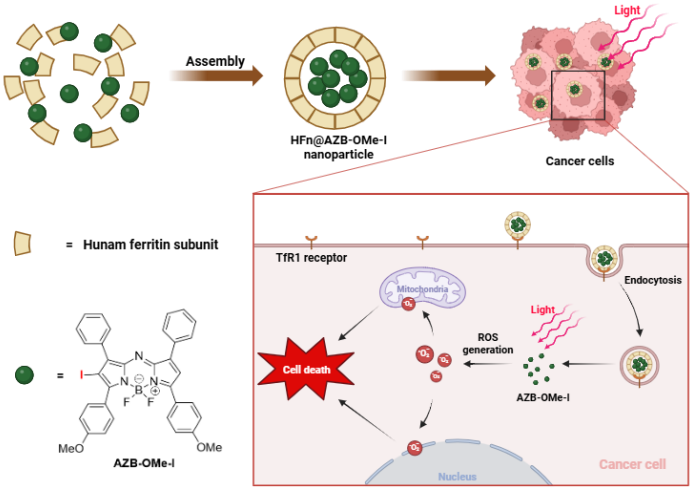

Figure 1. Self-assembled human ferritin nanocages serve as carriers for AZB-OMe-I molecules. This complex targets cancer cells, where it generates reactive oxygen species (ROS) upon photodynamic activation, leading to cell death.

GENE CHARACTERIZATION OF A PUTATIVE CIRCULAR DNA-ACTIVATING PROTEIN IN *Penaeus monodon*

Kanyapak Khaisri[1], Suparat Taengchaiyaphum[2], Kunlaya Somboonwiwat[1, *]
[1] Center of Excellence for Molecular Biology and Genomics of Shrimp, Department of Biochemistry, Faculty of Science, Chulalongkorn University, Bangkok, Thailand
[2] Aquatic Animal Health Research Team (AQHT), Integrative Aquaculture Biotechnology Research Group, National Center for Genetic Engineering and Biotechnology (BIOTEC), National Science and Technology Development Agency (NSTDA), Yothi office, Rama VI Road, Ratchathewi, Bangkok, Thailand
*e-mail: kunlaya.s@chula.ac.th

Abstract:

Endogenous Viral Elements (EVEs) are non-retroviral fragments inserted into a host genome following viral infection. They have been shown to possess specific antiviral activities. Previous studies on insects have suggested that EVEs are generated when viral mRNA is converted to viral copy DNA by a host reverse transcriptase, which is then integrated into the host genome by integrase. EVEs can be transcribed to small RNAs that target their cognate viruses via RNA interference (RNAi), limiting the infection and contributing to viral tolerance. It has been reported that WSSV-tolerant *Penaeus monodon* usually contains a small WSSV-EVEs region of 1,356 bp, referred to as high-frequency read fragments (HFRF). The conservation of WSSV-EVE may indicate its role in antiviral immune responses, but the exact mechanism of EVE biogenesis remains unclear. In this study, we characterized the circular DNA-activating protein (*Pm*CirDAP), which may be involved in this process. *Pm*CirDAP has two isoforms, both of which contain reverse transcriptase and RNase H domains, presumably functioning in converting viral RNA to viral copy DNA, and an integrase domain for genome integration. *Pm*CirDAP1 is highly expressed in hemocytes, lymphoid, and intestine, whereas *Pm*CirDAP2 is highly expressed in stomach, gill, and heart. As hemocytes are considered a key immune tissue, *Pm*CirDAP1 was further characterized. Its expression was down-regulated between 6 and 24 hours post-infection (hpi) and then slightly up-regulated at 48 hpi. This suggests that WSSV may suppress this host factor to prevent the generation of antiviral EVEs and subsequent RNAi defense, representing a viral immune evasion mechanism. The latter up-regulation could be part of the host's delayed effort to re-establish antiviral tolerance.

GENERATION OF TRUNCATED CD235a EXPRESSION CASSETTES FOR INVESTIGATING ITS ROLE IN MALARIA

Kumpanat Pomlok[1*], Suparat K. Lithanatudom[2], and Pathrapol Lithanatudom[3]

[1] Department of Microbiology, Faculty of Science, Silpakorn University, Nakhon Pathom, 73000, Thailand
[2] Program in Genetics, Faculty of Science, Maejo University, Chiang Mai 50290, Thailand
[3] Department of Biology, Faculty of Science, Chiang Mai University, Chiang Mai, 50200, Thailand
*e-mail: pomlok_k@su.ac.th

Abstract:

Plasmodium falciparum is the primary causative agent of malaria. Currently, several receptors on red blood cell surface have been reported to associate with parasite invasion, such as CD147, CD235a and CD108. While CD147 protein has been widely reported as the most important receptor for malaria invasion, the significance of CD235a has been largely overlooked. Besides, the critical binding site on CD235a involved in parasite invasion has yet to be investigated. Thus, plasmid constructs for the expression of truncated CD235a were generated, including cassettes for expressing native CD235a (450 bp) and three truncated variants of CD235a (402, 354, and 306 bp). According to protein expression results, data revealed three constructs for expressing variants in the glycosylated region (450, 402, and 354 bp) were capable of expressing themselves in HeLa cells. However, the failure of truncated CD235a expression (306 bp) could be reasoned by the loss of nucleotide sequence of CD235a spanning positions 106-153 in the glycosylated segment. This sequence loss may be significantly important for the protein folding process involved in its proper structural conformation and functional state. In conclusion, we obtained four constructs for CD235a variants expression, but three of four constructs were capable of expressing protein at the cell surface in HeLa, including a native form (450 bp) and two truncated forms (402 and 354 bp) of CD235a.

GLOBAL SPECIES DISTRIBUTION MODEL OF *Zanthoxylum rhetsa* DC. BASED ON MAXENT MODEL

Yosiya Chanta, Jantrararuk Tovaranonte*
School of Science, Mae Fah Luang University, Chiang Rai 57100 Thailand

*Corresponding author, e-mail: jantrararuk@mfu.ac.th

Abstract: *Zanthoxylum rhetsa (Roxb.)* DC, commonly known as Indian Prickly Ash, is a deciduous tree in the family Rutaceae, native to tropical and subtropical regions and widely distributed across Southeast Asia. It is especially valued for its aromatic fruits, which are traditionally used as spices and condiments. Species distribution models (SDMs) serve as effective tools for predicting suitable habitats, facilitating species introduction, cultivation, and conservation planning. This study aims to forecast the global potential distribution of *Z. rhetsa* and identify key environmental drivers influencing its habitat suitability. Using the MaxEnt model with 286 occurrence records, 19 bioclimatic variables, and several non-climatic factors, the analysis was performed under three thresholding approaches: Minimum Training Presence, Equal Training Sensitivity and Specificity, and 10th Percentile Training Presence. The predicted suitable habitat areas were 3.19% (7,060,914 km²), 1.17% (2,598,922 km²), and 0.29% (638,617 km²) of the global land area under the respective thresholds. The area under the curve (AUC) value is 0.986 indicating high model performance. The most suitable regions were found in Australia, followed by Asia, Africa, and The Americas. Precipitation of the Wettest Quarter (BIO16) and soil type emerged as the most influential environmental factors. These findings highlight the potential application of SDMs in guiding the conservation and sustainable utilization of *Z. rhetsa* worldwide.

KEYWORDS: MaxEnt, Species Distribution Model, *Zanthoxylum rhetsa*, Probability map

Green Synthesis of Cerium Oxide Nanoparticles and Its Antioxidant Properties

Napasorn Tanaatsawapon,[1] Patraporn Luksirikul,[2] and Kanlaya Prapainop Katewongsa[1,3,*]
[1]Department of Biochemistry, Faculty of Science, Mahidol University, Bangkok 10400, Thailand
[2]Department of Chemistry, Faculty of Science, Kasetsart University, Bangkok 10400, Thailand
[3]School of Materials Science and Innovation, Faculty of Science, Mahidol University, Bangkok, 10400, Thailand
*email: Kanlaya.pra@mahidol.ac.th

Abstract:

Cerium oxide (CeO_2) nanoparticles are metal oxide nanoparticles with several applications, including optoelectronic and opto-magnetic devices, electrocatalysis, electrochemical sensors, fuel cell conductors, and enhanced catalyst activity. The catalytic activity is strongly related to minimizing oxidative stress and reactive oxygen species (ROS). To enhance the antioxidant properties of CeO_2 nanoparticles, a green synthesis approach was employed—an environmentally friendly method that utilizes natural materials, specifically turmeric extract. Since turmeric extract is recognized for its strong antioxidant effects, it was employed to synthesize CeO_2 NPs (Tur-CeO_2 NPs).

The characterization of CeO_2 nanoparticles was performed using dynamic light scattering (DLS) to assess their size and zeta potential, and transmission electron microscopy (TEM) to determine their morphology. TEM results exhibited that CeO_2 nanoparticles have both spherical and rod-shaped morphologies at varying pH values. Before the breakdown of CeO_2 nanoparticles, the mean diameter was roughly 1000 nanometers, attributable to their aggregation, and the zeta potential was determined to be negative. However, after breakdown, the mean diameter decreases to a range of 200-700 nanometers, and the zeta potential becomes more positive. The antioxidant activity of CeO_2 NPs was assessed via the DPPH assay, which provides a general measure of free radical inhibition. The results exhibited a dose-dependent increase in percentage inhibition, ranging from 11% at the lowest concentration (15 µg/ml) to 79% at the highest concentration (1000 µg/ml), demonstrating the potential antioxidant effectiveness of CeO_2 NPs.

These findings demonstrate that CeO2 nanoparticles have broad potential, especially where their antioxidant properties provide therapeutic benefits.

INVESTIGATION OF PLGA NANOPARTICLE-MEDIATED INHIBITION OF AMYLOID-BETA FORMATION

Kaung Thant Sin,[1] Nontawat Buapheng,[2] Thitima Jianpinitnun,[2] Kanlaya Katewongsa[2,] *
[1]Biomedical Science Program, Faculty of Science, Mahidol University, Bangkok, 10400, Thailand
[2]Department of Biochemistry, Faculty of Science, Mahidol University, Bangkok, 10400, Thailand
*e-mail: kanlaya.pra@mahidol.ac.th

Abstract:
Alzheimer's disease (AD) is caused by the accumulation of amyloid-β (Aβ) peptides, which forms amyloid plaques and disrupts neurons; consequently, it causes loss of memory and cognitive function. Another factor that promotes AD is oxidative stress. Reactive oxygen species (ROS) can trigger the accumulation of Aβ and tau hyperphosphorylation, which are key mechanisms involved in the development of AD. Previous studies have shown the potential of PLGA nanoparticles as an AD treatment. Poly (lactic-co-glycolic acid) (PLGA) is a biocompatible polymer widely used in drug delivery systems due to its safety, tunable degradation rate, and ability to encapsulate both hydrophilic and hydrophobic molecules. In the context of AD, PLGA nanoparticles are particularly promising because they can cross the blood–brain barrier and can directly interact with Aβ peptides, reducing their aggregation and associated neurotoxicity. This research investigates the effects of PLGA nanoparticles on reducing amyloid beta (Aβ) formation in neuronal cells. The particles are produced by the single emulsion method, and both non-coated and chitosan-coated variations are studied. The synthesized non-coated PLGA nanoparticles have an average hydrodynamic diameter of 184.4 nm and a zeta potential of –7.1 mV, whereas the chitosan-coated particles measure 221 nm in size with a zeta potential of –5.8 mV. The ThT assay is used to evaluate Aβ aggregation, and the MTT assay is applied to determine cytotoxicity and cell viability in SH-SY5Y cell line (human neuroblastoma, ATCC). The results show that PLGA nanoparticles inhibit Aβ aggregation, as indicated by a marked decrease in fluorescence compared to 20 μM Aβ without the particles. Cytotoxicity testing of both non-coated and coated particles indicates cell viability above 90%, confirming that the particles are non-toxic to the cells.

ISOLATION OF HEAT-STABLE LYTIC BACTERIOPHAGES AGAINST CARBAPENEM-RESISTANT *Escherichia coli* FROM TROPICAL WASTEWATER IN THAILAND

Thanatera Petchleung,[1] Jitraphon Narawerawut,[1,3] Passorn Sae Jew,[1,3] Aye Mya Sithu Shein,[4] Apichaya Aryukarn,[4] Yaowarin Nakornpakdee,[2] Puey Ounjai,[5,*] Tanittha Chatsuwan[4,*]
[1]Biomedical Science Program, Department of Pathobiology, Faculty of Science, Mahidol University, Bangkok, Thailand
[2]Department of Pathobiology, Faculty of Science, Mahidol University, Bangkok, Thailand
[3]Department of Life Sciences, School of Life Sciences, University of Sussex, Brighton, United Kingdom
[4]Department of Microbiology, Faculty of Medicine, Chulalongkorn University, Bangkok, Thailand
[5]Department of Biology, Faculty of Science, Mahidol University, Bangkok, Thailand
*e-mail: puey.oun@mahidol.ac.th, Tanittha.C@chula.ac.th

Abstract:

Carbapenem-resistant *Escherichia coli* (CRE) has emerged as a critical global health threat, particularly in tropical regions where high environmental temperatures favor bacterial persistence and transmission. Bacteriophage therapy represents a promising alternative to antibiotics, yet the success of phage-based interventions relies on stability under challenging environmental conditions. Recognizing that hot tropical environments may serve as natural reservoirs for stable phages, in this work, we isolated and characterized lytic bacteriophages that specifically target CRE from wastewater in Thailand.

Multiple phages were obtained, exhibiting diverse plaque morphologies that ranged from small to large plaques, with or without halo zones, reflecting underlying genetic and functional diversity. Host range assays demonstrated broad infectivity, with phage ΦEC2000/6 displaying the widest spectrum, producing bacteriolytic activity against 36.8% (n = 7) of 19 clinical CRE isolates. All phages maintained high titers (up to 3.9×10^{15} PFU/mL) with <0.1-log reduction at 4–40 °C. Activity was lost at pH <3 or >11, while ΦEC1949/6 remained stable at pH 5–11 with only a 0.42-log reduction (4×10^{3}-1.5×10^{3} PFU/mL). The capacity to withstand hot and fluctuating environments highlights their adaptability and strengthens their potential for therapeutic application. These findings confirmed that wastewater from tropical environments serves as a rich reservoir for diverse and stable bacteriophages, potentially providing valuable candidates for phage therapy development against carbapenem-resistant *E. coli*.

MATERNAL GENETIC HISTORY OF LOLOISH SPEAKING HILL-TRIBES IN NORTHERN THAILAND

Dhammawit Haemanwichian[1], Wirunchana Kaweela[2], Tanapon Seetaraso[2], Natcha Chaisoung[2], Suwapat Sathupak[2], Jatupol Kampuansai [2,*]
[1]Chiang Mai University Demonstration School
[2]Department of Biology, Faculty of Science, Chiang Mai University, Chaing Mai, Thailand
*e-mail: Jatupol.K@cmu.ac.th

Abstract:

The Akha and Lahu are recognized as hill-tribe ethnic groups in Thailand. They speak languages belonging to the Sino-Tibetan linguistic family: Southern Loloish for the Akha and Central Loloish for the Lahu. Historical records indicate that these people migrated from their homeland on the Tibetan plateau over the last millennium, moving through southwestern China and northern Myanmar into northern Thailand. Despite their well-known unique cultures and languages, the genetic relationships between the Akha and Lahu remain unclear. This study investigates the maternal history of the Akha and Lahu in Chiang Mai and Chiang Rai provinces. Mitochondrial DNA control region analyses were conducted on 90 unrelated individuals from two Akha villages and two Lahu villages. Population pairwise differences (F_{st}) revealed significant genetic distinctions between the Akha and Lahu. A strong founder effect was observed in the Lahu village from Chiang Mai, with the lowest haplotype diversity at 0.7508±0.0710. The predominant mitochondrial lineages, haplogroup D4J in the Akha and D4e in the Lahu, suggest northern Asian ancestry. These findings enhance our understanding of the genetic differences, maternal lineage, and historical migrations of the Akha and Lahu populations in northern Thailand.

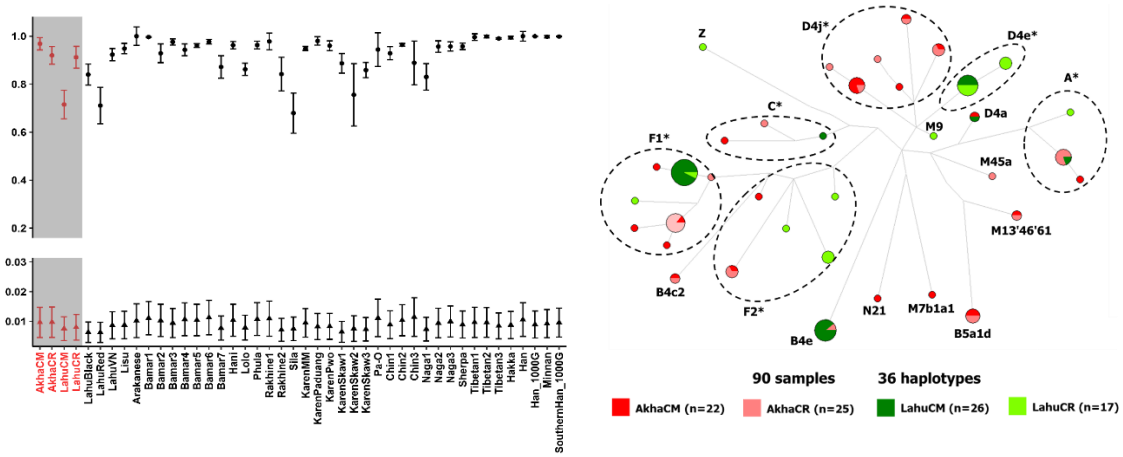

Figure 1.
Haplotype (h) and nucleotide (π) diversity (left)
and Median-Joining network of each mitochondrial DNA haplotype (right)

METABOLOMIC PROFILING OF THAI *Centella asiatica* (L.) Urb. ACCESSIONS REVEALS VARIATION IN LPS-ACTIVATED NITRIC OXIDE IN RAW264.7 CELLS

Samita Phothong[1], Thanaporn Thumyodsawat[2], Phontharat Channgam[2], Jira Jongcharoenkamol[3], Wanrachon Nukool[1], Marootpong Pooem[1], Kittisak Buddhachat[1,*]

[1]Department of Biology, Faculty of Science, Naresuan University, Phitsanulok, 65000 Thailand
[2]Naresuan University Secondary Demonstration School, , Naresuan University, Phitsanulok, 65000 Thailand
[3]Department of Pharmaceutical Chemistry and Pharmacognosy, Faculty of Pharmaceutical Sciences, Naresuan University, Phitsanulok, 65000 Thailand
*e-mail: kittisakbu@nu.ac.th

Abstract:

Centella asiatica (L.) Urb. is a medicinal plant valued for its anti-inflammatory, wound-healing, and collagen-stimulating activities, contributing to its importance as a source of raw materials for the pharmaceutical and nutraceutical industries. To identify elite accessions with superior bioactive potential, we evaluated 25 C. *asiatica* accessions collected from Thailand using a metabolomics-guided approach. Untargeted metabolite profiling was conducted by liquid chromatography–mass spectrometry (LC–MS) on ethanolic extracts at a concentration of 50 µg/mL. The extracts were further assessed for cytotoxicity and their ability to suppress nitric oxide (NO) production in lipopolysaccharide (LPS)-stimulated RAW264.7 macrophages. The average half-maximal inhibitory concentration (IC_{50}) of the extracts was 409.96 µg/mL, indicating low cytotoxicity. Most accessions demonstrated strong inhibition of NO production, except CMI, NKI, and NPT1. Metabolomic analysis revealed triterpenoids, flavonoids, phenolics, organic acids, sugars, and lipids as candidates linked to NO reduction, with moderate correlations observed for trisaccharides. These findings demonstrate variation in metabolite profiles and bioactivity among accessions and highlight metabolomics as a tool for selecting elite *C. asiatica* germplasm for medicinal applications.

Keywords: Metabolomics; Bioactive compounds; Multivariate analysis; Functional metabolites

Microplastic detection in freshwater gastropod from Mueang Nakhon Ratchasima District, Nakhon Ratchasima Province, community markets.

Natwalan Photphiphat,[1] Anchayanit Poonsree,[2] Pitchapa Keawmanee [3,*]
[1]Suranari Wittaya School, 248 Thanon Mittraphap, Nai Mueang, Mueang Nakhon Ratchasima District, Nakhon Ratchasima 30000
[2]Suranari Wittaya School, 248 Thanon Mittraphap, Nai Mueang, Mueang Nakhon Ratchasima District, Nakhon Ratchasima 30000
[3]Suranari Wittaya School, 248 Thanon Mittraphap, Nai Mueang, Mueang Nakhon Ratchasima District, Nakhon Ratchasima 30000
*e-mail: natwalanphotphiphat@gmail.com

Abstract:

Microplastics are plastic particles with a diameter of less than 5 millimeters, often caused by the decomposition or breakage of large plastic waste, caused by plastic that is created to be small. Nowadays, microplastic contamination is found in the environment. This affects the ecosystem and humans, especially in gastropod, where a large amount of microplastic contamination was found. This research objective is to investigate microplastic contamination in pond snail and apple snail by collecting samples of snail sold from community markets in Mueang Nakhon Ratchasima district, 5 sources to study. In addition, compare the number, size, type, color, and shape of microplastics found in snails with stereo light microscopy, fluorescence microscope, and infrared light analysis techniques (FTIR Micro- Spectrometer). The study found the spread and accumulation of microplastics in the pond and the apple snail from all the community markets. Pond snail from the water market found the most microplastics, amounting to 46.00 ± 7.00 pieces. Apple snails from Long Tong market found the most microplastics in the amount of 42.67 ± 10.79 pieces. Microplastics can be classified into 5 groups, including fibers, fragments, nurdles, films, and shapes that cannot be identified. The color of microplastics from all 5 colors of fluorescent endoscopy: black, yellow, red, green, and transparent. The nurdle microplastics were found in the highest number in the whole snail. Both 2 species were found in pond 28.60 ± 16.08 pieces and apple clams 34.60 ± 9.20 pieces and green is the most common color. Microplastics that accumulate in snail tissue may affect the health of consumers.

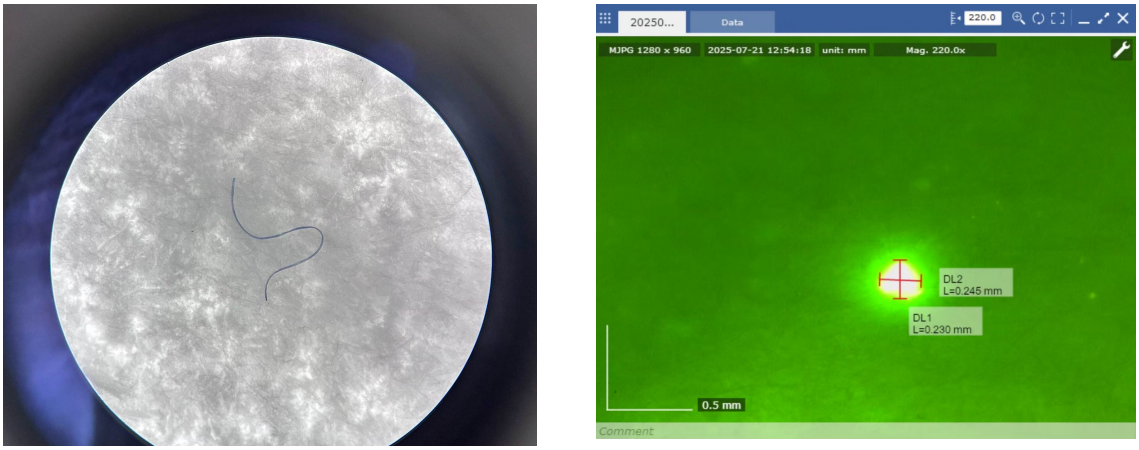

Figure 1.
Microplastics observed under a light microscope (left) and fluorescence microscopy (right)

Phytochemical profiling and chondroprotective activity of *Centella asiatica* (L.) Urb. extracts for the selection of elite accessions

Wanrachon Nukool[1], Puntritra Kamol[2], Nungruithai Suphrom[3], Kittisak Buddhachat[1,*]
[1]Department of Biology, Faculty of Science, Naresuan University, Phitsanulok, 65000, Thailand
[2]Biology Program, School of Science, University of Phayao, Phayao, 56000, Thailand
[3]Department of Chemistry, Faculty of Science, Naresuan University, Phitsanulok, 65000, Thailand
*e-mail: kittisakbu@nu.ac.th

Abstract:
Centella asiatica (L.) Urb. is a widely used medicinal plant valued for its therapeutic properties, particularly in skin care, wound healing applications and chondroprotection. In this study, a total of 25 *C. asiatica* ethanolic extracts was evaluated for their phytochemical profiles by quantifying four major bioactive compounds: asiaticoside, madecassoside, asiatic acid, and madecassic acid. The analysis revealed substantial variation among the samples, with the extract from Chiang Mai (CMI) exhibiting the highest concentrations of all four compounds. To further explore chondroprotective properties of these extracts, six representative samples were selected for biological evaluation using IL-1β-induced SW1353 chondrosarcoma cells, a model for cartilage inflammation and degradation. Gene expression analysis demonstrated that extracts from Lampang (LPG), Sakon Nakhon (SKN), and Sukhothai (STI) significantly downregulated the expression of pro-inflammatory and cartilage degradation-related genes, including *IL-1β*, *TNF-α*, *MMP3*, *MMP13*, and *IL-6*. Notably, these extracts exhibited relatively high levels of aglycones (asiatic acid and madecassic acid), suggesting that aglycon content may be associated with the reduction of inflammatory cytokine gene expression. These findings support the selection and cultivation of elite *C. asiatica* accessions as promising raw materials for the future development of herbal supplements aimed at promoting joint health and overall wellness.

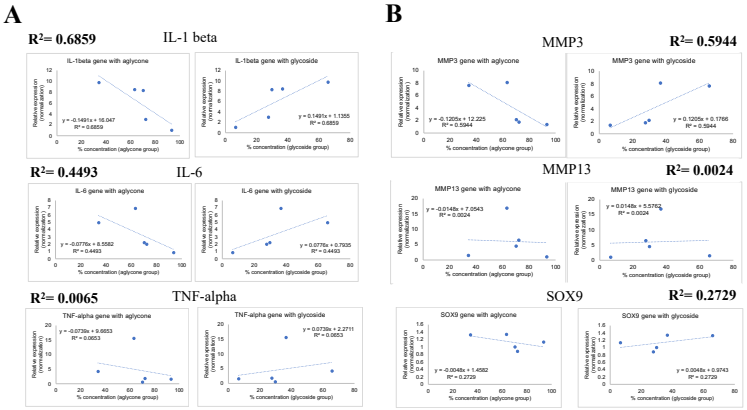

Figure 1.
Relationship between the chemical constituents of *C. asiatica* extract, specifically comparing the aglycone group and the glycoside group to their effects on the expression of genes associated with cartilage degradation, including inflammatory genes (IL-1β, IL-6, and TNF-α) (A), genes involved in extracellular matrix breakdown (MMP3 and MMP13) (B), and the gene responsible for collagen synthesis (SOX9) (B).

RAPID DNA EXTRACTION FOR DETECTING *Babesia* spp. USING RPA-CRISPR-CAS12A FOR POINT-OF-CARE TESTING

Suphaporn Paenkaew, Onnicha Sinthao, Thanawin Thaothim, Rongdej Tungtrakanpoung, Kittisak Buddhachat*
Department of Biology, Faculty of Science, Naresuan University, Phitsanulok, 65000 Thailand.
*e-mail: kittisakbu@nu.ac.th

Abstract:
Rapid and accurate detection of *Babesia* spp., the causative agents of babesiosis in animals, is critical for early diagnosis and disease management. Molecular diagnostics such as RPA-CRISPR-Cas12a offer high specificity and sensitivity but require DNA as the detection target for point-of-care testing. DNA extraction is an essential step, as commercial methods require centrifuge equipment and are time-consuming, thus unsuitable for field applications. In this study, we developed a simple, rapid, and efficient DNA extraction method by spotting blood on filter paper, treating with TE buffer, and applying heating, without the need for centrifugation. The process was completed within 15 minutes, and the extracted DNA was used in RPA-CRISPR-Cas12a detection at 37 °C within 1.5 hours. The assay demonstrated high specificity, with no cross-reactivity to related hemoparasites, and a limit of detection of 10^4 copies, comparable to that obtained using the commercial DNA extraction kit. Comparison of the diagnostic performance using real blood samples with the commercial method, based on bovine and canine blood, showed high concordance, with 95% accuracy, 100% precision, and a Cohen's kappa of 0.9. These results indicate that the rapid TE-based DNA extraction method is effective for *Babesia* spp. detection, as it provides DNA of sufficient quality for use as a target in RPA-CRISPR-Cas12a detection. Moreover, combining this rapid extraction with RPA-Cas12a offers strong potential for development in point-of-care applications.

REGULATION ON BIOFORTIFICATION IN *BRASSICA JUNCEA* MICROGREEN USING GAMMA-AMINOBUTYRIC ACID (GABA) UNDER CONTROLLED ENVIRONMENTS

Theeraphat Singto[1], Natnaree Sookyuen[2], Watsakorn Chaisombhat[3], Jitpanu Yamjabok[4,*], Patchara Praseartkul[4], Rujira Tisarum[4] and Suriyan Cha-um[4]

[1]*Princess Chulabhorn Science High School Lopburi, Khok Samrong, Lopburi, 15120,* Thailand
[2]*Princess Chulabhorn Science High School Chiang Rai, Mueang, Chiang Rai, 57000,* Thailand
[3]*Takuapasenanukul School, Takua Pa, Phang Nga, 82110,* Thailand
[4]National Center for Genetic Engineering and Biotechnology, National Science and Technology Development Agency, Khlong Luang, Pathum Thani 12120, Thailand
[*]*Corresponding author: jitpanu.yam@biotec.or.th*

Abstract

Brassica juncea microgreen is a short harvest cycle, high yielding and a good source of nutrients, which makes this species a promising superfood. This study aims to investigate role of gamma-aminobutyric acid (GABA) in enhancing iron biofortification in *B. juncea* microgreen. We hypothesized that GABA improves iron uptake in *B. juncea*. by root cell enlargement. To proof this, *B. juncea* microgreens were exposed to two $FeSO_4$ concentrations (0 and 0.2 µM) and three GABA concentrations (0 µM, 0.2 µM, and 0.5 µM) for two weeks under control conditions (set at 25 ºC and 12h photoperiod/12h dark). Growth parameters, photosynthetic pigment content and chlorophyll fluorescence were measured. The results showed that there were no statistically significant differences in *B. juncea* growth parameters ($p > 0.05$) between 0 µM $FeSO_4$ and 0.2 µM $FeSO_4$, as well as among three GABA concentrations. This indicates that *B. juncea* growth was not affected by either Fe or GABA treatment. Notably, Fe treatment significantly affected chlorophyll B content ($p = 0.033$), carotenoid content ($p = 0.030$), maximum photochemical quantum yield (F_v/F_m) ($p = 0.0003$) and photosystem II efficiency (Φ_{PSII}) ($p = 0.001$), regardless of GABA concentration. Comparing to 0 µM $FeSO_4$, Chlorophyll B and carotenoid decreased by 11.95 – 29.54 % and 10.04 – 25.21 %, whereas F_v/F_m and Φ_{PSII} increased by 1.18 – 3.57 % and 0 – 22.92 % in 0.2 µM $FeSO_4$ treated samples. This indicates that $FeSO_4$ treatment solely influences photosynthesis machinery without adversely affecting plant growth in *B. juncea*. In addition, GABA application does not induce any phenotypic changes at seedling stage of *B. juncea*. We conclude that Fe and GABA treatment are applicable for microgreen production of *B. juncea*. Still, further measurement of chemical composition, in particular for iron content, is required to elucidate the effect of iron treatment and the role of GABA in improved iron accumulation in *B. juncea*, as well as to determine the optimal treatment for producing high iron content *B. juncea* microgreen.

RISK OF SEQUENTIAL INVASIONS: INFLUENCE OF *Ageratina adenophora* ON GROWTH AND DEVELOPMENT OF *Bidens pilosa*

Neera Shrestha*, Chandra Prasad Pokhrel, Lal B. Thapa*, Ram Kailash Prasad Yadav

Central Department of Botany, Institute of Science and Technology, Tribhuvan University, Kirtipur, Kathmandu, Nepal

*Corresponding Email : shresthaneera3@gmail.com, lal.thapa@cdb.tu.edu.np

Abstract:

Bidens pilosa and *Ageratina adenophora* are the fast growing invasive herbs belonging to family Asteraceae and often found growing together in the invaded sites. Ecologically, when they grow together, they may compete for resources and potentially one may facilitate or suppress the growth and development of another. The nature and strength of these interactions remain poorly understood. The study investigated the effects of volatiles and mulching of *A. adenophora* on growth and development of *B.pilosa.* Seedlings of *B. pilosa* were grown in polyethylene pots (11cm height and 8.5 cm diameter) under two experimental conditions: (i) exposure to volatiles within a closed polyethylene chamber (25.5 cm × 35 cm) containing 100g of fresh leaves of *A. adenophora* and (ii) mulching treatment where chopped fresh leaves of *A. adenophora* were applied as 3 cm thick layer over the soil surface. Length and biomass of roots and shoots were measured. The leaf numbers were counted and biomass was also measured. Results showed the volatiles of *A. adenophora* are toxic for growth and development of roots of *B. pilosa* as the roots were very shorter by 82% and had low biomass (92%) in this treatment. Shoots under the chamber were 10.73±1.98 cm while they were ±1.87 cm outside the chamber. The shoots were comparatively thinner due to volatile effect but mulching showed positive effect on shoot biomass. Similarly, seedlings grown with mulching accumulated more amount of biomass than seedlings in control (35%), whereas volatiles reduced the biomass significantly in the leaves. Results indicate that *A. adenophora* volatiles can be harmful to co-existing *B. pilosa*, however, it can get benefit when *A. adenophora* leaves act as mulch and decompose over germinating seeds of *B. pilosa.* Hence, the interaction between these two weed species is antagonistic, and gives idea of interspecific co-existence and invasion dynamics. Overall, *B. pilosa* may emerge as a secondary invader as the mulching effect of *A. adenophora* may provide nutrients, water retention and shade effect. Thus, this study highlights the risk of sequential invasions.

SCREENING NINE CHILLI VARIETIES FOR BIOFORTIFICATION AND ENHANCED NUTRITIONAL VALUES BY SOIL DRENCHING IRON APPLICATION

Peemanut Phumma[1], Kongnahpat Jirojkhunathip[2], Jitpanu Yamjabok[3,*], Patchara Praseartkul[3], Rujira Tisarum[3] and Suriyan Cha-um[3]
[1]*Taweethapisek School, Bangkok Yai, Bangkok, 10600 Thailand*
[2]*Huahin School, Huahin, Prachuap Khiri Khan, 77110 Thailand*
[3]National Center for Genetic Engineering and Biotechnology, National Science and Technology Development Agency, Khlong Luang, Pathum Thani 12120 *Thailand*
[*]*Corresponding author: jitpanu.y@biotec.or.th*

Abstract:
Chilli is one of the most important spices, which widely played as major ingredient in Thai foods. In the Northern region of Thailand, leaves and young shoots of chilli are generally used as key ingredient for cuisine namely “Kang Care”. This culinary practice makes chilli a great candidate for microgreen production, which is an enriched biofortification for human health. Nevertheless, research on chilli microgreens remains limited. The aim of this study is to evaluate the potential for biofortification of nine chilli varieties through iron treatment. Fourteen-day-old seedlings were treated with $FeSO_4$ by soil drenching method at two concentration (0 and 0.2 mM), for seven days. Subsequently, microgreen samples were assessed for biomass yield, morphological traits, chlorophyll fluorescence, total carotenoid content and chlorophyll content. The results showed that 0.2 mM Fe treatment significantly increased shoot fresh weight (SFW) of chilli cv. Chinda by 39.66% (p = 0.029) but significantly decreased SFW of chilli cv. Yao by 18.11% (p = 0.029) when comparing to control Fe treatment (0 mM). Fe treatment significantly affected photosynthesis, with photosystem II efficiency (Φ_{PSII}) increasing by 26.91% in chilli cv. Khee Noo (p = 0.029) and by 39.48% in chilli cv. Mhundum Bang Chang (p = 0.029). Statistically significant reduced content of chlorophyll A (p = 0.034) and chlorophyll B (p = 0.0094) were only observed in chill cv. Kareang. In contrast, total carotenoids content was increased under Fe treatment in chilli cv. Yoa (48.44%, p = 0.029), whereas it was significantly reduced in chill cv. Kareang (33.83%, p = 0.029), Yak (p = 0.029), and chill cv. Khoapaa (28.6%, p = 0.029). In conclusion, nine chilli varieties have diverse phenotypic responses of microgreen to Fe treatment. Among these varieties, chilli cv. Chinda and chilli cv. Yoa identified as the promising candidates for chilli microgreen due to their high SFW and elevated carotenoid content. Therefore, the Fe content and other micronutrients in the chilli microgreens will further be quantified using ICP-MS analysis as important criteria to make a decision the best genotype in the near future.

SITE DIRECTED MUTAGENESIS OF α-GLUCOSIDASE FROM *Weissella cibaria*

Nida Singkorapoom*, Thatcheewa Apichatayanon, Watthanachai Saradhuldhat, Karan Wangpaiboon, Kuakarun Krusong
Center of Excellence in Structural and Computational Biology, Department of Biochemistry, Faculty of Science, Chulalongkorn University, Bangkok 10330, Thailand
*e-mail: nida.singkorapoom@gmail.com

Abstract:

α-Glucosidase is an enzyme that belongs to the Glycoside hydrolase family (GH) 13 that hydrolyzes carbohydrates at the α-1,4-glycosidic linkage to produce glucose. It is widely used in chemical synthesis to produce various glycosides, the treatment of disease such as type 2 diabetes, and the syrup production industry. α-Glucosidase from *Weissella cibaria* (*Wc*AG) is in the GH13_20 neopullanase subfamily, with a structure similar to the other enzymes within the subfamily. However, it has a distinct substrate preference compared to the other members of the subfamily, as it prefers to hydrolyze maltooligosaccharide that contain three to seven glucose molecules and acarbose, but not cyclic oliogosaccharides nor polysaccharides. *Wc*AG is a homodimer with a salt bridge gate formed by two amino acid residues located near the active site. We hypothesized that this salt bridge gate blocks the entry of larger carbohydrates, resulting in a unique substrate specificity of the enzyme. In this study, site-directed mutagenesis via PCR-overlap extension was performed to disrupt this gating mechanism. The mutant enzymes were expressed in *Escherichia coli* BL21(DE3) via induction using IPTG and purified using nickel column chromatography. The mutant enzymes showed enhanced activity toward acarbose, maltotetraose, and maltopentaose compared to the wild-type enzyme, while activity toward β-cyclodextrin was abolished. These findings highlight the structural role of the gating residues in determining substrate specificity of *Wc*AG, which improves the understanding of the structures of enzymes in this subfamily.

SPATIAL VARIABILITY OF CORAL RECRUITMENT AND REEF RESILIENCE ON SHALLOW REEF FLATS IN MU KO SURIN, PHANGNGA PROVINCE, ANDAMAN SEA

Makamas Sutthacheep*, Thamasak Yeemin, Wiphawan Aunkhongthong, Laongdow Jungrak, Charernmee Chamchoy, Sittiporn Pengsakun, Wanlaya Klinthong, Maneerat Sukkeaw,
Marine Biodiversity Research Group, Department of Biology, Faculty of Science, Ramkhamhaeng University, Huamark, Bangkapi, Bangkok, Thailand
*e-mail: smakamas@hotmail.com

Abstract:
Coral recruitment is a fundamental ecological process that underpins reef recovery, biodiversity maintenance, and long-term ecosystem resilience by ensuring the replenishment of coral populations, sustaining genetic diversity, and facilitating ecological connectivity across reef habitats. Successful recruitment not only drives the natural regeneration of degraded reefs but also serves as a key indicator of ecosystem health, reflecting the capacity of coral communities to persist and adapt under escalating climatic and anthropogenic stressors. This study investigated recruitment dynamics on shallow reef flats at Ao Mai Ngam, Ao Suthep, and Ao Pak Kaad within Mu Ko Surin National Park, Andaman Sea, as well as their implications for reef resilience. Field surveys conducted in 2024 employed belt transects (30 × 1 m) to estimate live coral cover and quadrats (16 × 16 cm) to quantify coral recruits (≤ 5 cm). Results revealed that the highest coral recruit density was recorded at Ao Mai Ngam (16.46 ± 1.19 recruits/m²), followed by Ao Suthep (14.04 ± 1.01 recruits/m²), while the lowest was observed at Ao Pak Kaad (9.20 ± 0.66 recruits/m²). Statistical analysis confirmed significant differences in recruitment density among sites ($F = 42.80$, $p < 0.05$), with Ao Mai Ngam supporting markedly higher densities than both Ao Suthep and Ao Pak Kaad. A total of 30 species of coral recruits were recorded across the study sites, with *Fungia*, *Porites*, *Acropora*, and *Pocillopora* emerging as the most dominant genera. The role of Ao Mai Ngam as a recruitment hotspot underscores its importance in maintaining coral population connectivity and its critical contribution to sustaining and enhancing reef resilience at the ecosystem level. These findings highlight the necessity of site-specific management strategies that safeguard recruitment hotspots while incorporating targeted restoration measures in degraded reef areas. By integrating protection and restoration, such approaches can reinforce the ecological processes that drive coral recovery, enhance population connectivity, and ultimately strengthen the adaptive capacity and long-term sustainability of coral reef ecosystems.

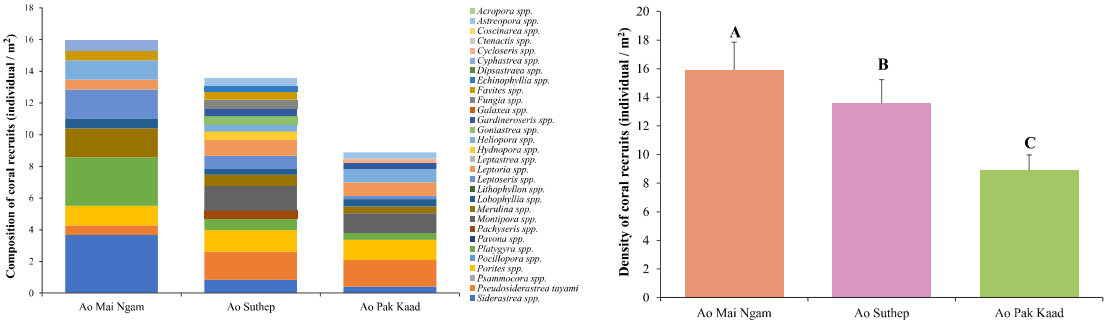

Figure 1.
Composition of coral species at each site (left)
Density of coral recruits at each site (right)

SUPPRESSION OF BANANA FUSARIUM WILT *Fusarium oxysporum* f.sp. *cubense* BY FROG SKIN-ASSOCIATED BACTERIA

Lela Susilawati,[1]* Arifah Khusnuryani[1], Olan Lusiana[1], Nabila Nur Shafira[1], Misbahul Munir[2]

[1]Department of Biology, Faculty of Science and Technology. UIN Sunan Kalijaga Yogyakarta, Jl. Marsda Adisutjipto No.1 Yogyakarta, 55281 Indonesia
[2]Herpetological Society of Indonesia, Jl. Ulin, Kampus Darmaga, Bogor, Jawa Barat 16680 Indonesia

*e-mail: lela.susilawati@uin-suka.ac.id

Abstract:

Fusarium wilt, caused by *Fusarium oxysporum* f. sp. *cubense* (Foc), is a major constraint to banana production in tropical regions and remains difficult to manage using conventional methods. This study explored the antifungal potential of cell-free filtrate (CFF) derived from ScD9 bacteria, isolated from the skin of the *Sumaterana crassiovis* frog, as a biocontrol agent against Foc in both *in vitro* and *in vivo* conditions. *In vitro* assays were conducted using CFF at concentrations of (v/v) 2%, 4%, and 6%, and included tests on mycelial growth and conidial germination. The results demonstrated significant antifungal activity, with the 6% CFF treatment showing the highest inhibition. *In vivo* experiments on banana plants further confirmed the biocontrol efficacy of 6% CFF, which significantly reduced both disease incidence and severity compared to untreated controls. Based on 16S rDNA sequence analysis and similarity search, isolate ScD9 identified as *Staphylococcus* sp. These findings indicate that CFF from *Staphylococcus* sp. strain ScD9 has promising potential as a sustainable biocontrol agent against Foc in banana, though further field evaluation is needed.

SYNCHRONOUS MOVEMENT AND MORTALITY OF EARTHWORMS IN CENTRAL NEPAL

Ankit Kumar Singh, Laxman Khanal*
Central Department of Zoology, Institute of Science and Technology, Tribhuvan University, Kathmandu 4418, Nepal
*e-mail: laxman.khanal@cdz.tu.edu.np

Abstract:
Earthworms are important ecological influencers that regulate soil nutrients, maintain soil quality, and sustain biogeochemical balance in terrestrial ecosystems. Their physiology, feeding habit, and movement have distinctly contributed on soil horizon. Usually, it shows movement in search of food and suitable habitat, however the previous report on synchronous mass movements of exotic earthworm species, discussed for probable factors associated on it. Meanwhile, observation on rapid emergence and mortality of earthworm species in their native locality are of immediate ecological concern to identify causative factors. Thus, we investigated mass movement and mortality of earthworm species at two different sites in central Nepal (Kathmandu and Lalitpur districts). Systematic sampling was conducted in 25 × 25 m² fixed plots once per week during the months of July and August for three consecutive years 2023-2025. From the area of mass movement, two different native species of *Eutyphoeus* spp. (Michaelsen, 1900) were reported based on morpho-anatomical comparisons; presence of tanylobous prostomium, lumbricine setae, male pores in XVIII, female pore in XIII, mid-ventral intestinal caeca in XXVI–XXVII, 3–6 pairs of supra-intestinal glands in XII and XXV, holandric testes, seminal vesicles in IX and XII, paired spermathecae without diverticula, and absence of lateral intestinal caeca. Mean density of movement was 97 individuals/m² in Lalitpur and 36.5 individuals/m² in Kathmandu, with average displacement speeds of 0.067 m/s and 0.055 m/s, respectively. Mortality rates averaged 29.88/m² in Lalitpur and 9.35/m² in Kathmandu, with juveniles comprising 98.5% of the population. Movements occurred within an altitudinal range of 1,850–2,350 m asl. Soil temperature, moisture, and nutrient content showed no significant differences ($p > 0.05$) between sites, eliminating these as explanatory factors. In contrast, soil erosion, road disturbance, and excess water runoff were positively correlated with migration rates and displacement speed, suggesting potential causal mechanisms that warrant further study. These findings demonstrate that synchronous mass movement and mortality of deep-burrowing *Eutyphoeus* species are likely responses to extreme rainfall and soil disturbance. Such events highlight the vulnerability of native Himalayan earthworms to hydrological and anthropogenic stressors, with broader implications for soil faunal diversity, nutrient cycling, and ecosystem functioning under changing climatic conditions.

USING NATURAL ANTIOXIDANT FROM *Centella asiatica* EXTRACT FOR CRYOPRESERVATION OF *Caenorhabditis elegans*

Korrawan Pipatanusone,[1] Thunchanok Tannikorn,[1] Tanawan Leeboonngame[2,*]
[1]Kamnoetvidya Science Academy, Thailand
[2]Department of Biology and Environmental Science, Kamnoetvidya Science Academy, Thailand
*e-mail: tanawan.l@kvis.ac.th

Abstract:

Cryopreservation is the process of preserving cells, tissues, organs, or living organisms at low temperatures to temporarily terminate biological activity and maintain their condition for a long time until needed. A major cause of reduced cell viability during freezing is excessive reactive oxygen species (ROS) accumulation, which disrupts the oxidant-antioxidant balance, leading to oxidative stress within the cells. This issue can be mitigated by antioxidants, which are found in various plants. *Centella asiatica* (Gotu kola) has been studied and found to contain bioactive compounds with antioxidant properties. This project aims to investigate the effects of *Centella asiatica* extract on *Caenorhabditis elegans* cryopreservation to determine the optimal conditions for enhancing the cryopreservation. *Centella asiatica* was extracted using two different solvents: 95% ethanol and water. The DPPH assays, an antioxidant determining test, showed more antioxidants in the ethanol extract than in the water extract. The extracts were then mixed with Nematode Growth Medium (NGM) agar at concentrations of 10, 50, 100, and 200 µg/mL—levels which past studies reported to exhibit insignificant cytotoxic activity—and used to pretreat *C. elegans* from the egg to L1 stage before freezing at -60 °C for 24 hours. The results showed that pretreatment with the extracts improves *C. elegans* survival after freezing. The ethanol extract enhances survival more effectively than the water extract, with 100 and 200 µg/mL ethanol extract significantly increasing survival rates ($p<0.05$). However, the motility assays, conducted at the adult stage, showed no significant difference between treated and untreated groups. Morphological abnormalities, the body length-to-width ratio lower than normal, were observed in the worms pretreated with water extract and the untreated group. Loss of DNA content was observed by DAPI staining only in the untreated group. This preliminary study shows that *Centella asiatica* can improve cryopreservation efficiency. In the future, it could be used to develop pretreatments that enhance cryopreservation efficiency and increase survival rates in cells, tissues, and whole organisms.

VISUALISATION OF LATENT DNA IN LIP-PRINTS WEARING LIPSTICKS

Pachaporn Khajornpop[1], Monrada Ngamapisit[1], Supitcha Hemwaranon[1], Piyamas Petcharoen[2],*
[1] Ratchasima Witthayalai School, SCiUS-Suranaree University of Technology (SUT), Nakhon Ratchasima, Thailand, 30000
[2] School of Biology, Institute of Science, Suranaree University of Technology (SUT), Nakhon Ratchasima, Thailand, 30000
*e-mail: piyamas@sut.ac.th

Abstract:
Diamond™ Nucleic Acid Dye (DD), in combination with a portable digital fluorescent microscope, has been developed as a promising tool for detecting latent DNA on forensic relevance, including lip-prints. Lip-prints are crucial in forensic investigations, allowing individual identification through DNA profiling or pattern analysis. However, research on latent DNA recovery from lip-prints wearing lipsticks remains limited, as the presence of cosmetic products may interfere with the DNA detection and visualisation. Previous research indicated that lip balm did not interfere with the DNA detection, whereas lip matte significantly impacted DNA detection. However, only one brand of each was analysed.

To address this limitation, this study broadened the evidence base by testing four lipstick types—lip gloss, lip balm, lip tint, and lip matte—each represented by two widely used brands. Three volunteers applied the tested lipstick and deposited their lips on cleaned glass slides. Then lip-prints were stained with DD and imaged with a portable fluorescence microscope. Images were assessed in ImageJ by quantifying ΔRGB/fluorescence contrast between stained cells and background. Each condition was replicated across donors and brands. Results showed that lip tint had the most significant impact on DNA visualisation, showing the highest RGB intensity colour difference analysed through ImageJ. In contrast, lip gloss had the least impact, as its formulation minimally interfered with DNA detection. This study presented valuable understandings into influence of DNA detection using DD staining in lip-prints wearing lipsticks.

C: ANALYTICAL CHEMISTRY

A DOPAMINE LEVEL DETECTION SENSOR USING METAL NANOMATERIALS ON MOLYBDENUM DISULFIDE AND GRAPHENE OXIDE ELECTRODES FOR KIDNEY DISEASE RISK ASSESSMENT

Kawissara Kanjanahirun,[1] Nanicha Kietrungnoppakun,[1,*] Patcharanun Kiattiwattanakorn[1]
Panyawut Rattanarom[1] and Asst. Prof. Dr. Sujittra Poorahong[2]
[1]Benjamarachutit school, Nakhon Si Thammarat, 80000 Thailand
[2]Department of Analytical Chemistry, School of Science, Walailak University,
Nakhon Si Thammarat
*e-mail: 43911@benjama.ac.th

Abstract:
Patients with impaired kidney function often exhibit abnormal dopamine secretion, leading to irregular urinary dopamine levels. These abnormalities are associated with chronic and acute kidney disease, pheochromocytoma, neuroblastoma, salt-sensitive hypertension, and complications from medications or L-DOPA–rich foods. In Thailand, the Health Data Center (HDC) reported 1,062,756 cases of chronic kidney disease in 2024. Early detection is essential to improve treatment outcomes and reduce mortality. However, the current standard method, High Performance Liquid Chromatography (HPLC), is expensive and time-consuming. This study aims to develop a rapid, sensitive, and cost-effective electrochemical sensor for dopamine detection. The sensor integrates metal nanoparticles synthesized on molybdenum disulfide (MoS_2) and graphene oxide (GO), with electrodes modified at a 1:1 GO:MoS_2 ratio. Differential Pulse Voltammetry (DPV) analysis demonstrated that current responses increased with dopamine concentration, while the half-wave potential slightly decreased due to surface accumulation. The sensor achieved a linear range of 0.2–1.2 mM (r = 0.9943), with sensitivity of 12.451 µA/mM, a limit of detection (LOD) of 1.1987 µM, and a limit of quantification (LOQ) of 3.8551 µM. Precision testing gave %RSD = 1.95%, confirming reproducibility. The results indicate that this sensor could be adopted as a reliable and efficient method for rapid urinary dopamine detection, with potential for integration into future clinical diagnostics.

A NON-ENZYMATIC ELECTROCHEMICAL URIC ACID SENSOR BASED ON AuPtNPs@OMC NANOCOMPOSITE MODIFIED SCREEN-PRINTED ELECTRODE COUPLED WITH FLOW INJECTION SYSTEM

Thanomwan Kueasom,[1,2,3] Thanawath Tuntiwongmetee,[1,2,3] Nuttakorn Junlapak,[1,2,3] Natha Nontipichet,[1] Panote Thavarungkul,[1,2,3] Suntisak Khumngern,[1], Apon Numnuam[1,2,3]*

[1]Center of Excellence for Trace Analysis and Biosensor, Faculty of Science, Prince of Songkla University, Hat Yai, Songkhla, 90110, Thailand

[2]Division of Physical Science, Faculty of Science, Prince of Songkla University, Hat Yai, Songkhla, 90110, Thailand

[3]Center of Excellence for Innovation in Chemistry, Faculty of Science, Prince of Songkla University, Hat Yai, Songkhla, 90110, Thailand

*e-mail: apon.n@psu.ac.th

Abstract:

A flow injection amperometric sensor for the non-enzymatic detection of uric acid (UA) was fabricated based on bimetallic alloy gold-platinum nanoparticles (AuPtNPs) and ordered mesoporous carbon (OMC). The bimetallic alloy AuPtNPs, as an excellent electrocatalyst towards UA oxidation, was decorated on the surface of OMC as an interesting supporting nanomaterial with high surface area, porosity, and good electroconductivity. Electrochemical characterization of the AuPtNPs@OMC revealed enhanced conductivity and a higher surface area of the modified electrode compared to the monometallic AuNPs@OMC and PtNPs@OMC. Furthermore, the amperometric response of the developed AuPtNPs@OMC sensor measured the UA concentration through the oxidation of UA and exhibited the highest sensitivity, with a linear range of 0.0025 – 1.0 mM. This improvement was ascribed to the synergistic effect of the AuPtNPs bimetallic alloy with excellent electrocatalytic activity and the highly porous structure of OMC. Moreover, this sensor tested the possible interferents for UA detection, like ascorbic acid and dopamine; these results indicated good selectivity of the AuPtNPs@OMC sensor toward UA. Therefore, this developing sensor has the potential application to measure UA in real samples.

A VOLTAMMETRIC SENSOR FOR CARBARYL DETECTION BASED ON AuNPs@OMC NANOCOMPOSITE MODIFIED GLASSY CARBON ELECTRODE

Kawisara Kommaless,[1,2,3] Nuttakorn Junlapak,[1,2,3] Natha Nontipichet,[1] Panote Thavarungkul,[1,2,3] Suntisak Khumngern,[1], Apon Numnuam[1,2,3]*

[1]Center of Excellence for Trace Analysis and Biosensor, Faculty of Science, Prince of Songkla University, Hat Yai, Songkhla, 90110, Thailand

[2]Division of Physical Science, Faculty of Science, Prince of Songkla University, Hat Yai, Songkhla, 90110, Thailand

[3]Center of Excellence for Innovation in Chemistry, Faculty of Science, Prince of Songkla University, Hat Yai, Songkhla, 90110, Thailand

*e-mail: apon.n@psu.ac.th

Abstract: An electrochemical carbaryl (CBR) sensor was developed by modifying an ordered mesoporous carbon (OMC) incorporated with gold nanoparticles (AuNPs) nanocomposite on a glassy carbon electrode (AuNPs@OMC/GCE). The three-dimensional structure of the OMC surface was functionalized with AuNPs through an in-situ chemical reduction method. The AuNPs@OMC nanocomposites were morphologically characterized by scanning electron microscopy (SEM) and transmission electron microscopy (TEM). The morphological analysis clearly confirms that AuNPs were uniformly formed and well-distributed on the surface of the OMC. The resulting AuNPs@OMC nanocomposites on GCE exhibited high sensitivity toward the oxidation of CBR owing to the synergistic effects of the enhanced high specific surface area, electrocatalytic activity, and rapid charge transfer. The developed sensor was studied for the optimal conditions to enhance the detection efficiency, including the amount of AuNPs@OMC and the effect of pH value. Under the optimized conditions, the AuNPs@OMC sensor for the detection of CBR exhibited a linear response from 2.0 to 10.0 mM with a low detection limit of 0.97 mM (3SD/slope). Therefore, it can be concluded that the developed AuNPs@OMC sensor exhibits promising analytical performance and has potential for future application in real sample measurement.

ACTIVATED CARBON IMPREGNATED DEEP EUTECTIC SOLVENT FOR SELECTIVE LITHIUM EXTRACTION FROM SPENT TERNARY LITHIUM-ION BATTERIES

Zaharaddeen Muhammad,[1,2], Panawan Vanaphuti[1], Apichat Imyim[1,*]
[1] Department of Chemistry, Faculty of Science, Chulalongkorn University, Bangkok 10330, Thailand
[2] Department of Chemistry, Faculty of Natural and Applied Sciences, Sule Lamido University Kafin-Hausa, Nigeria
Corresponding Author, E-mail: apichat.i@chula.ac.th

Abstract

The global transition to net-zero emissions has intensified the demand for critical raw materials, particularly lithium, which is essential for the production of lithium-ion batteries (LIBs). Despite its pivotal role, lithium recovery from spent LIBs remains insufficient (≤50%) compared to other transition metals (Co, Ni, & Mn >70%). In this study, a novel two-step process was developed, combining ultrasonic-assisted ethylenediaminetetraacetic acid (EDTA) leaching and selective adsorption using biomass-derived activated carbon (AC) impregnated with a hydrophobic deep eutectic solvent (HDES) at a 1:1 w/w ratio. Under ultrasonic conditions, EDTA functioned as both a leaching and masking agent, achieving leaching efficiencies of 98.5%, 98.1%, 97%, and 96.3% for Li^{+}, Mn^{2+}, Co^{2+}, and Ni^{2+}, respectively. Batch adsorption experiments demonstrated highly selective lithium extraction (99%) at optimized conditions (pH 12, 75 mg dosage, 2 h contact time). The adsorbent exhibited excellent reusability with minimal performance loss (≤1.5%) over five cycles and effective lithium desorption using mild acid treatment (0.7 M HCl). Kinetic, isotherm, and pH-dependent studies, together with detailed characterizations, confirmed that lithium adsorption is primarily governed by enolate-phosphoryl coordination. This method eliminates the use of volatile organic solvents and concentrated acids, addressing the limitations of conventional liquid-liquid extraction with HDES and traditional hydrometallurgical processes. This process offers a sustainable and environmentally benign pathway for lithium recovery, advancing resource conservation and the circular economy in battery recycling.

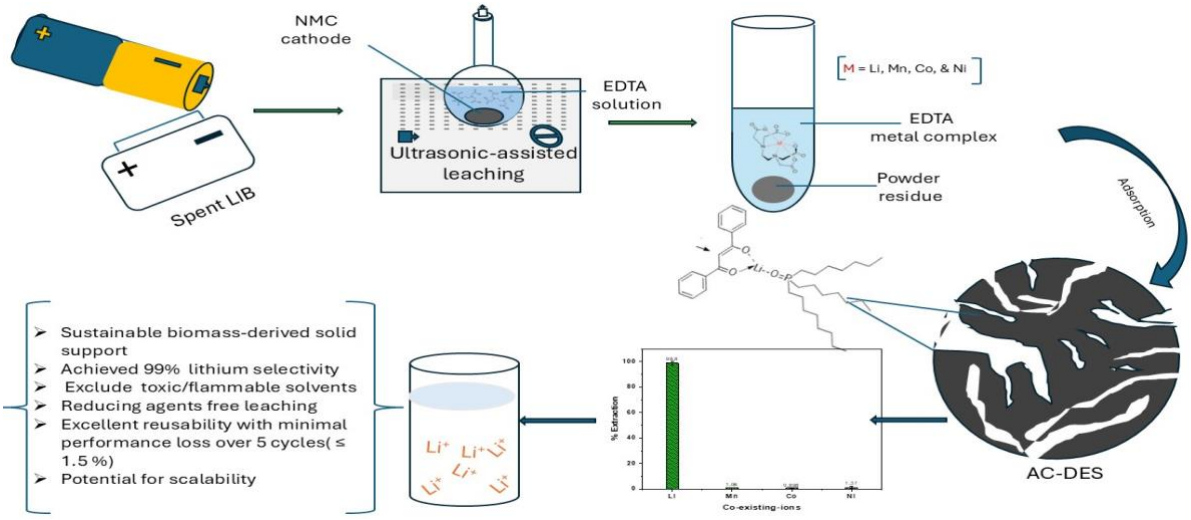

Figure 1: Two-step lithium extraction and recovery process using ultrasonic-assisted EDTA leaching and biomass-derived (AC-DES) solid support

AGGREGATION-BASED BIPHASIC FLUORESCENT RESPONSE OF SUGARCANE-DERIVED NITROGEN-DOPED CARBON DOTS TOWARD FORMALDEHYDE

Papontee Raungnay, Krittatham Uppagara, Satatorn Bowornnaowarak, Prasongporn Ruengpirasiri, PhD*
Kamnoetvidya Science Academy, Rayong, Thailand
*e-mail: prasongporn.r@kvis.ac.th

Abstract:
Formaldehyde, a class I carcinogen, is widely used for food preservation, tableware, and fumigation. Carbon dots (CDs), the carbon nanoparticle, are one of promising methods for detection of formaldehyde via fluorescence signal due to their unique photoluminescence properties, high selectivity and sensitivity. However, literature reports have conflicted: some systems show fluorescence enhancement upon FA exposure while others report quenching. Here we investigate the mechanisms that produce these opposing responses and demonstrate sugarcane-derived NCDs that exhibit a reproducible two-phase fluorescent response to FA. The extracted lignin from sugarcane bagasse and m-phenylenediamine (MPDA) was used to synthesize nitrogen doped carbon dots (NCDs) via hydrothermal method. Upon FA addition at pH 7, fluorescence intensity rises rapidly (within <10 s), then decays with apparent first-order kinetics while solution turbidity increases (OD_{600}). FT-IR of the precipitate reveals imine formation, consistent with FA reaction at surface amines. We propose a mechanistic sequence, firstly, rapid formation of surface imine/hydroxymethyl adducts disrupts hydrogen-bonding networks and transiently enhances emission (hydrogen-bond induced emission, HBIE), followed by slower imine-mediated crosslinking/aggregation that induces aggregation-induced quenching (AIQ). A simple kinetic model of F → M → A reproduces the rise-then-fall behavior. In dose–response tests the t = 10 min curve shows signal enhancement up to ≈60 ppm FA and quenching above that level, while at t = 60 min, the response is dominated by quenching over 0–500 ppm, with a limit of detection of 10.3 ppm (3σ/S) These results reconcile conflicting reports and illustrate how reaction kinetics and incubation time govern CD sensing behavior. With further optimization and selectivity studies, biomass-derived NCDs may be useful for real-time FA monitoring and imaging applications.

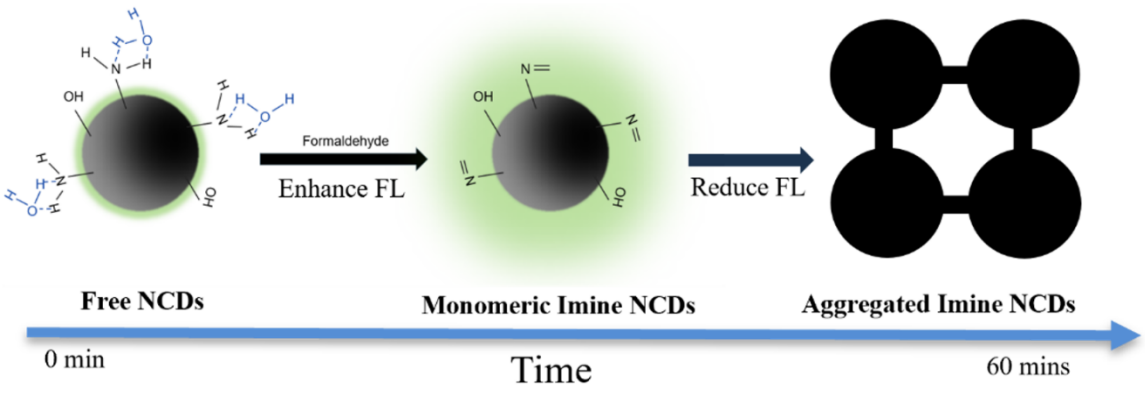

Figure 1. Proposed mechanism of fluorescence response of NCDs toward formaldehyde

CHEMICAL PROFILING FOR THE DISCRIMINATION OF COFFEE BEAN CULTIVARS BY LC-QTOF MS METABOLOMICS

Kanchana Watla-iad,[1,*] Plaipol Dedvisitsakul,[2] Natsaran Saichana,[2] Saowaluk Madkoksung[1]
[1]Coffee Quality Research Group, School of Science, Mae Fah Luang University, Chiang Rai 57100, Thailand
[2]Microbial Products and Innovation Research Unit, School of Science, Mae Fah Luang University, Chiang Rai, Thailand
*e-mail: kanchana.wat@mfu.ac.th

Abstract:
This study conducted metabolomic analysis of fourteen coffee bean varieties using liquid chromatography-quadrupole time-of-flight mass spectrometry (LC-QTOF) to characterize chemical profiles and establish varietal relationships. Green coffee samples, including Dwarf San Ramon, Geisha, Liberica, Typica, and various H-series cultivars, were collected from Royal Project Research Station Mae Hlod, Chiang Mai, Thailand. Sample preparation involved methanol extraction of 0.1g coffee powder with 1.5 mL methanol, 12-hour soaking, centrifugation at 1230 rpm for 10 minutes (repeated three times), and final volume adjustment to 5 mL. Stock solutions were diluted 50-fold before LC-QTOF analysis in positive and negative ionization modes. Multivariate statistical analysis was used via the MetaboAnalyst online program with hierarchical cluster analysis (Euclidean distance, Ward linkage) and Spearman correlation analysis. Heat map visualization illustrates metabolite distribution patterns across varieties. The analytical approach successfully differentiated coffee varieties based on metabolomic fingerprints, revealing distinct clustering patterns reflecting genetic and biochemical diversity. The results showed that Liberica, Dwarf San Ramon, H.D.T., and H.377/8 varieties exhibited significantly different metabolite profiles compared to other groups. This methodology provides valuable insights for coffee authentication, quality assessment, and breeding programs, contributing to the understanding of coffee cultivar diversity and applications in specialty coffee markets.

DETERMINATION OF SALICYLIC ACID BY A DISTANCE-BASED PAPER SENSOR

Piriyapong Saetang, Phimchaya Phutthaphongloet, Sasitorn Ngamprasertsuk,
Wijitar Dungchai*
University of Technology Thonburi, Prachautid Road, Thungkru, Bangkok 10140, Thailand
*e-mail: wijitar.dun@kmutt.ac.th

Abstract:

This study aimed to develop a distance-based paper sensor for the quantitative analysis of salicylic acid (SA), an active ingredient commonly found in various skincare products. The sensor was fabricated using Whatman No. 1 filter paper, patterned by laser printing and subsequently coated with ferric chloride hexahydrate ($FeCl_3 \cdot 6H_2O$) and polyethylenimine (PEI). These reagents form a coordination complex with salicylic acid, producing an orange-colored band, the length of which correlates with the SA concentration. Spectral analysis using a UV-Visible spectrophotometer revealed that the $FeCl_3 \cdot 6H_2O$ -SA complex exhibited maximum absorbance at 525 nm. Upon the addition of PEI, the maximum absorbance shifted to 460 nm, indicating the formation of a new complex. Optimization studies showed that a combination of 15.00 mM $FeCl_3 \cdot 6H_2O$ and 0.4% w/v PEI yielded the most reliable results, with a strong linear relationship between band length and SA concentration in the range of 2.00 - 18.00 mM. The derived calibration equation was $y = 0.0575x + 1.3917$ with a correlation coefficient (R^2) of 0.9960. The sensor's performance was further evaluated in the presence of commonly encountered cosmetic ingredients, including niacinamide, phenoxyethanol, EDTA, glycolic acid, and zinc sulfate. Most of these interferents had negligible effects on accuracy, except EDTA and zinc sulfate at higher concentrations. Application of the sensor to real cosmetic samples showed some deviations compared to the UV-Visible spectrophotometric method, likely due to matrix complexity. Nevertheless, the proposed device offers the advantages of low cost, operational simplicity, and acceptable accuracy in standard solution analysis, and demonstrates promising potential for future on-site testing applications.

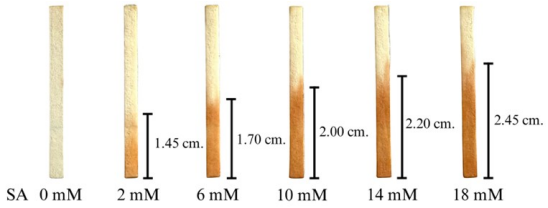

Figure 1.
Images of salicylic acid determination in the range of 0 – 18 mM with Distance-Based Paper Sensor at 15.00 mM $FeCl_3 \cdot 6H_2O$ and 0.4 %w/v of PEI.

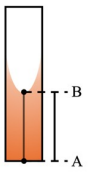

Figure 2.
The distance was measured from the center of the paper (A) to the end of the concave part of the colored band or the point where the color disappeared.(B)

DEVELOPMENT OF FLOW INJECTION AMPEROMETRIC SENSOR BASED ON SCREEN-PRINTED CARBON ELECTRODE MODIFIED WITH rGO-PDDA@PtNPs COMPOSITE FOR THE DETERMINATION OF H_2O_2

Neramit Nitichai,[1,2,3] Kanokkorn Sae-Tan,[1,2,3] Muktinan Saraban,[1,2,3] Natha Nontipichet,[1] Panote Thavarungkul,[1,2,3] Apon Numnuam,[1,2,3] Suntisak Khumngern[1]*
[1]Center of Excellence for Trace Analysis and Biosensor, Faculty of Science, Prince of Songkla University, Hat Yai, Songkhla, 90110, Thailand
[2]Division of Physical Science, Faculty of Science, Prince of Songkla University, Hat Yai, Songkhla, 90110, Thailand
[3]Center of Excellence for Innovation in Chemistry, Faculty of Science, Prince of Songkla University, Hat Yai, Songkhla, 90110, Thailand
*e-mail: suntisak.k@psu.ac.th

Abstract: Hydrogen peroxide (H_2O_2) is a strong oxidizing agent with effective bleaching and disinfecting properties. It is commonly used as an ingredient in hair dye products, bleaching agents, and acne treatments. However, excessive use can cause allergic reactions and skin irritation. Therefore, the development of simple and reliable analytical methods for detecting H_2O_2 is essential. In this study, a non-enzymatic electrochemical sensor combined with a flow-injection system was developed for the detection of H_2O_2. The sensor was based on a screen-printed carbon electrode (SPCE) modified with reduced graphene oxide-poly(diallydimethylammonium chloride)@platinum nanoparticles (rGO-PDDA@PtNPs). The synthesized nanocomposites exhibited excellent catalytic activity toward H_2O_2 reduction, showing high reduction current at low potentials. H_2O_2 was determined using amperometry at an applied potential of −0.20 V (*vs* Ag) in a flow injection system. The amount of prepared nanocomposite was optimized at 4.50 µg. The developed sensor exhibited good linearity between 0.5 µM and 15 mM. Moreover, the developed sensor exhibited excellent selectivity against possible interference presented in real samples. Hence, this sensor can be applied in the detection of H_2O_2 in real samples.

Development of paper sensors using dye compound to detect dopamine in sweat for point-of-care diagnosis of Parkinson's disease using fluorescent

Kanruthay Ruktaengam[1], Kanokket Juehom[1], Assoc. Prof. Dr. Boosayarat Tomapatanaget[2],
[1]Triam Udom Suksa School, Bangkok, Thailand
[2]Department of Chemical, Faculty of Science, Chulalongkorn University

Abstract

Dopamine is an essential biomarker for diagnosing neurological disorders, including Parkinson's disease. However, existing detection methods are often hindered by high costs, operational complexity, and time-consuming sample preparation. This study introduces a novel, cost-effective, and sensitive sensor for dopamine detection using pyrene boronic acid (**PBA**). The sensor harnesses the strong binding affinity between boronic acid and dopamine's diol groups, allowing for accurate and efficient detection under optimized conditions. Fluorescence spectroscopy confirmed the sensor's excellent sensitivity and selectivity, achieving a detection limit of 1×10^{-2} M. Through experiments varying the concentrations of **PBA** and dopamine, it was demonstrated that **PBA** at a minimum concentration of 1×10^{-3} M could reliably detect dopamine at concentrations as low as 1×10^{-2} M. Despite this constraint, the findings underscore the potential of the PBA-based sensor for real-time monitoring of dopamine levels. This research paves the way for advancements in biosensing technology, offering a practical solution for neurological diagnostics and expanding the accessibility of biomarker detection tools.

Keywords: Dopamine; Parkinson's disease; Pyrene boronic acid; Sweat; Catecholamines; Fluorescent

Introduction

Globally, Parkinson's disease affects approximately 10 million individuals, with an annual incidence rate of 10–20 new cases per 100,000 people. In Thailand, while the prevalence remains lower compared to Western countries, the number of cases is expected to rise due to the aging population, as the disease predominantly affects individuals over the age of 60.[WHO[1]]

For diagnosis of Parkinson's disease, the amount of dopamine (DA) in the nervous system is recognized as a critical biomarker; however, current methods for measuring dopamine levels face significant limitations. These include the need for specialized equipment, technical expertise, high costs, and time-intensive sample preparation processes [Fawsy[2],AANS[3]]. To address these challenges, this research aims to develop and optimize chemosensors, providing a more efficient, cost-effective, and accessible solution for dopamine detection.

Dopamine is categorized in the catecholamine group because the structure of dopamine contains both catechol and amine groups. For sensing of catechol moiety, boronic acid is normally used as a receptor because boronic acid can react with diol compounds and form boronate ester

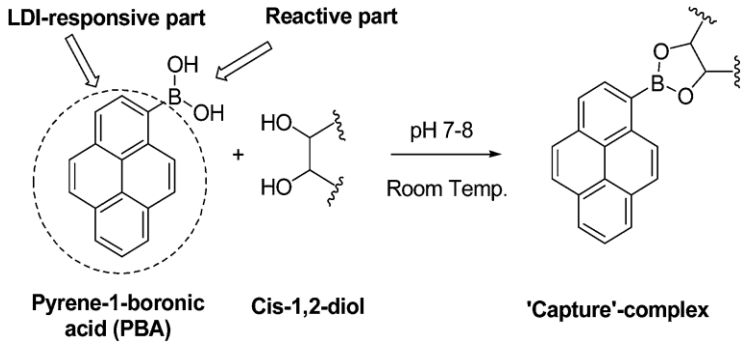

Figure 1.1 Reaction between boronic acid and diol group

Addy, P. S., Bhattacharya, A., Mandal, S. M., & Basak, A. (2014). Label-assisted laser desorption/ionization mass spectrometry Retrieved from https://doi.org/10.1039/C4RA07499H

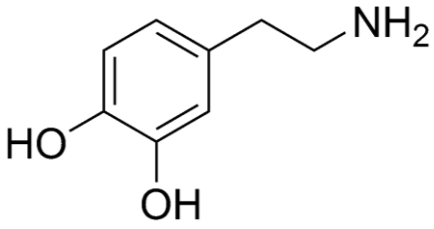

Figure 1.2 Dopamine structure

Cacycle. (2007). Dopamine chemical structure Wikimedia Commons. Retrieved from https://commons.wikimedia.org/wiki/File:Dopamine_chemical_structure.png

For example, Pyrene pyrene-boronic acid (**PBA**) has been used as a fluorescent sensor for dopamine sensing [Ellie[4]]. The structure of **PBA** is composed of a signal unit of fluorescent pyrene moiety and a receptor unit of the boronic acid functional group. The structure of dopamine contains a catechol group, which can react with boronic acid under slightly alkaline conditions to form a stable boronate ester anion. When boronic acid reacts with the catechol group, it induces a change in the electronic environment, affecting the pyrene moiety and leading to a change in the fluorescence signal properties. Typically, the interaction results in fluorescence quenching or shifts in the emission spectrum, caused by electron transfer or changes in the molecular environment. The fluorescence changes are proportional to the concentration of dopamine. As mentioned above, **PBA** has been attracted as a valuable tool for real-time dopamine detection in medical diagnostics and biochemical research.

There are a few reports regarding to the detection of dopamine by using the fluorescence sensor. In 2018, [Teo[5]] Teo et al. conducted the study "One-Step Production of Pyrene-1-Boronic Acid Functionalized Graphene for Dopamine Detection," which introduced an innovative dopamine sensor using graphene functionalized with pyrene-1-boronic acid (PBA). The researchers employed a molecular wedging technique to exfoliate graphite into graphene sheets while simultaneously incorporating **PBA** in a single step. The resulting PBA/graphene composite takes advantage of the boronic acid group's ability to bind with dopamine's diol groups, ensuring high sensitivity and selectivity in detection. The sensor demonstrated excellent electrochemical performance with minimal interference from other biomolecules. This streamlined synthesis approach reduces production complexity, making it cost-effective and scalable. The findings highlight the potential of PBA-functionalized graphene in biosensing applications, particularly for diagnosing neurological conditions like Parkinson's disease.

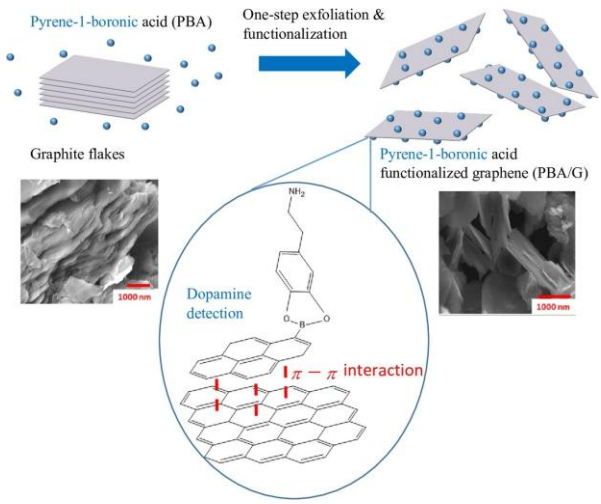

Figure 2. Electrons paired from the diol compound result in a neutral borate ester

Tajik, S., Taher, M. A., & Beitollahi, S. (2019). A novel electrochemical sensor based on poly (pyrocatechol violet) retrieved from https://ars.els-cdn.com/content/image/1-s2.0-S0254058419303256-egi10ZSNHQDZHR_lrg.jpg

The binding between boronic acid and diols compound was investigated by various pH of solution. The result exhibited that the binding constant between boronic acid and diol compounds decreases with the decrease in pH. At a pH lower than the pKa of boronic acid, the sp^2 hybridization of the boron atom is formed. In sp^2 hybridization, boron has only 6 valence electrons and can accept electrons paired from a diol compound, resulting in a neutral borate ester, as shown in Figure 3. When the pH of the solution increases and is higher than the pKa of boronic acid, the hybridization of the boron atom transforms to sp^3, resulting in a borate anion, which has a negative charge of the boron atom. In this hybridization of boron, the anionic boronic reacts with diol compounds, resulting in a borate ester anion, which has 8 valence electrons. Thus, the binding constant of boronic acid and diol compound in basic solution is higher than acidic solution

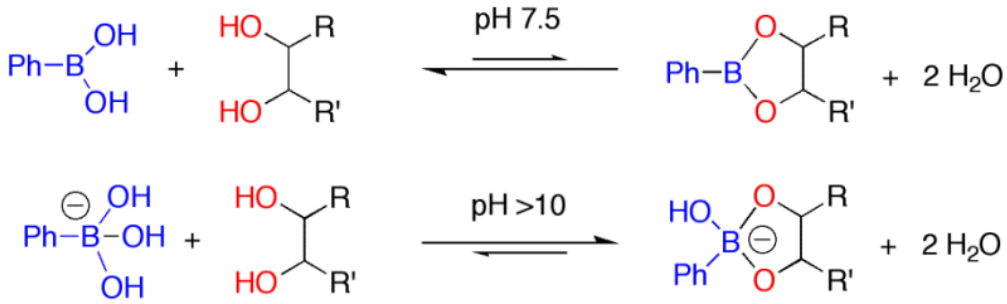

Figure 3. The formation of boronate ester and borate ester anion at varied pH
Pappin, B., Kiefel, M. J., & Houston, T. A. (2012). Boron-carbohydrate interactions. Retrieved from https://cdn.intechopen.com/pdfs/41107/InTech-Boron_carbohydrate_interactions.pdf

From the utilization of fluorescent chemosensory and properties of boronic acid, the **PBA** has been applied for the detection of dopamine, particularly in the context of Parkinson's diagnosis. Boronic acids can form reversible covalent bonds with diols, leading to changes in the fluorescent signal of pyrene. Therefore, researchers aim to develop a faster, more accurate test for measuring dopamine levels by fabrication of fluorescent dye on paper-based sensors as a point-of-care for measuring dopamine levels under the interaction between boronic acid in fluorophore and diol group-based catecholamine compound by using **PBA** fluorescent sensor. The quantitative and qualitative analysis of the sensing platforms towards analysts will be investigated for the benefit of the sensitivity of sensing platforms. If these studies are achieved and give excellent results, they will be developed to construct prototypes for sensing applications. It is an ideal platform for point-of-care (POC) testing in regions where limited resources are realized. This research will potentially provide the sensor prototype for pragmatic clinical diagnosis.

Theoretical and Conceptual Framework

1. Highly effective discrimination of catecholamine derivatives via FRET-on/off processes induced by the intermolecular assembly with two fluorescence sensors

1.1 Authors and Publishing Information

Anusak Chaicham, Somboon Sahasithiwat, Thawatchai Tuntulani and Boosayarat Tomapatanaget (2013)

1.2 Abstract

In 2013, Chaicham, A. et al developed a new sensing system based on intermolecular assembled complexes of two fluorescence sensors for discrimination types of biogenic amine derivatives as shown in the figure xxxx. Pyrene boronic acid (PBA) has been used as a first sensor for separation of biogenic amines composed of catechol group by using the specific covalent binding between boronic acid and catechol groups. PBAsensor shows the high effective identification of dopamine (DA), epinephrine (EPI) and norepinephrine (NE) because these biogenic amines have a catechol group in their molecule as shown in the figure xxx. The additional sensor coumarin aldehyde (CA) has been used for the separation of EPI from the other catecholamines by using the reaction between primary amine. Both structures of DA and NE have primary amines in their molecules; therefore, DA and NE are suitable catecholamines acting as guest linkers and assemblies formed between PBA and CA. The assembly of two fluorescence sensors via a catecholamine linker induces FRET-on and could discriminate structural similarity of catecholamines.

2. Boronic Acid Mediated Coupling of Catechols and N-Hydroxylamines: A Bioorthogonal Reaction to Label Peptides

2.1 Author and Publishing Information

Margaret K Meadows, Emily K Roesner, Vincent M Lynch, Tony D James, Eric V Anslyn

2.2 Abstract

In 2017, A simple method for combining 2-formylphenylboronic acid, catechol, and N-hydroxylamines was developed in water, forming boronate esters with compounds like l-DOPA. The reaction worked well alongside other chemical processes, such as copper-catalyzed alkyne-azide reactions and aminoether/carbonyl condensations, making it useful for complex chemical syntheses. The process was further simplified into a single-step reaction that combined boronate ester formation and aminoether condensation, successfully tested with a short peptide. This method is easy to use, reduces steps, and works efficiently, making it practical for building biomolecules. Its ability to function in water and its compatibility with biological systems make it valuable for research in chemistry, biology, and medicine.

3. Boronic acid-based fluorescent glucose sensors

3.1 Author and Publishing Information

Zhang, C., Zhang, Y., Wang, X., Yang, X., & Wang, Y

3.2 Abstract

In 2018, Zhang.C provided an in-depth overview of the progress in developing boronic acid-based fluorescent sensors for glucose detection. It highlights the unique ability of boronic acids to reversibly bind with diols, enabling effective glucose recognition. The paper categorizes different sensor designs, including small molecule sensors, polymer-based systems, and nanoparticle-integrated platforms, while detailing their mechanisms, sensitivity, and selectivity. Challenges such as interference from other sugars and pH sensitivity are discussed, alongside potential strategies to address these issues. The review concludes by outlining future research directions, focusing on improving sensor performance for practical use in medical diagnostics and continuous glucose monitoring.

4 Recent development of boronic acid-based fluorescent sensors

4.1 Author and Publishing Information

Guiqian Fang, Hao Wang, Zhancun Bian, Jie Sun, Aiqin Liu, Hao Fang, Bo Liu, Qingqiang Yao, Zhongyu Wu

4.2 Abstract

According to Guiqian Fang’s research in 2018, Boronic acids, as Lewis acids, have the ability to bind reversibly and covalently with 1,2- or 1,3-diols in aqueous solutions, forming five- or six-membered cyclic esters. This interaction induces significant fluorescence changes, making boronic acid compounds effective sensors for detecting carbohydrates and other substances. While previous reviews have addressed this topic, a surge of novel boronic acid-based fluorescent sensors has emerged in recent years. This paper highlights advancements from the past five years, focusing on sensors capable of detecting carbohydrates such as glucose, ribose, and sialyl Lewis A/X, as well as catecholamines, reactive oxygen species, and ionic compounds. Additionally, it explores emerging electrochemically related fluorescent sensors and new materials incorporating functionalized boronic acids, such as nanoparticles, smart polymer gels, and quantum dots. By summarizing and analyzing these innovations, the review aims to inspire further advancements in the design and application of boronic acid-based fluorescent sensors.

The findings from the research above have inspired the development of a paper-based diagnostic platform for Parkinson's disease. This tool uses boronic acid as a selective receptor for dopamine by incorporating boronic acid into the sensing mechanism, the platform enables

efficient detection of dopamine through measurable changes, such as fluorescence or colorimetric responses. The integration of advanced sensing chemistry into a paper-based format further enhances its accessibility and practicality for point-of-care applications.

Experimental Methodology

Equipment and Location

Equipment

- Beaker
- Micropipette
- Cuvette
- Fluorescence Spectrophotometry
- Eppendorf
- Hot plate
- Electronic balance
- 1-Pyreneboronic acid
- Sodium Hydroxide
- Sodium Thiosulfate
- HEPE Buffer
- Dopamine
- Sodium Chloride
- Methanol
- Deionized water

Location

Department of Chemistry, Faculty of Science, Chulalongkorn University, laboratory

Methodology

General

All materials and solvents were obtained from TCI, Sigma-Aldrich, Carlo Erba, and other suppliers as standard analytical grade and used without additional purification. Commercial-grade solvents, including methanol and deionized water, were utilized as received. The Blacklight photo box was utilized to monitor the brightness of the sensing materials in different conditions.

1. **Preparation of stock solution PBA and DA**

For the all experiment, 1×10^{-1} M and 1×10^{-3} M stock solutions of sensor **PBA** were prepared in methanol. A solutions of 1×10^{-1} M and 1×10^{-3} M of DA prepared in 5.0 x 10^{-2} M of HEPE buffer pH 6 containing sodium thiosulfate, and sodium chloride were prepared. The solution of 0.1 M sodium hydroxide was prepared in DI water. The stock solutions of **PBA** and DA were used in all experiments.

2. **Optimize concentration of sensor PBA**

A 1×10^{-1} M of **PBA** was diluted to be two concentrations of 1×10^{-2} M and 1×10^{-3} M in methanol. For each concentration, 900 µL of the **PBA** solution was transferred to a vial, followed by the addition of 100 µL of 1×10^{-1} M NaOH solution and the solution mixture is labeled as **PBA-OH**. The **PBA-OH** is continues diluted to be 5×10^{-3} M, 3×10^{-3} M, and 2×10^{-3} M by methanol.

3. **Study of naked eyes sensing of PBA sensor toward DA**

A stock solution of **PBA-OH** solution was prepared by adding 20 µL of 0.1 M sodium hydroxide in methanol into 180 µL of 1×10^{-3} M the sensor **PBA** in methanol. The mixture was stirred for 1 minute and labeled as a solution **PBA-OH**. Pipet 100 µL of the prepared **PBA-OH** solution and 100 µL of 5.0 x 10^{-2} M HEPES buffer pH 6 for blank solution in a microcentrifuge tube. The mixture solution was shaken for 1 minute prior to brightness measurement. For the complexation study with various concentrations of DA, 100 µL of the prepared PBA-OH solution in methanol was added with 100 µL of various DA concentrations in 0.05 m HEPES buffer pH 6, as shown in Table 1. For naked-eye detection, both solutions of **PBA-OH + Buffer** and **PBA-OH + DA** were examined in the fluorescent brightness under the black light excitation wavelength of 315 – 400 nm.

Table 1 Contents of each component in the sample portion of the microcentrifuge tubes

Entry / [Molar]	[PBA]	[NaOH]	[Na_2SO_3]	[NaCl]	[Dopamine]
1.	1×10^{-3}	1×10^{-1}	3.33×10^{-2}	6.67×10^{-3}	-
2.	1×10^{-3}	1×10^{-1}	3.33×10^{-2}	6.67×10^{-3}	0.5×10^{-3}
3.	1×10^{-3}	1×10^{-1}	3.33×10^{-2}	6.67×10^{-3}	1×10^{-2}
4.	1×10^{-3}	1×10^{-1}	3.33×10^{-2}	6.67×10^{-3}	1.5×10^{-2}
5.	1×10^{-3}	1×10^{-1}	3.33×10^{-2}	6.67×10^{-3}	2×10^{-2}
6.	1×10^{-3}	1×10^{-1}	3.33×10^{-2}	6.67×10^{-3}	2.5×10^{-2}

Result and Discussion

Figure 4 shows the strong green-fluorescent brightness of **PBA-OH.** Upon the addition of DA in the HEPES buffer solution of pH 6 2 x 10^{-3} M of **PBA-OH,** it exhibited a significant fluorescent darkness. This result is indicative of the reaction of **PBA-OH** and DA. For quantitative analysis by naked-eye studies, as shown in Figure 5, the lowest concentration of DA to react with PBA can induce fluorescent darkness, revealing the limit of detection (LOD). The results still displayed a green fluorescence brightness when the concentration of DA solution was lower than 1 x 10^{-2} M. This green fluorescence brightness was quenched when the concentration of DA was higher than 1 x 10^{-2} M. This result reveals that the detection limit of naked-eyes sensing of 1 x 10^{-3} M of PBA toward DA is 1 x 10^{-2}M.

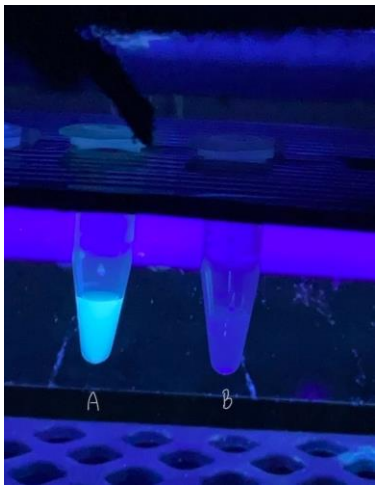

Figure 3. The green fluorescent brightness of 1×10^{-3} M **PBA-OH** (labeled A) and quenching of green fluorescence upon addition of 1×10^{-2} M of DA (labeled B)

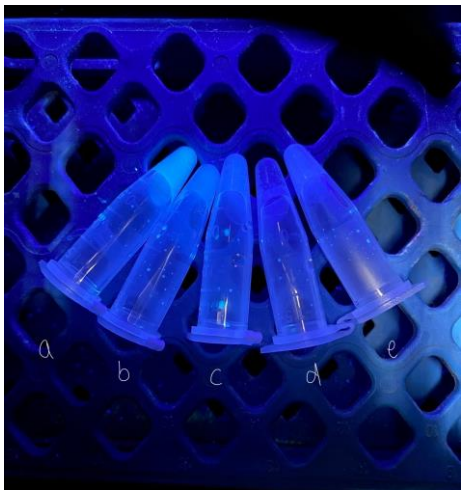

Figure 5. The limitation of naked-eyes detection of **PBA-OH** toward DA in various concentrations (concentration of DA is 5 × 10^{-3}M (a), 1 x 10^{-2}M (b), 1.5 × 10^{-2} M (c), 2 × 10^{-2} M (d), and 2.5 × 10^{-2} M (e)

PBA-OH showed strong green fluorescence in artificial sweat samples containing 2×10^{-3} M PBA and DA, without interference from the matrix. This confirms PBA-OH as a promising probe for DA detection in sweat.

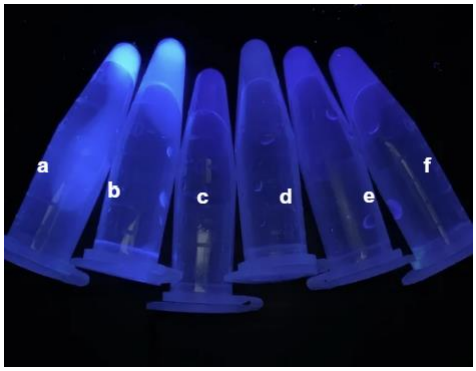

Figure 6: Naked-eye detection for analyzing PBA-OH interaction with dopamine (DA) at varying concentrations in artificial sweat as the following: no addition of DA (a), 5×10^{-3} M mol (b), 1×10^{-2} M (c), 1.5×10^{-2} M (d), 2×10^{-2} M (e), and 2.5×10^{-2} M (f). Under 365 nm black light.

The experiment using artificial sweat instead of HEPES buffer was applied to a paper-based platform. In this approach, 10 µL of PBA-OH (2×10^{-3} M) was mixed with 10 µL of DA solutions in artificial sweat at varying concentrations. Strong green fluorescence was observed in the absence of DA, similar to buffer-based experiments, while fluorescence was significantly quenched upon DA addition.

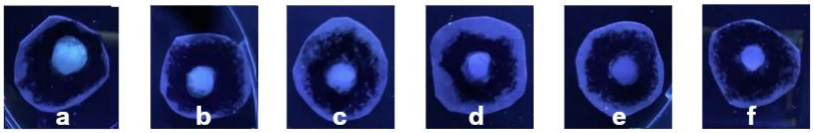

Figure 7: Paper-based naked-eye detection of PBA-OH toward DA in artificial sweat at various concentrations: no DA (a), 0.1896 mg (b), 0.3793 mg (c), 0.5689 mg (d), 0.7586 mg (e), and 0.9482 mg (f). Under 365 nm black light.

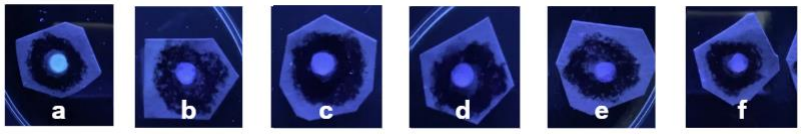

Figure 8: Paper-based naked-eye detection of PBA-OH toward DA in HEPES buffer solution 0.05M at various concentrations: no DA (a), 0.1896 mg (b), 0.3793 mg (c), 0.5689 mg (d), 0.7586 mg (e), and 0.9482 mg (f). Under 365 nm black light.

Discussion

Figure 9 presents the calibration curves of PBA with various concentrations of DA measured on paper substrates in two different media: 0.05 M HEPE buffer (yellow curve) and artificial sweat (green curve). The close similarity between the grayscale values of both curves demonstrates the high accuracy and reliability of the developed method. Furthermore, this consistency between the measurements in buffer and in a complex matrix like artificial sweat highlights the potential applicability of the method for real-world scenarios, particularly for non-invasive or wearable sensing platforms.

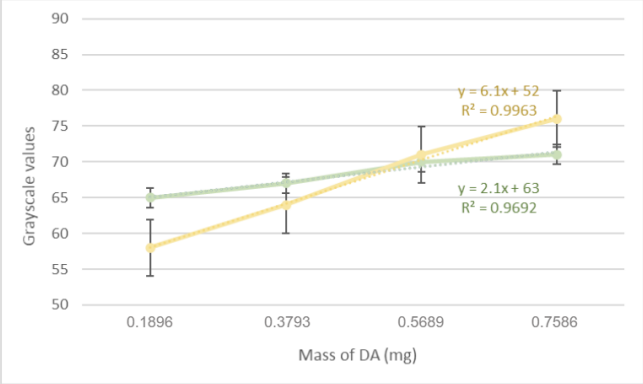

Figure 9: Calibration curve of PBA and various DA concentrations in HEPE buffer 0.05M on paper (Yellow curve) Calibration curve of PBA and various DA concentrations in artificial sweat on paper (Green curve)

Conclusion and Recommendation

We have successfully developed the naked-eye detection of dopamine by a small fluorescent probe based on pyrene boronic acid (PBA). Interestingly, the PBA shows strong green fluorescent brightness in the monomer manner under a concentration of 1×10^{-3} M. Upon adding the dopamine, the fluorescent darkness was remarkably observed with the limit of detection of 1×10^{-2} M of DA. PBA showed consistent fluorescence quenching upon dopamine addition in both liquid-based and paper-based experiments, including in artificial sweat. This highlights that PBA can be further developed for clinical diagnosis and portable testing.

Since the detection mechanism in this experiment relies on visual observation of fluorescence intensity, which directly correlates with dopamine concentration, it is recommended that the diagnostic application of this sensing platform be conducted in a dark

or low-light environment. Such conditions would minimize background light interference, thereby enhancing the clarity and contrast of the fluorescence signal for more accurate visual detection.

Reference

1. World Health Organization. (2022). News: Launch of WHO's Parkinson's Disease technical brief. WHO. https://www.who.int/news/item/14-06-2022-launch-of-who-s-parkinson-disease-technical-brief

2. Fawzy, A.(2019). A new validated HPLC method for the determination of levodopa: Application to study the impact of ketogenic diet on the pharmacokinetics of levodopa in Parkinson's participants [Doctoral thesis, School of Pharmacy, Pacific University, Hillsboro, OR, USA]. Pubmed. https://pubmed.ncbi.nlm.nih.gov/30203852/

3. American Association of Neurological Surgeons. (2024). Patient Content: Parkinson's disease. AANS.https://www.aans.org/patients/conditions-treatments/parkinsons-disease/#:~:text=Studies%20have%20shown%20that%20symptoms,muscle%20cells%20involved%20in%20movement

4. Teo Y. L., Gomaa A. M., H. Algarni, Cheewasedtham W., Rujiralai T., Chong K. F. (2019). One-step production of pyrene-1 - boronic acid functionalized graphene for dopamine detection. https://doi.org/10.1016/j.matchemphys.2019.04.029

5. Anusak, C., Somboon, S., Thawatchai, T. & Boosayarat, T.(2013). Highly effective discrimination of catecholamine derivatives via FRET-on/off processes induced by the intermolecular assembly with two fluorescence sensors (Doi: 10.1039/c3cc45077e) [Doctoral dissertation, Department of Chemistry, Faculty of Science, Chulalongkorn University, Bangkok, Thailand]. Chemcomm

6. Yanisa, S., Vithaya, R., Thawatchai, T., Vinich, P. & Boosayarat, T. (2015). Highly promising discrimination of various catecholamines using ratiometric fluorescence probes with intermolecular self-association of two sensing elements (Doi: 10.1039/c5ra10321e) [Docteral dissertation, A Department of Chemistry, Faculty of Science, Chulalongkorn University, Phyathai Road, Bangkok]. Royal Society of Chemistry

7. Pappin B., Milton J.K., & Todd A.H. (2012). Boron-Carbohydrate Interactions. http://dx.doi.org/10.5772/50630

8. Lei, P., Fan, Y., Shihao, X., Dan, L. & Changlong, J. (2024). Fluorescence sensing probe based on functionalized mesoporous MOFs for non-invasive and detection of dopamine in

human fluids (0039-9140) [Doctoral dissertation, Institute of Solid State Physics, Hefei Institutes of Physical Science, Chinese Academy of Sciences, Hefei, 230031, China]. ELSEVIER.

DROP-MIX-SEE: A CONVENIENT TEST KIT FOR ANALYSIS OF SALICYLIC ACID IN COSMETICS

Banthida Suntornwohan[1], Worakamon Suprom[1] and Sumonmarn Chaneam[1,2*]
[1]Silpakorn University, Faculty of Science, Department of Chemistry, Nakhon Pathom, 73000, Thailand
[2]Flow Innovation Research for Science and Technology Laboratories (FIRST Labs), Bangkok, 10400, Thailand
*e-mail: chaneam_s@su.ac.th

Abstract:
Salicylic acid (SA), also known as beta-hydroxy acid (BHA), is widely used in the cosmetic industry for its exfoliating and antimicrobial properties. It is frequently recommended by dermatologists for the treatment of acne and warts, and it also serves as a preservative to protect formulations, especially aqueous ones, from microbial growth. However, regulations strictly limit the allowable concentration of SA in cosmetics and skin care products. Improper use, either in the wrong product category or at excessive concentrations, may lead to regulatory violations and health risks to consumers. Excessive levels of SA may pose health risks to consumers. This work reports the development of a colorimetric test kit for detecting SA in cosmetics such as cleansers and serums. The method is based on the reaction between SA and copper(II) acetate under alkaline conditions, producing a green complex. The color intensity was captured and analyzed using a smartphone equipped with the Color Picker AR application. In RGB mode, the normalized intensity was calculated using (R + G + B)/B ratio, which was used to construct a calibration curve. The linear equation was obtained with a high correlation (R^2 = 0.9984). The reaction was adapted into a test kit for semi-quantitative analysis of SA. The procedure is simple and user-friendly, utilizing a “drop-mix-see” approach, with visual comparison of the generated color to a standard color chart. Finally, the sample analysis results were validated against high-performance liquid chromatography, demonstrating high accuracy and confirming the suitability of the test kit for real sample applications.

OPTIMIZATION OF ULTRASONIC-ASSISTED GREEN EXTRACTION OF HEAVY METALS FROM GALANGAL USING RESPONSE SURFACE METHODOLOGY

Banpot Klinpratoom,[1] Pattareeya Chaisaowong,[1] Phitchan Srichareon[2] and Nunticha Limchoowong[1,*],

[1]Department of Chemisty, Faculty of Science, Srinakharinwirot University, Bangkok 10110, Thailand

[2]Division of Health, Cosmetic and Anti-Aging Technology, Faculty of Science and Technology, Rajamangala University of Technology Phra Nakhon, Bangkok 10800, Thailand

*e-mail: nunticha@g.swu.ac.th

Abstract:

The utilization of galangal for consumption and medical purposes requires quality analysis of heavy metal contamination to ensure the protection of human health. Therefore, the aim of this research was to develop a green extraction method for quality analysis of heavy metal contamination (Lead (Pb), Cadmium (Cd), and Arsenic (As)) in galangal using ultrasonic-assisted extraction combined with optimization of extraction conditions via response surface methodology (UAE-RSM). A rotatable central composite design (CCD) was applied to design the experiment using three independent variables: A, dilute HNO_3 concentration (0.40–1.20 M); B, ultrasonic time (5-15 min); and C, acid volume (20–40 mL), in order to achieve a high percentage of extraction recovery (%recovery) for Atomic Absorption Spectrometric analysis. A quadratic regression model equation was used to predict the optimal conditions, and the analysis of variance (ANOVA) was performed to evaluate the goodness of fit of the model. The ANOVA results revealed that dilute HNO_3 concentration and acid volume had a significant influence ($p < 0.05$) on %recovery (response). The R^2 values of Pb, Cd, and As were 0.9878, 0.9866, and 0.9944, respectively. The optimal UAE-RSM conditions, which maximized %recovery, were found to be 0.68 M acid concentration, 11 min ultrasonic time, and 32 mL acid volume. The predicted values compared with the experimental values of %recovery for Pb, Cd, and As were 97.13 (95.17 ± 2.37), 102.09 (97.50 ± 5.13), and 103.26 (98.63 ± 0.25), respectively. Real sample analysis was further carried out by spiking metals into seven varieties of galangal. After extraction under the optimized conditions, the %recovery values were recorded in the range of 87.00–107.50. The UAE-RSM technique can be effectively applied for the extraction and analysis of heavy metal contamination in galangal with high %recovery. This technique is environmentally friendly and can be further utilized for quality analysis of heavy metals in food samples.

REAGENTLESS AND LABEL-FREE ELECTROCHEMICAL APTASENSOR USING POLYANILINE INCORPORATED WITH BATTERY-FREE NFC POTENTIOSTAT FOR ONE-STEP DETECTION OF SALIVARY CORTISOL

Chawin Srisomwat,[1,*] Supada Khonyoung,[1] Nuttanan Thanedsed,[1] Warawut Tiyapongpattana,[1] Sopon Butcha,[1] Orawon Chailapakul,[2]
[1] Department of Chemistry, Faculty of Science and Technology, Thammasat University, Pathumthani, 12121, Thailand
[2] Department of Chemistry, Chulalongkorn University, Pathumwan, Bangkok, 10330, Thailand
*e-mail: chawinsr@tu.ac.th

Abstract:
Cortisol serves as a vital biomarker for stress levels, but current evaluation methods are complex and resource intensive. Traditional detection approaches require elaborate procedures and sophisticated equipment, limiting their accessibility and practical application. There is a pressing need for user-friendly, cost-effective, and portable technologies that can efficiently monitor cortisol levels in real-world settings. We developed a reagentless and label-free electrochemical aptasensor for one-step detection of salivary cortisol, utilizing polyaniline (PANI) as an active conductive polymer and integrating it with a battery-free NFC potentiostat. The PANI-modified screen-printed electrode exhibited excellent conductivity and surface-enhancing properties, facilitating efficient aptamer immobilization and enabling reagentless electrochemical detection of cortisol without the need for additional redox reagents. The battery-free NFC integration enables seamless data transfer to mobile devices, providing real-time analysis capabilities. The proposed sensor achieved the linear range between 0.1 to 10 nM with a low detection limit of 27 pM or 33 minutes of analysis time and exhibited high selectivity for cortisol, which makes it suitable for patients with Addison's disease. Moreover, the good reproducibility of the five different devices (%RSD = 4.3) was accomplished. Also, the matrices in artificial saliva were not affected for cortisol detection. A performance comparison between commercial EmStat4s and our NFC-based potentiostat, in artificial saliva, validated the accuracy of the system with acceptable range (% recovery = 95 – 97; NFC, 91 – 107; EmStat4s). This innovative platform represents a significant advancement in point-of-care diagnostics by combining advanced conductive materials with modern electronics. The system's portability, cost-effectiveness, and user-friendly design make it particularly valuable for non-invasive stress monitoring through salivary analysis, opening new possibilities for accessible bioanalysis and personalized health monitoring.

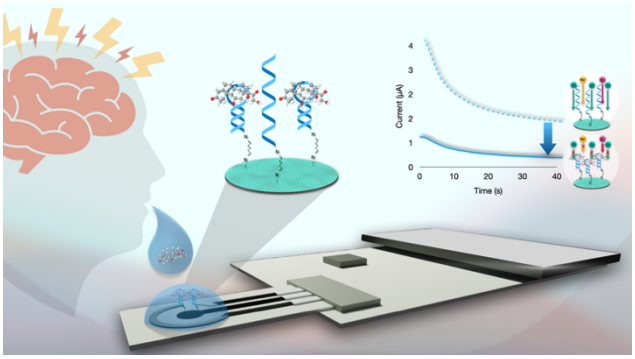

Figure 1. The proposed electrochemical aptasensor for salivary cortisol detection
(Leave a blank line before and after Figures.)

SIMULTANEOUS ELEMENTAL AND STRUCTURAL ANALYSIS OF HAIR SUBJECTED TO BLEACHING TREATMENTS

Natchaphon Sukphon, [1] Pannatorn Sukanan, [1] Kanokrat Sinknui [1]*
[1]Princess Chulabhorn Science High School Nakhon Si Thammarat, 120 M.1 Bangjak sub-district, Muang Nakhon Si Thammarat, Thailand 80330

*skanokrat208@gmail.com

Abstract:

The study investigates the effects of hair bleaching on hair composition and properties, with a focus on structural and dimensional changes in hair subjected to commercial bleaching treatments. Hair diameter was calculated using light interference principles and compared with Scanning Electron Microscopy (SEM) results. In addition, the elemental composition of hair was analyzed before and after bleaching using Energy Dispersive X-ray Spectroscopy (EDS). The results indicate that the diameters of natural hair and hair bleached once and twice are 50.00 µm, 44.77 µm, and 18.00 µm, respectively. The average reduction in hair diameter after the first and second bleaching treatments is 30.66% and 59.79%, respectively. Elemental analysis reveals a decrease in sulfur (S) and nitrogen (N) levels, indicating degradation of disulfide bonds in the keratin structure, while oxygen (O) content increases due to oxidation reactions. Furthermore, new elements such as sodium (Na), calcium (Ca), silicon (Si), and magnesium (Mg) were detected in bleached hair, suggesting either incorporation of bleaching chemicals or structural modifications. Unlike previous studies that focused solely on morphological or chemical aspects, this work provides a simultaneous investigation of elemental composition and structural changes, highlighting the combined effects of bleaching on both hair chemistry and morphology.

SYNTHESIS AND APPLICATION OF 3D GRAPHENE-BASED Fe_3O_4 NANOCOMPOSITE AS A MAGNETIC ADSORBENT FOR THE DETERMINATION OF PYRETHROIDS VIA MSPE-GC-ECD

Sirirat Phaisansuthichol[1]*, Suttipong Puangthong[1], and Naruephon Watthanaphap[2]
[1]Department of Chemistry, Faculty of Science, Maejo University, Chiang Mai 50290, Thailand
[2]Pesticide Residue Analytical Laboratory, Plant Protection Center, Royal Project Foundation, Chiang Mai, 50230, Thailand
*Corresponding author e-mail: phaisansuthichol@gmail.com

Abstract:

A three-dimensional graphene–magnetite nanocomposite (3D-G-Fe_3O_4) was successfully synthesized and employed as an efficient magnetic adsorbent for the determination of pyrethroid residues using magnetic solid-phase extraction (MSPE) followed by gas chromatography coupled with an electron capture detector (GC-ECD). The structural and morphological characteristics of the synthesized nanocomposite were elucidated using scanning electron microscopy (SEM) and Fourier-transform infrared spectroscopy (FT-IR).

To optimize the extraction parameters, a central composite design (CCD) integrated with response surface methodology (RSM) was utilized. The optimal MSPE conditions were as follows: 30 mg of 3D-G-Fe_3O_4, 20 mL of sample volume, 3.45 minutes of extraction time, and 4 mL of acetone as the desorption solvent.Under these optimized conditions, the method exhibited a linear calibration range of 0.01–0.30 mg L^{-1}, with correlation coefficients (R^2) exceeding 0.9983. The limits of detection (LOD, S/N = 3) and quantification (LOQ, S/N = 10) were determined to be 0.01 mg L^{-1} and 0.03 mg L^{-1}, respectively. The method demonstrated satisfactory precision, with intra-day relative standard deviations (RSDs) ranging from 5.05% to 7.02%, and recoveries between 93.0% and 112.9%.

Keywords: central composite design, magnetic three-dimensional graphene, GC-ECD

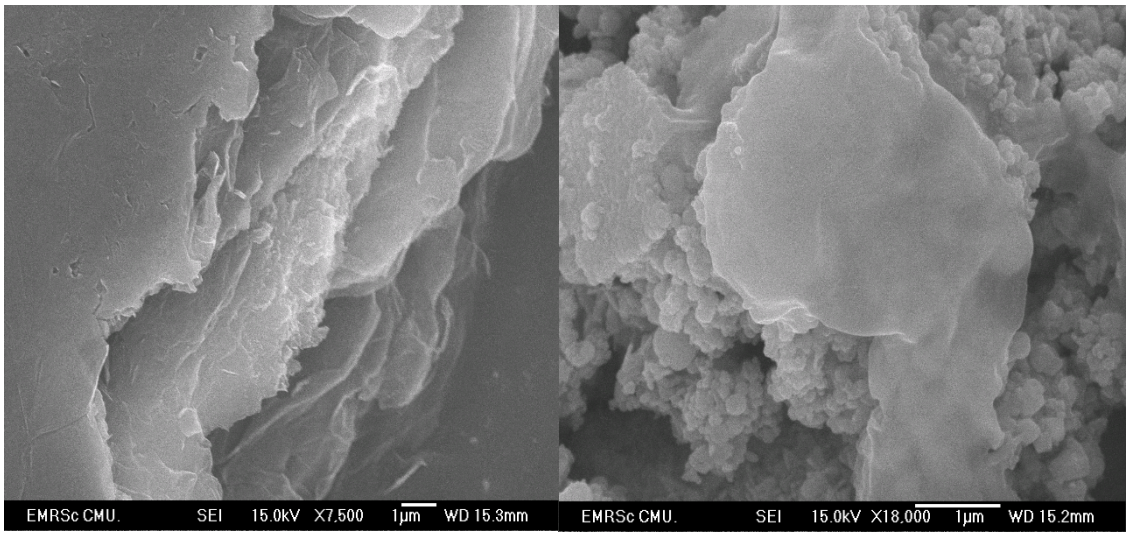

a. b.

Figure 1.
SEM micrographs of (a) graphene oxide showing its surface morphology and (b) 3D-G-Fe_3O_4 illustrating the deposition of Fe_3O_4 nanoparticles on the graphene oxide sheets.

C: INORGANIC CHEMISTRY

$CsPbBr_3$ QUANTUM DOT–POLYOXOMETALATE HYBRIDS FOR VISIBLE-LIGHT-DRIVEN SOLAR ENERGY CONVERSION AND STORAGE

Kona Sumi,[1] Yuji Akaishi,[2] Yusuke Inomata,[3] Tetsuya Kida,[3]*
[1] Department of Materials Science and Applied Chemistry, Kumamoto University, Japan
[2] Institute of Industrial Nanomaterials, Kumamoto University, Japan
[3] Faculty of Advanced Science and Technology, Kumamoto University, Japan
* tetsuya@kumamoto-u.ac.jp

Abstract:

While photovoltaic devices can convert photoenergy into electrical energy but are unable to store it. Here, we report the development of photoelectrochemical capacitors that can store electrical energy by utilizing polyoxometalates (POMs), which possess excellent reversible redox activity and high stability in their reduced state. However, the wide band gap of POMs severely restricts their photoelectrochemical applications. To overcome this limitation, we employed perovskite $CsPbBr_3$ quantum dots (QDs) as photosensitizers due to their strong absorption in the visible light region. Upon visible light irradiation, the QDs are photoexcited, and the generated electrons are transferred to the POMs.

Tetrabutylammonium (TBA^+) was combined with decatungstate $[W_{10}O_{32}]^{4-}$ as a counter cation to synthesize $TBA_4[W_{10}O_{32}]$ (POM) , which was dispersed in an organic solvent. The POM dispersion in acetonitrile was irradiated with UV light (Xenon lamp, λ =365 nm, 23 mW) , and UV-vis spectroscopy was used to evaluate its reduction behavior. $CsPbBr_3$ QDs were synthesized using the hot-injection method and coated with TiO_2 ($CsPbBr_3/TiO_2$ QDs) to improve durability. Finally, a mixed dispersion of QDs and POM in acetonitrile was irradiated with visible light (Xenon lamp, $\lambda \geq$420 nm, 263 mW) to assess the influence of QDs on the reduction of POM. Upon irradiation, the color of the solution changed from yellow to yellow-green, and a peak of POM^- was observed at around 620 nm. These results confirm successful photoinduced electron transfer from QDs to POMs under visible light irradiation, highlighting the potential of this hybrid system for integrated solar energy conversion and storage.

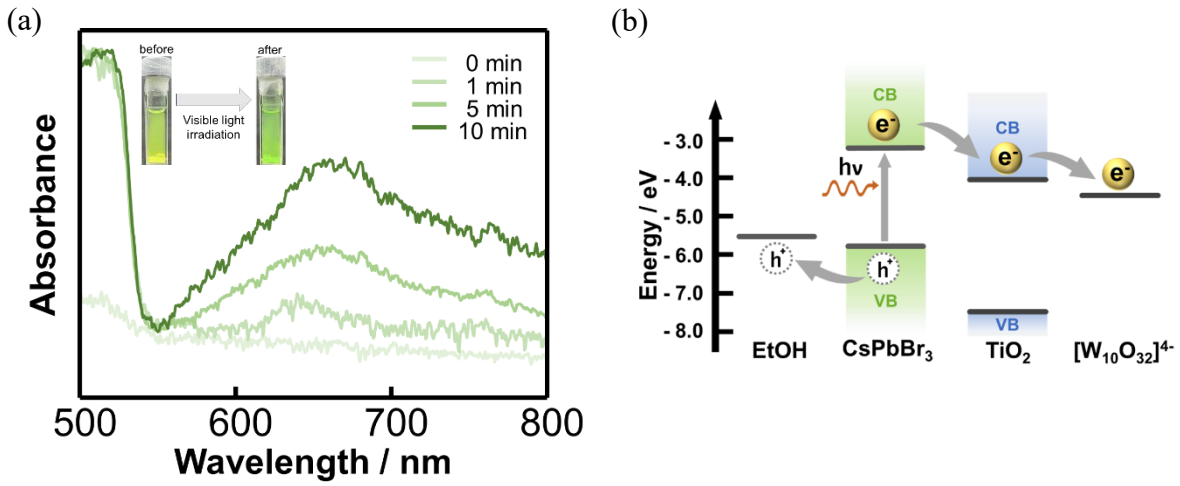

Figure 1. (a) Time dependent absorption spectral changes of the QDs/POM solution irradiated with visible light ($\lambda \geq$420 nm). (b) Band energy scheme of $CsPbBr_3/TiO_2$ nanocomposites together with the redox potentials of $[W_{10}O_{32}]^{4-}$.

References:

Nuket, P.; Akaishi, Y.; Yoshimura, G.; Vas-Umnuay, P.; Kida, T. Enhanced Interfacial Charge Transfer between CsPbBr3 Quantum Dots and Surface-Modified TiO2/FTO Photoanodes for Photocurrent Generation. *Materials Today Nano* **2022**, *18*, 100174. https://doi.org/10.1016/j.mtnano.2022.100174.

PET-DERIVED CARBON MATERIALS FOR FLUORESCENT MATERIALS AND MICROPLASTIC REMOVAL

Ekasith Somsook

NANOCAST Laboratory, Center for Catalysis for Advanced Sustainable Transformation (CAST), Department of Chemistry and Center of Excellence for Innovation in Chemistry, Faculty of Science, Mahidol University, Rama VI Rd, Bangkok 10400, Thailand

Email: ekasith.som@mahidol.ac.th

First, polyethylene terephthalate (PET) waste was transformed into high-performance quantum dots (QDs), combining technological innovation with a focus on environmental sustainability. The excellent fluorescence properties of the synthesized quantum dots were used to detect Fe^{3+} and F^- ions with high sensitivity and selectivity *via* "on-off-on" duality fashion. Also, the synthesized quantum dots exhibited a stable solid-state fluorescence enabling their use in solid-phase applications without the usual fluorescence loss common in other materials. The versatility and tunability of the synthesized materials were showcased by producing three different emission colors, achieved through the incorporation of different heteroatoms during synthesis process. Second, polyethylene terephthalate (PET) waste was transformed into activated carbon (PET-C) by means of a direct carbonization and subsequent KOH activation, without inert gases. PET-C was characterized and evaluated for microplastic (MP) removal, specifically targeting polystyrene (PS). Adsorption experiments revealed a maximal adsorption capacity of 139.57 $mg \cdot g^{-1}$ (0.5 g/L, 12 hours, 298 K), monolayer chemical adsorption is indicated by the Langmuir isotherm and pseudo-2^{nd}-order kinetics fitting. The procedure occurred spontaneously and exothermic, with robust pH stability. Removal mechanisms included π-π interactions, hydrogen bonding, hydrophobic interactions and electrostatic interactions supported by FTIR, XPS, and DFT calculations. PET-C demonstrated high efficiency in diverse water matrices with minimal anion interference and >80% removal efficiency retention after five cycles.

C: ORGANIC & MEDICINAL CHEMISTRY

ANTIOXIDANT POTENTIAL OF *Mimusops elengi* FLOWER EXTRACT: A BIOASSAY-GUIDED ISOLATION APPROACH

Nalittha Kaewfaed,[1] Khanitha Pudhom,[2] Siwattra Choodej[1,*]
[1]Department of Chemistry, Faculty of Science, King Mongkut's University of Technology Thonburi, Bangkok 10140, Thailand
[2]Department of Chemistry, Faculty of Science, Chulalongkorn University, Bangkok 10330, Thailand
*e-mail: siwattra.choo@kmutt.ac.th

Abstract:
Flowers of *Mimusops elengi* were extracted with methanol and fractionated using Diaion HP20 column chromatography. The antioxidant activity of each fraction was evaluated by the DPPH radical scavenging assay. The methanol-water fractions exhibited strong antioxidant activity with IC_{50} values ranging from 44.4 ± 1.2 to 86.1 ± 1.9 µg/mL, which is comparable to ascorbic acid (IC_{50} value of 41.2 ± 1.9 µg/mL). NMR analysis revealed the presence of flavonoid glycosides as the major constituents, with characteristic signals of flavonoids at 6.5-8.0 ppm and sugar moieties at 4.0-5.5 ppm. In contrast, the methanol- and acetone-eluted fractions showed very weak (IC_{50} value of 563.0 ± 2.7 µg/mL) and no detectable (IC_{50} value of > 1000 µg/mL) activity, respectively, and were found to contain triterpenes as the predominant compounds, characterized by typical signals of multiple singlet methyl groups at 0.7-1.5 ppm. These results highlight flavonoid glycosides as the key antioxidant constituents of *M. elengi* flowers, demonstrating a bioassay-guided approach for the identification of bioactive natural products from traditional Thai medicinal plants.

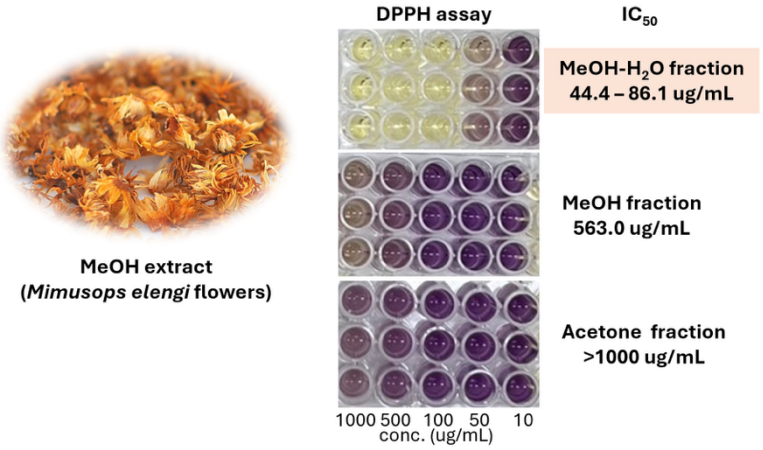

CHEMOENZYMATIC SYNTHESIS OF 3-HALOCHROMONES VIA OXIDATIVE α-HALOGENATION OF ENAMINONES IN TPGS-750-M MICELLES

Chisanu Krongyut[1], Jakkarin Limwongyut[1,*], Nittaya Wiriya[1], Anyanee Kamkaew[1], Ailada Jantasin[1], Rung-Yi Lai[1,*]
Suranaree University of Technology Nakhon Ratchasima 30000 Thailand
*e-mail: jakkarin@g.sut.ac.th, rylai@sut.ac.th

Abstract:

The synthesis of chromones has garnered significant attention due to the widespread presence of the chromone scaffold in bioactive compounds and natural products. Among these, 3-halochromones serve as versatile intermediates for constructing a variety of valuable chromone-based derivatives. Traditionally, these compounds are synthesized via oxidative α-halogenation of *o*-hydroxy enaminones, a process that typically relies on toxic and corrosive reagents. Herein, we report an alternative, environmentally friendly approach using vanadium-dependent chloroperoxidase from *Curvularia inaequalis* (*Ci*VCPO) to catalyze oxidative α-halogenation in an aqueous medium with H_2O_2/KX (X = Cl, Br, I). By employing a micellar system formed with the surfactant TPGS-750-M, the substrate concentration could be raised to 50 mM without compromising yield, significantly minimizing the need for organic solvents. Substrate scope studies reveal that both bromination and chlorination favor electron-donating substituents, while moderate electron-withdrawing groups are also well tolerated (20 examples). Iodination is also feasible under these conditions; however, its slower conversion rate suggests a need for further optimization. Interestingly, iodination proceeds even in the absence of *Ci*VCPO, albeit with lower efficiency, likely due to in situ generation of I_2. Overall, this chemoenzymatic strategy offers a sustainable and efficient method for synthesizing a broad range of 3-bromo- and 3-chlorochromones, with potential for further development in iodination chemistry.

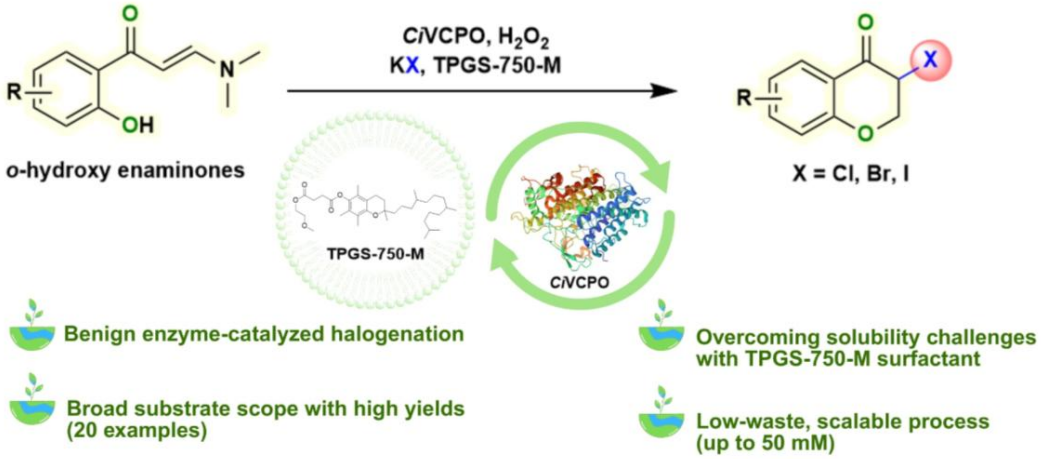

DEVELOPMENT OF SKIN LOTION FROM THE PEELS OF *Passiflora edulis* Sims AND *Hylocereus undatus*

Ratchaneekorn Kaewpraju,[1,*] Parinda Soragul,[1] Parinuch Chumkaew[2]
[1]PSU Wittayanusorn Surat Thani School (SCiUS), Surat Thani 84000, Thailand
[2]Prince of Songkla University, Surat Thani Campus, Surat Thani 84000, Thailand
*e-mail: Pim72630@gmail.com

Abstract:
The natural extracts from agricultural waste materials have gained increasing attention in terms of economy, sustainability, beauty and health because they contain bioactive compounds or phytochemicals that are nutritious and beneficial to health, beauty and well-being. Nowadays, agricultural waste materials are utilized as an ingredient in skincare products due to their higher safety compared to chemical substances. In addition, dragon fruit (*Hylocereus undatus*), and passion fruit (*Passiflora edulis*) have been intensively studied and found to be rich sources of vitamins, flavonoids and phenolic compounds, which are effective antioxidants and oxidation inhibitors. This research aimed to extract peels of dragon fruit (*H. undatus*), passion fruit (*P. edulis*), and mixed dragon fruit and passion fruit, and to study the physical properties (appearance, layer separation, color, and pH) and to develop skincare product formulations. In the study, two techniques of extraction (maceration and reflux) using methanol as a solvent were investigated. The solvent was removed under reduced pressure to afford the maceration extracts of *P. edulis* (33.10 % yield), *H. undatus* (25.85 % yield) and mixed fruits (35.49 % yield) and the reflux extracts of *P. edulis* (24.44 % yield), *H. undatus* (20.63 % yield) and mixed fruits (24.06 % yield). The results showed that the maceration method provided higher yield of crude extracts than the reflux method. Qualitative analysis of the phytochemical constituents showed the presence of the following secondary metabolites: terpenoids (Salkowski test), flavonoids (Ammonia test), steroids (Liebermann–Burchard test), phenols (Ferric chloride test), saponins (Foam test), tannins (Ferric chloride test) and anthraquinones (Borntrager's test). The body lotion was prepared using a lotion base with three different concentrations of the maceration and reflux extracts of the mixed fruits at 1 %, 2.5 %, and 5 %. The mixed fruit peel extract was selected due to the presence of more diverse bioactive compounds, which may provide improved antioxidant capacity and functional performance relative to single fruit extracts. The pH values of the lotions from both maceration and reflux extracts at above concentrations were in the range of 4.78-5.29. The heating-cooling cycle test was used to estimate the stability of the lotion in terms of both chemical and physical properties. The results revealed that the skin lotion containing 1% extract showed a smooth and uniform texture, while the 2.5% and 5% formulations were slightly thicker and gel-like. The lotions at all concentrations remained stable without phase separation or precipitation during the heating–cooling cycles, indicating good physical stability under temperature stress.

FABRICATION OF POLYVINYL ALCOHOL AND SODIUM ALGINATE HYDROGELS WITH BIURET REAGENT FOR PROTEIN DETECTION IN AQUEOUS GELATIN AND UREA SOLUTION

Kasidth Rungbannaphan,[1] Pornchanok Thipsurat,[1] Atsadaporn Thangprasert,[2,*]
Pakorn Pasitsuparoad [3]
[1]PSU. Wittayanusorn Surat Thani, Surat Thani, 84000, Thailand
[2]Faculty of Science and Industrial Technology, Prince of Songkla University, Surat Thani Campus, Surat Thani, 84000, Thailand
[3]Faculty of Technology and Environment, Prince of Songkla University, Phuket Campus, Phuket, 83120, Thailand
*e-mail: a.thangprasert@gmail.com

Abstract:

Chronic kidney disease (CKD) commonly occurs in patients with chronic illnesses and the elderly, and many CKD-related deaths are due to delayed diagnosis and treatment. Elderly patients who do not undergo regular health check-ups may unknowingly be at risk. Previous studies have utilized hydrogels in diapers and also employed them in detecting diabetes through sweat; however, these two applications have yet to be combined. In this study, polyvinyl alcohol (PVA) and sodium alginate (SA) were mixed at different ratios as follows: 100:0, 75:25, 50:50, 25:75, and 0:100, namely P100S0, P75S25, P50S50, P25S75, and P0S100, respectively. The hydrogels were fabricated via a freeze–thaw process followed by soaking in a $CaCl_2$ solution overnight. The morphology and molecular organization of the hydrogels were observed and characterized using FTIR and SEM. The swelling and degrading behaviors of the hydrogels were also evaluated. FTIR results confirmed chemical interactions in hydrogels such as hydroxyl, carboxylic, and carbonyl groups. SEM images showed a porous structure with a nonhomogeneous pore size distribution. Large and low-density pore distribution correlates with SA loading. Moreover, increasing SA loadings also increases water absorption and degradation but reduces mechanical strength and hydrogel stability. The protein detection was investigated using colorimetry of Biuret solutions. A calibration curve was acquired from gelatin solution, 0.25 - 10 ppm. The samples were tested with simulated solutions using urea as an interference. The results showed good correlation in gelatin solutions, but high deviation was shown in urea simulated solutions. The hydrogels developed in this study are intended to be used as prototypes for detecting protein levels in CKD patients' urine and for creating diapers for elderly CKD patients in the future.

GREEN SYNTHESIS OF PYRROLIDINE DERIVATIVES VIA 1,3-DIPOLAR CYCLOADDITION IN HYDROPHOBIC DEEP EUTECTIC SOLVENTS

Nattawadee Nimsawang, Lalita Radtanajiravong*
Department of Chemistry, School of Science, University of Phayao, Phayao 56000, Thailand
*e-mail: lalita.ra@up.ac.th

Abstract:
Synthesis of pharmaceutical pyrrolidine derivatives *via* 1,3-dipolar cycloaddition of azomethine ylides and alkenes is often associated with non-benign synthetic conditions. To address environmental concerns, the use of green and recyclable solvents presents a sustainable alternative to traditional toxic organic solvents. In this study, we evaluated the effectiveness of terpene-based deep eutectic solvents (DESs) in facilitating thermal cycloaddition reactions. This method afforded the desired pyrrolidine products in yields ranging from 23% to 93%. A broad scope of aryl aziridines and alkene substrates was well tolerated. Additionally, the DES system demonstrated good recyclability, retaining high performance over five cycles with minimal degradation.

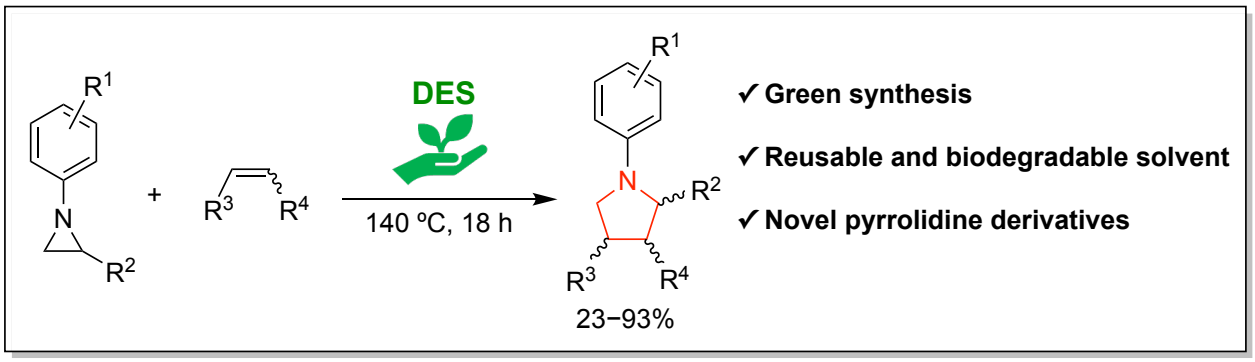

Figure 1. Synthesis of pyrrolidines *via* 1,3-dipolar cycloaddition in terpene-based deep eutectic solvents.

SCREENING OF THAI MEDICINAL PLANTS FOR ANTIMICROBIAL AND ANTIOXIDANT ACTIVITIES: POTENTIAL APPLICATION IN CHITOSAN-BASED HYDROGEL FOR ORAL CARE

Patcharakorn Raksasee,[1] Safira Minham,[1] Kornkanok Ubolchollakhet,[2] Netnapa Chana[3,4,*]
[1]Paphayompittayakom School (SCiUS-Thaksin University), Phatthalung 93210, Thailand
[2]Department of Rubber and Polymer, Faculty of Engineering, Thaksin University, Phatthalung Campus, Phatthalung 93210, Thailand
[3]Department of Biological Science, Faculty of Science and Digital Innovation, Thaksin University, Phatthalung Campus, Phatthalung 93210, Thailand
[4] Innovative Material Chemistry for Environment Center, Department of Chemistry, Faculty of Science and Digital Innovation, Thaksin University, Phatthalung Campus, Phatthalung 93210, Thailand
*e-mail: netnapa@tsu.ac.th

Abstract:
Post-dental extraction complications remain significant challenges in dental practice, necessitating effective therapeutic agents. This study screened leaves of selected Thai medicinal plants for antimicrobial and antioxidant properties and evaluated their incorporation into chitosan-based hydrogel systems for oral wound care. Leaves of four Thai medicinal plants (*Psidium guajava*, *Piper betle*, *Tridax procumbens*, and *Chromolaena odorata*) were extracted using water and ethanol solvents. Extracts were evaluated for antioxidant activity using DPPH assay and antimicrobial efficacy against *Streptococcus mutans*, *Staphylococcus aureus*, and *Escherichia coli* using disc diffusion method. Promising extracts were incorporated into chitosan hydrogels and assessed for bioactive compound release and maintained biological activities. *P. guajava* aqueous and ethanol extracts, along with *P. betle* ethanol extract, exhibited potent antioxidant activities (IC_{50}: 14.46–15.59 µg/mL). *P. guajava* aqueous extract demonstrated the strongest antimicrobial effect against all tested pathogens, with inhibition zones of 17.44 ± 0.13 mm against *E. coli*, 13.86 ± 0.09 mm against *S. mutans*, and 13.58 ± 0.08 mm against *S. aureus*. The activity against *S. mutans* was comparable to chlorhexidine (25.8 ± 0.4 mm) as positive control. When incorporated into chitosan hydrogels, *P. guajava* extract retained biological activity with burst release characteristics (2.4 mgGAE/mL at 6h, 67% antioxidant activity). Chemical profiling by LC-MS/MS analysis revealed phenolic compounds including flavonoid derivatives contributing to bioactivities. The findings demonstrate the potential of Thai medicinal plants, particularly *P. guajava*, as natural bioactive agents for oral care. The successful incorporation into chitosan hydrogel systems suggests a promising platform for developing therapeutic formulations for dental extraction wound management.

SYNTHESIS OF CAERULOMYCIN A ANALOGUES

Pansachon Intamalee,[1] Arthit Chairoungdua,[2] Rungnapha Saeeng[1,3,*]
[1]Department of Chemistry and Center of Excellence for Innovation in Chemistry, Faculty of Science, Burapha University, Chonburi 20131, Thailand
[2]Department of Physiology, Faculty of Science, Mahidol University, Bangkok 10400, Thailand
[3]The Research Unit in Synthetic Compounds and Synthetic Analogues from Natural Product for Drug Discovery (RSND), Burapha University, Chonburi 20131, Thailand
*e-mail: rungnaph@buu.ac.th

Abstract:
Caerulomycin A, a marine-derived natural product from *Actinoalloteichus cyanogriseus*, exhibits diverse biological activities, including antibacterial, antifungal, antitumor, and cytotoxic effects. In this study, a six-step synthetic route to Caerulomycin A was developed from commercially available reagents, affording an overall yield of 28%. Since the oxime ether moiety is considered a privileged group in medicinal chemistry, being present in numerous scaffolds with broad biological and pharmaceutical properties, we designed structural modifications of Caerulomycin A at the oxime functionality through incorporation of various benzyl ether substituents. The resulting oxime ether derivatives were subsequently evaluated for their cytotoxic activity against six human cancer cell lines. Some synthetic derivatives demonstrated notable activities against SH-SY5Y and KKU-M213 cancer cells (IC_{50} = 4.59-8.05 μM).

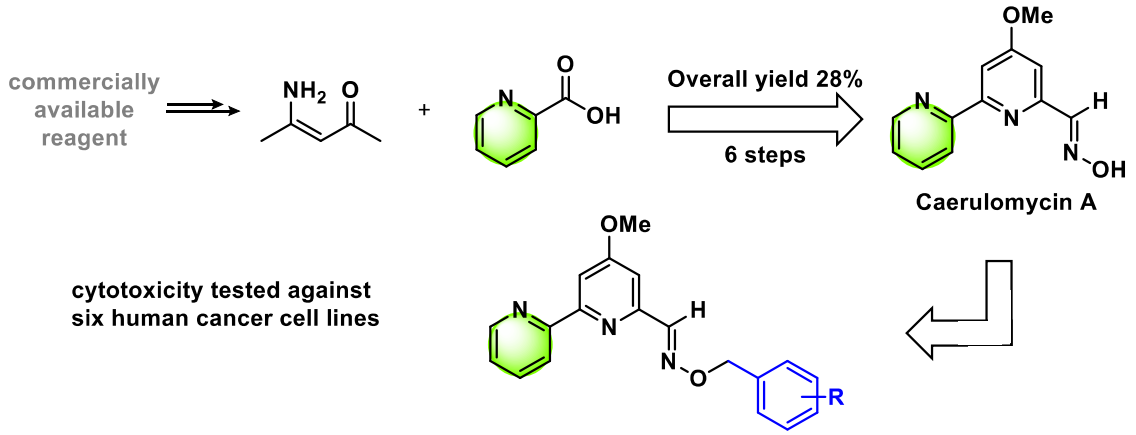

Figure 1.
Total synthesis of oxime ether Caerulomycin, A analogues employing commercially available reagents.

C: PHYSICAL & THEORETICAL CHEMISTRY

A DENSITY FUNCTIONAL THEORY INVESTIGATION INTO THE SELECTIVITY MECHANISMS OF STARCH ESTER TRANSESTERIFICATION

Phakthada Pitavaratorn*, Chinnathee Saisith
Kamnoetvidya Science Academy, Rayong, Thailand
*E-mail: Phakthada.bb@gmail.com

Abstract:
Starch is a renewable and biodegradable polymer, but its applications are limited by low thermal stability, high water sensitivity, and weak mechanical properties. Transesterification can enhance its performance by replacing hydroxyl groups with ester groups. The effectiveness of this process is expressed as the degree of substitution (DS), which represents the average number of hydroxyl groups per anhydroglucose unit (AGU) that are replaced by ester. Experimental studies reveal that vinyl esters achieve DS values of 2.20–2.63, compared with only ~0.45 for methyl esters under identical conditions. Despite extensive experiments, the molecular-level reasons behind this phenomenon remain unclear. Density Functional Theory (DFT) reveals electronic structures, thermodynamic, and kinetic details underlying this difference that experiments alone cannot capture. Thus, this study employs DFT with B3LYP functional and 6-311G+(d,p) basis set. The calculations were simulated on the model reaction where starch is represented by 8-glucose-monomer amylose. Analysis of reaction pathways, Gibbs free energies, and molecular orbitals corroborates the experiment. Additional influences, such as steric hindrance, were also analyzed for their contributions. These results clarify why vinyl esters demonstrate higher reactivity and provide molecular insights into how ester structure governs transesterification efficiency. Such understanding supports the advancement of starch-based materials for biodegradable plastics, adhesives, and coatings. Beyond practical implications, the results also contribute to fundamental knowledge, supporting young researchers and students in the field.

COMPUTATIONAL INVESTIGATION OF NOVEL ULTRAFLEXIBLE BORON-OXIDE ZEOLITIC FRAMEWORKS

Worapruch Chupong,[1] Saranathorn Sangkaew,[1] Ukrit Keyen[2,*]
[1]Kamnoetvidya Science Academy, Wang Chan, Rayong, 21210 Thailand
[2]Computation and Modelling Laboratory (CML-KVIS), Department of Chemistry, Kamnoetvidya Science Academy, Wang Chan, Rayong, 21210 Thailand
*e-mail: ukrit.k@kvis.ac.th

Abstract:

This research project focuses on enhancing the structural flexibility of zeolites while preserving their intrinsic porosity, with the goal of designing boron oxide frameworks that maintain zeolite topologies. Zeolites, microporous aluminosilicate crystals made of Si, O, and Al, are crucial in industrial catalysis but suffer from rigidity that limits selective adsorption. In this work, we developed a generalizable computational strategy by directly constructing boron oxide frameworks from crystallographic information files (.cif) of zeolites. The strategy determines the centroid positions of symmetry-equivalent sites to define boron atom locations, enabling systematic substitution of $[SiO_4]^{4-}$ units with $[B_2O_5]^{4-}$ units composed of planar BO_3 groups similar to α-B_2O_3. Utilizing first-principles quantum mechanical calculations with Quantum ESPRESSO, we optimized the structures and assessed their stability. Our results show that the boron oxide frameworks are noticeably more flexible than the original zeolites, as seen in their flatter energy–volume curves. The pore size distribution also points to a clear trend that the new frameworks lean toward larger pores while still holding on to their zeolite framework. On the stability side, thermodynamic analysis through solution energy calculations confirm stability relative to quartz and α-B_2O_3. Ongoing work includes bond angle distribution, radial distribution, phonon density of states, band structure, and adsorption–diffusion simulations, which will provide a more complete understanding of the local structure, dynamical stability, and catalytic potential of these frameworks. Altogether, these findings highlight a new class of boron oxide materials that retain the zeolite shape but achieve far greater flexibility and also retain stability. With upcoming results expected to confirm their tunable properties and catalytic advantages, this approach has the potential to reshape the design of porous materials and establish them as strong candidates for future catalytic applications.

MECHANISTIC INVESTIGATION OF ZnO/Ag SYSTEMS VIA DIRECT MODULATION OF ANTIMICROBIAL ACTIVITY USING STACKED Ag–ZnO NANOCUBE "NANOAPARTMENTS" AND NANOWIRE "NANOCONDOMINIUMS"

Papangkorn Phongchamnaphai,[1] Pannatad Ophasmongkolchai,[1] Purin Kittijit,[1] Peerasit Lueang-urai,[1] Ukrit Keyen,[1,2]* Yutichai Mueanngern[1,2]*
[1]Kamnoetvidya Science Academy (KVIS), Rayong 21210, Thailand
[2]Department of Chemistry, Kamnoetvidya Science Academy (KVIS), Rayong 21210, Thailand
*e-mail: yutichai.m@kvis.ac.th

Abstract:

ZnO is a photocatalyst with prominent antibacterial properties due to its ability to produce reactive oxygen species (ROS). ZnO/Ag interfaces are proposed to display enhanced photocatalytic performance due to the ability of Ag to absorb visible light. Two nanomaterial heterostructures were designed: nanoapartments, composing of stacked monolayers of ZnO and Ag nanocubes, and nanocondominiums, composing of stacked monolayers of ZnO and Ag nanowires. The role of the ZnO/Ag interfaces and their crystal structure on the system's performance are studied by measuring antibacterial activity. ZnO and Ag nanocubes and nanowires were synthesized, and ZnO/Ag nanostructures were constructed via the Langmuir-Blodgett technique. Characterization through TEM, SEM, and EDS confirmed the structural and morphological properties of the nanostructures. D-spacing from these images were measured, and electron diffraction was performed to characterize the crystal structure. Antibacterial activity was evaluated against *Escherichia coli* via optical density measurements. Photocatalytic performance was assessed through the degradation of methylene blue under visible light to further confirm the attribution of antibacterial activity to the mechanism of ROS generation. Both the nanoapartment and nanocondominium structures exhibited higher antibacterial and kinetic rate of photocatalysis than pure ZnO or pure Ag nanoparticles. XPS analysis was performed to confirm the charge transfer from Ag to ZnO, revealing that photoirradiation reduces ZnO (Zn^{2+}) to metallic Zn, and oxidizes metallic Ag to Ag^{+}, confirming the transfer of electrons from Ag to ZnO's conduction band. Periodic ab-initio DFT calculations within the GGA-PBE functional and atomic pseudopotentials were implemented to investigate the mechanism of the ROS generation reaction on the ZnO surface kinetically and thermodynamically, relative to a ZnO/Ag heterostructure, showing the heterostructure to be the more kinetically favorable pathway.

NON-COVALENT INTERACTIONS GOVERNING SUBSTRATE BINDING IN GH27 α-GALACTOSIDASE–CATALYZED TRANSGLYCOSYLATION

Keawalin Puntupin[1], Kotchaphan Thaya[1], Wijitra Jitonnom[1, 2], Jitrayut Jitonnom[2*]
[1]Demonstration School University of Phayao, Phayao 56000, Thailand
[2]Unit of Excellence in Computational Molecular Science and Catalysis, and Division of Chemistry, School of Science, University of Phayao, Phayao 56000, Thailand
*e-mail: jitrayut.018@gmail.com

Abstract:
α-Galactosidase, a member of the glycoside hydrolase family 27 (GH27), catalyzes the hydrolysis of α-1,6-glycosidic bonds in carbohydrate molecules and plays a key role in glycan metabolism. In this study, we investigated the non-covalent interactions (NCIs) governing the stability of enzyme–substrate complexes during transglycosylation catalyzed by α-galactosidase. Three disaccharides (melibiose, lactose, and sucrose) were examined as acceptor molecules of the transglycosylation in both the wild-type (WT) enzyme and two variants (W188A and F235A). NCI analysis was performed by reprocessing molecular dynamics simulation data, visualizing structures in VMD, and generating interaction plots using NCIweb. This approach provides molecular-level insights into the roles of key residues and NCIs in shaping substrate binding and catalytic outcomes. The results reveal that hydrogen bonds, van der Waals forces, and steric effects contribute to substrate binding at the enzyme active site with different NCI patterns observed between the WT and the mutants: WT forms stronger and more favorable interactions that support efficient catalysis, whereas alanine mutants weaken key interactions leading to reduced binding stability. These findings highlight the importance of NCIs in substrate recognition, binding stability, and hence enzyme reactivity, offering useful insights for future enzyme engineering and drug development.

D: MATHEMATICS / STATISTICS / COMPUTER SCIENCE / DATA SCIENCE / AI

A NONSTANDARD PROOF OF MICHAEL'S SELECTION THEOREM

Supanat Jumpalek,[1] Athipat Thamrongthanyalak,[2,*]
[1,2]Department of Mathematics and Computer Science, Faculty of Science, Chulalongkorn University, Thailand, 10330
*e-mail: athipat.th@chula.ac.th

Abstract:
Let $D \subseteq R^k$. A set-valued map $F : D \Rightarrow R^m$ is a function $F : D \to P(R^m)$. We say that F is lower semicontinuous if for any $x \in D$ and open set $V \subseteq R^m$, if $V \cap F(x) \neq \emptyset$, then there exists a neighborhood U of x such that $F(x') \cap V \neq \emptyset$ for all $x' \in U$. Micheal's Selection Theorem states that every lower semicontinuous set-valued map with nonempty, closed, and convex set values has a continuous selection. In this talk, we are going to show an alternative proof of Micheal's Selection Theorem via nonstandard analysis.

A STUDY OF MINIMUM SECURE DOMINATING SETS IN CYCLE AND PATH GRAPH

Chanon Bumpeng,[1,*] Viramon Hataiwaseewong,[1] Apirat Wanichsombat,[2]
Phattaraphorn Hama,[1]
[1]PSU Wittayanusorn Suratthani School, Thailand
[2]Prince of Songkla University, Surat Thani Campus, Thailand
*e-mail: chanonza2569@gmail.com

Abstract:

In graph theory, the Domination Number (DN) is a parameter used to find the smallest set of vertices, called a Dominating Set (DS), that can cover all the vertices in a graph. This concept is applied in many real-world situations. For example, it can help reduce the number of wireless network access points needed to cover an area efficiently, which helps lower installation costs. The Secure Domination Number (SDN) is a variation of DN that focuses on network security. It can be used in planning the placement of antivirus or spam protection software on network devices to ensure all devices are protected from malware or spam attacks. This study want to find the patterns of a Secure Dominating Set , which is a secure dominating set with size equal to the SDN (γ_s -Secure Dominating Set: γ_s -SDS). The focus is on cycle and path graphs, exploring all possible secure dominating sets and analyzing the patterns found. The results show that, in cycle graphs, especially those with an odd number of vertices, there is a close pattern for create SDS. The total number of γ_s -SDS can be counted using a formula that depends on the number of vertices and the different induced distance sequences in the graph. In path graphs, a method for building SDSs was also found, but no formula has been discovered yet for counting all possible γ_s -SDS.

APPLICATION OF P-MEDIAN MODEL FOR SCHOOL SERVICE AREA ANALYSIS: A CASE STUDY OF EDUCATIONAL SERVICE AREA 2, NAKHON PATHOM, THAILAND

Sirirat Phongpipattanapan *
Department of Liberal Arts, Mahidol Wittayanusorn School, Nakhon Prathom, Thailand
*e-mail: sirirat.pan@mwit.ac.th

Abstract:
Inefficient planning of school service areas, which often results in students commuting outside their designated zones, leads to problems such as excessive travel distances, school overcrowding, and the suboptimal use of educational resources. This research, therefore, aims to apply the P-median model to analyze and optimize the school service areas within Educational Service Area 2, Nakhon Pathom. The study uses a mathematical model with the objective function of identifying p school locations that minimize the total weighted distance from student groups to their nearest assigned school. The model's core objective function is to (Minimize $Z = \sum_{i \in I} \sum_{j \in J} h_i d_{ij} x_{ij}$), where h_{ij} is the actual number of students residing near origin point i, d_{ij} is the actual distance between student group i and school j, and x_{ij} is a binary decision variable (1 if student group i is assigned to school j; 0 otherwise).The model operates under the constraint that each student group is assigned to exactly one school.The analysis was conducted using real-world data from 120 primary schools and approximately 5,000 students, with the model being processed through mathematical programming and spatial analysis performed using a Geographic Information System (GIS). The results show that the model selected 50 optimal school locations, which successfully reduced the average student travel distance from 3.8 to 2.4 kilometers. Furthermore, the solution helped alleviate overcrowding and better aligned student distribution with individual school capacities. The study demonstrates that the P-median model is a systematic and effective tool for data-driven educational policy planning. Recommendations include extending the model's application to other educational service areas, ensuring regular data updates, and promoting GIS and quantitative analysis skills among educational administrators to enhance management efficiency.

Design and Implementation of a Web-Based Carbon Footprint Assessment System for Sustainable Event Management

Tanawat Chumwong[1] , Chompoohnek Ponuy[1] , Woranittha Sotorn[1] , Chinnapong Angsuchotmetee[2*],
[1]PSU.Wittayanusorn School, Songkhla 90110 Thailand
[2]Division of Computational Science, Faculty of Science, Prince of Songkla University, Songkhla 90110 Thailand
e-mail: chinnapong.a@psu.ac.th

Abstract:
This work presents the development of a web-based system for assessing the carbon footprint of events in Thailand. Traditional assessments often require experts and on-site checks, which are not always possible for schools or small organizations. Our system makes the process more accessible by letting event organizers enter key information such as the number of participants, travel, energy use, and materials involved in their event. The system then calculates greenhouse gas (GHG) emissions using emission factors that are scientifically verified by certified experts, ensuring that the results are based on reliable standards. The system was built using Python with the Django Framework, Django ORM for database management, and Chart.js for clear data visualization. To test the system, we collected data from small, medium, and large school events. The results showed that GHG emissions increase sharply with event size. For example, a small event produced about 910 $kgCO_2e$, while a large event produced more than 11,600 $kgCO_2e$. The tool also estimated how many trees would be needed to offset these emissions, helping users better understand the impact of their activities. These findings reveal that even normal school or community events generate a significant amount of GHG, which many organizers may not realize. By raising awareness and providing simple recommendations, the system encourages students, teachers, and organizations to plan activities in a more sustainable way and to follow low carbon event practices that support greener and more responsible event management.

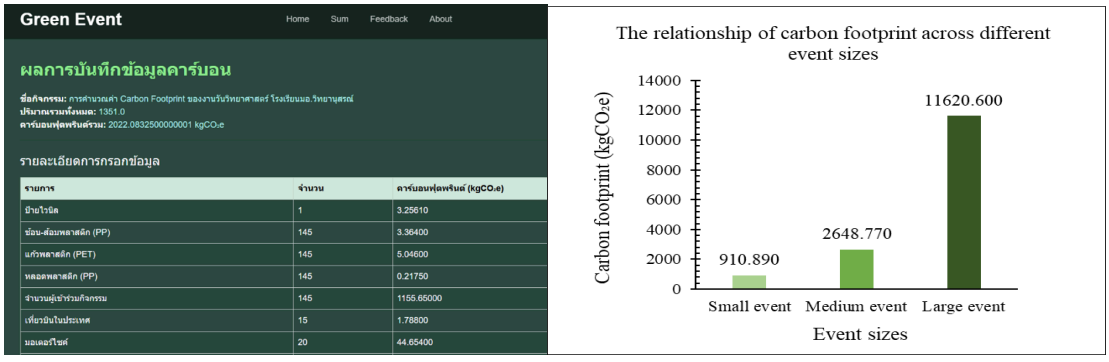

Figure 1 (left) Screenshot of "Green Event" a Web-Based Carbon Footprint Assessment System for Sustainable Event Management
(right) Data collection on the carbon footprint of school events of different sizes

DRONE ATTACHMENTS FOR DETECTING VICTIMS IN THE EARTHQUAKE-PLANZONE USING IMAGE PROCESSING TECHNIQUES

Phichamon Udomvittayakhai,[1,*] Kingfa Saeyong,[1] Nathaphon Boonnam[2]
[1]PSU Wittayanusorn Surat Thani School (SCiUS), Thailand
[2]Prince of Songkla University, Surat Thani Campus, Thailand
*e-mail: pichamol221@gmail.com

Abstract:
Finding disaster victims is crucial for rescue operations after a disaster. Traditional methods, such as physical searches, and the use of SAR dogs, can be resource-intensive, and untimely. Nowadays, there is a safer and more modern approach. Using drones with attachments can detect victims more effectively. This research focuses on improving an image processing system using a Raspberry Pi 4, and a camera module attached to a drone to detect victims in earthquake planzones. It enables swift detection of survivors and respectful recovery of deceased, enhancing safety for rescue teams and supporting affected communities. The process begins by collecting dataset from Kaggle and Roboflow for creation of machine-learning model using 800 labeled images dataset . The YOLO models are compared with 5n, 8n, and 11n performance from training and validation set with a ratio of 80:20 to determine the most effective prey detection system. We attach Raspberry Pi 4 and a camera module to evaluate simulated scenarios in both open environments and obstructed areas. Also, we enhance it until its accuracy achieves a 90 percent. Finally, the attachment was attached to a drone to enhance operational capabilities. From the experimentation, we found that the YOLOv5n model is the most suitable for the resources of the Raspberry Pi 4 and compatible with other accessories. The drone attachment can detect humans in both open environments and obstructed areas with Accuracy, Precision, Recall, and F1-score values at 94.96, 97.92, 92.00, and 94.86 percent, respectively along with mAP@0.5 at 0.977.

Model	Accuracy (%)	Precision (%)	Recall (%)	F1-score (%)	mAP@0.5
YOLOv5n	94.96	97.92	92.00	94.86	0.977
YOLOv8n	93.95	97.87	90.00	93.76	0.936
YOLOv11n	90.39	98.34	82.44	89.94	0.915

Table 1. Accuracy comparison table of all 3 versions of YOLO models

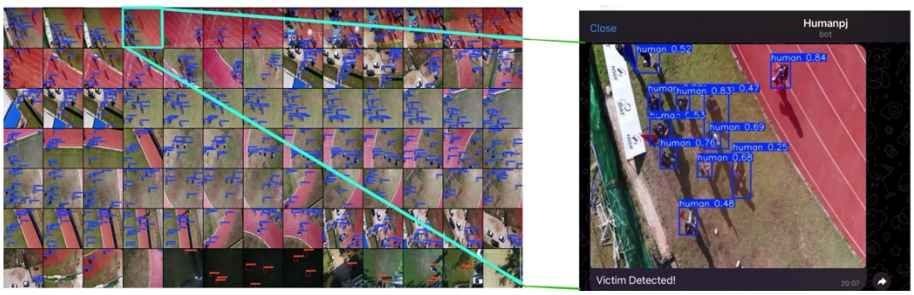

Figure 1. Telegram notifications when victims are detected in open environments

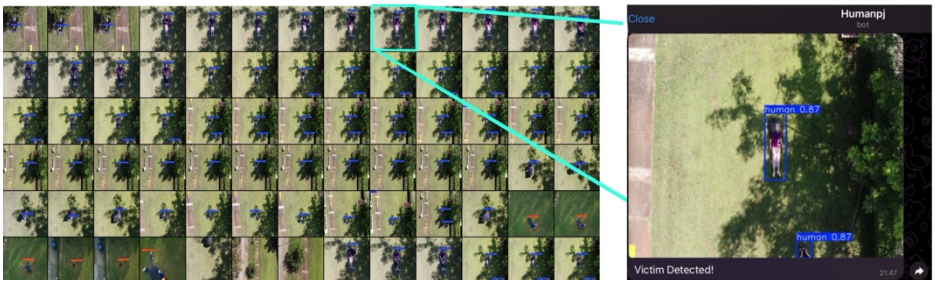

Figure 2. Telegram notifications when victims are detected in obstructed areas by covering some part of body and in low light

The system can detect victims at a height of 5-20 meters. Also, the system demonstrated that the attachment can work for 3 hours, with a response time of 4 seconds (Since the camera on). The results show that using the drone attachments for victims detection is effective, allowing timely assistance through Telegram notifications and facilitating the recovery of deceased. It also reduces risks for rescuers during searches.

PONGJIT: AN ADAPTIVE BIOFEEDBACK SYSTEM FOR ENHANCING STUDENT FOCUS AND MITIGATING LEARNING BURNOUT

Thakorn Kreaboonma[1], Sujika Churprayoon[1]
and Asst. Prof. Dr. Worawan Diaz Carballo (Marerngsit)[2,*]
[1]Department of Computer, Bunyawat Witthayalai School, Lampang 52000, Thailand
[2]Department of Computer Science, Faculty of Science and Technology,
Thammasat University, Lampang 52190, Thailand
*e-mail: ktharkorn@gmail.com

Abstract:
Student burnout and diminished concentration represent significant challenges in modern education, directly impacting learning engagement and academic outcomes. To address this, PongJit was developed as a novel technology-enhanced learning tool. This intelligent ecosystem interfaces with wearable devices to create a real-time, adaptive biofeedback loop. By combining virtual reality (VR) with AI-driven analysis, the system provides an intuitive and immersive user experience, enabling seamless data collection and feedback delivery. By analyzing heart rate variability (HRV) and other physiological signals, the system dynamically adjusts ambient auditory tones and visual stimuli—such as background color, brightness, and ambient soundscape—to restore students' attention levels. HRV, commonly used as an indicator of autonomic balance, was adopted here as a proxy for mental focus, reflecting parasympathetic modulation during sustained cognitive engagement. The AI models powering PongJit were trained and deployed on the LANTA High-Performance Computing (HPC) infrastructure, enabling low-latency physiological data analysis and real-time environment adaptation even under multi-user workloads. Through research trials and data collection with 30 high-school participants over four weeks, the system demonstrated significant increases in HRV and reductions in self-reported stress compared to a baseline session without adaptation. These results indicate a direct positive impact on students' capacity for sustained learning. PongJit offers a new paradigm for educational technology, shifting from static applications to dynamic systems that autonomously optimize the learning environment. All environmental adjustments occur automatically through AI–VR–HPC synergy, requiring no manual intervention. It contributes to the field of technology-enhanced learning by showing how intelligent biofeedback and HPC-driven AI can be integrated into the educational ecosystem to foster a more resilient and focused generation of learners.

PYTHOPIA : GAMIFICATION OF PYTHON LEARNING THROUGH A 3D GAME

Weerapat Piti [1], Prach Khamnurak[1], Piyanart Chotikawanid [2,*]
[1]PSU Wittayanusorn Surat Thani School, Surat Thani 84000, Thailand
[2]Faculty of Science and Industrial Technology, Prince of Songkla University, Surat Thani Campus, Surat Thani 84000, Thailand
*e-mail: piyanart.ko@psu.ac.th

Abstract:

Coding is a crucial skill for 21st century students, enabling them to create instructions or programs that drive computers to perform tasks efficiently. This skill is especially important for Gen Z and Gen Alpha, who have grown up immersed in a technology-driven world. However, not all students enjoy learning to code, as they often find it less engaging and perceive it as overly complicated. Game-based learning has been shown to enhance student engagement and motivation, a method referred to as gamification. Building on this concept, this research addresses the challenges in programming education by developing PYTHOPIA - a 3D educational game designed to teach Python programming through engaging and interactive experiences. The game was developed using the Unity engine and programmed in C#. It is designed as a 3D third-person perspective game, where players are tasked with completing missions by locating and assembling the correct code blocks to achieve their objectives. The code blocks are Python instructions, and each level has varying levels of content and difficulty. This game will reduce the complexity of coding concepts and customize the experience to be appropriate and interesting for Gen Z learners, focusing on 3D platforms on computers to maximize engagement. The game mechanics were designed to reinforce basic Python programming principles, while the pre- and post-game assessments measured knowledge acquisition, retention, and engagement levels using a T-Test. The sample consisted of two groups of 30 students, aged 13-16, who did not have sufficient background in Python coding. The first group received Python instructions only through a teacher and video as part of the traditional teaching method, while the second group received the same instruction and played the game. Preliminary results indicate that game-based learning significantly increases students' motivation and understanding of programming concepts. The post-game assessment further emphasized the game's effectiveness by demonstrating significantly higher retention rates and improved Python proficiency in the first group, with a statistically significant increase in test scores (P-value = 6.47×10^{-12}), while no significant improvement was found in the second group. This research demonstrates the potential of gamification to revolutionize programming education by combining entertainment with education, fostering technological innovation and equipping them with critical skills for the 21st century.

THE 360° ALZHEIMER'S THERAPY ECOSYSTEM: AI-POWERED SOFTWARE ARCHITECTURE FOR PERSONALIZED NEUROTHERAPY

Thakorn Kreaboonma[1], Nawaphorn Tanatiratorn[2], Sujika Churparyoon[1], Kanokpitch Moungsrijan[3], Ratchapon Peebanmai[1], Apinya Takaewpun[1] and Asst. Prof. Dr. Worawan Diaz Carballo (Marerngsit)[4,*]
[1]Bunyawat Witthayalai School, Lampang 52000, Thailand
[2]Prasarnmit Demonstration School (Secondary), Bangkok 10110, Thailand
[3]Lomsakwittayakhom School, Phetchabun 67110, Thailand
[4]Thammasat University, Lampang 52190, Thailand
*e-mail: zenova.teams@gmail.com

Abstract:
Alzheimer's therapy in Thailand faces two major challenges: limited personalization and language-cultural mismatch. To address these, our team from Mae Moh, Lampang has developed a self-learning neurotherapy ecosystem powered by the LANTA HPC-based AI engine and Wangchan, Thailand's large language model. The AI core dynamically integrates EEG, GSR, and Apple HealthKit data with personalized conversational therapy in Thai, creating culturally relevant emotional engagement. The Wangchan-LANTA hybrid architecture enables the AI to both analyze patient emotional responses and autonomously adjust visual, auditory, and linguistic stimuli in real time. This "Thai AI using Thai resources" framework strengthens data privacy, accelerates learning by 25%, and provides natural Thai-language interaction unmatched by foreign models. In a pilot study (n = 10, aged 65–82), participants achieved a 40% improvement in MoCA memory recall after six weeks of adaptive therapy. Developed under the Lampang Sandbox Wellness Initiative, this copyrighted innovation (2025) marks Thailand's first locally powered AI system for Alzheimer's rehabilitation—bridging neuroscience, HPC, and Thai-language intelligence for inclusive elder care.

THE GEOMETRY OF RANDERS CYLINDERS OF REVOLUTION WITH NON-CONSTANT NAVIGATION DATA ALONG MERIDIANS

Natnicha Rakbumrung,[1,*] Chayapon Chainarong,[1] Asst. Prof. Dr.Rattanasak Hama [2]
[1] PSU. Wittayanusorn Surat Thani School, Thailand
[2] Faculty of Science and Industrial Technology, Prince of Songkla University, Surat Thani Campus, Thailand
*e-mail: natnicha8814@gmail.com

Abstract:

The study of differential geometry involves examining surfaces and shapes using calculus and linear algebra. It helps explain how objects bend and twist. Examples include calculating optimal flight paths for airplanes, studying the curvature of surfaces, and analyzing the shortest paths on surfaces known as geodesics. One specific area of research is the study of the cut locus, which is the set of cut points. A cut point of a point p is a point that can be connected to p by more than one geodesic. For example, on a sphere, the cut point of a given point is its antipodal point. In this research, the focus is on studying the structure of the cut locus on surfaces of revolution surfaces where the Gaussian curvature is not constant. The researcher uses Descartes' rule of signs to study the structure of the cut locus by expressing the Gaussian curvature as a polynomial function. The results of the research provide necessary conditions for describing the structure of the cut locus on surfaces of revolution. Through this study, the researcher identifies examples of surfaces of revolution where the cut locus is the meridian on the opposite side.

E: ENERGY / ENVIRONMENTAL & EARTH SCIENCE / MATERIALS SCIENCE / CHEMICAL TECHNOLOGY

Adsorption of Carbon Dioxide Gas from Chitosan and Calcium Oxide Composite

Thanchanok Sangwara,[1] Warissara Rattana,[1] * Saranyoo Klaiklay,[2] Yutthapong Pianroj,[2] Apiluck Eiad-Ua[3]
[1]PSU. Witthayanusorn Surat Thani, Surat Thani, 84000, Thailand
[2]Faculty of Science and Industrial Technology, Prince of Songkla University, Surat Thani
[3]King Mongkut's Institute of Technology Ladkrabang
*e-mail: 2445@psuwitsurat.ac.th

Abstract:

Global warming is a worldwide issue caused by greenhouse gases, especially carbon dioxide (CO_2), from human activities such as industrial processes. This causes the Earth's temperature to rise and seriously affects the environment and living beings. Adsorption is an alternative solution for efficiently capturing CO_2 using recyclable natural materials, offering energy and cost savings while being easy to control and non-polluting. However, the methods to solve this problem do not focus enough on important details, such as the best temperature for CO_2 adsorption or the optimal mix of materials.

This project investigates a CO_2 adsorbent composite material. It uses calcium oxide (CaO) from oyster shells and chitosan from tilapia fish scales. Experiments are conducted under different conditions to determine the optimal temperature and material composition. CaO–chitosan composite materials were prepared by blending CaO powder with chitosan at ratios of 10%, 20%, and 30% (w/w). The structure, surface area, and porosity characteristics of the composite were analyzed using Scanning Electron Microscopy (SEM) and a Surface Area and Porosity Analyzer (BET). At this stage, the study focused on model-based analysis and adsorption characterization rather than actual CO_2 adsorption experiments, and the findings from this model will be applied in future work to guide experimental design, optimize adsorption conditions, and improve the practical performance of CaO–chitosan composites for CO_2 capture. The results showed the CO_2 adsorption capacity, revealing that the adsorbent composed of calcium oxide and 30% chitosan exhibited the highest adsorption efficiency. This suggests a sustainable method for reducing greenhouse gases in the air.

An Integrated Bioremediation System Combining Biocomposite-Zeolite Adsorption Beads and Agricultural Waste-Enhanced Microbial degradation for Industrial dye Wastewater Treatment

Chayachon Jiemwetwittayaporn,[1] Warinthip Suwanratsamee,[2] Thanasan Nilsu[3,*]
[123]Kamnoetvidya Science Academy
*e-mail: chayachon.j@kvis.ac.th, warinthip.s@kvis.ac.th, thanasan.n@kvis.ac.th

Abstract:

The textile industry is a major source of freshwater pollution, largely from dye-contaminated wastewater containing toxic, persistent chemicals. Conventional physicochemical treatments are often unsustainable, producing hazardous residues and high carbon emissions. This study presents an integrated, eco-friendly treatment system combining adsorption with biodegradation. Dye adsorption was performed using calcium alginate beads reinforced with 4% cellulose and 4% zeolite, which exhibited strong stability, low swelling, and efficient removal of model dyes. These CAZ-Beads achieved removal of 96.78% of Congo red (1000 ppm, azo dye) and 93.00% of alizarin red (2000 ppm, anthraquinone dye) within 20 hours. For biodegradation, bacterial strains isolated from soil and water were screened for dye-degrading capacity and laccase activity. *Bacillus* sp. and *Lysinibacillus* sp. demonstrated the highest performance, degrading up to 94.8% of azo dyes and 80.9% of anthraquinone dyes using palm oil wastewater and molasses as low-cost nutrient sources. Additionally, PEI-coated CAZ-Beads exhibited adsorption capacities up to 9 times higher than unmodified beads and enabled dye desorption through pH-dependent elution. FT-IR confirmed azo bond cleavage, while toxicity tests showed no harmful effects on seed germination. These results highlight bead-based adsorption combined with bacterial degradation as a promising strategy for sustainable treatment of industrial dye wastewater.

ASSESSMENT OF CARBON CAPTURE USING UNMANNED AERIAL VEHICAL COMBINED WITH IMAGE PROCESSING TECHNOLOGY

Supakarn Kumfoo,[1,*] Thanapon Mahaparn,[1] Chavisa Panyanukij,[1] Supet Jirakajohnkool[2] and Nutthapol Junkaew[2]
1 Science Classrooms in University - Affiliated School Project, Thammasat University - Suankularb Wittayalai Rangsit School Center (SCiUS TU-SKR), Faculty of Science and Technology, Thammasat University, Khlong Laung, Pathum Thani, 12120, Thailand
2 Department of Sustainable Technology of Rural Technology, Faculty of Science and Technology, Thammasat University, Khlong Laung, Pathum Thani, 12120, Thailand
*e-mail: supakarn.karn.kumfoo@gmail.com

Abstract:

The extensive greenhouse gas emissions have contributed to global warming and escalated into the climate change crisis. Thailand aims to achieve carbon neutrality by 2050 and net-zero greenhouse gas emission by 2065. Therefore, the Greenhouse Gas Management Organization (TGO) was established along with the T-VER program, which is a program under TGO. The amount of greenhouse gases that is stored or captured is quantified as "carbon credits," which can be used to offset the carbon emissions of the organizations. Nowadays, assessing the carbon sequestration is conducted through field surveys, and calculating the carbon sequestration afterwards is done by taking an allometric equation.

This research aims to study the differences in carbon sequestration potential among 30 sampled trees through field measurements and UAV data combined with image processing technology to provide an innovative way to assess the carbon sequestration. The study shows that UAVs can be used to obtain tree height accurately, due to the 1.88% mean difference between field-survey data and drone data, which is highly acceptable. However, there is a low correlation ($r = 0.178$) between NDVI and carbon sequestration, indicating that NDVI is weakly related to carbon sequestration and is influenced by the timing of flight. Moreover, the regression analysis using NDVI and Htree as predictors for biomass and carbon sequestration yielded a low R-squared value (10.2%), suggesting the need for additional variables along with optimizing the seasonal timing of drone flight. Although UAV methods are faster than field surveys, reliable carbon estimations require methodological advancements and field data integration for future applications.

ASSESSMENT OF WATER QUALITY FLUCTUATION TRENDS IN INNER-CITY CANALS IN CONDITION OF CLIMATE CHANGE AND SEA LEVEL RAISE

Nguyen Ngoc Diep [2] **, *Bui Viet Hung*** [1,*]
[1]University of Science, Vietnam National University, Ho Chi Minh City, Vietnam
[2]University of Labor and Affair (Branch 2), Ho Chi Minh City, Vietnam
*e-mail: bvhung@hcmus.edu.vn

Abstract:
In assessing the trend of regional water quality change, climate change scenarios are always the choice in many studies. This is understandable when climate change scenarios describe the specific conditions of the hydrological regime and the level of socio-economic development of the region in the future. However, simulating water quality by mathematical models is still challenging when many processes of changing the content of water components are determined through regional experiments. The study applies detailed statistical methods - often used in temperature forecasting for climate change scenarios - combined with multivariate regression analysis to establish a water quality dataset according to the scenarios (RCP2.6, RCP4.5 and RCP8.5) with the full number of components in the formula for calculating the water quality index (WQI). The results of the study show that the correlation (R^2) varies depending on the type of substance and the monitoring location, but remains at a reasonable level. Based on the water quality parameter set according to climate change scenarios, the study identifies the trend of self-improvement of water quality. This result is very valuable for urban water management, especially in planning drainage systems and constructing treatment facilities to support sustainable improvement of water quality in the context of changing climate conditions.

Introduction:
In the IS92 emission scenario assessment report (IPCC, 1995), the IPCC pointed out that emission scenarios need to reflect the following issues: (1) Estimating future emissions; (2) Updating the latest information on changes in the world economic situation; (3) Expanding the socio-economic development range; (4) Examining new trends and assessing the level of technological change; (5) Assessing the consequences of socio-economic development; (6) Reflecting emission commitments related to the UN Framework Convention on Climate Change.

Normally, in terms of emission levels, there are 3 main scenarios (IPCC, 1995):

- High emission scenario (RCP2.6 - low development) is characterized by independence, protection of local characteristics, continued regional population growth, regionally oriented economic development, slow and separate technological change and economic growth per capita;
- Medium emission scenario (RCP4.5 - medium development) is characterized by average economic development, slow and asynchronous technological change. Also aimed at environmental protection and social equity;
- Low emission scenario (RCP 8.5 - high development) has rapid changes in economic structure towards service and information economy, reducing the intensity of material consumption; developing clean technologies and efficient use of resources; focusing on global solutions for economic, social and environmental sustainability.

To establish data sets for climate change and sea level rise scenarios, according to IPCC (1995), there are many different methods depending on the level of information and

data available such as on hydrometeorology, socio-economic development. To build climate change scenarios for each region, country and territory (IPCC, 1995), it is necessary to "downscale" the simulation space (simulation grid) of global models, that is, to create information at the regional scale. There are two main approaches to downscaling: statistical methods and dynamic methods. In addition, there is a less used approach that is to interpolate directly from the output of AOGCM (IPCC, 1995).

The two main methods in downscaling are as follows (1) Dynamic method (MIKE11 model set of DHI) simulates the hydrological regime according to the climate change and sea level rise scenarios; (2) Statistical method is based on the view that environmental factors (climate, quality ...).

The statistical downscaling method has the advantage of being simple and does not require large computer resources, so it can be applied to many different global climate model results tests (IPCC, 1995). Another advantage is that this method can be used to provide information for a specific location, which is essential for studies on the impact of climate change (Bui H. V etc., 2025).

Water quality (WQ) includes a combination of different components such as physical, chemical and biological. The state of water quality (level of pollution) depends on and fluctuates according to the speed of economic and social development (pollutants) and flow conditions (impacts on improvement trends) (Le, 2004, Pham H. T. M., 2009).

To recognize the trend of quality improvement, it is necessary to fully consider the natural impact processes (flow hydrological regime) on the chemical - physical - biological processes of water sources through the concept of self-cleaning ability or self-improvement of water quality (Pham, 2009, Tran, 2010, Thomann, 1987). Natural systems (hydro-meteorological conditions) may change and the above quality improvement trends will also be affected and transformed (Cawthron, 2023, Thomas, 2009).

Considering climate change and sea level rise conditions is also included in many studies assessing environmental quality, including water environment. It is common to consider climate change and sea level rise scenarios for specific cases such as salinity intrusion or changes in sediment and sand content, and few studies mention quality components such as organic matter such as BOD_5 or physical matter such as pH ... (Nguyen D. T., 2005). These water quality components are simulated or evaluated for changes on the "base" of hydrological conditions simulated according to climate change and sea level rise scenarios.

Water quality data sets are often considered as the consequences of waste discharge during socio-economic development into water sources with corresponding levels of wastewater collection and treatment. The climate change and sea level rise scenarios for establishing data sets of quality parameters will be suitable for the speed/level of socio-economic development from low to high, corresponding to the levels of water collection and treatment, including: (1) RCP2.6 - low socio-economic development, high emissions - the level of water quality after treatment meets the low standard requirements; (2) RCP4.6 - medium socio-economic development, medium emissions - the level of water quality after treatment meets the medium standard requirements; (3) RCP 8.5 - high socio-economic development, medium low emissions - the level of water quality after treatment meets the high standard requirements (IPCC, 1995, Bui H. V. etc., 2025).

Research on assessing the quality of inner-city canal water sources in Ho Chi Minh City is quite rich and diverse in terms of applied methods (from models to WQI index, receiving capacity and self-cleaning capacity...). The main reason for the above problem is that the city has a dense inner-city canal system with 5 main inner-city canals: Nhieu Loc Thi Nghe canal, Tam Luong - Vam Thuat - Ben Cat canal, Tau Hu Ben Nghe canal, Tan Hoa - Lo Gom canal and Kenh Doi - Kenh Te canal. The quality of canal water sources is monitored

annually with quite high frequency (1 - 3 months for 1 measurement). Ho Chi Minh City is a fast-growing and large city in Vietnam. With a large population and a developed economy, canals in the city receive a huge amount of waste, creating pressure on the quality of water sources.

Methodology:

a. Research area.

The inner-city canal system of Ho Chi Minh City (HCMC) includes (1) Nhieu Loc Thi Nghe canal, (2) Tan Hoa Lo Gom canal, (3) Tau Hu Ben Nghe canal, (4) Tham Luong Ben Cat Vam Thuat canal and (5) Kenh Doi Kenh Te canal (See Figure 1).

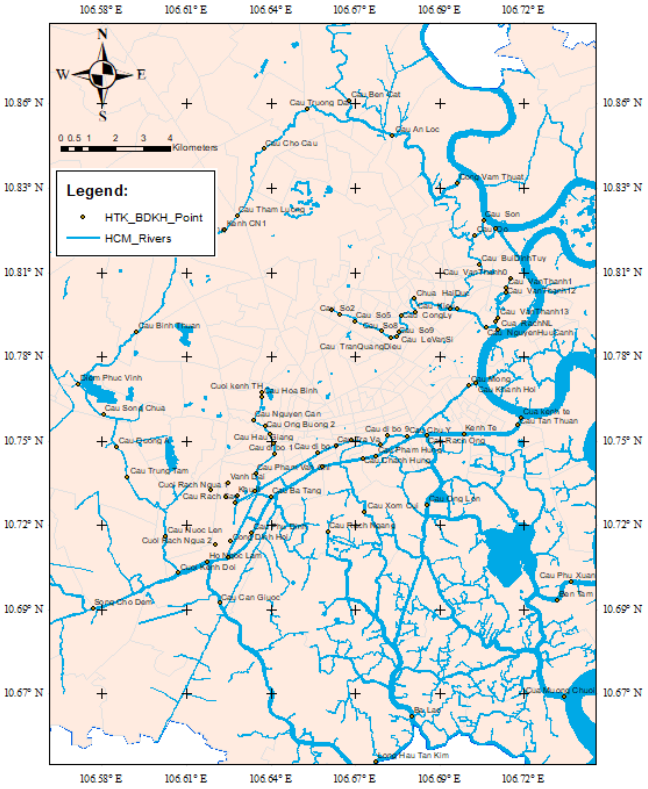

Figure 1. Inner-city canal system and monitoring points of Ho Chi Minh City

b. Water quality and flow data on inner-city canals for the period 2012-2023.

The data set of water quality for the period 2012-2023 together with the results of flow regime simulation (Q flow, U velocity, Z water level) at monitoring locations on the inner-city canal system of Ho Chi Minh City.

The data set of water quality and the results of flow regime simulation above are inherited from the results of the topic "Assessing the self-cleaning capacity of inner-city canal water sources in Ho Chi Minh City, considering the impact of the operation of the tide-prevention sluice system and climate change" (Bui H. V. et al., 2025) (See Table 1 and Table 2).

Table 1. The flow's factors (Q-m^3/s, U-m/s, Z-m) at the Dien Bien Phu Bridge monitoring position in Nhieu Loc Thi Nghe Canal (2019 example)

Month	$Q_{Low\ tide}$	$Z_{Low\ tide}$	$U_{Low\ tide}$	$Q_{High\ tide}$	$Z_{High\ tide}$	$U_{High\ tide}$
01	73.53	1.15	0.39	53.68	1.24	0.25

02	62.88	1.26	0.40	50.79	0.99	0.22
03	63.88	1.35	0.41	49.79	0.89	0.22
04	96.02	1.36	0.46	48.80	1.12	0.25
05	53.95	1.39	0.38	47.96	0.96	0.22
06	55.20	1.47	0.36	43.69	0.78	0.21
07	95.37	1.20	0.45	49.45	1.27	0.26
08	53.30	1.23	0.37	48.61	1.12	0.22
09	54.59	1.30	0.36	44.30	0.94	0.22
10	95.37	1.20	0.45	49.45	1.27	0.26
11	53.30	1.23	0.37	48.61	1.12	0.22
12	54.59	1.30	0.36	44.30	0.94	0.22

(Source: Bui H. V. and etc., 2025)

Table 2. The low tidal water quality data set is at Dien Bien Phu monitoring position in Nhieu Loc Thi Nghe canaal (2019 example)

Month	The low tidal periods										
	T°C	pH	TSS	NTU	NH_4^{3-}	PO_4^-	DO	COD	BOD_5	Coliform	E. Coli
1	29.7	6.41	31.6	27.5	3.21	0.08	2.31	11.0	4.96	142000	20000
2	29.6	6.46	40.5	45.4	0.14	0.04	4.54	40.8	24.9	26000	13000
3	30.0	6.78	31.7	22.9	0.28	0.06	3.39	28.2	14.4	23000	3900
4	30.5	6.36	16.4	38.2	1.22	0.04	3.35	18.6	10.6	64000	12000
5	31.5	6.67	33.8	33.4	0.81	0.02	3.30	21.9	10.8	33000	8100
6	31.3	7.53	68	24.2	0.01	0.01	1.88	25.0	8.0	9300	2700
7	30.1	7.16	22	39.8	0.56	0.03	2.13	23.0	8.0	15000	2800
8	29.8	7.21	25	23	0.75	0.08	3.13	15.0	6.0	93000	21000
9	30.7	6.95	29	34.6	0.01	0.07	3.09	14.0	5.0	23000	15000
10	30.0	7.1	34	39.8	1.21	0.1	0.5	11.0	4.0	39000	14000
11	30.8	7.28	21	63.2	5.69	0.35	1.12	16.0	8.0	93000	29000
12	30.7	7.17	11	10	6.44	0.08	0.61	25.0	10.0	43000	2300

(Source: Bui H. V. and etc., 2025)

c. Establishing a set of water quality indicators according to the downgrading - statistical method

Building a set of water quality data according to climate change scenarios (with 3 development levels including low development, medium development and high development). Corresponding to the development scenarios of the city as above combined with the plan to improve the level of domestic wastewater treatment in the city.

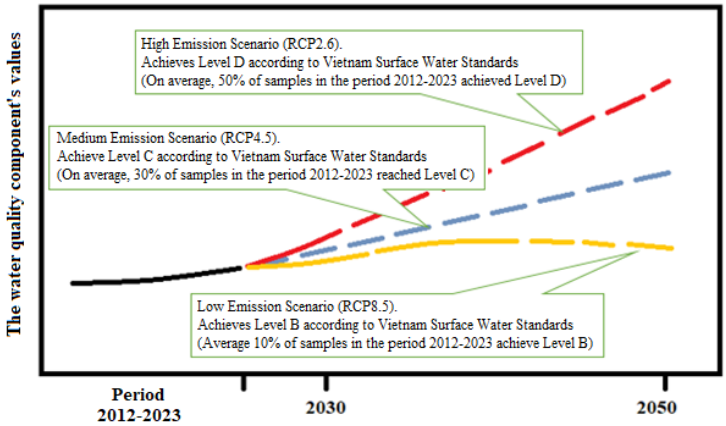

Figure 2. Guidelines for establishing water quality datasets according to climate change scenarios

Analysis of trends of water quality data set in the period 2012-2023 with the condition of domestic wastewater treatment level corresponding to 3 climate change development

scenarios corresponding to level D (50% of component samples meet), C (30% of component samples meet) and B (20% of component samples meet), wastewater is collected and treated at 100% as shown in Figure 2 and Table 3 below.

Table 3. Simulation scenario statistics

No	Year/ CC scenarios	Boundary data for MIKE models and water quality
1	RCP2.6 (2050)	+ Vung Tau water level margin 2020 + %H (cm) (RCP2.6-2050) + Low development scenario corresponding to the level of domestic wastewater treatment of 100% reaching level D of QCVN 08:2023/BTNMT and the average value of water components belonging to group 50% of the samples of the data set meeting standard D in the period 2012-2023
2	RCP4.5 (2050)	+ Vung Tau water level margin 2020 + %H (cm) (RCP4.5-2050) + Medium development scenario with wastewater treatment level of 100% reaching level C of QCVN 08:2023/BTNMT, the values of water components according to this scenario are within 30% of the samples of the data set meeting standard C in the period 2012-2023
3	RCP8.5 (2050)	+ Vung Tau water level margin 2020 + %H (cm) (RCP8.5-2050) + High development scenario with wastewater treatment level of 100% reaching level B of QCVN 08:2023/BTNMT, the values of water quality components according to this scenario are within 10% of the samples of the data set meeting standard B in the period 2012-2023

To establish a water quality dataset for climate change and sea level rise scenarios, the study applied the correlation equation between water quality components and flow components according to the scenario, economic situation and selected quality dataset (full measurements during the year and all locations in the region). The correlation formula simulates water quality according to climate change and sea level rise scenarios as follows (Bui H. V. etc., 2025):

$$Y_j = A_{flow}\, Q_{flow} + A_{ptkt}\, GDP_j + \Sigma_i\, A_{position\ (i)}\, y_{(i)} + A_o \qquad (01)$$

Where are:

Q_{flow} – Flow rates are calculated based on scenarios. (m^3/s);

GDP – Projected economic growth rate by scenario (%)

$y(i)$ – Corresponding water quality component values of the selected year

A – correlation coefficient of the respective components

Criteria for evaluating the correlation level of the results of the data set establishment: by the correlative coefficient (R2) between the 20% observation data set and their recalculated results through the correlation equation of the remaining 80% data set (See Table 4 – Example of the correlative coefficients of some water components at some observation locations on NLTN canal).

Table 4. The values of multivariate correlative coefficient R^2 at the observation locations

Position / Component	Cau So 1	Chua Hai Duc	Cau Thi Nghe 2	Cau Le Van Si	Cau Dien Bien Phu
pH	0.60	0.94	0.87	0.91	0.94
TSS	0.66	0.87	0.75	0.86	0.82
Turbidity	0.80	0.85	0.74	0.87	0.85
$N\text{-}NH_4^+$	0.58	0.75	0.73	0.72	0.78
$P\text{-}PO_4^{3-}$	0.55	*0.27*	*0.46*	*0.40*	*0.48*

DO	0.64	0.93	0.85	0.89	0.91
COD	0.55	0.83	0.56	0.80	0.72
BOD_5	*0.49*	0.76	0.58	0.72	0.68
Coliform	0.87	*0.34*	0.73	*0.29*	0.73
E. Coli	0.94	0.71	0.96	0.70	0.97

d. Assessment of the quality of canal water sources according to the index

The method of calculating and using the VN_WQI index in assessing water quality is carried out according to the instructions in Decision 1460/QD-TCMT of the General Department of Environment, Ministry of Natural Resources and Environment. The water quality water quality index (VN_WQI) is used to assess the quality of inner-city canal water sources in Ho Chi Minh City as follows (Bui H. V. etc., 2025):

$$VN\_WQI = \frac{WQI_I}{100} x \left[\frac{1}{k}\sum_{i=1}^{k} WQI_{IV} \; x \frac{1}{l}\sum_{j=1}^{l} WQI_{VI}\right]^{\frac{1}{2}} \quad (2)$$

In which:

WQI_I: Calculation results of pH parameters

WQI_{IV}: Calculation results of organic group parameters (BOD_5, COD...)

WQI_{VI}: Calculation results of physical group parameters (TSS and turbidity)

Classification of water quality according to VN_WQI index as follows (See Table 5):

Table 5. VN_WQI level and suitability for intended use

WQI's values	Level of WQ	Fit for purpose
91 - 100	Very good	Good for domestic water supply purposes
76 - 90	Good	Used for domestic water supply purposes but requires appropriate treatment measures
51 - 75	Normal	Used for irrigation and other similar purposes
26 - 50	Weak (pollution)	Water is polluted. Used for navigation and other similar purposes
10 - 25	Hard pollution	Water is polluted hardly, need treatment measures in the future
< 10	Extreme pollution	Water is polluted extremely, need to have measures to fix and handle

(Source: Decision No 1460/QĐ-TCMT)

e. Method for assessing the self-cleaning capacity of water sources

The study applied the dissolved oxygen decomposition process and the corresponding simulation equation is the Street-er-Phelpse equation (Nguyen D.T., 2005; Bui L.T. etc., 2013). The equation is as follows:

$$D_t = \frac{k_1 L_O}{k_2 - k_1}\left(e^{-k_1 t} - e^{-k_2 t}\right) + \frac{k_3 N_O}{k_2 - k_3}\left(e^{-k_3 t} - e^{-k_2 t}\right) + \frac{SOD}{k_2 H}\left(1 - e^{-k_2 t}\right) + D_O e^{-k_2 t} \quad (3)$$

Where are:

k_1 – Oxygen depletion coefficient due to composition BOD_5;

$k_1 = (0.125 \sim 0.5)\,(H/2.45)^{-0.434}(q)^{(T-20)}$ When depth (h)<2.45 m (4)

$k_1 = (0.125 \sim 0.5)\,(q)^{(T-20)}$ When depth (h) ≥ 2.45 m (5)

k_2 – Oxygen diffusion coefficient into water;

$k_2 = 3.3\,U\,H^{-1.33}\,(1.0241)^{(T-20°)}$ (6)

k_3 – Oxygen depletion coefficient due to composition NH_4;

$k_3 = (0.005 \sim 1.0)\ (1.0241)^{(T-20°)}$ (7)

U and H is the velocity and depth of flow at the observation points on the channel;

D_t – oxygen depletion level in the stream;

L_o, N_o, D_o, SOD is the initial concentration value of BOD_5; NH_4; Oxygen and oxygen demand of bottom sludge.

$SOD = (0.006 \sim 0.45)\ (1.065)^{(T-20°)}$ (8)

The formula for evaluating the self-cleaning capacity of a water source is the ratio between the coefficients of the oxygen diffusion and depletion processes (oxygen fluctuation ratio) as follows:

$$f = k_2 / k_1 \quad (9)$$

The classification of self-cleaning capacity of water sources is shown in Table 6

Table 6. Classification of self-cleaning capacity of water sources according to oxygen fluctuation ratio

Levels	The critical values	The level of self-cleaning capacity
1	$10 \leq f$	Very good
2	$4 \leq f < 10$	Good
3	$2 \leq f < 4$	Normal
4	$f < 2$	Weak, water is polluted

f. Method for assessing the trend of water quality improvement

The study applied the matrix method to assess the trend of water quality improvement between the levels of water quality (Table 5) and its self-cleaning capacity (Table 6). It summarized on Table 7. The classification of improvement levels in assessing the trend of water quality improvement is summarized in Table 8 below.

Table 7. Matrix for assessing the trend of water quality improvement based on the level of self-purification ability and the current quality status of water sources

		The levels of self-cleaning capacity of water resource			
The levels of water quality	***Levels***	*Very good*	*Good*	*Normal*	*Weak*
	Very good	Very good	Very good	Good	Good
	Good	Very good	Good	Good	Unclear
	Normal	Good	Good	Unclear	Unclear
	Weak	Good	Unclear	Unclear	Decline
	Very weak	Unclear	Unclear	Decline	Decline
	Extreme	Unclear	Decline	Decline	Decline

(Source: Dang and etc., 2018; Bui H. V and etc., 2025)

Table 8. Classification of water quality change trend levels

No	Levels	Meaning
1	Very good	It has a very good self-improvement tendency. Water is not polluted.
2	Good	It has good self-improvement tendency. Water shows no signs of pollution.
3	Unclear	The trend of quality improvement is unclear. Water quality levels fluctuate up and down and water is often polluted.
4	Decline	Water quality tends to decline and is often at a level of

severe pollution.

(Source: Dang and etc., 2018; Bui H. V and etc., 2025)

Results and Discussion:

a. Building the set of water quality parameters for climate change and sea level rise scenarios in the study area

To establish a water quality dataset for climate change scenarios (2050), the study applied the MIKE 11 mathematical model simulating according to Table 3. In addition, the study analyzed and hypothesized the economic growth rate of Ho Chi Minh City at low (under 4%), medium (about 7%) and high (10%) levels, using the water quality measurement dataset of the canal system in 2015 and 2017. Applying the correlation equation (1) to establish a dataset of water quality parameters for 2050. The results of the flow simulation in the river system, canals in Ho Chi Minh City and the water quality dataset at the monitoring points corresponding to the climate change and sea level rise scenarios were inherited from the results of the topic "Assessing the self-purification capacity of water sources in inner-city canals in Ho Chi Minh City, considering the impact of the operation of the tidal sluice system and climate change" (Bui H. V. etc., 2017). 2025) (See Table 9 and Table 10).

Table 9. Flow regime (Q-m^3/s, U-m/s, Z-m) at monitoring points of Dien Bien Phu Bridge on Nhieu Loc Thi Nghe canal (Example: for RCP 8.5)

Months	$Q_{L.tide}$	$Z_{L.tide}$	$U_{L.tide}$	$Q_{H.tide}$	$Z_{H.tide}$	$U_{H.tide}$
01	133.26	1.96	0.88	68.26	1.80	0.49
02	74.73	2.02	0.73	67.09	1.56	0.42
03	76.52	2.12	0.71	61.09	1.29	0.41
04	133.74	2.11	0.89	67.78	1.65	0.49
05	75.21	2.17	0.73	66.61	1.41	0.42
06	77.14	2.29	0.71	60.47	1.12	0.41
07	132.64	1.80	0.88	68.88	1.96	0.49
08	74.11	1.85	0.72	67.71	1.73	0.42
09	75.90	1.96	0.70	61.71	1.45	0.42
10	132.64	1.80	0.88	68.88	1.96	0.49
11	74.11	1.85	0.72	67.71	1.73	0.42
12	75.90	1.96	0.70	61.71	1.45	0.42

(Source: Bui H. V and etc., 2025)

Table 10. Water quality data set at Dien Bien Phu Bridge, Nhieu Loc Thi Nghe canal during low tide (Example: for RCP 8.5)

Month	The case of low tide										
	T°C	pH	TSS	NTU	NH_4^{3-}	PO_4^-	DO	COD	BOD_5	Coliform	E. Coli
1	27.7	6.6	20.9	8.3	0.2	0.1	2.6	10.1	5.2	2000	16.4
2	27.9	6.6	31.0	9.7	0.1	0.1	2.5	14.8	5.9	3000	90.0
3	29.3	6.7	23.0	8.5	0.1	0.1	2.3	11.4	5.7	21000	200.0
4	30.4	6.7	17.4	12.3	0.1	0.1	2.5	8.9	3.8	5000	29.0
5	30.9	6.5	16.7	11.6	0.2	0.1	2.1	9.8	3.6	2000	29.0
6	29.9	7.0	16.0	11.7	0.1	0.0	2.4	4.6	4.8	3000	17.1
7	29.6	6.7	14.5	12.3	0.1	0.0	2.4	6.1	3.6	5000	900.0
8	29.6	6.6	16.0	11.3	0.8	0.1	2.7	13.6	5.7	2000	22.0
9	29.6	6.5	26.9	14.4	0.1	0.1	2.3	9.2	4.4	2000	15.0
10	29.3	6.5	13.9	10.9	0.1	0.1	1.5	9.4	4.6	3000	43.0
11	29.1	6.2	16.0	12.3	1.4	0.1	2.3	11.0	4.3	3000	15.0
12	29.0	6.7	16.7	8.8	0.1	0.0	1.9	6.6	3.2	5000	60.0

(Source: Bui H. V and etc., 2025)

b. Assessing the quality of canal water sources according to the VN_WQI index

Among the methods for assessing canal water quality according to regional climate change and sea level rise scenarios such as assessing socio-economic development conditions, management conditions, wastewater collection and treatment, and expectations about the level of surface water quality achieved according to current standards (Cawthron, 2023; Bui H. V et al., 2025), assessment according to the purpose of use of QCVN 08:2023/BTNMT through indicators as equation (1) with scenarios such as Table 3 is often considered and applied.

The results of calculating WQI for the current status and climate change scenarios are calculated according to formula (1) shown in Figure 3 below.

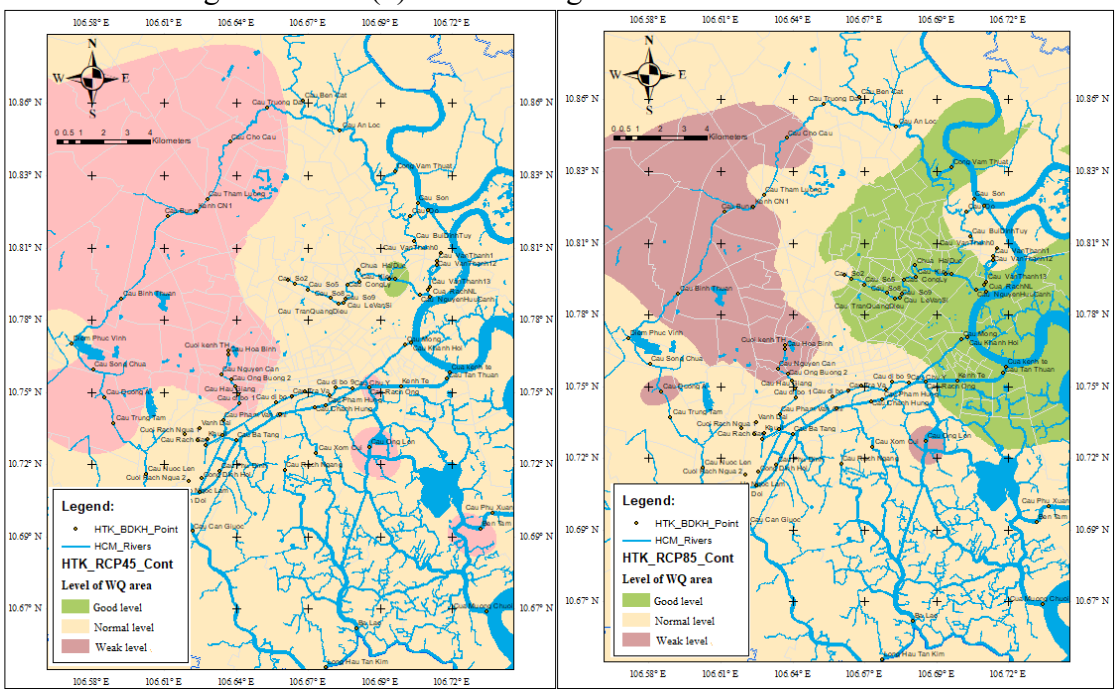

Figure 3. Zoning of water quality levels in inner-city canals of Ho Chi Minh City according to climate change scenarios (RCP4.5 and RCP8.5)

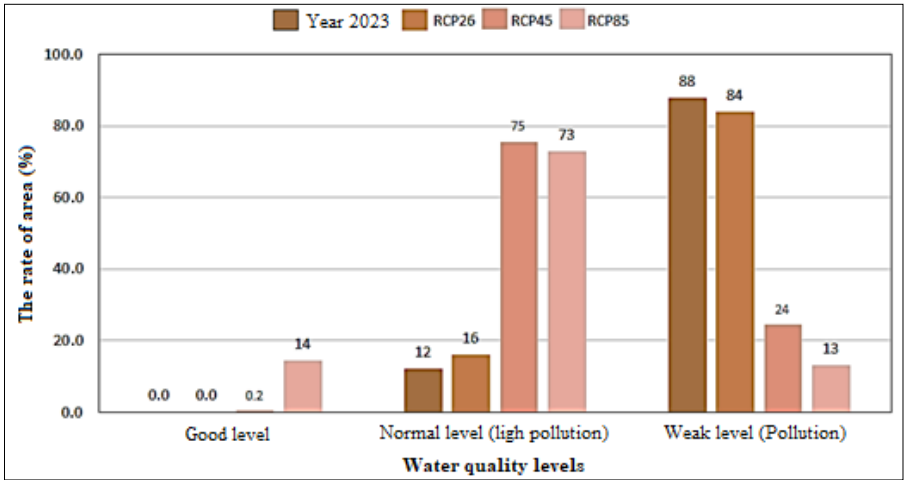

Figure 4. Changes in the area ratio of water quality zones in inner-city canals according to climate change scenarios

Figure 3 shows that the water quality of inner-city canals also depends on different locations such as near the Saigon River (a “clean” water source), the urban center. The Figure also shows the region of water quality zones are also different and tend to differ according to

the level of development.

For example, the area of weak level (canal water is polluted) gradually decreases and concentrates in the central area of the inner-city canal system corresponding to the assessment scenarios (from current (2023) to all climate change scenarios such as RCP2.6, RCP4.5 and RCP8.5 with the respective area ratios of 84%, 24% and 13% per the inner-city canal basin (See Figure 4).

c. Assessment of the self-cleaning capacity of canal water sources

Based on the current status and climate change and sea level rise scenarios, the study simulated the flow regime in the inner-city canal system of Ho Chi Minh City. The results of the flow factor value (flow rate - Q (m^3/s), velocity U (m/s) and water level H (m)) at the water quality monitoring locations on the canals were determined and summarized as Table 8 (Example for RCP8.5).

From the build water quality data set as Table 9 (Example for RCP8.5) and the simulated flow factors (flow rate - Q (m^3/s), velocity U (m/s) and water level H (m)) as Table 8 (Example for RCP8.5), the Streeter-Phelpse equation (3) was applied to determine the oxygen diffusion and depletion coefficients to calculate the oxygen fluctuation rate *(f)* at each monitoring location of each canal. The calculation results are summarized in the figure below (See Figure 5).

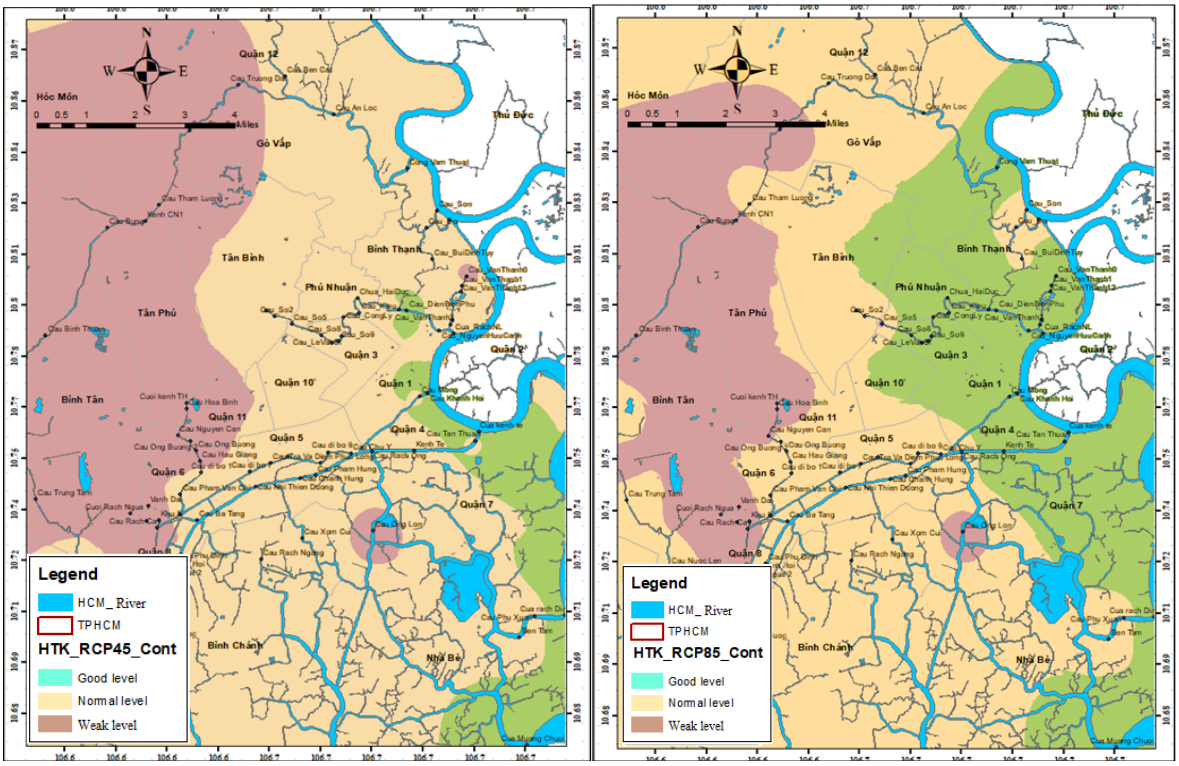

Figure 5. Zoning of self-cleaning capacity levels in inner-city canals of Ho Chi Minh City according to climate change scenarios (RCP4.5 and RCP8.5)

Figure 5 shows that, from the high development scenario (RCP8.5) to the low development scenario (RCP2.6 and RCP4.5), the water surface area of canals with poor/average self-cleaning ability gradually decreases and is concentrated in the central area of the inner-city canal system (where the water is moderately to heavily polluted), the water surface area with good self-cleaning ability gradually expands from the riverside area inwards. The proportion of water surface area with average self-cleaning ability corresponding to the scenarios gradually decreases from 61% to 20% and 4% (See Figure 7). In contrast to the proportion of area with average self-cleaning ability, the proportion of area

with good self-cleaning ability gradually increases in the direction of development from the Saigon River inwards (See Figure 5 and Figure 6).

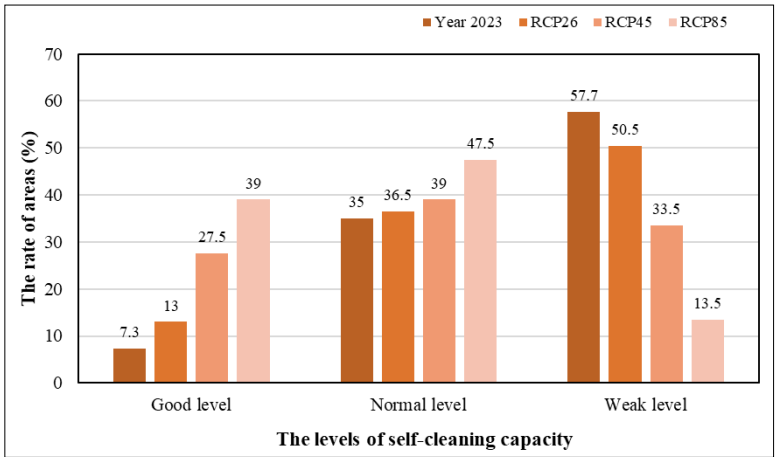

Figure 6. Changes in the area ratio of level's self-cleaning capacity zones in inner-city canals of Ho Chi Minh City according to climate change scenarios

d. Assessment of the level of improvement trends in the quality of inner-city canal water sources in Ho Chi Minh City

From the analysis results on the scope and area ratio of water quality areas and self-cleaning capacity according to the above climate change scenarios, it can be seen that the above factors depend a lot on the location of the area (adjacent to a large river, located in the central area of the inner city) even though there are good conditions for water quality, 100% wastewater collection and treatment and the level of socio-economic development. However, there is a general trend in the level of improvement in both quality and self-cleaning capacity from the current scenario to the highly developed climate change scenario (RCP8.5) (See Figure 7).

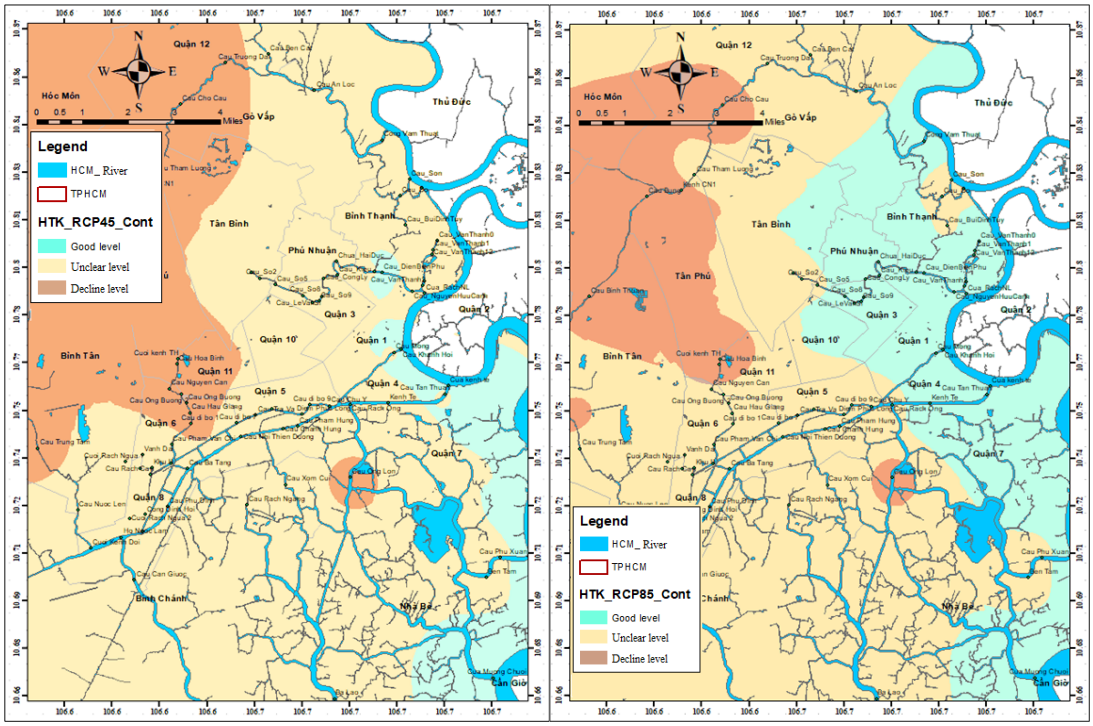

Figure 9. The changes of self-improvement trends in water quality in inner-city canal areas of Ho Chi Minh City according to climate change scenarios (RCP4.5 and RCP8.5)

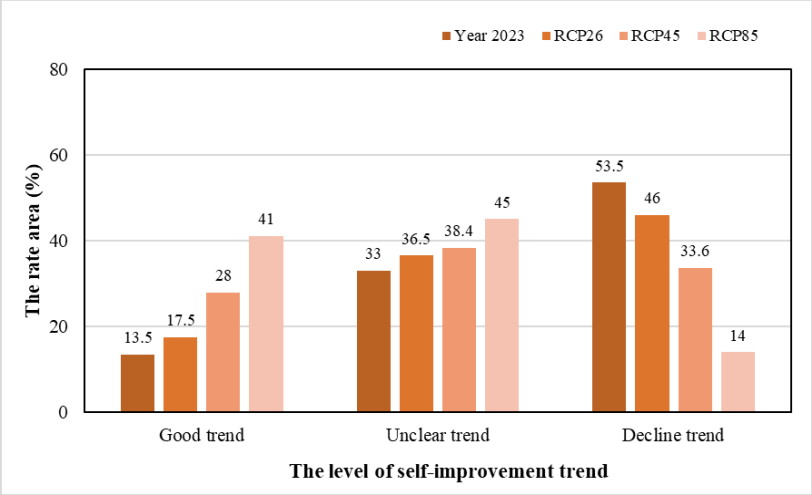

Figure 10. Changes in the proportion of areas with a tendency to improve the quality of inner-city canals in Ho Chi Minh City according to climate change scenarios

Similar to the regional changes in water quality (Figures 5) and self-cleaning capacity (Figures 8), the direction and rate area of change in areas with a tendency to improve water quality increases gradually from the RCP2.6 to RCP8.5 scenarios (See Figure 10). The central inner-city area, including the area between Tham Luong, Ben Cat and Vam Thuat canals and Tan Hoa and Lo Gom canals, is still an area with a tendency to decline in water quality, and is also a heavily polluted area with poor self-cleaning ability, although the conditions for wastewater collection and treatment reach 100% and the composition of substances in the water source meets the standards QCVN 08:2023/BTNMT. The main cause of the problem in this area is the slow flow and very weak tidal influence from the Saigon River.

Conclusion:

The research results have provided very meaningful information for environmental management agencies in Ho Chi Minh City on the main issues that directly and significantly affect the problem of surface water pollution in the inner city area of the City: (1) surface water quality depends greatly on the flow coefficient or the level of influence of the tide from the Saigon River, (2) collection must reach 100% and treatment must meet quality standards for all wastewater sources before discharging into the environment and (3) it is necessary to focus on solutions to improve the flow and environment for canals in the inner city area. The initial research has established a water quality data set with full components for the corresponding climate change scenarios. The research has also provided trend areas to improve surface water quality in Ho Chi Minh City.

Acknowledgements. This article is based on research results funded by Ho Chi Minh City National University (VNU-HCM) under grant number C2023-18-26".

References

IPCC (1995). Climate Change 1994 - Radiative Forcing of Climate Change and An Evaluation of the IPCCIS92 Emission Scenarios. *Reports of Working Groups I and III of the Intergovernmental Panel on Climate Change, forming part of the IPCC Special Report to the*

first session of the Conference of the Parties to the UN Framework Convention on Climate Change. (climate_change_1994.pdf)
Bui H. V., Pham H. V., Le A. H., & Pham H. T. (2025). Assessment of the self-purification capacity of inner-city canal water sources in Ho Chi Minh City, considering the impact of the operation of the tidal sluice system and climate change. *University of Science, VNU-HCM*.
Nguyen D. T. (2005). *Mathematical model for flow and water quality in the canal system. Southern Institute of Water Resources Planning*. Agriculture Publishing House. 234 pages.
Thomann R V and Mueller J A, (1987), Principles of Surface Water Quality Modeling and Control, Harper International Edition, New York
Thomas V B, John A M, Marc G V C and Mani V D (2009). *A Simple Field Technique for Accurate Reaeration Estimates in Aquatic Systems*. Lake and Reservoir Management, 15:3, 185-199, DOI: 10.1080/07438149909354116
Le T., Nguyen H. Q. (2004). *Environment of Dong Nai - Saigon River Basin*, Science and Technology Publishing House, 2004
Pham H. T. M. (2009). Development of Water Quality Indices for Surface Water Quality Evaluation in Vietnam, *Thesis for Ph.D.'s Degree, Korea*.
Tran P. T. N. (2010). *Study on the current pollution status of Ba Bo canal and solutions*, Van Lang Private University, June 2010. (http://docx.vn/tai-lieu/24449/Slide-o-nhiem-o-kenh-Ba-Bo.tailieu).
Cawthron (2023). *Factsheet: Calculating water quality trends in rivers and lakes. Land, Air, Water Aotearoa* (LAWA). https://www.lawa.org.nz/. Published Date 22 SEP 2023.
Bui L. T., Nguyen H. D., Le H. T. (2013). *Determining the self-cleaning capacity of canal and river systems using the Saigon River as a research example*. Journal of Meteorology and Hydrology, February 2013

BIOCOMPOSITE FROM DURIAN RIND AND ORANGE PEEL AS A NATURAL POLYMER MATRIX FOR ADVANCED WOUND DRESSING

Thanyathorn Lohabunditwong[1,*]
[1]The Newton Sixth Form, Thailand
*e-mail: aunging.research@gmail.com

Abstract:
Thailand faces pressing environmental challenges arising from infectious and organic waste, contributing to greenhouse gas emissions and persistent plastic pollution. Valorization of agricultural residues into high-value biomedical products offers a sustainable solution.
In this context, we developed a novel, advanced nonwoven wound dressing fabricated entirely from discarded durian rinds and orange peels, transforming problematic organic waste into a valuable biomedical product. Scanning electron microscopy revealed that the dressing possesses a fibrous texture with nanometer-sized pores, which not only facilitate fluid absorption but also provide a promising platform for future incorporation of nano scale active ingredients designed to accelerate wound healing processes.
In comparative absorbency tests using 0.9% normal saline solution (NSS), the prototype advanced nonwoven wound dressing (1 × 2.5 cm) demonstrated 3.9-fold higher uptake than a commercial reference (Tensoplast®), supporting superior fluid management and effective handling of wound exudate. The material exhibited excellent flexibility, maintaining its shape and integrity after repeated bending, indicating the robustness necessary for practical applications. Furthermore, antioxidant activity measured by the DPPH assay confirmed the retained presence of natural phytochemicals capable of mitigating oxidative stress, a key factor in promoting faster wound healing. Biodegradability evaluation demonstrated that the dressing begins to decompose within 24 hours of soil exposure, illustrating its environmental friendliness and potential to reduce the medical waste burden.
Crucially, this advanced wound dressing functions without synthetic chemicals or additives, offering a safer, more sustainable alternative that supports the healing process through intrinsic bioactivity and biocompatibility. Although these initial results are highly promising and consistent with Sustainable Development Goals (SDGs), further rigorous in vivo studies and clinical evaluations are necessary to validate its therapeutic efficacy and to investigate the benefits of integrating nanoactive compounds for enhanced functionality.
This innovation exemplifies a successful intersection of environmental sustainability and biomedical advancement, presenting strong potential for scalable industrial production and application, while simultaneously addressing pressing environmental and public health challenges.

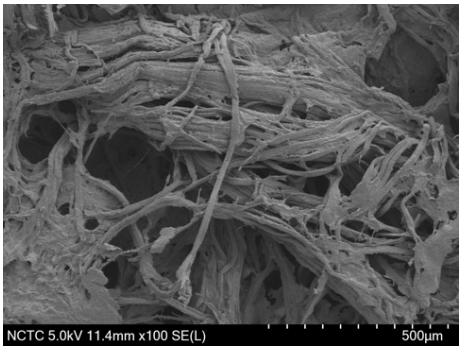

CHARACTERISTICS OF CLAY MINERALS RELATED TO ION-ADSORPTION RARE EARTH ELEMENT DEPOSIT FROM GRANITIC ROCKS IN PHANG NGA AREA, SOUTHERN THAILAND, SE ASIA TIN BELT

A-lin Suksawat[1,2], Thirawat Tukpho[1], Montree Sirimongkonpun[1], Tawatchai Chualaowanich[2], Alongkot Fanka[1,3,*]

[1]Department of Geology, Faculty of Science, Chulalongkorn University, Bangkok 10330, Thailand

[2]Department of Mineral Resources, Rama VI Rd., Ratchathewi, Bangkok 10400, Thailand

[3]Applied Mineral and Petrology Research Unit (AMP RU), Department of Geology, Faculty of Science, Chulalongkorn University, Bangkok 10330, Thailand

*e-mail: alongkot.f@chula.ac.th

Abstract:

Ion-adsorption type Rare Earth Element (REE) deposits are considered environmentally sustainable sources of critical metals for green and high-tech applications. This study investigates the clay mineral phases containing REEs and associated with REE-bearing minerals in weathered granitic rocks, including Lam Pi granite and Kata Beach granite, from the Phang Nga area, southern Thailand, part of the Southeast Asian tin belt. The granitic rocks are characterized by porphyritic texture, together with the main mineral assemblages of quartz, K-feldspar, plagioclase, biotite, muscovite, and accessory minerals including monazite, zircon, apatite, titanite, tourmaline, and cassiterite. Weathered granitic soil profiles are well defined as A, B, and C horizons in the Kata Beach granite and B horizon in the Lam Pi granite. The A horizon is primarily associated with gibbsite. The B horizon with well-reported high REE concentration, especially Lam Pi granitic soil, is enriched in clay minerals, including kaolinite, halloysite, gibbsite, and vermiculite. In the C horizon, clay minerals are mainly kaolinite, halloysite, illite, vermiculite, and gibbsite. Moreover, cerianite, the dominant REE-bearing phase, is observed in the upper part of the B horizon associated with kaolinite and gibbsite. At the same time, rhabdophane is the main phase in the lower part of the B horizon, commonly associated with kaolinite and halloysite. These results indicate that intense tropical weathering of granitic rocks in the Phang Nga area enhances the mobilization of REEs and subsequent adsorption onto clay minerals, leading to the development of ion-adsorption type REE deposits.

CHARACTERISTICS OF RARE EARTH ELEMENT MINERALS RELATED TO LITHIUM-BEARING PEGMATITES IN KANCHANABURI AREA, WESTERN THAILAND: IMPLICATION FOR RARE EARTH ELEMENT POTENTIAL

Chawin Chaywong[1], Ganokwan Saripun[1], A-lin Suksawat[1,2], Montree Sirimongkonpun[1], Thirawat Tukpho[1], Kritsada Sukkamol[1], Sukritta Jesrichai[1], Varinthorn Bovornkitpakorn[1], Alongkot Fanka[1,3]*

[1]Department of Geology, Faculty of Science, Chulalongkorn University, Bangkok, 10330, Thailand

[2]Department of Mineral Resources, Rama VI Rd., Ratchathewi, Bangkok 10400, Thailand

[3]Applied Mineral and Petrology Research Unit (AMP RU), Department of Geology, Faculty of Science, Chulalongkorn University, Bangkok, 10330 Thailand

*e-mail: alongkot.f@chula.ac.th

Abstract:

Rare earth elements (REEs) are crucial resources for modern computer and electronic industries. The REEs occur in numerous types of rocks, including granitic rocks and pegmatites. This study focuses on the characteristics, including petrography and mineral chemistry, of REE minerals in Li-bearing pegmatites in the Kanchanaburi area, Western Thailand, part of the Southeast Asia tin belt. The Li-bearing pegmatites are composed of essential minerals, including plagioclase, K-feldspar with clear perthitic texture, quartz, and lepidolite, along with muscovite, apatite, columbite-tantalite, xenotime, monazite, thorite, and zircon as accessory minerals. The mineral assemblages of columbite-tantalite, xenotime, monazite, and thorite are well-defined as REE-bearing minerals that can serve as the primary source of REEs in the Li-pegmatites in this area. The results indicate that the Li-bearing pegmatite can be the main source of LREEs (La, Ce) from monazite and HREEs (Y, Dy, Er, Yb) from columbite-tantalite, xenotime, and thorite.

COMPARATIVE LITERATURE REVIEW OF LITHIUM-BASED AND ZINC-BASED BATTERIES: TOWARD A SAFER AND MORE SUSTAINABLE ENERGY FUTURE

Suppasate Chunhachai[1,*]
[1]Department of Chemical Technology, Faculty of Science, Chulalongkorn University, Thailand
*e-mail: suppasate.chu@hotmail.com

Abstract:

The global push for reliable and sustainable energy storage technologies has heightened the focus on electrochemical batteries, particularly lithium-ion batteries (LIBs) and zinc-based batteries (ZBs). This literature review analyses and compares both technologies in terms of performance, cost, safety, environmental impact, scalability, and material availability. While lithium-ion batteries dominate the current market owing to their high energy density and cycle life, they also pose significant challenges such as flammable organic electrolytes, limited lithium reserves, high extraction costs, and toxic waste. In contrast, zinc-based batteries, including zinc-ion and zinc-air, offer distinct advantages. Zinc is naturally abundant, cost-effective, and environmentally friendly. Zinc batteries utilize aqueous electrolytes, enhancing their safety and recyclability. Recent studies have focused on overcoming zinc batteries' historical drawbacks, such as dendrite formation and limited rechargeability, through novel electrode materials, ionic conductivity analysis, and molecular dynamics simulations. These simulations have contributed to understanding the structural dynamics and diffusion mechanisms of Zn^{2+} ions in different electrolyte systems, such as zinc triflate and zinc TFSI. Through a comprehensive synthesis of scientific papers, this review supports the growing consensus that zinc-based batteries are a promising alternative for stationary and low-to-medium power applications. The research highlights not only their improved electrochemical performance but also their superior safety profile and environmental sustainability. The conclusion recommends further investment in zinc battery research and development as a pathway toward scalable, cost-effective, and greener energy storage solutions for future global needs.

CONTROLLED RELEASE OF HOLY BASIL ESSENTIAL OIL NANOEMULSION ENCAPSULATED IN GELATIN/CARBOXYMETHYL CELLULOSE HYDROGEL FOR WOUND CARE

Shehbaz AMEER[1], Pranut POTIYARAJ[1], Tu Minh TRAN VO[1]*
[1]Department of Materials Science, Faculty of Science, Chulalongkorn University, Bangkok 10330, Thailand
Email: minhtu.t@chula.ac.th, Phone: +66 82 924 1525

Abstract:

Controlled drug release is a key challenge in drug delivery systems (DDSs). Hydrogels, such as gelatin and carboxymethyl cellulose (CMC), are used in DDSs for their biocompatibility. Holy basil essential oil (HBEO) is a therapeutic agent known for its antioxidant, anti-inflammatory, and wound healing properties. However, its clinical use is limited by poor aqueous solubility, volatility, and instability. Nanoemulsion (NE) is an effective strategy to overcome these limitations. In this study, 1% HBEO in 0.5% polyvinyl alcohol (PVA) aqueous solution formulation yielded nanosized droplets (182 ± 3 nm, PDI = 0.286) and showed sustained release, with 92% drug release over 30 h, compared to the rapid release for 1% HBEO in water. To further enhance stability and controlled delivery, the HBEO nanoemulsion (HBEONE) was incorporated into a gelatin/CMC hydrogel matrix (3:1), crosslinked using glutaraldehyde (GA). The resulting hydrogel exhibited a swelling ratio of 8 (g/g) and HBEO loading capacity of 67.5%. MTT assay revealed L929 fibroblast viability with HBEO/gelatin/CMC hydrogel, which was observed with less cytotoxicity compared to the natural release of HBEONE without a hydrogel matrix. These results demonstrate the HBEONE-loaded gelatin/CMC hydrogel as a robust platform for controlled delivery and wound care applications.

Introduction

Achieving controlled release of therapeutic agents remains a major challenge in conventional drug delivery. Traditional administration methods often cause large fluctuations in plasma drug concentrations, resulting in reduced therapeutic efficacy and an increased risk of side effects due to peak–trough variations. To address these limitations, drug delivery systems (DDSs) have been developed to transport drugs more precisely within the body, enhancing their stability, bioavailability, and therapeutic efficacy[1], [2]. On the other hand, DDSs aim to maintain consistent drug levels over time and deliver therapeutic agents to targeted sites. Among various therapeutic agents, natural bioactive agents such as essential oils (EOs) have gained significant attention due to their multifaceted pharmacological properties and biocompatibility [3]. EOs are volatile, plant- derived mixtures composed of terpenes, phenolics, and other secondary metabolites, and their incorporation into DDSs can enhance their stability, bioavailability, and targeted therapeutic action. One notable example is holy basil essential oil (HBEO), extracted from *Ocimum tenuiflorum* (Tulsi), a medicinal plant traditionally used widely [4], [5]. Due to such broad pharmacological potential, HBEO is considered a promising natural therapeutic agent[6], [7]. However, its practical use is limited due to inherent challenges like volatility, poor aqueous

solubility, oxidation, degradation and potential risk at high concentrations [8]. Therefore, a formulation capable of protecting EOs from degradation factors is necessary. To address the drawbacks of HBEO, including poor solubility, instability, and low bioavailability, nanoemulsion technology offers an effective delivery strategy. These formulations are biphasic systems consisting of an aqueous continuous phase and an oil-based dispersed phase, stabilized by surfactants to ensure droplet uniformity and prevent coalescence [9]. Modern preparation techniques such as ultrasonic emulsification [10], high-pressure homogenization [11], and microfluidization [12] are commonly employed to reduce droplet size and achieve a stable nanoscale dispersion. Among various nanoemulsion preparation methods, ultrasonic probe emulsification is considered one of the most efficient techniques for nanoemulsion fabrication[13], [14]. In previous studies, nanoemulsions of EOs from cananga odorata were prepared by ultrasonic emulsification for enhanced herbicidal potential [15], similarly cinnamon and thyme essential oil nanoemulsions were prepared by the same method to improve their antifungal [16] and antibacterial [17]activities, respectively. In nanoemulsion formulation, the aqueous component is typically referred to as the watery phase, which was designed not only as pure water but also as a diluted polymer solution, a strategy intended to reduce the volatility and evaporation of EOs components during emulsification[9], [10], [11], [12], [13], [14], [15], [16], [17]. Recent studies have demonstrated the effective use of water-soluble polymers such as polyethylene glycol (PEG)[18] and polyvinylpyrrolidone (PVP) [19] in essential oil-based nanoemulsion systems to enhance their performance and therapeutic potential. In addition to PEG and PVP, polyvinyl alcohol (PVA) is also particularly notable for its excellent film-forming ability[20], emulsification properties, and capacity to stabilize dispersed oil droplets[21]. There remains limited research on the use of aqueous solutions of PVA for the development of EOs nanoemulsions. Thus, present study aims to investigate the feasibility of using PVA as a continuous watery phase to produce nanoemulsion of HBEO using an ultrasonic probe. But nanoemulsion alone face challenges like fast evaporation, instability and short retention time on the targeted sites. Therefore, to overcome this limitation mostly nanoemulsions are incorporated into suitable carrier that can hold the nanoemulsion to the targeted site. Hydrogels are the ideal carrier due to their high-water content and biocompatibility [22]. Gelatin derived from the collagen, it offers excellent biocompatibility, biodegradability and mechanical strength, which make it suitable for biomedical carriers[23]. On the other hand, CMC is a derivative of cellulose, which is a white color water soluble polymer and have been used in pharmaceuticals as a thickener and stabilizer. CMC provides flexibility and enhances the swelling capacity to the hydrogel[24]. The combination of gelatin/CMC results in stable, elastic and highly absorbent hydrogel that is capable of long, slow, and extended release of the loaded therapeutic agents [25], [26], [27]. To increase its further structural integrity, this hydrogel chemically crosslinking approach was selected instead of physical crosslinking because physical crosslinking often is reversible and exhibits poor stability. Glutaraldehyde (GA) crosslinker was used as the chemical crosslinker, it reacts with the amino acid group of gelatin and hydroxyl groups of CMC, forming a covalent bond. For example, Bigi et al. reported that increasing GA concentration from 0.05% to above 1 wt% significantly enhanced the Young's modulus and reduced the swelling ratio of gelatin films, confirming that higher crosslink density leads to a more compact and mechanically resilient network[28]. However, despite the extensive use of gelatin-based scaffolds, there remains limited research on its application in hybrid

gelatin/CMC hydrogels designed to encapsulate and control the release of essential oil nanoemulsions. Therefore, this study aims to develop and evaluate a gelatin/CMC hydrogel loaded with HBEONE for enhanced stability, prolonged release, and sustained therapeutic efficacy.

1. Experimental

1.1. Materials

Gelatin with a Bloom strength of 200, pharmaceutical grade, was obtained from Spectrum Chemical Mfg. Corp. Carboxymethyl cellulose (CMC), with a degree of substitution of 0.7, was purchased from Merck Ltd. Thailand). Glutaraldehyde (GA) 25% and polyvinyl alcohol (PVA) with M_w of 115,000 Da and a hydrolysis level of 98–99%, were supplied by Loba Chemie Ltd. Holy Basil Essential Oil (HBEO) was sourced from TCFF Ltd, Thailand. Other reagents and chemicals were of analytical grade.

1.2. Preparation of HBEO Nanoemulsion (HBEONE)

HBEO Nanoemulsions (HBEONE) were prepared following a previously reported method with slight modifications[15]. Initially, HBEO was mixed with Tween 80 in a 1:1 (w/w) ratio and magnetically stirred for 15 minutes to form a coarse emulsion. The coarse emulsion mixture was subjected to the aqueous (watery) phase consisted of polyvinyl alcohol (PVA) solutions at varying concentrations of 0%, 0.5%, 1%, and 2% (w/w), using an ultrasonic probe to obtain a fine and stable nanoemulsion. During sonication, the beaker was placed in an ice bath to dissipate the heat generated by the ultrasonic process.

1.3. Fabrication of HBEONE-entrapped gelatin/CMC hydrogels

The hydrogels were fabricated using a previously reported method with some modifications [26], as summarized in Figure 1. A 10 %(w/w) gelatin solution was prepared in deionized (DI) water at 60 °C under gentle stirring. Separately, a 1 % CMC solution was prepared at room temperature. Both solutions were then mixed at 50 °C for 30 minutes under constant stirring to obtain gelatin/CMC precursor blends in different weight ratios, as shown in Table 1. Glutaraldehyde (GA) at 0%, 0.5%, 1.0%, and 2.0% (w/w) of the total solution was used as a crosslinking agent, and the mixture was stirred thoroughly to ensure homogeneous dispersion. The resulting solution was cast into a Teflon mold and allowed to set at room temperature to form the hydrogel. After that, the crosslinked hydrogels were washed with DI water and 70 % ethanol to remove unreacted crosslinker GA. Next, gelatin/CMC hydrogels were soaked in 1% (w/w) HBEONE to fully absorb. HBEONE loaded-hydrogels were rinsed with DI water 3 times, and subsequently blotted with tissue paper to remove surface water [20], [26].

Table 1 Different formulations of gelatin/CMC hydrogel

Samples	Gelatin/CMC ratio	GA (% w/w)
S1	1/0	1
S2	3/1	1
S3	1/1	1
S4	0/1	1
S2-1	3/1	0
S2-2	3/1	0.5
S2-3	3/1	2

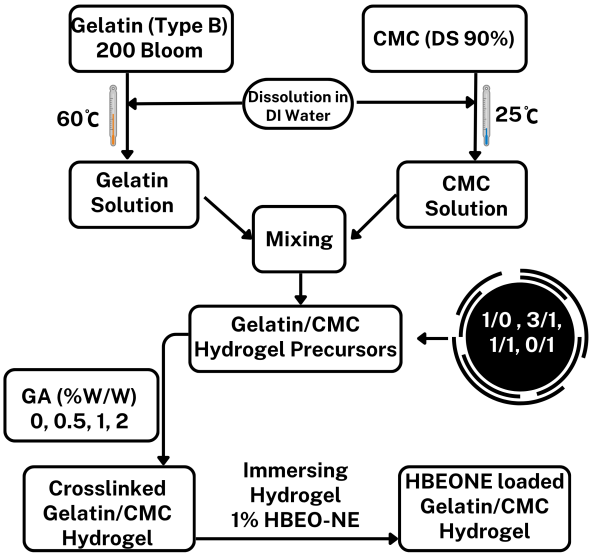

Figure 1 Schematic diagram of the fabrication of HBEONE-crosslinked gelatin/CMC hydrogel

1.4. Characterization of HBEONE and gelatin/CMC hydrogels loading HBEONE

1.4.1. HBEONE droplet size and stability

The droplet size distribution and polydispersity index (PDI) of the HBEO-NE were determined using a dynamic light scattering (DLS) instrument (Zetasizer, Malvern Panalytical, UK) to evaluate stability as well as uniformity of HBEONE . Samples were diluted with DI water in a 1:9 ratio to avoid the multiple scattering effect. 2 mL diluted sample was transferred into a cuvette for analysis. Measurements were conducted at 25 °C and a fixed scattering angle of 165°. Each sample was analyzed in triplicate, and the average droplet size and PDI were recorded.

The stability of the HBEONE was assessed by centrifuging 10 mL samples at 10,000 rpm for 20

minutes (25 °C). Afterward, samples were stored in sealed bottles at 4 °C and 25 °C for 8 weeks.

1.4.2. Characterization of gelatin/CMC hydrogels

Chemical structure confirmation

Attenuated Total Reflectance–Fourier Transform Infrared (ATR-FTIR) spectroscopy was performed to identify the functional groups and the interactions of gelatin, CMC, HBEONE, and HBEONE-loaded gelatin/CMC hydrogels. 32 scans per sample over the spectral range of 4000–400 cm^{-1} were recorded with a resolution of 2 cm^{-1}[15].

Thermal stability of gelatin/CMC hydrogels

Differential Scanning Calorimetry (DSC) was performed to check the stability, thermal transition and the effect of the incorporation of HBEO-NE in gelatin/CMC hydrogels systems. The analysis was performed over a temperature range of 0–210 °C at a heating rate of 10 °C/min under a nitrogen atmosphere (flow rate: 20 mL/min).

Morphology observation

The cross-sectional morphology of pure gelatin, gelatin/CMC composite, and HBEONE-loaded CMC/gelatin hydrogel was investigated using scanning electron microscopy (SEM, JEOL JEM-6335F). Before imaging, samples were lyophilized to preserve their internal structural details. These dried samples were coated with a thin layer of gold using a sputter coater to increase conductivity[29]. SEM images were captured to evaluate the interconnectivity within the hydrogel matrix.

Swelling Degree

The swelling behavior of gelatin, CMC, and combined gelatin/CMC hydrogels was evaluated to check the water absorption capacity. The swelling tests were conducted in phosphate-buffered saline (PBS) at 35 °C to simulate the physiological conditions[29]. The hydrogels were immersed in PBS until equilibrium, and the swelling degree was calculated using the following equation:

$$\text{Swelling degree} = \frac{W_s - W_d}{W_d} \quad (1)$$

where W_s is the weight of the swollen material, and W_d is the weight of the dry material.

Antioxidant test

The antioxidant potential of HBEONE-loaded gelatin/CMC hydrogel was evaluated using the DPPH (2,2-diphenyl-1-picrylhydrazyl) radical scavenging assay[29]. A 0.1 mM DPPH solution was prepared in ethanol. HBEONE-loaded hydrogel was immersed in the PBS solution at pH 7, and 3 ml sample was taken out after intervals. Each sample was mixed with DPPH solution and incubated in the dark for 30 minutes. Absorbance was measured at 517 nm using a UV-Vis spectrophotometer. Ethanol served as the blank condition, and the DPPH solution was used as the control. The DPPH radical scavenging activity was calculated using the following equation:

$$\text{Scavenging Activity (\%)} = \left(\frac{A_{Control} - A_{Sample}}{A_{Control}}\right) \times 100 \quad (2)$$

where $A_{Control}$ is the absorbance of the DPPH solution without the sample, and A_{Sample} is the absorbance after the sample was added. The antioxidant activities of the HBEONE-loaded and blank hydrogels were compared to assess the retention of bioactivity of HBEO after encapsulation.

HBEONE entrapment efficiency and in vitro release study

HBEO entrapment efficiency was evaluated by the previously reported method with modifications[30]. HBEONE-loaded gelatin/CMC hydrogel was cut into pieces of 0.6 cm × 3 cm and 1.95 mm thickness and placed into a UV-Vis cuvette, and the absorbance was measured at 278 nm. The absorbance was compared against a pre-established calibration curve to determine the amount of HBEO (ppm) entrapped within the hydrogel matrix. In Figure 2, the presence of HBEO was confirmed by measuring the intensity of its characteristic absorption peak at 278 nm in the UV–Vis spectrum. The absorption spectrum of the HBEO-NE–loaded hydrogel exhibited a prominent peak at 278 nm, indicating the successful incorporation of HBEO within the hydrogel matrix. The release behavior of HBEO from the HBEONE-loaded gelatin/CMC hydrogels was conducted in 100 mL of PBS (pH 7.4) maintained at 37.0 ± 1 °C to mimic body temperature.

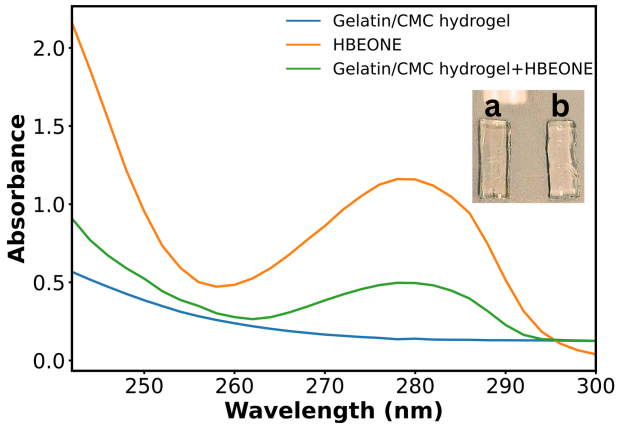

Figure 2 UV–vis spectra of the gelatin/CMC hydrogel and gelatin/CMC/HBEONE hydrogel with 2.1 and 1.95 mm thickness, respectively, and HBEONE at 166.7 ppm; the appearance of gelatin/CMC hydrogels (a) without HBEONE and (b) with HBEONE (the insert picture).

At intervals, 3 mL samples were withdrawn and replaced with fresh PBS to maintain constant volume. The amount of HBEO released was quantified by UV–Vis spectrophotometry at 278 nm. All release experiments were performed in triplicate (n = 3), and results are reported as mean ± standard deviation. The initial 60% release data were fitted to the following kinetic models to elucidate the mechanism of HBEO release from the hydrogel matrix [31]:

Korsmeyer–Peppas model

$$\left(\frac{M_t}{M_\infty}\right) = K\, t^n \quad (3)$$

where M_t is the amount of HBEO released at time t, M_∞ is the total release at equilibrium, K is the release rate constant, and n is the release exponent (Fickian if $n \leq 0.45$, non-Fickian if $0.45 < n < 1$).

Zero-order model

$$C_t/C_0 = k_0 t \quad (4)$$

First-order model

$$\log C_t = \log C_0 - \frac{k_1 t}{2.303} \quad (5)$$

Higuchi model

$$C_t/C_0 = k_h\, t^{0.5} \quad (6)$$

where C_t represents the amount of drug released at time t, C_0 denotes the initial drug concentration within the hydrogel, k_0, k_1, and k_h correspond to the respective release rate constants, and n is the release exponent that characterizes the mechanism of drug release.

1.4.3. Cytotoxicity evaluation using MTT Assay

The cytotoxicity of HBEONE and HBEONE-loaded gelatin/CMC hydrogel was checked using MTT (3-(4,5-dimethylthiazol-2-yl)-2,5-diphenyltetrazolium bromide) assay. 100 µL of L929 fibroblast cell suspension solution was seeded into 96-well plates at a density of 5×10^4 cells/mL and incubated at 37 °C in a humidified atmosphere containing 5% CO_2 for 24 h to allow cell attachment. After incubation, the culture medium was replaced with fresh medium containing the prepared hydrogel extracts, and cells were further incubated for 48 h. Subsequently, MTT solution (0.5 mg/mL) was added to each well, and the plates were incubated for an additional 4 h to allow the formation of formazan crystals. The supernatant was then carefully removed, and 100 µL of DMSO was added to each well to dissolve the formazan crystals completely. The absorbance was measured at 570 nm using a microplate reader, and cell viability (%) was calculated using the following equation:

$$\text{Cell Viability} = \left(\frac{A_{\text{Sample}}}{A_{\text{Control}}}\right) \times 100\ (\%) \quad (7)$$

Where $A_{Control}$ is the absorbance of the untreated conditions without samples. A_{Sample} is the absorbance of the treated sample.

A one-way analysis of variance (ANOVA) with Tukey's test was used to determine the statistical significance among groups. The level of significance was set at $p^* < 0.05$, and all analyses were conducted using SPSS version 30.0.0 software. All data are presented as the mean ± standard deviation (SD) of three independent replicates.

2. Results and Discussion

2.1. Impact of emulsification conditions on nanoemulsion characteristics

As shown in Table 2 and Figure 3, the size and stability of HBEONE were notably affected by varying PVA concentrations. When formulated in DI water without PVA, the NE exhibited the smallest droplet size of 124 nm with a moderate PDI of 0.269. The incorporation of PVA significantly influenced both droplet size and dispersion stability. At 0.5% PVA, the droplet size increased to 182 nm with a PDI of 0.286, while further increasing the concentration to 1% PVA resulted in improved homogeneity (PDI = 0.242) but a larger droplet size of 244 nm, which slightly exceeded the typical nanoemulsion range (10–200 nm). At 2% PVA, the droplet size further increased to 394 nm with a higher PDI of 0.302, likely due to excessive polymer content promoting droplet aggregation in the aqueous phase. Furthermore, the HBEO release was achieved with approximately 92% cumulative release at equilibrium when the nanoemulsion was prepared using a 0.5% PVA aqueous phase.

Table 2 Effect of PVA concentrations on the size, stability, and release of HBEO from HBEONE

Oil Phase	Watery Phase (PVA solution)	Droplet Size (nm)	Polydispersity index (PDI)	Release of HBEO at Equilibrium (%)
1 %	0%	124±3	0.269±0.05	85±3
	0.5%	182±3	0.286±0.05	92±3
	1%	244±3	0.242±0.05	88±3
	2%	394±3	0.302±0.05	85±3

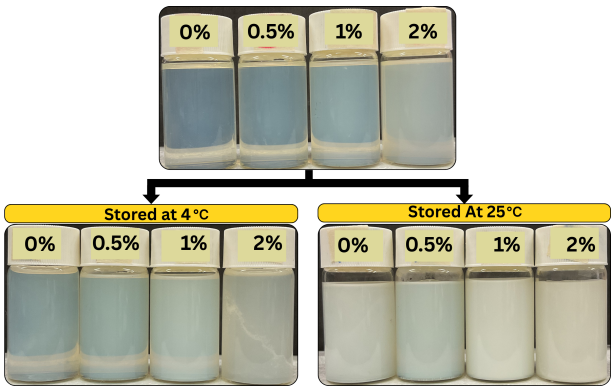

Figure 3 Stability comparison of HBEONE at 4°C and 25°C after 8 weeks of storage.

2.2. Characterization of HBEONE entrapped gelatin/CMC hydrogels

FTIR analysis of the composite hydrogels

FTIR analysis was performed to investigate the interactions between gelatin, CMC, and the crosslinked gelatin/CMC hydrogel, both with and without the incorporation of HBEONE (Figure 4). The spectrum of neat gelatin displays an absorption band at around 3267 cm^{-1}, corresponding to the stretching vibration of –OH and –NH groups involved in hydrogen bonding. The amide I band appears at 1629 cm^{-1}, attributed to C=O stretching vibration, confirming the characteristic protein backbone. In the spectrum of pure CMC, a strong –OH stretching band is observed at 3350 cm^{-1}. When gelatin and CMC were blended (S2-1), the –OH/–NH stretching peak was at 3280 cm^{-1} and it was slightly shifted to a lower wavenumber, indicating the formation of hydrogen bonding between the hydroxyl groups of CMC and the amide groups of gelatin by increasing the crosslinker GA to 2 %. As highlighted in the yellow-shaded region, the significant absorption features appeared around 2952 cm^{-1}, which are attributed to the C–H stretching of aliphatic constituents of HBEO, emphasizing the successful incorporation of HBEONE into the hydrogel matrix. However, these peaks exhibited a slight reduction in intensity at 2% GA compared to 1% GA, suggesting a lower HBEONE entrapment due to the denser and more compact crosslinked

network.

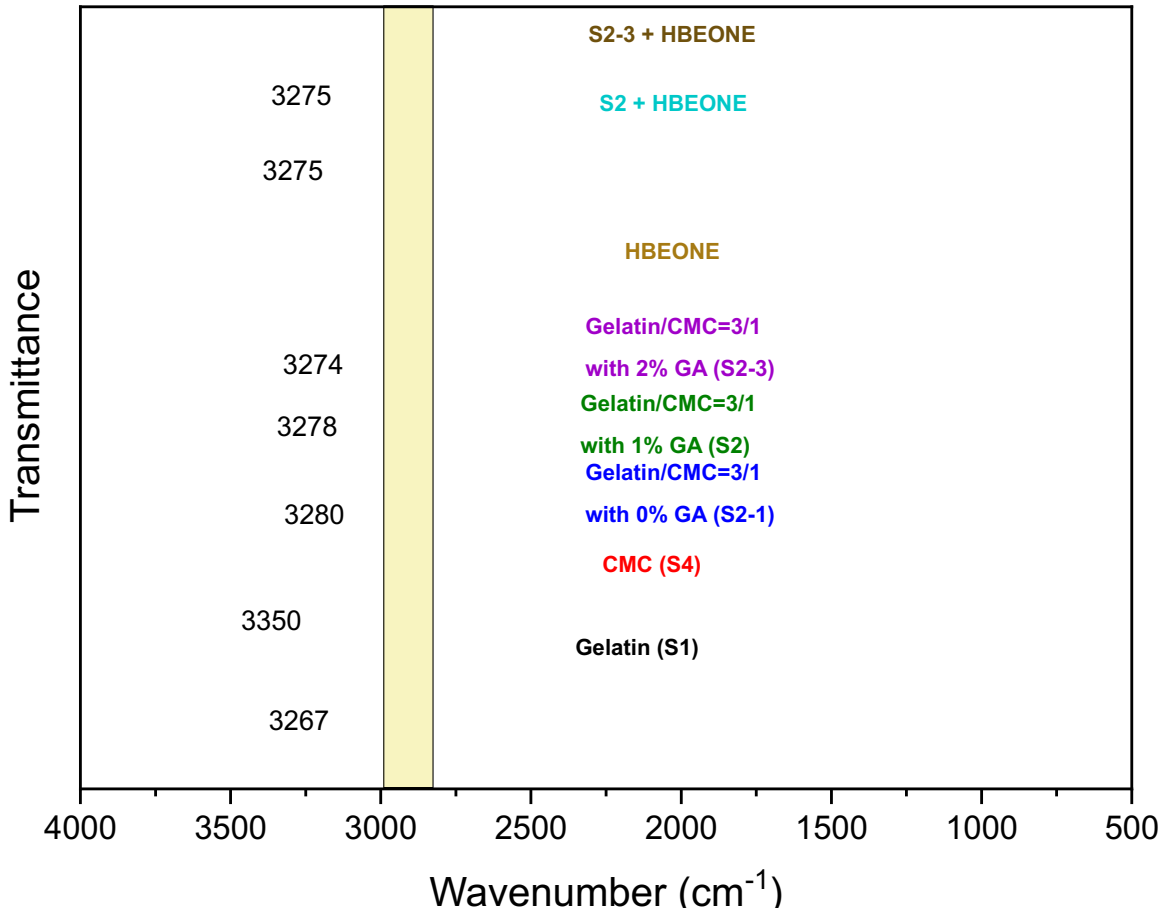

Figure 4 FTIR spectra of gelatin/CMC hydrogels showing the effect of the incorporation of HBEO

Thermal properties of gelatin/CMC hydrogel

DSC thermograms of the gelatin/CMC hydrogels with varying crosslinker GA concentrations and with/without HBEO nanoemulsion incorporation are presented in Figure 5. The pristine gelatin/CMC hydrogel (S2-1, 0% GA) exhibited 1st endothermic transition around 110–120 °C, corresponding to the helix–coil transition of gelatin and bound water evaporation. The second endothermic peak appeared at 165°C, corresponding to the melting temperature (T_m) of gelatin/CMC hydrogel. With increasing GA concentration from 0% to 2%, a slight shift of the T_m toward higher values was observed, indicating the improvement in thermal stability. However, upon incorporation of HBEO nanoemulsion into the gelatin/CMC (S2) matrix crosslinked with 1% GA, a remarkable decrease in the Tm was detected. This reduction suggests that the embedded nanoemulsion droplets disrupted the polymer–polymer hydrogen bonding and partially interfered with the crosslinking network, leading to a more flexible structure and reduced thermal resistance

[32].

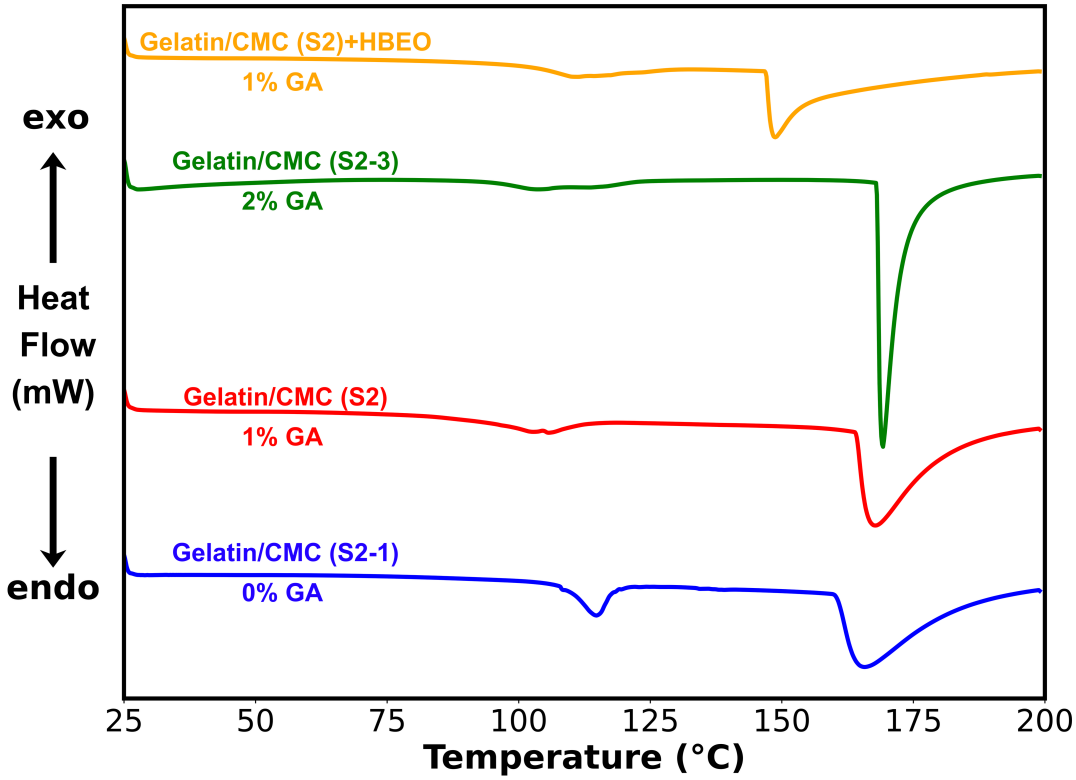

Figure 5 DSC thermogram of gelatin/CMC hydrogels varying concentrations of GA

Morphological observations

The cross-sectional morphology of the hydrogels was examined by scanning electron microscopy (SEM), as shown in Figure 6. The neat gelatin (S1) hydrogel exhibited a relatively smooth and less porous structure. Upon incorporation of CMC into the hydrogel matrix (sample S2), the morphology became more porous, reflecting improved water absorption and interconnectivity between the polymer chains. With a further increase in CMC content (sample S3), SEM images revealed a looser and more open network structure, suggesting enhanced flexibility and swelling capacity due to reduced intermolecular interactions within the hydrogel matrix. Moreover, the cross-sectional images showed that increasing the GA concentration from 1% to 2% produced a denser and more compact internal structure, consistent with higher crosslinking density and reduced pore volume [33]. Following the incorporation of HBEONE into the hydrogel matrix, the morphology became irregular, attributed to the distribution of nanoemulsion droplets within the polymer network.

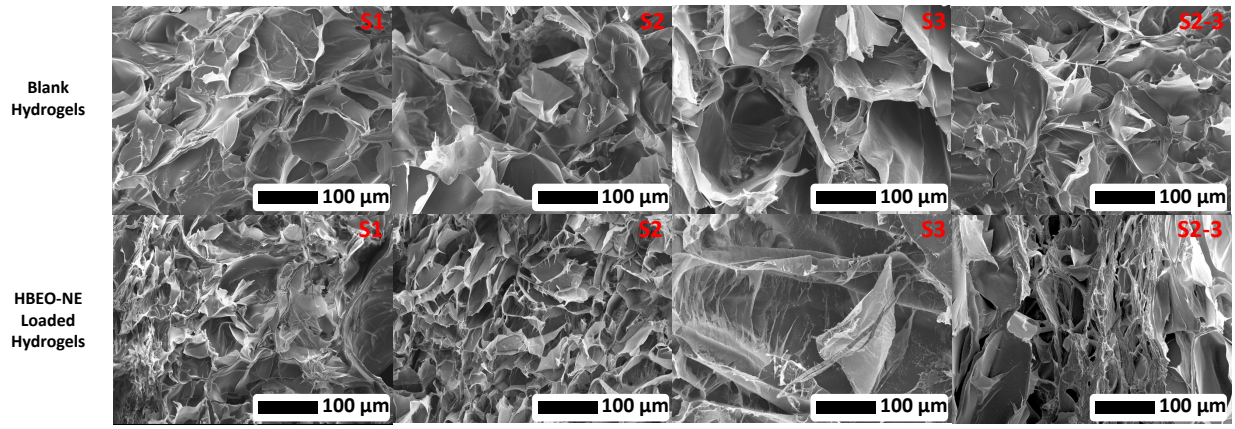

Figure 6 Cross-sectional morphology of hydrogels (S1)gelatin, (S2) gelatin/CMC(3/1) 1% GA, (S3) gelatin/CMC(1/1) 1% GA, (S2-3) gelatin/CMC (3/1) 2% GA

Swelling behavior of gelatin/CMC hydrogels

The swelling behavior of the Gelatin/CMC hydrogel studied over a 24-hour duration was shown in Figure 7a**.** All samples swelled quickly in the first 4 hours, then slowed down and eventually reached equilibrium. The swelling depended on the hydrogel composition. Pure gelatin (S1) with 1% glutaraldehyde (GA) showed the lowest swelling ratio. Adding carboxymethyl cellulose (CMC) at a 1:1 ratio (S3), the swelling degree was enhanced 2.5 times compared to neat gelatin (S1). This result indicates the hydrophilic CMC showed more water absorption [20]. On the other hand, increasing crosslinker GA from 1% to 2 % reduced the swelling ratios of gelatin/CMC (3/1) from 8(g/g) to 6.5(g/g), respectively. Furthermore, the swelling behavior of HBEONE-loaded hydrogels showed a moderate decrease compared to unloaded hydrogels, which can be attributed to the partial occupation of the hydrogel pores by HBEONE droplets, thereby restricting water absorption and swelling.

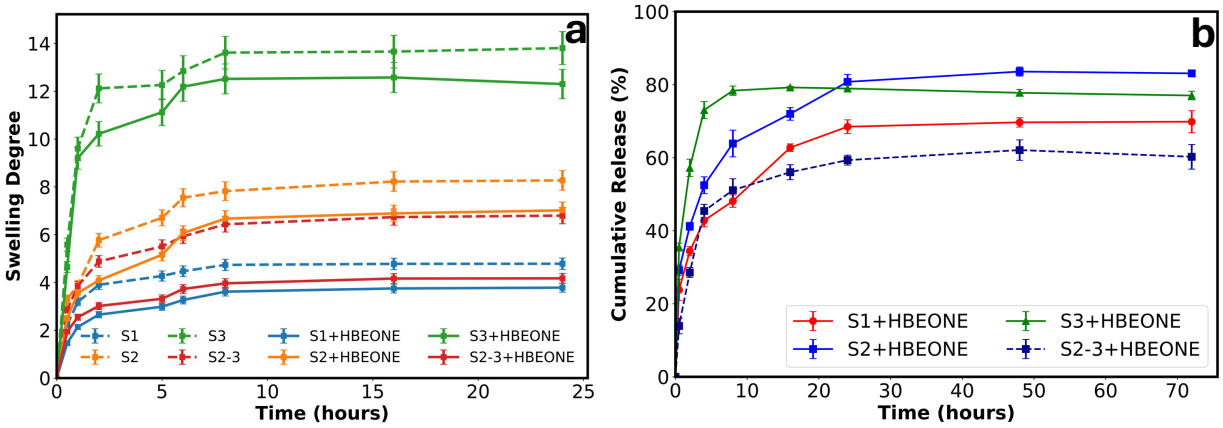

Figure 7 (a) Swelling behavior of different hydrogels and **(b)** in vitro HBEO release study of hydrogels

In vitro HBEO release study from composite hydrogels

The in vitro release profiles of HBEONE-entrapped gelatin/CMC hydrogel formulations were shown in Figure 7b**.** Among all hydrogels, the S3 formulation with a higher CMC amount showed the quick release (80% release in first 10 hours) . In contrast, S1, S2, and S2-3 displayed lower release of the HBEO. Since S3 contains the highest CMC content which enhanced the porosity and makes it easy to uptake the HBEONE and easier diffusion as compared to the neat gelatin. Furthermore, the hydrogel prepared with 2% crosslinker GA (S2-3) demonstrated the lowest swelling and reduced uptake of the HBEONE compared to the 1% crosslinker formulation, thus it had a slow release of HBEO. variation in HBEONE loading are shown in Table 3.

To understand the release mechanism of these hydrogel systems, the release profiles of the resulting hydrogels were fitted to several kinetic models, as summarized in Table 4. The correlation coefficient (R^2) values indicate that Korsmeyer–Peppas models best fit the release data, suggesting that the drug release follows diffusion-controlled and Fickian mechanisms. As a result, these findings revealed that the HBEO release from gelatin and gelatin/CMC hydrogels was primarily governed by a diffusion mechanism based on Korsmeyer–Peppas with $n < 0.45$ [26].

Table 3 gelatin/CMC hydrogels and their HBEONE loading capacities

Sample	Gelatin/CMC Ratio	GA (%)	HBEONE Loading (%)
S1	1/0	1	58
S2	3/1	1	67.5
S3	1/1	1	72.7
S2-3	3/1	2	55.4

Table 4 Fitting parameters of different kinetic models for HBEO release from gelatin/CMC hydrogels entrapping HBEONE

Sample	Zero-order	First-order	Higuchi	Korsmeyer–Peppas		
	r^2	r^2	r^2	k_{KP}	n	r^2
S1	0.61	0.68	0.82	0.30	0.230	0.96
S2	0.60	0.72	0.81	0.37	0.222	0.95
S3	0.23	0.24	0.42	0.49	0.141	0.71
S2-3	0.45	0.52	0.67	0.23	0.284	0.84

Antioxidant activity of HBEONE-loaded hydrogel

As shown in Figure 8, the HBEONE-loaded hydrogel exhibited a markedly higher radical-scavenging activity than the blank hydrogel throughout the 72 hours. The antioxidant inhibition increased steadily from about 20% at 1 h to nearly 60% at 24 h, maintaining that level up to 72 h, indicating a sustained release of HBEO's phenolic constituents. In contrast, the blank hydrogel showed negligible activity (<5%), confirming that the antioxidant effect arose solely from the encapsulated HBEO.

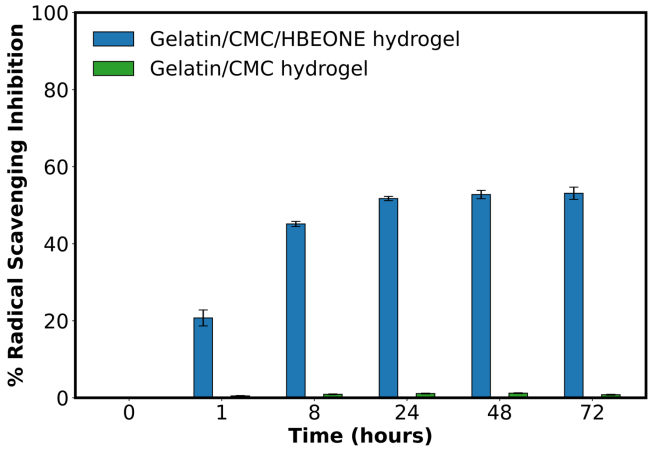

Figure 8 Comparison of antioxidant activity of HBEONE-entrapped gelatin/CMC hydrogel and the gelatin/CMC hydrogel

2.2.1. Cytotoxicity test (MTT assay)

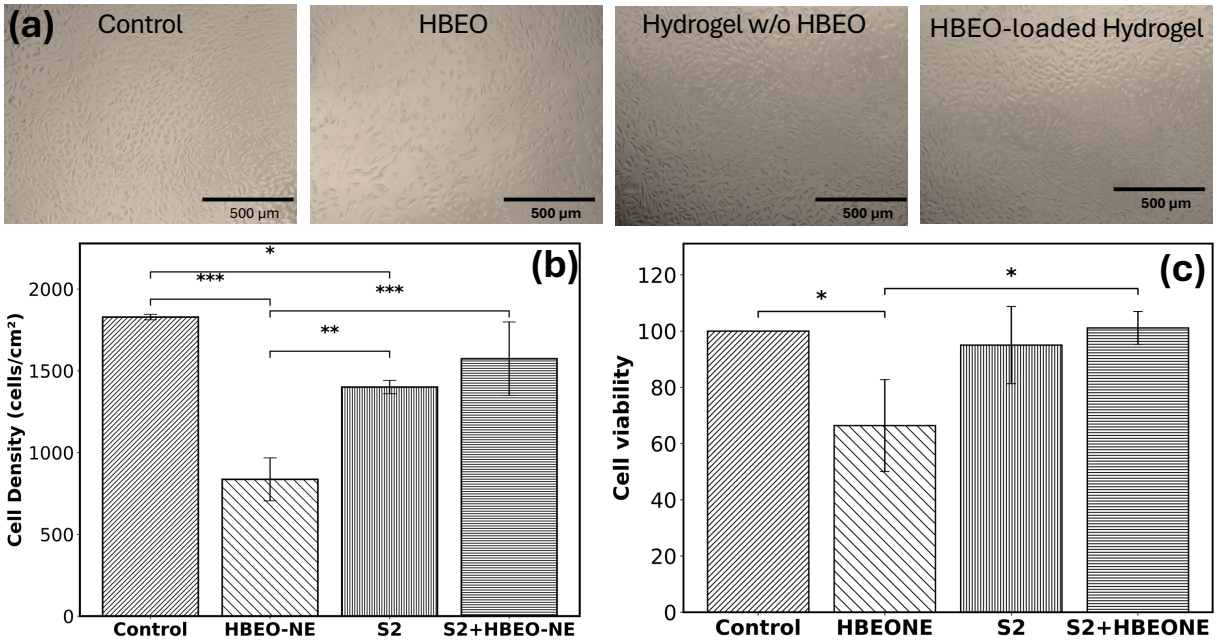

Figure 9 (a) The microscopy images, **(b)** % cell density, and **(c)** cell viability of control, HBEO, hydrogel S2, and S2+HBEONE sample. Data are presented as mean ± SD (n = 3). Statistical analysis was performed by one-way ANOVA followed by Tukey's post-hoc test, with the criterion for statistical significance as follows: * significant at $p < 0.05$, ** significant at $p < 0.01$, and *** significant at $p < 0.001$

The cytotoxicity of HBEO, gelatin/CMC hydrogel, and HBEONE-loaded gelatin/CMC hydrogel was assessed using the MTT assay, as shown in Figure 9. Microscopic observations revealed that the hydrogel-treated groups supported uniform cell distribution and morphology, indicating good cell attachment and proliferation comparable to the control group. In contrast, cells treated with pure HBEO exhibited a marked decrease in cell number, showing approximately 66.4% viability relative to the control. This reduction may be attributed to the burst release of HBEO, leading to temporary cytotoxic effects and possible apoptosis. These results confirm that encapsulating HBEO-NE within the gelatin/CMC hydrogel effectively mitigates its direct cytotoxicity while maintaining biocompatibility, providing a safer and more suitable platform for biomedical applications.

3. Conclusion

The integration of HBEO nanoemulsion into a gelatin/CMC hydrogel addressed the limitations of free HBEO by improving its solubility, stability, and controlled release. The HBEONE (1% HBEO in 0.5% PVA) achieved nanosized droplets (182 ± 3 nm, PDI = 0.286) with a sustained 92% release. Once dispersed in the gelatin/CMC (3:1) network, the composite hydrogel combined high water uptake (swelling ratio ≈ 8 g/g) with substantial loading (≈ 67.5%), supporting prolonged HBEO availability. Functionally, the system preserved HBEO's sustained antioxidant response while reducing cytotoxicity versus free HBEO in L929 cells, indicating that nanoencapsulation and matrix-mediated diffusion effectively mitigate concentration spikes that can trigger apoptosis.

References

[1] D. Braatz, M. Cherri, M. Tully, M. Dimde, G. Ma, E. Mohammadifar, F. Reisbeck, V. Ahmadi, M. Schirner, R. Haag , "Chemical Approaches to Synthetic Drug Delivery Systems for Systemic Applications," Angewandte Chemie International Edition, vol. 61, no. 49, p. e202203942, Dec. 2022,

[2] R. Langer, "Drug delivery and targeting," Nature, vol. 392, no. 6679 Suppl, pp. 5–10, Apr. 1998,

[3] D. P. de Sousa, R. O. S. Damasceno, R. Amorati, H. A. Elshabrawy, R. D. de Castro, D. P. Bezerra, V. R. V. Nunes, R. C. Gomes, and T. C. Lima, "Essential Oils: Chemistry and Pharmacological Activities," Biomolecules, vol. 13, no. 7, Jul. 2023,

[4] A. P. Raina, A. Kumar, and M. Dutta, "Chemical characterization of aroma compounds in essential oil isolated from 'Holy Basil' (Ocimum tenuiflorum L.) grown in India," Genetic Resources and Crop Evolution, vol. 60, no. 5, pp. 1727–1735, Jun. 2013,

[5] A. Bhatnagar and R. Pimoli, “Chemical composition of the essential oil of Ocimum sanctum L. growing in Garhwal region of Uttarakhand, India,” International Journal of Herbal Medicine, vol. 13, no. 2, pp. 43–46, Jan. 2025,

[6] P. Singh, B. B. Basak, V. J. Patel, R. Sarkar, K. C. Patel, and G. N. Motaka, “Integration of Biochar with Chemical Fertilizers Improves the Economic Yield, Quality of Holy Basil (Ocimum sanctum L.) and Soil Health,” Journal of Soil Science and Plant Nutrition, vol. 24, no. 4, pp. 6404–6417, Dec. 2024,

[7] S. Chalkual, “Bioactive compounds from holy basil (ocimum tenuiflorum L.) against angiotensin-converting ENZYME2 (ACE2),” Chulalongkorn University Theses and Dissertations (Chula ETD), Jan. 2023,

[8] M. W. Imam and S. Luqman, “Unveiling the mechanism of essential oil action against skin pathogens: from ancient wisdom to modern science,” Archives of microbiology, vol. 206, no. 8, Aug. 2024,

[9] R. J. Wilson, Y. Li, G. Yang, and C. X. Zhao, “Nanoemulsions for drug delivery,” Particuology, vol. 64, pp. 85–97, May 2022,

[10] A. A. C. Toledo Hijo, R. E. Guinosa, and E. K. Silva, “Ultrasound emulsification energy strategies impact the encapsulation efficiency of essential oils in colloidal systems,” Journal of Molecular Liquids, vol. 358, p. 119179, Jul. 2022,

[11] Y. Shi, M. Zhang, K. Chen, and M. Wang, “Nano-emulsion prepared by high pressure homogenization method as a good carrier for Sichuan pepper essential oil: Preparation, stability, and bioactivity,” LWT, vol. 154, p. 112779, Jan. 2022,

[12] Z. Xing, Y. Xu, X. Feng, C. Gao, D. Wu, W. Cheng, L. Meng, Z. Wang, T. Xu, X. Tang, Fabrication of cinnamon essential oil nanoemulsions with high antibacterial activities via microfluidization, Food Chemistry, vol. 456, Oct. 2024.

[13] L. Zhou, W. Zhang, J. Wang, R. Zhang, and J. Zhang, “Comparison of oil-in-water emulsions prepared by ultrasound, high-pressure homogenization and high-speed homogenization,” Ultrasonics Sonochemistry, vol. 82, p. 105885, Jan. 2022,

[14] R. Song, Y. Lin, and Z. Li, “Ultrasonic-assisted preparation of eucalyptus oil nanoemulsion: Process optimization, in vitro digestive stability, and anti-Escherichia coli activity,” Ultrasonics Sonochemistry, vol. 82, Jan. 2022,

[15] C. Laosinwattana, N. Somala, J. Dimak, M. Teerarak, and N. Chotsaeng, "Ultrasonic emulsification of Cananga odorata nanoemulsion formulation for enhancement of herbicidal potential," Scientific Reports, vol. 15, no. 1, pp. 1–17, Dec. 2025,

[16] P. Pongsumpun, S. Iwamoto, and U. Siripatrawan, "Response surface methodology for optimization of cinnamon essential oil nanoemulsion with improved stability and antifungal activity," Ultrasonics Sonochemistry, vol. 60, p. 104604, Jan. 2020,

[17] Z. Yang, Q. He, B. B. Ismail, Y. Hu, and M. Guo, "Ultrasonication induced nano-emulsification of thyme essential oil: Optimization and antibacterial mechanism against Escherichia coli," Food Control, vol. 133, p. 108609, Mar. 2022,

[18] Y. Weerapol, S. Manmuan, N. Chaothanaphat, S. Okonogi, C. Limmatvapirat, S. Limmatvapirat, and S. Tubtimsri, "Impact of Fixed Oil on Ostwald Ripening of Anti-Oral Cancer Nanoemulsions Loaded with Amomum kravanh Essential Oil," Pharmaceutics, vol. 14, no. 5, p. 938, May 2022,

[19] N. M. Deghiedy, N. M. Elkenawy, and H. A. Abd El-Rehim, "Gamma radiation-assisted fabrication of bioactive-coated thyme nanoemulsion: A novel approach to improve stability, antimicrobial and antibiofilm efficacy," Journal of Food Engineering, vol. 304, p. 110600, Sep. 2021,

[20] V. S. Ghorpade, R. J. Dias, K. K. Mali, and S. I. Mulla, "Citric acid crosslinked carboxymethylcellulose-polyvinyl alcohol hydrogel films for extended release of water soluble basic drugs," Journal of Drug Delivery Science and Technology, vol. 52, pp. 421–430, Aug. 2019,

[21] M. S. Manga, L. Higgins, A. A. Kumar, B. T. Lobel, D. W. York, and O. J. Cayre, "Exploring effects of polymeric stabiliser molecular weight and concentration on emulsion production via stirred cell membrane emulsification," Polymer Chemistry, vol. 14, no. 45, pp. 5049–5059, Nov. 2023,

[22] E. J. Delgado-Pujol, G. Martínez, D. Casado-Jurado, J. Vázquez, J. León-Barberena, D. Rodríguez-Lucena, Y. Torres, A. Alcudia, and B. Begines, "Hydrogels and Nanogels: Pioneering the Future of Advanced Drug Delivery Systems," Pharmaceutics 2025, Vol. 17, Page 215, vol. 17, no. 2, p. 215, Feb. 2025,

[23] R. Andreazza, A. Morales, S. Pieniz, and J. Labidi, "Gelatin-Based Hydrogels: Potential Biomaterials for Remediation," Polymers 2023, Vol. 15, Page 1026, vol. 15, no. 4, p. 1026, Feb. 2023,

[24] W. ; Zhang, Y. ; Liu, Y. ; Xuan, M. A. Correa-Duarte, W. Zhang, Y. Liu, Y. Xuan, and S. Zhang, "Synthesis and Applications of Carboxymethyl Cellulose Hydrogels," Gels 2022, Vol. 8, Page 529, vol. 8, no. 9, p. 529, Aug. 2022,

[25] N. Kreua-Ongarjnukool, S. T. Niyomthai, K. Sarodom, T. Lothong, and N. Soomherun, "Hybrid Gelatin/Carboxymethyl Cellulose Hydrogel Loaded Copper (II) Ion for Medical Applications," Materials Science Forum, vol. 1009, pp. 3–8, 2020,

[26] F. Sahar, A. Riaz, N.S. Malik, N. Gohar, A. Rasheed, U.R. Tulain, A. Erum, K. Barkat, S.F. Badshah, S.I. Shah, "Design, characterization and evaluation of gelatin/carboxymethyl cellulose hydrogels for effective delivery of ciprofloxacin," Polymer Bulletin, vol. 80, no. 11, pp. 12271–12299, Nov. 2023,

[27] Z. Soleimani, H. Baharifar, N. Najmoddin, and K. Khoshnevisan, "Evaluation of Carboxymethyl Cellulose/Gelatin Hydrogel-Based Dressing Containing Cefdinir for Wound Healing Promotion in Animal Model," Gels 2025, Vol. 11, Page 38, vol. 11, no. 1, p. 38, Jan. 2025,

[28] A. Bigi, G. Cojazzi, S. Panzavolta, K. Rubini, and N. Roveri, "Mechanical and thermal properties of gelatin films at different degrees of glutaraldehyde crosslinking," Biomaterials, vol. 22, no. 8, pp. 763–768, Apr. 2001,

[29] A. Kaolaor, K. Kiti, P. Pankongadisak, and O. Suwantong, "Camellia Oleifera oil-loaded chitosan nanoparticles embedded in hydrogels as cosmeceutical products with improved biological properties and sustained drug release," International Journal of Biological Macromolecules, vol. 275, p. 133560, Aug. 2024,

[30] T. M. Tran Vo, T. Piroonpan, C. Preuksarattanawut, T. Kobayashi, and P. Potiyaraj, "Characterization of pH-responsive high molecular-weight chitosan/poly (vinyl alcohol) hydrogel prepared by gamma irradiation for localizing drug release," Bioresources and Bioprocessing, vol. 9, no. 1, Dec. 2022,

[31] S. Bhunchu, P. Rojsitthisak, and P. Rojsitthisak, "Kinetic study of chitosan-alginate biopolymeric nanoparticles for the controlled release of curcumin diethyl disuccinate," Journal of Metals, Materials and Minerals, vol. 27, no. 2, Dec. 2017

[32] Y. Qin, W. Li, D. Liu, M. Yuan, and L. Li, "Development of active packaging film made from poly (lactic acid) incorporated essential oil," Progress in Organic Coatings, vol. 103, pp. 76–82, Feb. 2017,

[33] G. Mugnaini, R. Gelli, L. Mori, and M. Bonini, “How to Cross-Link Gelatin: The Effect of Glutaraldehyde and Glyceraldehyde on the Hydrogel Properties,” ACS Applied Polymer Materials, vol. 5, no. 11, pp. 9192–9202, Nov. 2023,

Determination of Earthquake Magnitude, Direction, and Occurrence Time Using Trigonometric Functions and the Scientific Method with Comparison to Actual Earthquakes.

Chaiyawat Musikapan[1,*], Ratinan Boonklurb[2]
[1] Engineer of Nitta Kid Charoen D Co., Ltd. and Iris Mechatronics Co., Ltd., Thailand
[2] Department of Mathematics and Computer Science, Faculty of Science, Chulalongkorn University, Thailand
*e-mail: chaiyawat.cuengineer@gmail.com

Abstract:

This study analyzes earthquake data recorded by the United States Geological Survey (USGS) from 2005 through March 2025, encompassing earthquake magnitudes, locations, and occurrence times. A novel methodology, together with a corresponding set of equations, was developed by integrating trigonometric calculations with the equation of time to reveal intrinsic relationships among seismic events. The proposed model simultaneously determines earthquake magnitude, direction, and occurrence time. Validation against actual seismic records revealed strong agreement between the model's calculations and observed earthquake data, achieving average accuracies of 98.73% for magnitude, 75.23% for earthquake direction vectors, and 95.25% for earthquake occurrence time.

DEVELOPMENT OF A MULTILAYERED ALUMINA-SIC CERAMIC COMPOSITE FOR ENHANCED FRACTURE RESISTANCE IN ARMOR APPLICATIONS

Pheeranat Leangthanarerx[1,2], Uraiwan Intatha[1,2], Nattakan Soykeabkaew[1,2], Nattaya Tawichai[1,2,*]
[1]School of Science, Mae Fah Luang University, 333 M1, Muang, Chiang Rai, 57100, Thailand
[2]Center of Innovative and Materials for Sustainability (iMatS), Mae Fah Luang University, Thailand
*e-mail: nattaya.taw@mfu.ac.th

Abstract:
This study develops a new multilayered alumina-silicon carbide (Al_2O_3-SiC) composite to improve the fracture resistance of traditional ceramic armor. The structure consists of 41 tape-cast alumina layers separated by four SiC-rich interfacial layers, designed to promote crack deflection and control their growth. The composite was made using tape casting, stacking, lamination, uniaxial pressing (100–500 kN), and sintering across a temperature range (1,550–1,650°C). Mechanical performance was tested through flexural testing, while microstructure and crystallography were analyzed with scanning electron microscopy (SEM) and X-ray diffraction (XRD). Results show that the multilayer structure significantly enhances mechanical properties; the sample sintered at 1,650°C reached a maximum flexural stress of 42.75 MPa, a 59% increase over a pure alumina matrix (26.92 MPa). Additionally, sintering temperature was identified as a key factor, increasing density from 1.94 g/cm³ at 1,550°C to 2.24 g/cm³ at 1,650°C. Microstructural and mechanical analyses confirm the effectiveness of the multilayer design in improving overall properties and fracture resistance performance.

DEVELOPMENT OF CONDUCTIVE MOF GAS SENSORS FOR VOCs DETECTION

Shumpei Goto,[1] Muhammad Sohail Ahmad,[2] Yusuke Inomata,[1] Tetsuya Kida[2,*]
[1]Department of Applied Chemistry and Biochemistry, Kumamoto University, Kumamoto, 860-8555, Japan
[2]Institute of Industrial Nanomaterials, Kumamoto University, Kumamoto 860-8555, Japan
*e-mail: tetsuya@kumamoto-u.ac.jp

Abstract:

Metal-organic frameworks (MOFs) have attracted considerable attention in recent years as gas sensing materials due to their high specific surface area and porosity, which endow them with excellent gas adsorption properties. Among them, Cu_3(hexahydroxytriphenylene (HHTP))$_2$ has attracted much attention because it shows a electrical conductivity, featuring a two-dimensional π-conjugated structure and interlayer π–π stacking, which contributes to its high charge transport properties. These properties make MOF materials a promising candidate for gas sensing applications based on resistance measurements.

In this study, we aimed to develop a sensor capable of highly sensitive detection of volatile organic compounds (VOCs) at mild operating temperatures. $Cu_3(HHTP)_2$ was synthesized via a hydrothermal method. Its crystallinity was confirmed by X-ray diffraction (XRD), and its morphology was investigated using scanning electron microscopy (SEM). As shown in Figure 1a, the SEM image reveals that the synthesized $Cu_3(HHTP)_2$ consists of nanorod-like particles with an average diameter of 60 nm. This nanostructure is expected to facilitate gas diffusion and enhance surface interactions. The specific surface area and pore size were also evaluated using Brunauer-Emmett-Teller (BET), with values of 579.49 m^2/g and 2.59 nm, respectively. To fabricate the sensor devise, the specific amount of the synthesized MOF was dispersed in an acetone suspension and deposited onto an alumina substrate with gold comb electrodes via spin coating to fabricate the sensing device. Resistance measurements were conducted at 180 °C using hydrogen, acetone, ethanol, toluene, NO_2 (each at 50 ppm). As shown in Figure 1b, the $Cu_3(HHTP)_2$-based sensor exhibited a promising response to VOCs at relatively low temperatures. These results demonstrate that $Cu_3(HHTP)_2$ exhibits high sensitivity and stable gas response even at relatively low temperatures, indicating its potential as a promising material for VOC gas sensor applications.

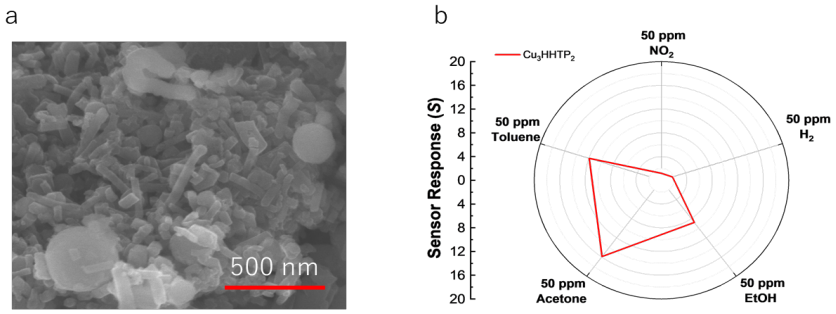

Figure 1. a). SEM image of $Cu_3(HHTP)_2$ b). Sensing performance of Cu_3HHTP_2 for VOCs and NO_2 under dry atmosphere at 180 °C

Effect of Polyethylene Oxide Concentration on Solvation Structure and Ion Dynamics in $NaClO_4$ Electrolytes

Ali Hassan,[1] Manaswee Suttipong[1,*]
[1]Department of Chemical Technology, Faculty of Science, Chulalongkorn University, Bangkok, 10330, Thailand
*Corresponding author: manaswee.s@chula.ac.th

Abstract

Polymer-based electrolytes are promising candidates for next-generation sodium-ion batteries (SIBs), yet the molecular role of polymer concentration in governing solvation and ion transport remains insufficiently understood. In this work, we employ molecular dynamics (MD) simulations to investigate fluorine-free sodium perchlorate ($NaClO_4$) electrolytes in propylene carbonate (PC) and diethyl carbonate (DEC) with polyethylene oxide (PEO) contents ranging from 0 to 20 wt% (0, 1, 5, 10, and 20 wt%). Structural analyses based on radial distribution functions and coordination numbers show that increasing PEO concentration strengthens Na^+ coordination with polymer oxygens while simultaneously weakening Na^+-ClO_4^- interactions, thereby reorganizing the solvation environment. This stabilization of the solvation shell comes at the expense of reduced polymer segmental mobility, resulting in a trade-off between solvation strength and ion diffusion. Dynamical analyses reveal that PEO addition lowers Na^+ diffusivity compared to polymer-free systems, although intermediate PEO concentrations can optimize the balance between ionic conductivity and mechanical stability. By bridging atomistic solvation behavior with macroscopic transport properties, these insights offer molecular-level design guidelines for developing safer and more efficient SIB electrolytes.

Electrochemical CO2 reduction using monoatomic graphene copper composite oxide catalysts

Shingo Morikawa[1], Yusuke Inomata[2], Armando T. Quitain[3], Tetsuya Kida[2]*,

1.Graduate School of Science and Technology, Kumamoto University, Kumamoto, 860-8555, Japan
2.Faculty of Advanced Science and Technology, Kumamoto University, Kumamoto, 860-8555, Japan
3.Center for International Education, Kumamoto University, Kumamoto, 860-8555, Japan
*tetsuya@kumamoto-u.ac.jp

Abstract:

In recent years, from the perspective of global environmental conservation, among technologies that convert CO2 emitted by humans into valuable substances, electrochemical CO2 reduction reactions (CO2RR) that are expected to achieve high conversion rates under ambient temperature and pressure conditions have garnered significant attention. Graphene oxide, with its numerous chemically reactive sites, is widely utilized as a catalyst carrier. Its single-atom structure has the potential to maximize the utilization efficiency of elements and introduce new chemical properties.

In this study, we evaluated the performance of single-atom catalysts derived from graphene oxide composite with copper by creating GDE electrodes and conducting CO_2RR. The single-atom catalysts derived from graphene oxide composite with copper were synthesized from graphene oxide and copper sulfate solution. The prepared single-atom catalysts were characterized using TEM and LSV measurements. Gas-phase components were analyzed using GC-BID, and liquid-phase components were analyzed using HPLC, with the FE values of each generated substance compared. Additionally, the CO_2 activity of the catalyst synthesized in this study was confirmed based on the LSV measurement results. Carbon monoxide reached a maximum at 30 mol%, but little effect of potential was observed. The FE value of formic acid increased as the negative potential increased.

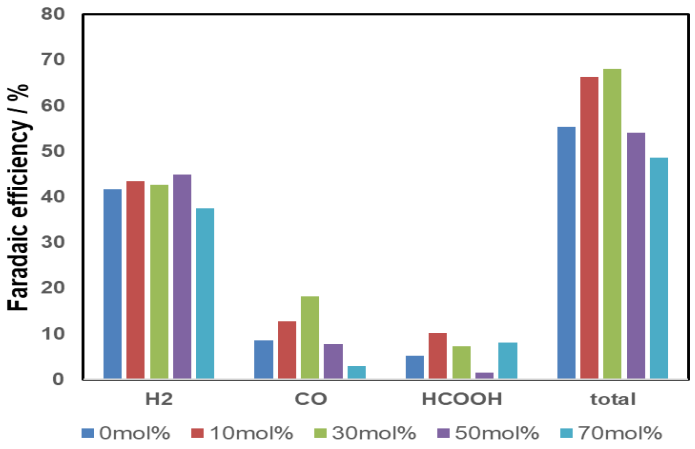

Figure 1. Faraday efficiency of each substance produced (H_2, CO, HCOOH, Total) when electrolyzed at -1.9V.

Enhancement of Essential Oil Extraction from Anise (*Pimpinella anisum*) via Microwave Hydrodistillation with Maceration Pre-Treatment

Dian Purnami Handayani[1], Arin Pashadiera Mellina[1], Siti Zullaikah[1], Mahfud Mahfud[1]*, Heri Septya Kusuma[2]
[1]Department of Chemical Engineering, Institut Teknologi Sepuluh Nopember, Surabaya, Indonesia
[2]Department of Chemical Engineering, Universitas Pembangunan Nasional Veteran, Yogyakarta, Indonesia
*e-mail: mahfud@chem-eng.its.ac.id

Abstract

Enhancing essential oil extraction is central to improving process efficiency, lowering energy and solvent inputs, and strengthening the sustainability profile of natural-product manufacturing. While microwave hydrodistillation (MHD) accelerates the release of volatiles via dielectric heating, mass-transfer limitations in intact plant matrices can still cap recoveries; a targeted pre-treatment that weakens the matrix offers a practical route to close this performance gap. This work addresses that gap by evaluating maceration as a simple, low-temperature pre-treatment to enhance subsequent MHD performance.

Anise (*Pimpinella anisum*) seeds, widely valued for their aromatic essential oil and diverse applications, were extracted in this study using two strategies to assess the effect of pre-treatment: conventional microwave hydrodistillation (MHD) and maceration-microwave-assisted hydrodistillation (MMHD).

Experiments varied microwave power (300, 450, 600 W), feed-to-solvent ratio (F/S), and time; extractions used water as solvent, and were run up to 180 min with periodic sampling. The maceration pre-treatment (aqueous, controlled agitation and temperature) was designed to increase solvent penetration and pre-weaken cellular structures before dielectric heating.

MMHD consistently outperformed MHD. At the identified operating window, 450 W, F/S 0.14 g·mL^{-1}, and 180 min, MMHD achieved a 2.49% oil yield versus 2.08% for MHD. The improvement is attributed to enhanced cell-wall disruption and reduced mass-transfer resistance, enabling faster and more complete release of volatiles under microwave heating. These gains are aligned with green-processing principles by enabling higher yield at moderate power and without additional organic solvents, supporting efficiency, scalability, and responsible production.

ENHANCING SUPERHYDROPHOBICITY OF PAPER VIA GAS-PHASE SILYLATION USING HEXADECYLTRIMETHOXYSILANE AND TITANIUM (IV) ISOPROPOXIDE

Patcharawarin Sathapornwajana[1], Kuntinee Suvarnakich[1,2], Kamonwan Pacaphol[1,2*]
[1]Pulp, Paper and Packaging Technology Program, Faculty of Science, Chulalongkorn University, Bangkok 10330, Thailand
[2]Department of Imaging and Printing Technology, Faculty of Science, Chulalongkorn University, Bangkok 10330, Thailand
*e-mail: kamonwan.p@chula.ac.th

Abstract:
The shift to paper packaging is driven by concerns over plastic's non-biodegradability and environmental impact. Although paper is biodegradable, it exhibits poor water resistance. Various coatings have been developed to address this drawback; however, because these coatings remain only on the surface, protection is limited to the outer layer. This study aimed to enhance the water resistance of paper through chemical vapor deposition silylation using different volumes of hexadecyltrimethoxysilane (HDTMS) in the gas phase, which can penetrate the paper structure more effectively than surface coatings. Titanium (IV) isopropoxide (TTIP) was introduced as a catalyst via spray coating at varying concentrations. The results demonstrated that applying only HDTMS at 28 mL/m² of paper surface, without TTIP, successfully generated a hydrophobic surface with a water contact angle of 115° ± 5 on both sides of the paper. Furthermore, the incorporation of 10% v/v TTIP of the paper weight with a 30-min curing time yielded a superhydrophobic surface, achieving a water contact angle of up to 151° ± 3 on both sides. The evidence of silylation was comprehensively confirmed by FTIR, XRF, and SEM analyses. These findings highlight the potential of gas-phase silylation for significantly enhancing paper hydrophobicity in packaging applications.

Graphical abstract

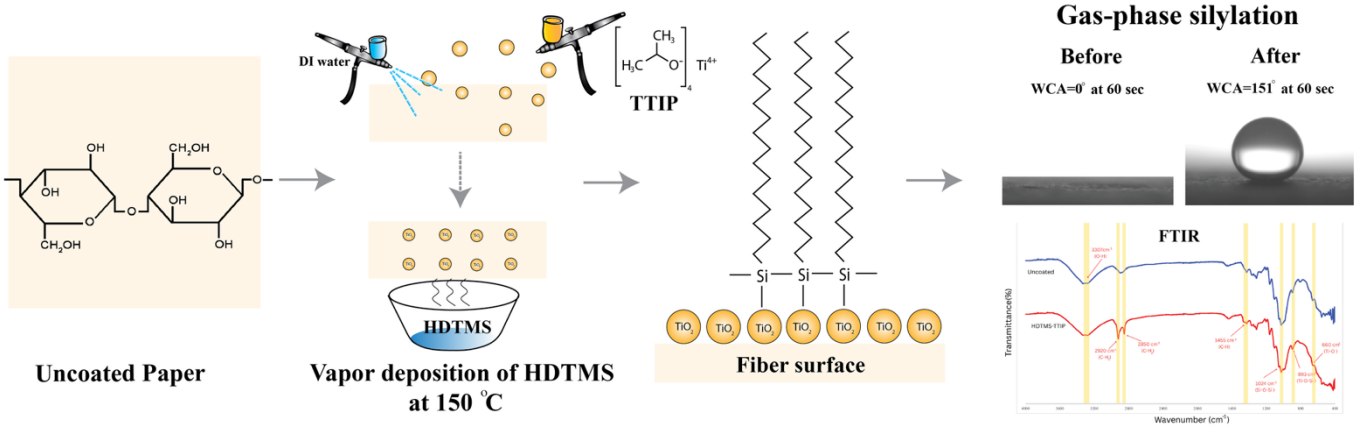

FABRICATION OF BLACK ZIRCONIA CERAMIC FOR JEWELRY APPLICATIONS FROM DENTAL ZIRCONIA BLOCK SCRAP RECYCLING

Thanakorn Wasanapiarnpong [1,*], Prane Junlar [2], and Sittinun Tawkaew [3]
[1] Upcycled Materials from Industrial and Agricultural Wastes Research Unit, Department of Materials Science, Faculty of Science, Chulalongkorn University, Bangkok, Thailand
2 Department of Science Service, Ministry of Higher Education, Science, Research and Innovation, Bangkok, Thailand
3 Department of Chemical Engineering, Faculty of Engineering, Srinakharinwirot University, Bangkok, Thailand
*e-mail: thanakorn.w@chula.ac.th

Abstract:
This research aimed to prepare high-value black zirconia ceramics for jewelry applications by utilizing waste zirconia blocks from denture production. The waste material was wet-milled in a porcelain ball mill using alumina balls, with the addition of 2.5wt% CoO and 2.5wt% MnO_2 as black colorants. After 24 hours of milling, a fine zirconia powder mixture with an average particle size of approximately 2 μm was obtained. The dried powder was sieved through a 100-mesh screen to ensure homogeneity. The zirconia powder was then uniaxially pressed into specimens using a hydraulic press at 50 MPa: cylindrical pellets (20 mm diameter) and rectangular bars (80 × 10 × 5 mm) The green bodies were sintered at 1500 °C with a heating rate of 5 °C/min and a soaking time of 1 hour. The sintered samples were then tested and characterized bulk density, water absorption, Vickers hardness, three-point bending strength, phase composition by XRD, microstructure by SEM, color measurement, and gloss analysis. The results showed that the ceramics exhibited high density, very low water absorption (0.12%), an average hardness of 7.63 GPa, fracture toughness of 3.24 $MPa \cdot m^{1/2}$, and flexural strength of 465.84 MPa. While colorant additions reduced mechanical properties compared to pure zirconia, the values achieved remain suitable for decorative jewelry applications. Furthermore, after grinding and polishing, the samples presented an attractive black appearance, making them highly suitable for use as jewelry materials.

GEOLOGICAL INSIGHTS INTO ORE GENESIS AND ANCIENT METALLURGY IN KHON KAEN GEOPARK, THAILAND: GEOCHEMICAL AND PETROGRAPHIC EVIDENCE FROM SLAG, LATERITES, AND HOST ROCKS

Vimoltip Singtuen, [1,*] Ajcharanan Nakdee,[1] Burapha Phajuy, [2]

[1] Department of Geotechnology, Faculty of Technology, Khon Kaen University, Khon Kaen 40002 Thailand
[2] Department of Geological Sciences, Faculty of Science, Chiang Mai University, Chiang Mai 50200 Thailand

*e-mail: vimoltipst@gmail.com

Abstract:
Khon Kaen Geopark hosts extensive accumulations of ancient iron slag, with individual deposits reaching several tons, typically located on stream terraces. Despite their abundance, the origin and production context of these slag deposits remain insufficiently understood. This study investigates the spatial distribution, mineralogical characteristics, and geochemical signatures of the slag and surrounding materials to evaluate the potential for historical iron smelting. Macrographic analysis identifies distinct pyrometallurgical textures—including dense, porous, flow-banded, and glassy morphologies—indicative of high-temperature metallurgical processing. Some slag samples also contain remnants of furnace materials, further supporting smelting activity. Two types of laterite—nodular and recemented—were observed in the vicinity. Portable X-ray fluorescence (pXRF) analysis reveals evidence of aluminium alteration phases and early-stage lateritization in local soils and sandstones. Geochemical profiles reflect a weathering continuum characterized by a saprolitic zone exhibiting iron leaching and supergene enrichment near the groundwater table. The parent rocks are Fe-rich reddish sandstones, including arkose and lithic arkose, associated with the Nam Phong and Phu Kradung formations of the Khorat Group. Oxidative weathering driven by water, oxygen, carbon dioxide, and organic acids facilitated the formation of iron-enriched profiles. Fe_2O_3 concentrations in lateritic samples range from 36.12 to 60.56 wt%, comparable to global lateritic iron ores, suggesting that sufficient iron resources were locally available to support ancient smelting practices within the region.

Green Diesel Production from Sludge Oil with Ni/SiO_2 Catalysis

Yawo Ewoxo,[1] Siti Zullaikah,[2]*
[1,2] Department of Chemical Engineering, Institut Teknologi Sepuluh Nopember (ITS), Kampus ITS, Keputih, Surabaya, 60111 Indonesia
*e-mail: s.zullaikah@its.ac.id

Abstract:
The use of food-based feedstocks for producing green diesel has raised persistent concerns, as it directly competes with the food sector and puts a strain on economic stability. Consequently, the present study investigates sludge oil, a byproduct of crude palm oil refinery with a high oil content (approximately 36.5%). The sludge oil is composed of triglycerides, free fatty acids, fatty acid methyl esters, and other compounds, which have demonstrated considerable potential as a renewable feedstock for catalytic hydrotreating. The utilization of sludge oil entails the extraction of silica with a purity of 91.8% from rice husk ash, which is then employed as a support for nickel catalysts. The successful impregnation of 7.44 wt% Ni is achieved through this method. The catalytic performance of Ni/SiO_2 was assessed in a hydrotreating reactor under varying operation conditions, including temperature (250-300°C), reaction time (3-5 h), and catalyst loading (3-7 g). The optimization process was executed through the implementation of response surface methodology, employing a Box-Behnken design. The study revealed that the interaction between reaction time and catalyst loading had the most significant influence on hydrocarbon yield, with the optimal conditions determined as 261 °C, 3.67 h, 4.86 g of catalyst, and 5 MPa H_2. Under these conditions, the process yielded 89.62% hydrocarbons, with 83.19% of the yield comprising diesel-range (C_{15}–C_{18}) hydrocarbons and 16.81% lighter fractions (C_{12}–C_{14}). Free fatty acids conversion followed first-order kinetics, with an activation energy of 35.13 kJ/mol. It is noteworthy that the green diesel obtained exhibited a cetane number of 62, which was higher than the commercial HVO from PT. Pertamina, which has a cetane number of 56.2. The present findings demonstrate that industrial sludge oil can function as a viable and sustainable feedstock for green diesel production, thereby validating the efficacy of Ni/SiO_2 derived from rice husk ash.

LIGHT-ACTIVATED VOC GAS SENSORS USING DOPED METAL OXIDES

Papitchaya Khunjan,[1] Tetsuya Kida[2,*]
[1]Department of Applied Chemistry, Graduate School of Science and Technology, Kumamoto University, 860-8555 Kumamoto, Japan
[2] Faculty of Advanced Science and Technology, Kumamoto University, 860-8555 Kumamoto, Japan
*e-mail: tetsuya@kumamoto-u.ac.jp

Abstract:

Volatile organic compounds (VOCs) are major contributors to indoor air pollution and serve as biomarkers for non-invasive medical diagnostics. Metal oxide semiconductor (MOS) gas sensors, especially those based on SnO_2, are commonly used due to their high sensitivity. However, their requirement for high operating temperatures, around 300 °C, limits their use in portable and low-power devices. This study explores the possibility of stable and high-response operation by doping SnO_2 with 5 wt% of Pt, Co, and Ni, combined with light irradiation. Ethanol, acetone, and toluene were selected as target gases. Operating temperature from 250 °C to 50 °C, most doped sensors showed poor recovery, making it difficult to calculate reliable responses. Interestingly, under UV irradiation, SnO_2 showed very good recovery toward ethanol even at 50 °C. This improvement can be attributed to the photoactivation of the SnO_2 surface by UV light, which enhances surface reactions with VOC molecules and enables efficient sensing at lower temperatures.

Magnetic CuFe-LDH/Activated Carbon Composite Derived from Coffee Ground for Efficient Removal of Dyes and Antibiotics from Water

Krongkhwun Chaiyapat1,[1] Korawan Thongnim1,[1] Pruettiphong Phiromrak1,[1]
Sornchai Intachai2[2,*]
[1] Paphayompittayakom School (SCiUS-Thaksin University), Phatthalung, 93210, Thailand
[2] Innovative Material Chemistry for Environment Center, Department of Chemistry, Faculty of Science and Digital Innovation, Thaksin University, Phatthalung campus, Phatthalung, 93210, Thailand
*e-mail: sonchai.i@tsu.ac.th

Abstract:
Water pollution is a global problem caused by human activities, particularly wastewater release from textile dyeing factories and hospitals containing dyes and antibiotics. Although various technologies exist, the simultaneous removal of positively and negatively charged pollutants with easy material recycling remains challenging. This research developed a magnetic composite of CuFe-layered double hydroxide (CuFe-LDH) and activated carbon (AC) derived from spent coffee grounds (Coffea arabica L.) via a solid-state reaction, an eco-friendly method without hazardous waste. The composite was characterized using XRD, FT-IR, EDX, Zeta potential, VSM, and BET, confirming the integration of CuFe-LDH with AC through electrostatic attraction in a high-surface-area structure containing minor CuO, FeOOH, and Fe_3O_4 impurities.The composite was applied for removing toxic pollutants: cationic dye (malachite green), anionic dye (aniline blue), and antibiotic (amoxicillin). Wastewater samples (100 ppm, 100 mL) were treated by adsorption (0.20 g adsorbent) and photocatalysis under visible light (0.05 g catalyst). The material achieved removal efficiencies of 52–75% (malachite green), 67–80% (aniline blue), and 47–65% (amoxicillin). Photocatalytic degradation reached 87–100%. Importantly, the magnetic composite could be reused up to five cycles with high efficiency, demonstrating strong potential for wastewater treatment of cationic, anionic, and zwitterionic contaminants.

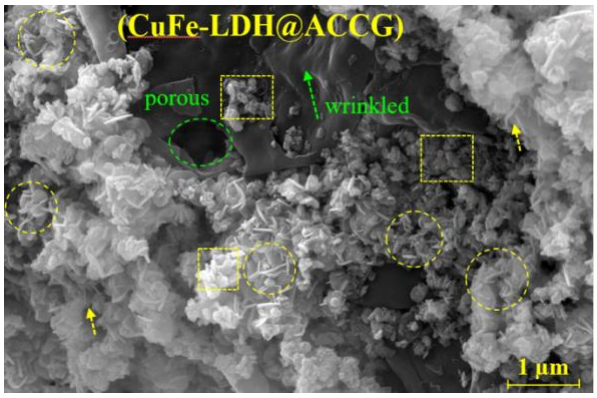

Figure 1.
Show the morphology of composite material

MECHANICAL AND PHYSICAL PROPERTIES OF *Pleurotus Ostreatus* MYCELIUM-BASED COMPOSITES FOR SUSTAINABLE WALL PANELS

Goodwill Ragui,[1] Sitthi Duangphet,[2] Somwan Chumphonhphan [2, *]
[1]School of Science, Mae Fah Luang University, 333 M1, Muang, Chiang Rai, 57100, Thailand
[2]Center of Innovative and Materials for Sustainability (iMatS), School of Science, Mae Fah Luang University, Thailand
*e-mail: somwan@mfu.ac.th

Abstract:
As the world looks for greener building solutions, mycelium-based composites are emerging as a promising alternative to traditional materials. In this study, we explored the use of Pleurotus ostreatus, better known as the Black Pearl Oyster mushroom and locally grown in Thailand, to create sustainable wall panels. The composites were formed using four different blends of sawdust and coconut coir (100:0, 90:10, 80:20, and 70:30 ratios), making use of agricultural byproducts that are widely available in the region. Once grown and dried, the panels were tested for their strength and durability through compression, flexural, and impact tests, and their practical performance was further assessed by measuring density and moisture absorption.

The results showed that compressive stress at maximum force ranged from 0.10 to 0.25 MPa, with the highest value observed in the 90:10 composition. The moisture content before drying varied between 52.88% and 62.87%, while the density of the composites decreased from 256.03 kg/m^3 (100:0) to 183.63 kg/m^3 (70:30) as coconut coir content increased. These findings demonstrate that varying the sawdust-to-coir ratio directly affects both mechanical and physical performance, allowing the material to be tailored for specific wall panel applications. Overall, the use of locally sourced Pleurotus ostreatus mycelium and agricultural residues shows strong potential for producing eco-friendly wall panels that reduce dependence on conventional materials while supporting sustainable Thai bio-based innovations.

Microencapsulation of Zingiber *cassumunar* Roxb. Essential Oil using Poly-L-lactic Acid for Enhanced Stability

Methakriat Sirival,[1] Sutiam Kruawan,[2] Nattika Thanuthong,[3] Rujikarn Sirivantharat[3,*]

[1]Department of Chemical Technology, Faculty of Science, Chulalongkorn University, Bankok 10330, Thailand
[2]Faculty of education, Dhonburi Rajabhat University, Bangkok 10600 Thailand
[3]Department of General Science, Faculty of Science and Engineering, Kasetsart University Chalermphrakiat Sakon Nakhon Province Campus, Sakon Nakhon 47000, Thailand
*e-mail: rujikarn.s@ku.th

Abstract:
This research studied the encapsulation process of *Zingiber cassumunar* Roxb. essential oil using poly-L-lactic acid (PLLA). The preparation of shell capsules of PLLA containing essential oil was accomplished by using techniques of solvent evaporation with molecular weight of the PLLA at 77,000, 140,000 and 200,000 g/mol, and various weight ratios of the PLLA polymer to essential oil at 90:10, 70:30 and 60:40. Regarding the experiment, it was found that the preparation of the method using the ratio PLLA with molecular weight 140,000 g/mol per essential oil at the weight ratio 90:10 resulted in a maximum encapsulation efficiency of 97.03%. This microcapsule was observed with optical microscope OM), scanning electron microscope (SEM), UV-Visible spectrophotometer and fourier transform infrared spectroscopy (FT-IR). The highest release rate was 0.54 mg at a molecular weight and ratio of PLLA 140,000 g/mol to essential oil 60:40 at 120 min. These research results can be applied to other fields regarding preserving the properties of essential oils for extended durations, e.g., the application of essential oil capsules to be applied in medicine, spa and skin scrub.

Microwave-Assisted Chemical Activation of Rice Husk-Derived Activated Carbon for Solketal Synthesis

Teemaporn Choochem, Montakarn In-karn, Pesak Rungrojchaipon*
Industrial Chemistry, School of Science, King Mongkut's Institute of Technology Ladkrabang, Bangkok, Thailand
*e-mail: pesuk.ru@kmitl.ac.th, mmmontakarn092@gmail.com

Abstract:

This research focuses on adding value to agricultural waste materials by using rice husk as the primary raw material for activated carbon (AC) synthesis. The process begins by converting the rice husk into activated carbon using sulfuric acid (H_2SO_4) at a concentration of 18 M. The carbon is then chemically activated with copper (II) chloride ($CuCl_2$) and phosphoric acid (H_3PO_4) in a weight ratio of 1:1 and 1:4, respectively, and the samples were calcined at of 600 and 800 °C for 2 hours under a nitrogen gas atmosphere to prevent oxidation. After activation, the AC was further modified by microwave heating (700 W, 5 rounds of 5 minutes each) to enhance surface area and pore structure, to enhance the surface area and porous structure of the carbon. Following the treatment, the samples are analyzed for their properties using techniques such as BET, TGA, FT-IR, and SEM to evaluate surface area, pore volume, thermal stability, and surface functional groups. Additionally, methylene blue and iodine adsorption tests are performed to confirm the adsorption efficiency. Moreover, the catalytic performance of the prepared AC was investigated in the acetalization of glycerol with acetone to produce solketal synthesis process from glycerol and acetone, utilizing its surface acidity to promote the reaction. This study demonstrates that rice husk-derived AC can act as both an efficient adsorbent and a sustainable catalyst, providing a low-cost pathway for value-added chemical synthesis

Mineralization of Cu-Mo porphyry deposit in Phetchabun Province, Central Thailand

Natdanai Chaloeicheep,[1] Chawin Chaywong,[1,*] Kanlayarat Sonsrong,[1] Sukritta Jesrichai, [1] Sirawit Kaewpaluk[2]
[1]B.Sc. Program in Geology, Department of Geology, Faculty of Science, Chulalongkorn University, Bangkok, 10330, Thailand
[2]Applied Mineral and Petrology Research Unit (AMP RU), Department of Geology, Faculty of Science, Chulalongkorn University, Bangkok 10330, Thailand
*e-mail: chawin.chaywong@gmail.com

Abstract:
Copper (Cu) has recently been recognized as one of the critical minerals serving as a raw material for modern and renewable technology. In Thailand, several Cu deposits are in operation; however, the Cu-Mo porphyry depositional style is less focused on and has no operation yet. Therefore, a Cu-Mo porphyry deposit in Phetchabun Province was the focus of this study. The study aims to characterize mineral assemblages, mineralization style, and paragenesis stages in this deposit. Based on petrographic observation, mineralization occurs as veinlets and stockwork styles hosted by granodiorite and basaltic andesite. At least 4 mineralization veins were observed and identified, namely: 1) qtz-clay-chl-py-cpy-mo vein (Vein I), 2) qtz-chl-py-cpy vein (Vein II), 3) clay-py-qtz-cpy-sp vein (Vein III), and 4) qtz±sulfides vein (Vein IV). Additionally, veins I, II, and III can be characterized as the main mineralization stages. Alteration minerals in this prospect consist of quartz and sericite, which can be identified as sericic alteration. In addition, REE-bearing minerals, comprising zircon and monazite, were observed in the granodiorite host rock. These minerals can be used to investigate geochronology and the appropriate magma chemistry for Cu-Mo mineralization, which can be applied to future Cu-Mo exploration.

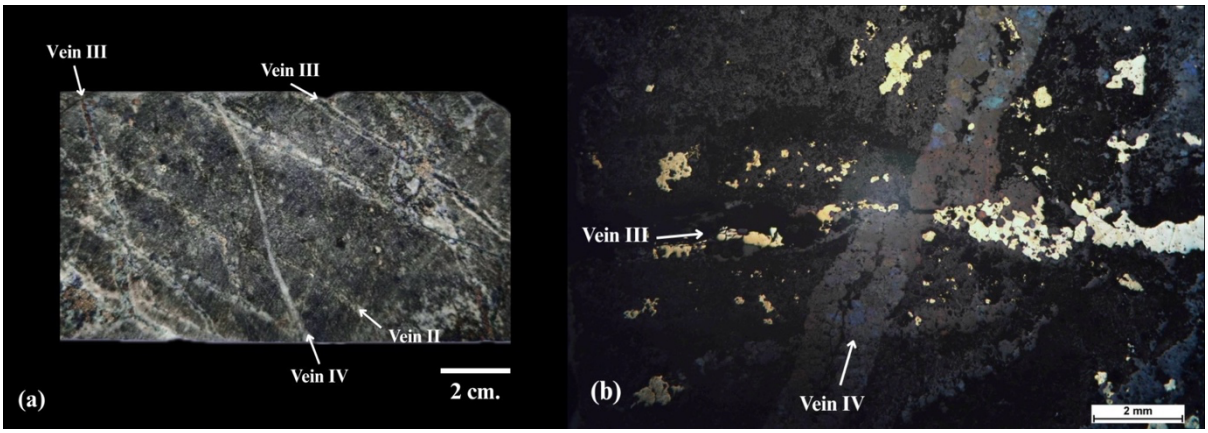

Figure 1.
Representative sample of Cu-Mo porphyry deposit showing (a) Photograph of a core sample presenting the intersection of Vein I, II, and III; (b) Photomicrograph of the sample that contains Vein III and Vein IV

MODULATION OF ANTIMICROBIAL EFFECT ON VANADIUM-PROMOTED CASSAVA/CHITOSAN BIOPOLYMER FILMS USING WHITE-LIGHT IRRADIATION

Pawarisa Ngamroj[1], Natthakit Phophuttharaksa[1], Natputthiya Chavanalikigorn[2], Yutichai Mueanngern[2, *]
[1]Kamnoetvidya Science Academy, Rayong, 21210, Thailand
[2]Department of Chemistry, Kamnoetvidya Science Acadamy, Rayong, 21210, Thailand
*e-mail: yutichai.m@kvis.ac.th

Abstract:
Biopolymer films fabricated from chitosan and cassava starch were modified by vanadium soaking and white-light irradiation and its antimicrobial properties were studied. Vanadium-soaked and irradiated film had the highest activity, which was 1.4-fold greater than the vanadium-soaked film and 1.1-fold greater than the control film. This result suggests that vanadium and irradiation interacted synergistically to enhance antimicrobial performance. After soaking, the films turned yellow, showing that vanadium was mainly in a high oxidation state, while irradiation changed the color to green due to partial reduction of vanadium to lower oxidation states. Scanning electron microscopy (SEM) revealed clear morphological changes on the film surface after vanadium incorporation and irradiation, suggesting that these treatments may have influenced the internal structure or polymer interactions. Transmission electron microscopy (TEM) showed bacterial cell wall ruptures after contact with the irradiated films while Energy Dispersive Spectroscopy (EDS) confirmed an elevated release of vanadium into the bacterial solution. The lower oxidation state of vanadium can react with oxygen to form reactive oxygen species (ROS) such as superoxide radicals ($O_2^{\bullet -}$), which damage bacterial membranes and speed up cell death. Although vanadium can be toxic in large amounts, previous reports on similar systems reveal low release of vanadium from these film, making them a promising biodegradable antimicrobial material.

MORPHOMETRIC EVIDENCE OF TRANSIENT LANDSCAPE ADJUSTMENT ALONG THE PHETCHABUN FAULT ZONE, CENTRAL THAILAND

Thitima Wongthibet[1], Pichawut Manopkawee[1,*]

[1]Department of Geological Sciences, Faculty of Science, Chiang Mai University, Chiang Mai, Thailand
*e-mail: pichawut.m@cmu.ac.th

Abstract:

Landscape evolution in tectonically active regions reflects the interplay of tectonics, climate, and lithology. The Phetchabun Mountain Ranges and adjacent intermontane basin in central Thailand provide a natural setting to examine landscape response to tectonic forcing in an extensional regime. Due to the complex Paleogene–Neogene tectonics, the area preserves evidence of differential uplift and transient topographic adjustment. This study analyzed 94 watersheds using high-resolution DEMs and morphometric indices, including channel steepness, longitudinal profiles, knickpoint mapping, and chi-plots. The Results reveal a systematic north–south decline in basin-averaged channel steepness and elevation, consistent with spatial variations in rock uplift. Prominent slope-break knickpoints indicate transient conditions where incision signals have not fully propagated upstream. Geomorphic evidence confirms active deformation along the Phetchabun Fault Zone (PFZ), although limited chronological data are not sufficient to determine the rate of incision and rock uplift. Tectonic activity is identified as the primary control on regional morphology, with climate, lithology, and sediment supply exerting lesser influences. Stronger uplift in the north is linked to Paleogene normal faulting, while weaker uplift in the south reflects multistage rifting and less resistant lithologies. The differential uplift along the PFZ is shown to govern long-term topographic development, with river systems serving as sensitive indicators of transient tectonic adjustment. These findings highlight the dominant role of tectonics in shaping the Phetchabun landscape and provide a framework for applying similar morphometric approaches in other tectonically active regions.

MULTIFUNCTIONAL NANOCAPSULE-INTEGRATED POLYESTER AND MICRO-POLYESTER TEXTILES ENHANCED WITH CHITOSAN AND SILVER PARTICLES FOR ANTIBACTERIAL ACTIVITY AND SUSTAINED FRAGRANCE RELEASE

Chananchida Sukchaiya, Miyuki Sato, Adis Khetubol, Janjira Maneesan,*
Kamnoetvidya Science Academy, Rayong, Thailand
*e-mail: janjira.m@kvis.ac.th

Abstract:

In today's world, where health, hygiene, and environmental sustainability are increasingly valued, the demand for high-performance and functional sportswear continues to rise. However, a persistent problem is the unpleasant odor caused by sweat and bacterial growth. This study focuses the practical development of multifunctional sportswear fabrics with antibacterial and aromatic properties by using chitosan, silver ions, and peppermint-oil nanocapsules. Polyester and micro polyester fabrics were coated through various methods to achieve odor control, bacterial inhibition, and long-lasting fragrance release. Structural analysis using FT-IR, SEM, and TGA confirmed the structure of subtances and successful coating. Nanocapsules exhibited stable spherical morphology (60-80 nm) and thermal stability up to 250 °C. The modified fabrics exhibited over 95% inhibition of *E. coli* and *B. cereus*. We additionally washed the fabrics five times and compared the remaining antibacterial efficiency of each coating method. The fabrics coated with chitosan, silver ions, and nanocapsules (Methods 2 and 3 with nanocapsules) showed the best durability, maintaining over 95% inhibition of *B. cereus* and 65-85% inhibition of *E. coli* after washing. To visualize and explain the bonding mechanism, a computational simulation illustrated that polyester–chitosan bonds were the most stable (-884 to -886 Eh), while nanocapsule-silver bonds ruptured first, matching the experimental results. Overall, this study demonstrates a quantitatively verified, eco-friendly textile system with strong antibacterial performance, durable coating, and sustained fragrance which is an innovation toward sustainable multifunctional sportswear.

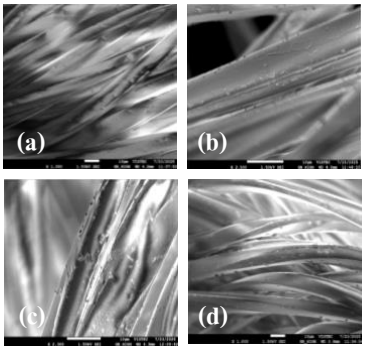

Figure 1. Scanning Electron Microscopy (SEM) micrographs of coated fabrics

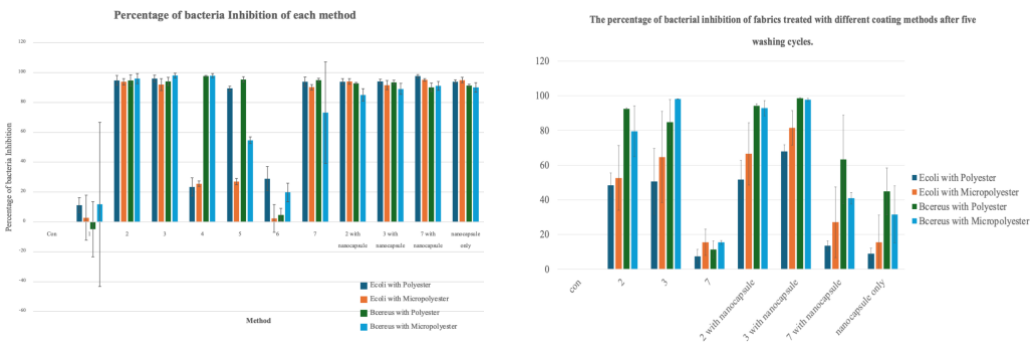

Figure 2. Antibacterial inhibition of fabrics treated with different methods before (left) and after five washing cycles (right)

NANOPOROUS CARBON COMPOSITE MATERIALS FROM BANANA TRUNK AND LABEL VIA HYDROTHERMAL-CARBONIZATION FOR CEMENT UTILIZATION

Vorawit Yuenyong, Khanatsanan Intaraprasert, Monthakarn Chanthip, Damrong Mingkhwankeeree, Narutchai Thongprasert, Apiluck Eiad-Ua*
Department of Nanoscience and Nanotechnology, School of Integrated Innovative Technology, King Mongkut's Institute of Technology Ladkrabang.Bangkok, Thailand
Suratthani School, Mueang Suratthani,Suratthani Bangkok, Thailand
*E-mail: apiluck.ei@kmitl.ac.th

Abstract:
This study aims to develop nanoporous carbon (NPC) materials from banana trunks and waste polyvinyl chloride (PVC) plastic labels through hydrothermal carbonization (HTC) to enhance the properties of cement. PVC and banana trunks were mixed in ratios of 9:1, 8:2, 7:3, 6:4, and 5:5 (PVC:banana trunk) and subjected to HTC at temperatures of 200–260°C for 8 hours to form a nanoporous carbon structure. The resulting material was washed to remove impurities and then ground into a fine powder using ball milling before undergoing carbonization at 600–900°C under a nitrogen atmosphere (originally for 1 hour). The carbonized powder was then mixed with cement at different ratios, such as 1:4:0.2 and 1:4:0.4. The composite was cast and tested for structural properties and compressive strength using analytical techniques including FTIR, XRD, Raman spectroscopy, SEM, and TGA. Test results showed that the produced NPC had a high surface area, a uniform porous structure, and good dispersion within the cement matrix. This led to increased cement strength and a denser microstructure, demonstrating that using banana trunks and waste plastic as raw materials for NPC production not only improves construction material performance but also offers a sustainable option for waste management.

Keywords: Nanoporous Carbon, Hydrothermal Carbonization, Polyvinyl Chloride (PVC), Banana trunk

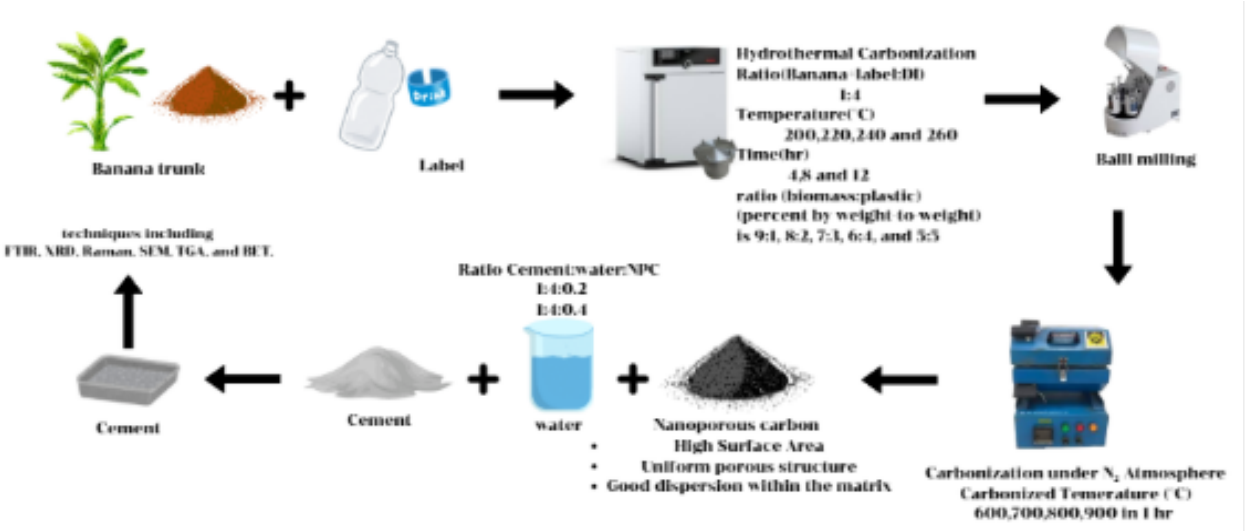

Figure 1.
Scheme diagram of research experiment

Novel Flexible Electrochemical Sensors for Visualized Clinics

Jia Zhu, Yuan Lin

School of Material and Energy, University of Electronic Science and Technology of China, Chengdu 610054, China

Abstract

Real-time, non-invasive, and continuous monitoring of physiological and biologic conditions has great clinical implications in both health management and disease treatment. A plausible way towards this goal is to leverage the state-of-the-art flexible electronics technology that combines excellent mechanical pliability and electronic functionalities. Despite tremendous advances in flexible electronics technology, non-invasive and continuous monitoring of trace amounts of biomarkers in various biofluids remains a formidable challenge. In this talk, I will introduce strategies for designing high-performance flexible electrochemical sensors for real-time biomarker monitoring, including leveraging highly reactive porous structures, catalytic materials, and field effect transistor (FET) configurations, as well as their clinical implications. In this regard, novel laser fabrication and large-scale transfer printing were innovated for the scalable production of highly sensitive, reliable, flexible electrochemical sensors towards glucose, amino acid, and hormone. Furthermore, field effect-based sensing and amplification mechanisms were incorporated into electrochemical sensors to push their detection limit from μM to nM. Collectively, our research aims to advance flexible electrochemical sensors for visualized clinical care, including early diagnosis and management of diseases, by leveraging the cutting-edge and interdisciplinary knowledge of materials science and biomedical engineering.

Keywords: flexible electronics, biosensors, biomarkers, electrochemical sensing

One-pot Synthesis of Zeolite A and NaX from Rice Husk Ash via Microwave-Assisted Hydrothermal Process

Chonlada Ouamsi,Chanisara Chuachaona,Pimpisa Thavorn,Pesak Rungrojchaipon*
Applied Chemistry, School of Science, King Mongkut's Institute of Technology Ladkrabang, Bangkok, Thailand
*e-mail: pesak.ru@kmitl.ac.th,65050180@kmitl.ac.th

Abstract:
Rice Husk Ash (RHA) is an agricultural waste material that possesses valuable properties as a highly pure silica source, where waste valorization enables the sustainable recovery of silica. In this study, we report the utilization of RHA to directly synthesize two high-value crystalline aluminosilicates, zeolite A and zeolite NaX, via a one-pot microwave-assisted hydrothermal method under controlled conditions. The synthesis was carried out using silica derived from RHA and aluminum hydroxide as the aluminum source. Prior to synthesis, RHA underwent an essential acid-washing pre-treatment step to remove impurities and ensure the quality of the silica precursor. The synthesized zeolites were thoroughly characterized using various analytical techniques: X-ray Diffraction (XRD) was used to confirm the crystal structure and purity, Scanning Electron Microscopy (SEM) was employed to observe the morphology, and X-ray Fluorescence (XRF) was used to determine the elemental composition. Additionally, the utility of zeolite syntheses was evaluated by studying their adsorption capacity of Methylene Blue (MB) dye from aqueous solutions. In summary, this work demonstrated a successful synthesis approach to convert RHA into a high-performance porous material in a sustainable manner for application in wastewater treatment and environmental remediation.

keywords: Rice Husk Ash (RHA), Zeolite Synthesis, Microwave-assisted Hydrothermal Method, Adsorption,Wastewater Treatment

OPTIMIZATION OF WATER CONTENT IN $CH_3NH_3PbI_3$ AND MICROPIPETTE-ASSISTED FABRICATION FOR HIGH-PERFORMANCE PEROVSKITE SOLAR CELLS

Paparwalin Wayupa,[1] Nonpawit Koheng,[1] Sarawut Siracosit,[2] Chanisara Chooseng,[3] Watcharaphol Paritmongkol,[3,*] Suranan Anantachaisilp[1,*]

[1]Kamnoetvidya Science Academy, Pa Yup Nai, Wangchan District, Rayong 21210, Thailand
[2]Department of Materials, University of Oxford, Park Rd., Oxford OX1 3PH, United Kingdom
[3]School of Molecular Science and Engineering, Vidyasirimedhi Institute of Science and Technology, Pa Yup Nai, Wangchan District, Rayong 21210, Thailand

e-mail: suranan.a@kvis.ac.th watcharaphol.p@vistec.ac.th

Abstract:

Perovskite solar cells (PSCs) have emerged as a promising alternative photovoltaic technology due to their high power conversion efficiency (PCE). However, their sensitivity to moisture remains a major challenge, affecting both stability and reproducibility. Although many studies have explored the role of water, the effect of trace amounts remains unclear. Previous reports indicate that even small amounts of water in precursor solutions can strongly influence device performance. This study investigates the effect of water concentrations lower than 70 ppm (specifically 0-60 ppm) added to DMF:DMSO solvent mixtures used in $CH_3NH_3PbI_3$ precursor preparation. Water content was precisely quantified using Karl Fischer titration. Perovskite films were fabricated via spin coating combined with an antisolvent method, and solar cells were completed through thermal evaporation. Water concentrations within an optimal low range yielded larger crystal grains with fewer grain boundaries, resulting in enhanced charge transport and improved PCE. This improvement is attributed to hydrogen bonding between hydroxyl groups (–OH) in water and iodide ions (I^-), which influences nucleation and crystal growth. Since the antisolvent dropping step in perovskite film formation is highly sensitive to timing and droplet consistency, a micropipette-assisted system was developed using a servo motor for controlled solution delivery. Under optimized dispensing conditions, the proportion of high-quality films increased approximately fourfold, while the variation in PCE decreased by 50%, demonstrating improved reproducibility and reduced human error. These findings highlight the importance of controlling trace water levels in precursor solvents and adopting automated techniques to improve film quality and consistency in perovskite solar cell fabrication.

PLATINUM-DECORATED SnO_2 NANOCRYSTALS FOR HIGHLY SENSITIVE DETECTION OF VOLATILE ORGANIC COMPOUNDS (VOCs)

Reira Takase,[1] Yusuke Inomata,[2] Tetsuya Kida[3,*]
[1]Department of Materials Science and Applied Chemistry, Kumamoto University, Kumamoto, 860-8555, Japan
[2]Faculty of Advanced Science and Technology, Kumamoto University, Kumamoto, 860-8555, Japan
[3]Institute of Industrial Nanomaterials, Kumamoto University, Kumamoto 860-8555, Japan,
*tetsuya@kumamoto-u.ac.jp

Abstract:
Semiconductor metal oxides (SMOx)-based gas sensors detect target gases based on changes in electrical resistance caused by gas adsorption and surface reactions. SMOx are widely used as sensing materials due to their high sensitivity to harmful chemical substances even at ppm-level concentrations. In this study, we focused on tin oxide (SnO_2) as the sensing material because of its low cost, non-toxicity, and high thermal and chemical stability. To improve sensing performance, platinum (Pt) was loaded onto SnO_2 nanocrystals. Both SnO_2 and Pt-loaded SnO_2 were synthesized by a hot-soap method. The synthesized samples were coated on an alumina substrate by screen printing. Their gas sensing properties were evaluated toward 50 ppm ethanol under dry air at different temperatures. The measurements involved ten repeated cycles of flowing air for 30 min followed by ethanol for 30 min, and the average response was calculated as $S = R_{air} / R_{gas}$. 3 wt% Pt-loaded SnO_2 showed the highest response (S=1,198) at 300 °C (Fig. 1). Compared with SnO_2, Pt-loaded SnO_2 exhibited a 3.9-fold increase in sensor response, suggesting that Pt loading on SnO_2 nanocrystals is an effective approach to improve the sensor response to ethanol gas.

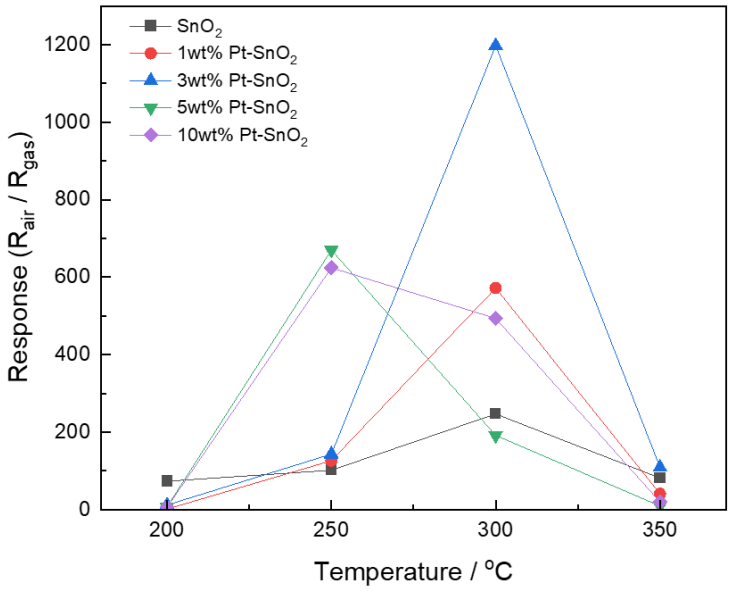

Figure 1. Sensor Response of SnO_2 and Pt-Loaded SnO_2 to 50 ppm Ethanol under Dry Conditions at different temperatures.

POST-TREATMENT OF PALM OIL MILL EFFLUENT USING IMMOBILIZED *Chlorella vulgaris*

Soravit Sukchuay[1], Ploypitcha Pattarapongpetch,[1]* Papitchaya Srithep,[2]
[1]PSU Witthayanusorn Suratthani School (SCiUS), Thailand
[2]Prince of Songkla University, Surat Thani Campus, Thailand
*e-mail: pharidapt78@gmail.com

Abstract:
Palm Oil Mill Effluent (TPOME) remains unsuitable for discharge due to excessive organic matter and nitrogen levels. *Chlorella vulgaris* was immobilized in 2% and 4% sodium alginate, creating a mixture with 2% and 4% sodium alginate concentrations to evaluate its efficacy in TPOME treatment. The results indicated that the 4% concentration achieved the highest biomass density ($6.10 \times 10^5 \pm 3.05 \times 10^4$ cells/mL), while chlorophyll a and carotenoid concentrations reached 2.60 ± 0.05 mg/L and 0.50 ± 0.02 mg/L, respectively. Ammonia and Chemical Oxygen Demand (COD) removal efficiencies were 83.1% ± 2.5% and 53.3% ± 1.8%, respectively. After 12 days, 4% concentration beads exhibited minimal shrinkage (3.00 ± 0.14 mm), demonstrating greater stability than the 2% concentration. These findings indicate that *Chlorella vulgaris* immobilized in 4% sodium alginate is an effective approach for TPOME remediation while simultaneously enhancing biomass production.

PREPARATION AND PHYSICAL PROPERTIES OF POLYURETHANE WASTE/MODIFIED EPOXIDIZED NATURAL RUBBER BLEND

Sa-Ad Riyajan*
[1] Department of Chemistry, Faculty of Science and Technology, Thammasat University, Klongluang, Patumthani, Thailand, 12120
*e-mail: saadriyajan@hotmail.com

Abstract:
A polyurethane foam waste/modified epoxidized natural rubber (MENR) was successfully developed using low-cost, biodegradable, and renewable natural rubber/cassava starch. The modified polyurethane foam waste/MENR efficiently delayed the nutrient release. The maximum swelling ratio was found when using 10% PUW and its value was 560%. The degree of epoxidation in the ENR was about 25% by mole. The tensile properties of PU/MENR had the highest value at 10% PU, with the tensile properties of 18.5 MPa. The PU-added sample was uniform and had pores formed was observed by SEM. Herein matrix swollen capacity and nutrient controlled-release behaviors of the sponge in water were investigated. The amount of urea was encapsulated in matrix was about 50% by weight. The results showed the PUW/MENR successfully transformed with excellent agricultural properties. Urea released longevity of the sponge reached more than 50 days. This research prepared porous waste materials such as polyurethane foam waste, natural rubber, and tapioca starch. This research will not only provide a theoretical basis. But this research helps to develop the urea fertilizer-controlled release when using PU/MENR as polymer matrix.
The rate of urea release from the polyurethane waste/modified epoxidized natural rubber blend at 10%PUW was about 90.2% within 30 h. The biodegradation level of PUW/MENR samples after three months of burial was 80-95%.

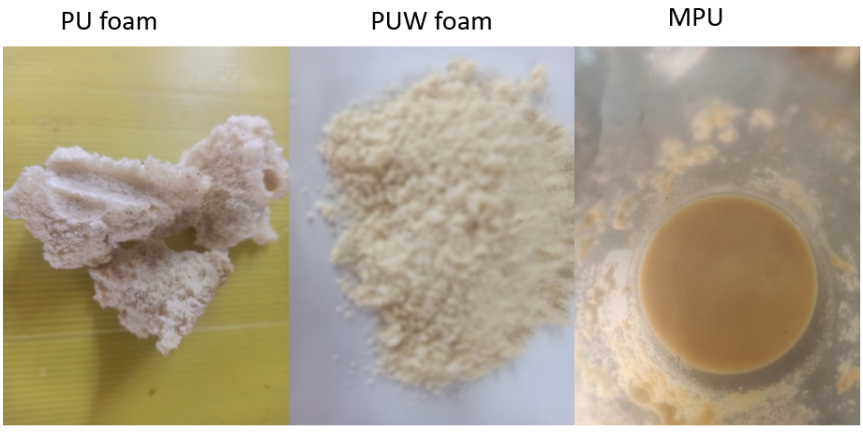

Figure 1.
PU foam, PUW foam, and MPU

PREPARATION OF CHITOSAN/RICE HUSK SILICA/CALCIUM ALGINATE COMPOSITE USE IN CONTROLLED DRUG DELIVERY SYSTEMS FOR FOLIC ACID

Ponpomkwan Chanhom,[1] Chayanan Manawongcharoen,[1] Nutatcha Yowcharoensuk,[1] Phuwit Suwannatain,[1] Jidapa Pimthong,[2] Sakdinun Nuntang[2,*]

[1] Chiang Mai University Demonstration School, Chiang Mai, 50200, Thailand
[2] Industrial Chemistry Innovation Program, Faculty of Science, Maejo University, Chiang Mai 50290, Thailand

*e-mail: Sakdinun.nt@gmail.com

Abstract:
In this study, preparing chitosan/rice husk silica/calcium alginate (CH/RHS/CA) composite was employed as drug delivery for folic acid (FA). The silica particles were achieved from silica precursor obtained from rice husk. Folic acid was attached to the surface of silica particles through direct bonding and bonding through chitosan. Then, X-ray diffraction, N_2 adsorption-desorption analysis, Fourier transform infrared spectroscopy and scanning electron microscopy were used to study the surface and structure of these composite materials. This was done to confirm that silica particles had a chitosan coating and folic acid conjugation and coating with calcium alginate. The CH/RHS/CA/FA composite exhibited a higher drug loading percentage than the pure rice husk silica. The CH/RHS/CA composite exhibited a high folic acid loading of 87.51%. In addition, the effects of the type of silica, pH, time, and temperature on the release of folic acid were also investigated. According to the study, the CH/RHS/CA bead with high folic acid loading exhibited the highest folic acid content, releasing 43.54 mg/g at pH 7 and room temperature over 1 h.

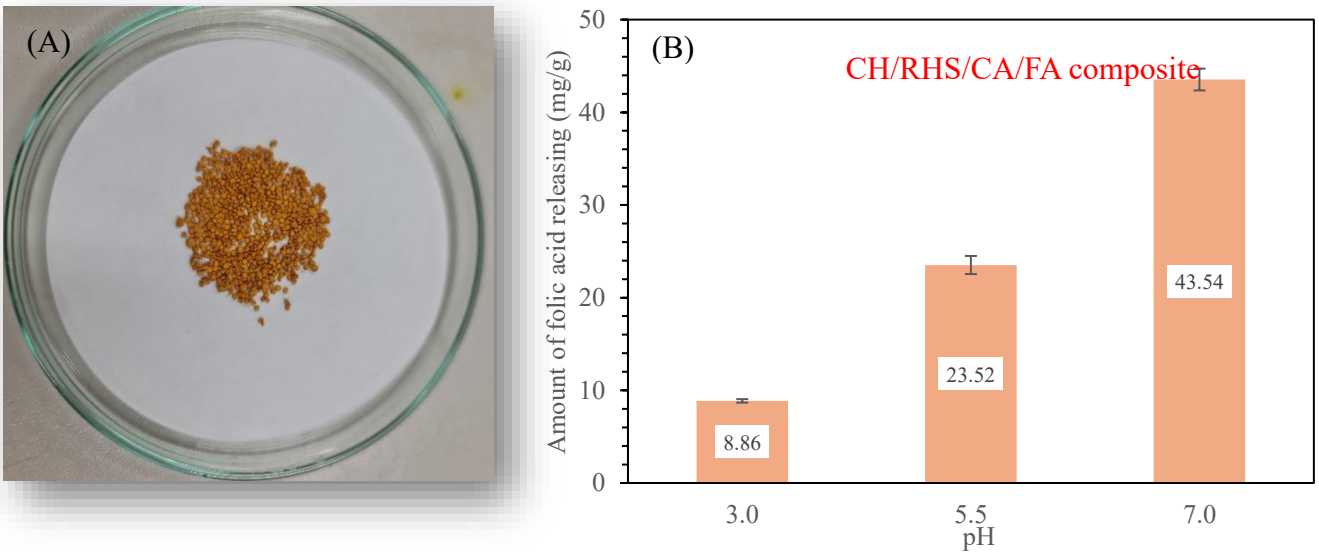

Figure 1.
(A) CH/RHS/CA/FA composite (B) pH effect on folic acid releasing process of CH/RHS/CA/FA composite.

Silica Particles Derived from Rice Husk via Solvent Extraction for Reinforcing Natural Rubber in Soft Cast Applications.

Athitiya Pranprasoet[1] , Chompunuch Boontawee[2]*
Princess Chulabhorn Science High School Nakhon Si Thammarat , Nakhon Si Thammarat , THAILAND
*e-mail: 6606177@pccnst.ac.th

Abstract:

Development of reinforced soft casts utilized silica extracted from rice husk through a solvent extraction method (N Setyawan et al., 2021), focusing on optimizing the silica-to-natural-rubber ratio to achieve suitable splint properties while adding value to agricultural waste. Characterization of the synthesized silica was performed using Fourier Transform Infrared Spectroscopy (FTIR), with results compared to commercially produced silica. Mechanical evaluation of splint materials was conducted using natural rubber latex concentrated to 60% via centrifugation. Dispersion of compounding agents and preparation of five latex formulations containing silica at 0, 1, 2.5, 5, and 10 phr enabled property testing, including tensile and tear strength and density measurements. Fourier Transform Infrared Spectroscopy analysis confirmed that rice-husk-derived silica possessed structural and compositional properties comparable to commercial silica. The formulation containing 2.5 phr silica exhibited the most favorable mechanical performance, with tensile strength of 0.0250 N/mm², tear strength of 8.07 N/mm, and density of 0.32 g/cm³, indicating optimal suitability for soft cast production.

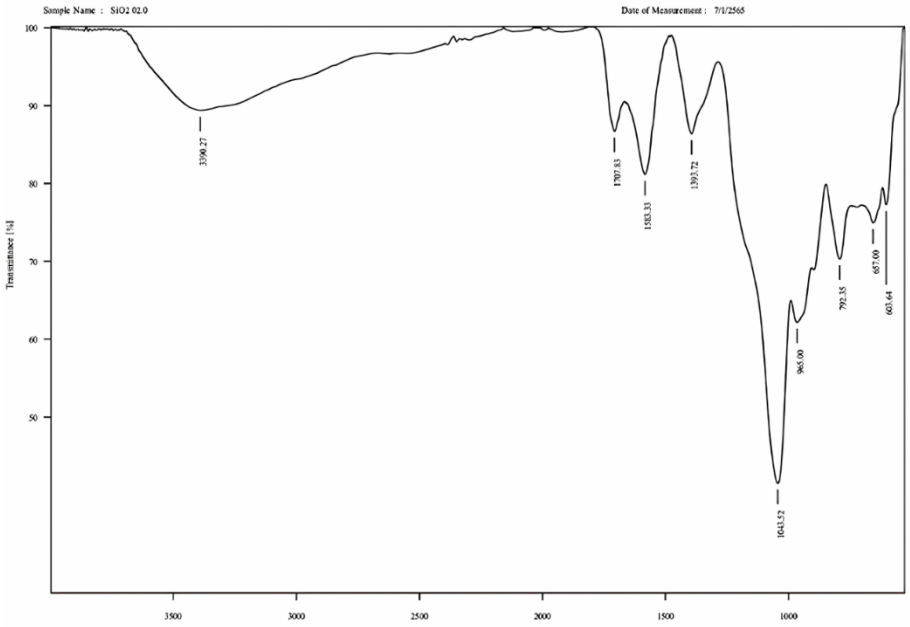

Figure 1. FTIR spectrum analysis of using silica extracted from rice husk via a solvent extraction method

SOLID ELECTROLYTE-TYPE ELECTROCHEMICAL GAS SENSORS WITH MOF-BASED ELECTRODE CATALYSTS FOR N_2O AND CO DETECTION

Mana Yamaguchi,[1] Sohail Ahmad,[2] Yusuke Inomata,[3] Tetsuya Kida[2,*]
[1] Graduate School of Science and Technology, Kumamoto University, Japan
[2] Institute of Industrial Nanomaterials, Kumamoto University, Japan
[3] Faculty of Advanced Science and Technology, Kumamoto University, Japan
*e-mail: tetsuya@kumamoto-u.ac.jp

Abstract:

Electrochemical gas sensors have several advantages over other types of sensors including their wide tunable target gases, high sensitivity, low cost, and easy fabrication. Other desirable requirements for gas sensors include chemical stability, high gas selectivity, and no temperature dependence. In particular, electrochemical gas sensors using solid electrolytes are promising due to their simple detection mechanism and high gas selectivity.

In this study, graphene oxide (GO) membrane is used as solid electrolyte and coupled with Metal-Organic Frameworks (MOFs). The GO membranes are inexpensive and abundant raw materials and have the advantage of high proton conductivity at room temperature. When the target gas molecules come into contact with the sensing electrode's surface, specific electrochemical reactions take place, leading to changes in the electrical properties of the electrode. The development sensing electrode was important to optimize the selectivity, sensitivity, stability, response time, and integration capabilities of electrochemical gas sensors. MOF serve as the sensing electrode catalyst, aiming to develop a highly gas-selective electrochemical sensor. MOFs have been attracting significant attention in gas sensor applications because their structure, conductivity and change transfer reaction can be tailored by selecting organic ligands and metal centers.

The sensor device, shown in Figure 1a, was fabricated to evaluate the gas sensor characteristics, and NiCo-BDC (Ni and Co ions are coordinated with 1,4-H_2BDC (1,4-benzenedicarboxylic acid)) is used as a sensing electrode (SE) catalyst. This sensor showed high selectivity and concentration dependency for N_2O gas (Figure 1b). Furthermore, the sensor using NiCu-CAT as the detection electrode catalyst showed high selectivity for CO. This suggests that the selectivity of sensors can be controlled by MOF species. Simultaneously, the mechanism on the sensing performance was investigated by DRIFTS measurements.

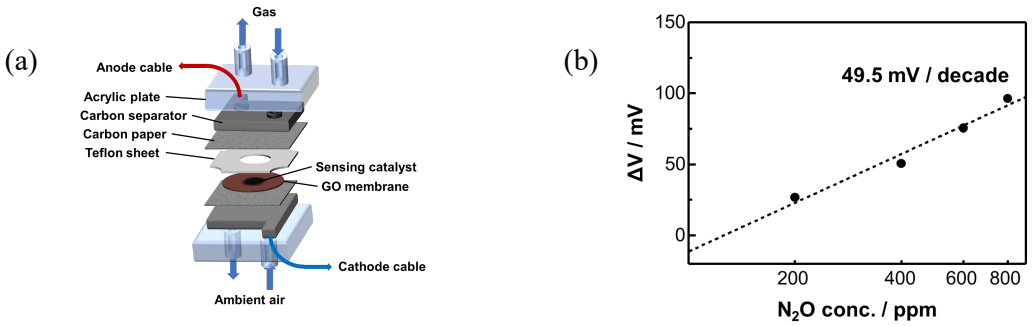

Figure 1.
(a)Schematic of the sensor device using NiCo-BDC and (b) dependence of sensor response on N_2O concentration.

SPENT COFFEE GROUND/RICE HUSK AND RECYCLED PAPER-BASED MYCELIUM BIOCOMPOSITES FOR SUSTAINABLE ROAD GUIDEPOSTS

Pimpet Sratong-on,[1,2] Kanyarat Puttawongsakul,[1,2] Nawin Kanthawee,[1] Sutep Joy-A-Ka,[3] Supaluk Prapan[1,*]
[1]Composite Materials and Lightweight Structure Laboratory, Faculty of Engineering, Thai-Nichi Institute of Technology, Bangkok, 10250, Thailand
[2]Department of Engineering Technology, Faculty of Engineering, Thai-Nichi Institute of Technology, Bangkok, 10250, Thailand
[3]Material Properties and Failure Analysis Laboratory, Thailand Institute of Scientific and Technological Research (TISTR), Pathum Thani, 12120, Thailand
*e-mail: supaluk@tni.ac.th (Supaluk Prapan)

Abstract:
Mycelium biocomposites (MBC) are novel sustainable materials with specific strength, biodegradability, and fire retardancy comparable to hydrocarbon foams. However, their properties are highly dependent on the substrate. Here, we investigated the potential of using high-content spent coffee grounds (SCG) mixed with rice husks (RH) and pure recycled paper (RP) as substrates for MBCs intended for road guidepost materials. *Pleurotus ostreatus* mycelium was cultivated on three compositions: SCG:RH at 50:50, 80:20 weight ratios, and 100% RP. Compression (ASTM D3501), water absorption, and fire-retardant tests (modified UL-94) were conducted, with porosities evaluated by X-ray Micro-CT. MBC/RP exhibited the highest specific strength (6.29 N·m/kg), significantly superior to MBC/SCG80-RH20 (2.23 N·m/kg) and MBC/SCG50-RH50 (1.52 N·m/kg). However, MBC/RP showed a rapid initial water absorption rate (11.5 mg/s) and reached 200% saturation at 72 hours. This high absorption was attributed to the fibrous RP substrate creating highly interconnected pores (52.87%). Conversely, MBC/SCG-RH composites, despite having greater overall porosities (58.27%-62.61%), showed much lower initial absorption rates (≤ 0.21 mg/s) and reached lower saturation (130% at 96 hours), suggesting a greater proportion of closed pore structures. MBC/RP self-extinguished within 25 mm without dripping, while MBC/SCG-RH composites exhibited prolonged afterglow and extensive burning. The superior mechanical properties of MBC/RP suggested its suitability for use as a core material to enhance the specific rigidity of flexible para-rubber guidepost. Future work should investigate its degradation under outdoor conditions.

SURFACE MODIFICATION OF ACTIVATED CARBON FROM RICE HUSK VIA PHYSICAL AND CHEMICAL PRETREATMENTS FOR CATALYTIC APPLICATION IN SOLKETAL PRODUCTION

Sopida Kaewsuk,* Pesak Rungrojchaipon
Applied Chemistry, School of Science, King Mongkut's Institute of Technology Ladkrabang, Bangkok, Thailand
*e-mail: shoopnigdyaok@gmail.com

Abstract:
This study investigates the preparation of acid catalysts from rice husk-derived activated carbon for solketal synthesis. Two pretreatment methods, physical and chemical, were examined. In the physical pretreatment route, rice husk was carbonized at 600 °C and activated with KOH (RH-KOH) or $CuCl_2$ (RH-$CuCl_2$) at a 1:4 ratio and 800 °C. RH-$CuCl_2$ exhibited the highest surface area, acidity, and lowest bulk density, which were further enhanced by sulfuric acid treatment (AC-$CuCl_2$/H_2SO_4), resulting in superior methylene blue adsorption. Using AC-$CuCl_2$/H_2SO_4 as a catalyst, solketal synthesis from glycerol and acetone (1:4 molar ratio) at 60 °C for 3 h achieved 82.84% glycerol conversion, 86.72% selectivity, and 71.85% yield. In the chemical pretreatment route, rice husk was carbonized with concentrated sulfuric acid and subsequently activated by microwave-assisted treatment with KOH or $CuCl_2$ (1:4), further improving surface properties. Catalyst characterization was carried out using Boehm titration, iodine number, BET surface area analysis, TGA, FTIR, and SEM. Overall, the results demonstrate that rice husk-derived activated carbon is an effective and sustainable catalyst for solketal production.

SUSTAINABLE MOLECULARLY IMPRINTED BIOPOLYMERS FOR SELECTIVE ADSORPTION OF TETRACYCLINE

Pattareeya Chaisaowong,[1] Banpot Klinpratoom,[1] Phitchan Srichareon[2] and Nunticha Limchoowong[1,*],
[1]Department of Chemisty, Faculty of Science, Srinakharinwirot University, Bangkok 10110, Thailand
[2]Division of Health, Cosmetic and Anti-Aging Technology, Faculty of Science and Technology, Rajamangala University of Technology Phra Nakhon, Bangkok 10800, Thailand

*e-mail: nunticha@g.swu.ac.th

Abstract:
This study presents the synthesis and characterization of magnetic molecularly imprinted composite biopolymers (MIP) designed for the rapid and selective adsorption of tetracycline contaminants in food and environmental samples. The MIPs were fabricated via a one-pot sonochemical-assisted coprecipitation method, integrating chitosan, cellulose, and β-cyclodextrin as biopolymer matrices with Fe_3O_4 magnetic nanoparticles as the core. Characterization techniques including FTIR, XRD, TEM, and TGA confirmed the successful formation, structural stability, and magnetic responsiveness of the composite. Adsorption studies demonstrated fast kinetics facilitated by ultrasonication, with optimal tetracycline binding at pH 6 and a maximum monolayer adsorption capacity of 141.4 mg/g following the Langmuir isotherm model, indicative of homogeneous binding sites. The MIP exhibited excellent selectivity and reusability over seven cycles with efficient desorption using methanol-acetic acid, maintaining high recovery and enrichment of tetracyclines from milk, pork, tap water, and dental wastewater samples. The system showed resilience to varying ionic strengths and solvent volumes, confirming its robustness for practical application. Overall, the developed magnetic MIP composite offers a promising approach for selective, efficient, and reusable monitoring of antibiotic residues in diverse aqueous matrices.

SYNTHESIS OF ACTIVATED CARBON FROM EGG SHELL FOR CIPROFLOXACIN ANTIBIOTIC REMOVAL

Chetnipat Kunawong,[1] Punnawat Pengthong,[1] Phuktharin Phaisanthanaphat,[1] Napaphat Datpratoom,[1] Chanokchon Anukul,[2] Sakdinun Nuntang[2,*]

[1] Montfort College, Chiang Mai, 50000, Thailand
[2] Industrial Chemistry Innovation Program, Faculty of Science, Maejo University, Chiang Mai 50290, Thailand

*e-mail: Sakdinun.nt@gmail.com

Abstract:
Due to ineffective pharmaceutical wastewater treatment, the aquatic environment is exposed to antibiotic contaminants released by the pharmaceutical industries. These substances are harmful to both humans and aquatic life. This study's purpose is to evaluate the adsorption capacity of activated egg shell as an adsorbent for removing the antibiotic ciprofloxacin (CIP) from an aqueous solution. The egg shell-based activated carbon was successfully synthesized by the simple chemical activation process. Phosphoric acid (H_3PO_4), sodium hydroxide (NaOH) and zinc chloride ($ZnCl_2$) were used as activation agents. XRD pattern revealed the hexagonal structure of activated carbon. The functional group presents in activated carbon was identified using FT-IR spectroscopy. N_2 adsorption–desorption analysis displayed BET surface area of 15-30 m^2/g. The findings demonstrated these materials exhibited a superior removal of ciprofloxacin (> 60%).

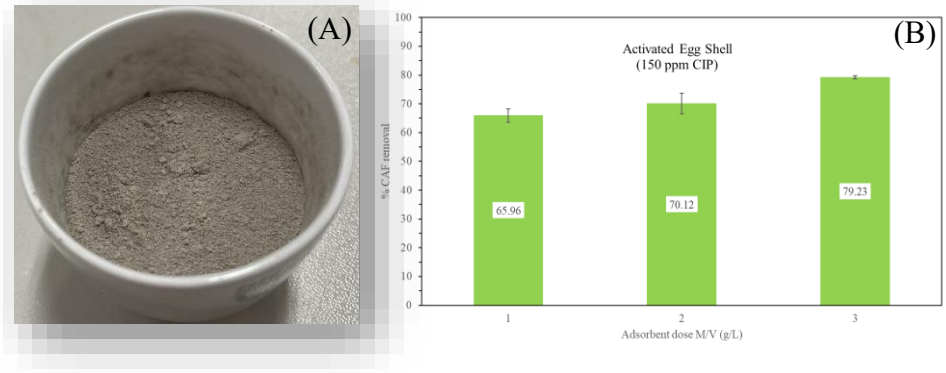

Figure 1.
(A) Activated egg shell (B) CIP removal using activated egg shell in various adsorbent dose.

SYNTHESIS OF HYDROXYAPATITE FROM FLUE GAS DESULFURIZATION GYPSUM FOR ADSORPTION OF Cd^{2+} AND Pb^{2+}

Sukrit Sarati[1,2], Uraiwan Intatha[1,2], Sitthi Duangphet[1,2], Nattakan Soykeabkaew[1,2], Nattaya Tawichai[1,2,*]

[1]School of Science, Mae Fah Luang University, 333 M1, Muang, Chiang Rai, 57100, Thailand

[2]Center of Innovative and Materials for Sustainability (iMatS), Mae Fah Luang University, Thailand

*e-mail: nattaya.taw@mfu.ac.th

Abstract:

A novel method has been developed to valorize flue gas desulfurization (FGD) gypsum, a waste product from coal-fired power plants, by converting it into hydroxyapatite (FGD-HAP) through a hydrothermal process at 150 °C for 24 hours with a fixed calcium-to-phosphorus (C/P) ratio of 1.67. XRD confirmed a well-crystallized hydroxyapatite of more than 80%. The FTIR spectra showed characteristic PO_4^{3-} and OH^- vibration bands, further verifying the successful synthesis of hydroxyapatite. SEM and BET revealed a porous morphology and a high specific surface area, facilitating effective metal ion interaction. The cadmium and lead concentrations were analyzed using inductively coupled plasma optical emission spectroscopy (ICP-OES) to evaluate adsorption efficiency. The FGD-HAP exhibited exceptional adsorption capacities for heavy metals, achieving 270 mg/g for Pb^{2+} and 40 mg/g for Cd^{2+}. These capacities are competitive with or superior to hydroxyapatite derived from conventional sources like eggshell or bone ash. The exceptional performance, particularly for Pb^{2+}, is attributed to a highly effective dissolution-precipitation mechanism, leading to the formation of stable lead phosphate phases. This work establishes FGD gypsum not as a waste but as a sustainable and superior precursor for synthesizing effective adsorbents, offering a circular economy solution for both industrial waste management and environmental remediation.

SYNTHESIS OF POLYVINYL ALCOHOL/Ag-NPs BIOCHAR/SODIUM ALGINATE GEL BEADS AND THEIR ANTIBACTERIAL ACTIVITY AGAINST GRAM POSITIVE BACTERIA

Supanan Wanitlertthanasarn,[1] Laphatrada Thambancha,[1] Napaphat Pripwai[1], Jiratchaya Ruechai[1], Jidapa Pimthong,[2] Sakdinun Nuntang[2,*]

[1] Montfort College, Chiang Mai, 50000, Thailand
[2] Industrial Chemistry Innovation Program, Faculty of Science, Maejo University, Chiang Mai 50290, Thailand

*e-mail: Sakdinun.nt@gmail.com

Abstract:
In this study, polyvinyl alcohol/silver nanoparticle-carrying biochar/alginate gel beads (PVA/Ag-NPs-C/SA) were designed for suppressing gram positive bacteria. The biochar prepared from corn husk was loaded with nano silver particles as the filler, alginate as the substrate, and polyvinyl alcohol (PVA) as the additive to enhance the mechanical properties. Their structure and morphology were characterized by X-ray diffraction (XRD, Brunauer-Emmett-Teller (BET) specific surface area and Fourier transform infrared spectroscopy (FTIR). The results indicated that silver nanoparticles were successfully loaded onto the corn husk biochar. The composite material displayed an amorphous carbon structure and possessed a high BET surface area of 45.5 $m^2 g^{-1}$. Furthermore, it demonstrated higher stability in aqueous solutions than the composite hydrogel material without Ag-NPs biochar but showed lower swelling in the aqueous solution. Their antibacterial activities were against gram-positive bacteria such as *Staphylococcus aureus (S. aureus)* and *Staphylococcus epidermidis (S. epidermidis)* examined by tablet colony counting method and optical density (OD) method. The results showed that the PVA/Ag-NPs-C/SA composite was more effective and had superior antibacterial performance than initial corn husk biochar which indicated that PVA/Ag-NPs-C/SA composite has good properties for antibacterial gram-positive bacteria.

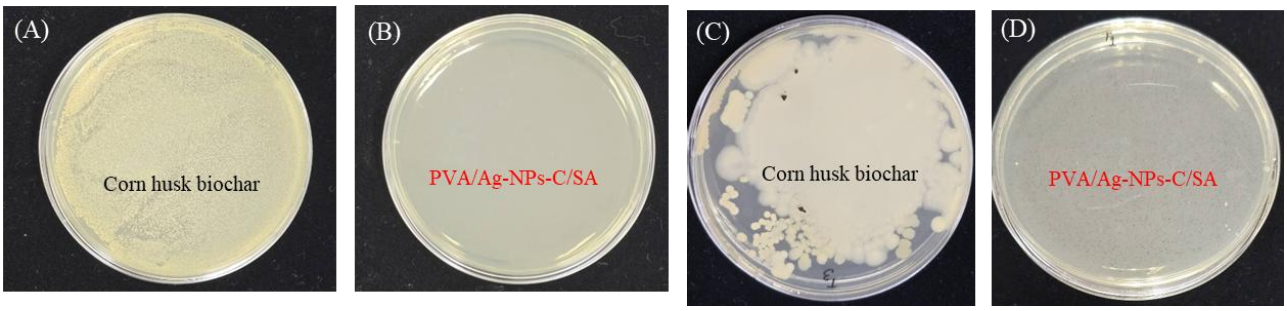

Figure 1.
Inhibition tests against *S. aureus* (A) (B) and *S. epidermidis* (C) (D) of Corn husk biochar and PVA/Ag-NPs-C/SA material.

SYNTHESIS, STRUCTURAL ANALYSIS, AND THERMAL PROPERTIES OF A BIMETALLIC NICKEL-MANGANESE GLYCEROLATE

Tikamporn Yimsri, Manutsanan Phromsorn, Pesak Rungrojchaipon*
Industrial Chemistry, School of Science, King Mongkut's Institute of Technology Ladkrabang, Bangkok, Thailand
*e-mail: pesak.ru@kmitl.ac.th, 65050718@kmitl.ac.th

Abstract:
This study focuses on synthesis and characterization of nickel-manganese glycerolate from nickel(II) acetate tetrahydrate and manganese(II) acetate tetrahydrate reacting with glycerol. The precursor to glycerol molar ratios investigated were 1:2, 1:20 and 1:200, with reactions conducted using heating mantle methods at temperatures 120, 140 and 160 °C. Product yields were compared under these conditions. The synthesized materials were characterized by XRD, SEM, FTIR, TGA and Particle Analysis. The results confirmed that nickel-manganese glycerolate was successfully obtained at molar ratios of 1:20 and 1:200, as evidenced by characteristic peaks in the spectra. Both precursor ratio and reaction temperature strongly influenced the product yield, with the highest yields achieved at 160 °C for the 1:20 and 1:200 conditions. Particle size analysis revealed that the 1:20 molar ratio produced the largest average particle size among the tested conditions.

Ternary and Quaternary Amorphous Oxide Nanoparticles for Selective Acetone Gas Detection

Yu Jono,[1] Yusuke Inomata,[2] Tetsuya Kida [3,*]
[1]Graduate School of Science and Technology, Kumamoto University, Japan
[2]Faculty of Advanced Science and Technology, Kumamoto University, Japan
[3]Institute of Industrial Nanomaterials, Kumamoto University, Japan
*e-mail: tetsuya@kumamoto-u.ac.jp

Abstract:

Semiconductor gas sensors detect low-concentration gases using changes in electrical resistance caused by gas adsorption and reaction on the material surface. Although acetone detection using semiconductor gas sensors is non-invasive, challenges remain, including high operating temperatures, low selectivity, and unclear sensing mechanisms. Therefore, we focus on amorphous In-Sn-Zn oxide (ITZO) nanoparticles and amorphous Ga-In-Sn-Zn oxide (GITZO) nanoparticles. These amorphous multi-metal oxides nanoparticles consist of randomly arranged metal atoms, which are expected to increase the number of defect sites and acetone adsorption. Since acetone interacts with Lewis acid sites, increasing the number of these sites on p-block metal oxides is expected to improve detection performance.

In this study, we compared amorphous ITZO nanoparticles with amorphous GITZO nanoparticles. GITZO was synthesized using the hot soap method. The GITZO sensor showed the highest sensor response (R_{air}/R_{gas} = 79) at a low temperature of 250°C, compared to conventional single metal oxide sensors (such as SnO_2 and ZnO). Additionally, the sensor response ratio for acetone versus ethanol (a typical interfering gas of acetone) at 10 ppm was highest for GITZO, demonstrating its acetone selectivity (Fig. 1b). We investigated the sensing mechanism by performing gas adsorption analysis, temperature-programmed desorption (TPD), *operando* diffuse reflectance Fourier transform infrared spectroscopy (DRIFTS) under gas flow, and UV-Vis spectroscopy. These analyses revealed that the sensor response is related to the partial oxidative decomposition of acetone adsorbed on Lewis acid sites on the material surface. The enhanced sensor response and selectivity of GITZO compared to ITZO are attributed to the increased number of Lewis acid sites and higher catalytic activity induced by quaternization.

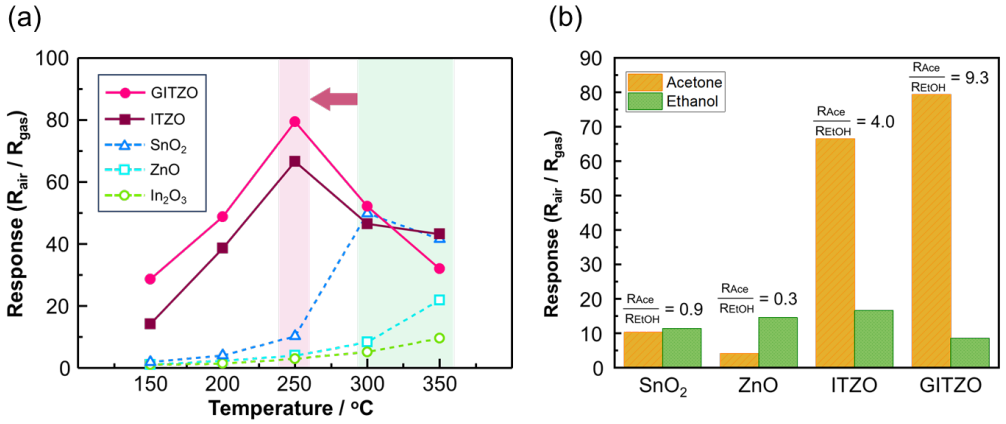

Figure 1. (a) Temperature dependence of the sensor response to 10 ppm acetone at 150°C to 350°C and (b) Gas selectivity to 10 ppm acetone and 10 ppm ethanol at 250°C.

The Geochemical Identity and Provenance of Black Spinel Gem (Nil) in Kanchanaburi, Thailand.

Piyatida Sangtong,[1,]*Janjira Sratongyung[2]

[1]Geoscience program, Mahidol University Kanchanaburi Campus, Thailand
[2]Science Laboratory for Education Division, Mahidol University Kanchanaburi Campus
*e-mail: Piyatida.san@mahidol.ac.th

Abstract:

The gem material of Thailand is deposited particularly in Chanthaburi and Kanchanaburi. The host rock is in Cenozoic basalts that have different gem materials (e.g., spinel, sapphire, pyroxene, and zircon). The black gem in Kanchanaburi is well-known and locally commonly known as "*Nil Muang Kan*" which is a recognition comparable to black diamond. Nil is considered to have originated in Kanchanaburi, consisting mainly of clinopyroxene and spinel. In this research study on the chemical composition of 3 types commonly known: Nil Sian or Nil Tako (black pyroxene), Nil Tun (black spinel), and Nil Tid Lak (Magnesium spinel). There are chemical composition that represents the host basalt is formed from a primary magma. The spinel group in the isomorphous series: Spinel series (aluminum), Magnetite series (ferric iron), Chromite series (chrome). The spinel classification diagram displayed as Nil Sian and Nil Tun range in Al-magnetite and Fe-spinel. In addition, Nil Sian has an outstanding Ca-value that represents clinopyroxene. On the other hand, Nil Tid Lak consists mainly of Fe, Ti, and V. The outstanding of Fe-value is a signature of black spinel in Kanchanaburi. The identity of black spinel is consistent with the occurrence of mineral deposits in the western region of Thailand. Although the nature of its occurrence and geological characteristics require further evidence to confirm it. However, the unique geological event of tectonic and basalt origin makes *Nil Muang Kan* more special.

TYPE MORPHIC FEATURES OF NATIVE GOLD FROM PLACER GOLD DEPOSITS IN BANG SAPHAN AREA, SOUTHERN PART OF THAILAND

Ladda Tangwattananukul*, Sarita Wongin

Department of Earth Sciences, Faculty of Science, Kasetsart University, Bangkok 10900, Thailand.

*e-mail: fscildt@ku.ac.th

Abstract:
In Thailand, the Bang Saphan area is well known for native gold panning, as secondary gold is transported and deposited with sediments in debris flows or rivers. However, the specific characteristics of secondary gold, including its transport processes and association with host rocks, have not yet been reported in published studies. This study aims to investigate the characteristics of secondary gold, including its size, shape, and concentrations of gold and iron, to determine the relationships between different morphologies, gold color variations, and associated heavy minerals. Secondary gold can be classified into three types and ten morphological categories based on color, shape, and size. Type I is characterized by red-yellow coloration, containing approximately 90 wt% Au, <1 wt% Ag, and ~10 wt% Fe. Type II is yellow, containing ~90 wt% Au, ~10 wt% Ag, and <1 wt% Fe. Type III is orange-bronze, containing <90 wt% Au, ~1 wt% Ag, and >10 wt% Fe. Morphologies of secondary gold are classified as lumpy–globular, irregular, nuggets, dendritic, subdiscoidal, teardrop, cornflake, elongated, botryoidal, and plate, occurring in various sizes. The most common forms are lumpy–globular, nuggets, and teardrops. Gold primarily coats quartz, hematite, and ilmenite, whereas cassiterite and wolframite remain uncoated due to differences in chemical interactions, stability, and surface properties. In summary, secondary gold in the Bang Saphan area is associated with Si, Fe, Cu, Sn, Zr, W, and Zn. These heavy minerals influence both the color and quantity of gold.

ZINC GLYCEROLATE SYNTHESIZED VIA MICROWAVE AND METHANOL-ASSISTED REFLUX METHODS: COMPARATIVE CHARACTERIZATION AND THERMAL STABILIZATION IN PVC

Thanakorn Teekasung,* Pesak Rungrojchaipon
Applied Chemistry, School of Science, King Mongkut's Institute of Technology Ladkrabang, Bangkok, Thailand
*e-mail: 66056037@kmitl.ac.th

Abstract:
Zinc glycerolate (ZnGly) was synthesized using two different approaches: a microwave-assisted method and a methanol-aided conventional reflux process. Zinc oxide (ZnO) and glycerol (Gly) were employed as precursors, with zinc acetate serving as the catalyst. A ZnO:Gly molar ratio of 1:7 was applied in the microwave synthesis, whereas the reflux method utilized an approximate ratio of 1:6.7. Methanol was introduced as a co-solvent in the reflux system to enhance solubility and improve reaction efficiency. The microwave-assisted synthesis produced a yield of 76.75% ZnGly at 80 °C for 60 min, while the methanol-aided reflux method achieved a significantly higher yield of over 90% at 70 °C for 30 min. Compared with previously reported reflux syntheses, the developed method required a lower reaction temperature and shorter processing time, demonstrating superior energy efficiency and process optimization. The crystalline structure and chemical bonding of ZnGly were confirmed by X-ray diffraction (XRD) and Fourier-transform infrared spectroscopy (FTIR), which revealed characteristic diffraction peaks and Zn–O–C vibrational bands typical of zinc glycerolate. When incorporated into polyvinyl chloride (PVC) as a thermal stabilizer, reflux-synthesized ZnGly extended the initial discoloration time from approximately 10 min for pure PVC to about 28 min, while microwave-synthesized ZnGly delayed it to around 20 min at 180 °C. These results indicate that ZnGly, particularly when synthesized via the methanol-aided reflux route, provides enhanced thermal stabilization performance. Overall, this study demonstrates that combining methanol-aided low-temperature reflux synthesis with microwave-assisted synthesis offers high-yield, energy-efficient, and sustainable strategies for ZnGly production and highlights its potential application in polymer thermal stabilization.

F: FOOD SCIENCE AND TECHNOLOGY/AGRICULTURAL SCIENCE

Formulation of Bioactive Coating from Mangosteen Peel Tannin Extract for Retarding Fruit Quality Deterioration

Kotchaphan Sangsriin[1,*],Klowkarimook Lookin[2],Nichakamon kaewnoona[3], Boonyaporn Chukiatchat[4]
Princess Chulabhorn Science High School Nakhon Si Thammarat, 120 M.1 Bangjak Sub-district, Muang Nakhon Si Thammarat, Thailand
*6606137@pccnst.ac.th

Abstract:

This study aimed to investigate the antioxidant potential of tannin extract from mangosteen peel in inhibiting vitamin C oxidation and to develop it into a bioactive coating for extending the shelf life of fruits. The research was motivated by postharvest fruit deterioration, a major cause of economic losses, and the underutilization of mangosteen peel, an agricultural by-product abundant in bioactive tannins with antioxidant properties. The study hypothesized that mangosteen peel tannin extract could inhibit vitamin C oxidation and, when incorporated into bioactive films, enhance the preservation of fruits.

Tannin extract was obtained through ethanol extraction. The inhibitory effect of the extract on vitamin C oxidation was evaluated by measuring the absorbance at 265 nm using a spectrophotometer.The results showed that a concentration of 0.59% w/v achieved 50% inhibition (IC_{50}). This information was used to formulate bioactive films composed of gelatin, chitosan, sorbitol, and tannin extract. Three formulations were prepared, cast into thin films, and assessed for physical properties and coating performance.

Apples coated with the films were stored at 25 °C for 14 days. The F1 formulation (gelatin 2.00% w/v, chitosan 1.50% w/v, sorbitol 0.20% w/v, tannin extract 0.59% w/v) exhibited the best performance, showing minimal film porosity, reducing weight loss by 49.65%, suppressing flesh discoloration by 20.89%, maintaining tissue density by 27.53%, and increasing soluble solids content by 2.11% compared with uncoated controls.

In conclusion, mangosteen peel tannin extract shows significant potential as an antioxidant agent for bioactive coatings, effectively extending the shelf life of fruits. This approach not only reduces postharvest losses but also offers a sustainable strategy for valorizing agricultural by-products and enhancing the econ omic value of local fruit resources.

BIOCONVERSION OF MEALWORM (*Tenebrio molitor*) FRASS BY BLACK SOLDIER FLY LARVAE (*Hermetia illucens*) SIGNIFICANTLY IMPROVED QUANTITY AND QUALITY OF AQUAFEED PROTEIN

Panitta Boonsrirat,[1] Nutt Nuntapong,[1] Aekkaraj Nualla-ong,[2] Karun Thongprajukaew,[3,*]
[1]Aquatic Science and Innovative Management Division, Faculty of Natural Resources, Prince of Songkla University, Songkhla 90110, Thailand
[2] Division of Biological Science, Faculty of Science, Prince of Songkla University, Songkhla 90110, Thailand
[3]Applied Aquatic Animal Nutrition Laboratory, Division of Health and Applied Sciences, Faculty of Science, Prince of Songkla University, Songkhla 90110, Thailand
*e-mail: karun.t@psu.ac.th

Abstract:

This study investigated the bioconversion of mealworm frass (MF) by black soldier fly larvae (BSFL; *Hermetia illucens*) and evaluated its potential as a high-quality aquafeed protein. The experiment was conducted using a completely randomized design, comprising two treatments and quadruplicate sets of samples. The frass from mealworm was efficiently converted by BSFL over a 10-day period under optimized substrate utilization (1: 5 *w*/*w* of BSFL per MF, 65 ± 5% relative humidity). Proximate analysis revealed significantly increased crude protein (244 ± 2 vs 487 ± 3 g/kg of dry matter), ether extract (10.7 ± 0.2 vs 24.4 ± 0.4 g/kg of dry matter), ash (111 ± 1 vs 121 ± 1 g/kg of dry matter), crude fiber (170 ± 1 vs 224 ± 1 g/kg of dry matter) contents, and gross energy (14.2 ± 0.1 vs 15.0 ± 0.1 kJ/g) in BSFL frass (BF) relative to MF, suggesting enhanced nutrient concentration through larval growth and development ($p < 0.001$). Conversely, a reduction in nitrogen-free extract contents (466 ± 2 vs 145 ± 3 g/kg of dry matter) was observed during bioconversion. Essential and non-essential amino acid profiles were similar between MF and BF, reflecting preserved protein balance ($p > 0.05$). Fourier transform infrared spectroscopy analysis highlighted changed spectra characteristic and increased α-helix/β-sheet ratios and β-turns in BF relative to MF ($p < 0.05$), indicative of protein denaturation and conformational change favorable for digestion. *In vitro* protein digestibility of BF was significantly improved when screening using digestive enzymes from economic important fish, Nile tilapia (*Oreochromis niloticus*) ($p < 0.001$). These data suggest that BF is an alternative protein source that can be used in aquatic animal feeds.

EFFECT OF ANGKAK (FERMENTED RED RICE) ADDITION ON THE PHYSICAL AND SENSORY QUALITY OF RETORTED LAMB SAUSAGES DURING ROOM TEMPERATURE STORAGE

Ade Luthfi Ramadhani, Pradita Iustitia Sitaresmi, Ali Agus, *Endy Triyannanto

Department of Animal Products Technology, Faculty of Animal Science, Universitas Gadjah Mada

**Coressponding email*: endy.triyannanto@ugm.ac.id

ABSTRACT :

This research aimed to determine the effects of *Monascus purpureus* (angkak) addition, storage duration, and their interaction on the physical and sensory qualities of retorted lamb sausages. Angkak was incorporated into the formulation at levels of 0%, 1%, 1.5%, and 2%. The sausages were subsequently stored at room temperature for 0, 7, 14, and 21 days. The physical parameters tested included pH, water holding capacity (WHC), tenderness, and color (analyzed for lightness, redness, and yellowness). Sensory attributes measured were color, taste, aroma, texture, and overall acceptability. Physical quality data were analyzed using a factorial Completely Randomized Design (CRD) Analysis of Variance (ANOVA), with Duncan's New Multiple Range Test (DMRT) used for follow-up analysis. Sensory data utilized the non-parametric Kruskal-Wallis test, with DMRT for significant differences. The analysis of physical quality demonstrated the comprehensive influence of Angkak, revealing that its addition had a significant effect ($P<0.05$) on pH, WHC, lightness, redness, and yellowness. This indicates that angkak addition substantially modifies the stability and color characteristics of the sausages. In contrast, storage duration also showed a significant effect ($P<0.05$), primarily influencing pH, WHC, lightness, and yellowness. Furthermore, the combined interaction between angkak addition and storage time was critical, as it significantly affected ($P<0.05$) pH, WHC, lightness, redness, and yellowness. The sensory analysis further highlighted Angkak's dominant role: angkak addition and its interaction with storage duration significantly affected ($P<0.05$) all sensory attributes measured: color, taste, aroma, texture, and overall acceptability. Conversely, storage duration alone had a significant effect ($P<0.05$) only on the taste of the lamb sausages. These results strongly emphasize that the incorporation of angkak is the primary factor driving changes in the overall sensory profile. In conclusion, these findings establish that the addition of Angkak is highly effective in formulating retorted lamb sausages, as it significantly influences nearly all physical parameters and exhibits a broad, dominant effect across all measured sensory qualities. This suggests that angkak can be utilized to improve formulation and potentially enhance the stability and shelf-life of retorted lamb sausages during room temperature storage.

Keywords: *Monascus purpureus*, sausage, lamb sausage, storage, retort pouch

Evaluation of probiotic *Bacillus* against pathogenic bacteria in seabass (*Lates calcarifer*)

Achiraya Nuisee[1], Natwarat Netnopparat[1], Patima Permpoonpattana[2]*, Orathai Dangsawa[3]*
[1]PSU Wittayanusorn Surat Thani School
[2]Department of Agricultural Science and Technology, Faculty of Innovative Agriculture, Fisheries and Food, Prince of Songkla University, Surat Thani Campus
[3]Sciencetific Laboratory and Equipment Center, Prince of Songkla University, Surat Thani Campus
*e-mail: achirayanuisee@gmail.com

Abstract:

This study aimed to evaluate the potential of probiotic *Bacillus* sp. bacteria in inhibiting pathogenic bacteria in seabass. Four *Bacillus* sp. isolates, namely KP5, KNSH11, PWR04, and SHPS6, were tested for their ability to form spores. The results showed that the spore formation efficiencies of the four isolates were 95.44%, 87.38%, 85.30%, and 78.27%, respectively. Antibiotic susceptibility testing of four bacterial isolates using the disc diffusion method showed that all were susceptible to gentamicin. Chloramphenicol was also effective, especially against KP5 and SHPS6. SHPS6 and PWR04 were resistant to ampicillin and cloxacillin, while KNSH11 showed resistance to ampicillin. KP5 showed no resistance to any of the tested antibiotics. The acid and bile salt tolerance test showed acid survival rates higher than 74% and bile salt survival rates higher than 75%. The ability to inhibit pathogenic bacteria was tested using the agar well diffusion method with cell free supernatant (CFS) from the four *Bacillus* sp. isolates. It was found that the CFS from KP5, KNSH11, and PWR04, when cultured in Tryptic Soy Broth (TSB) for 24 hours, could inhibit *Pseudomonas aeruginosa*. The CFS from SHPS6, when cultured in Nutrient Broth (NB) for 72 hours, inhibited the pathogenic isolate PTFOR09. The study also tested the ability of the *Bacillus* sp. isolates to inhibit biofilm formation by pathogenic bacteria in seabass. The results showed that the CFS of all isolates was able to inhibit biofilm formation by pathogenic bacteria in seabass, including *Pseudomonas aeruginosa*, *Staphylococcus aureus*, *Vibrio parahaemolyticus*, and the pathogenic isolate PTFOR09. Therefore, this study suggests that all four *Bacillus* sp. isolates have probiotic properties and can inhibit pathogenic bacteria in seabass. These probiotics can be used in aquaculture practices and the animal feed industry to improve fish health and prevent diseases.

GENOME-WIDE ASSOCIATION STUDY (GWAS) REVEALS ENDOSPERM-SPECIFIC GENES (*OsEnS*) AND *Wx* GENE REGULATING SEED STORAGE PROTEIN (SSP) IN RICE GRAIN (*Oryza sativa* L.)

Piyamongkol Mangkalasane[1,4], Parin Taweechotworakul[4], Thanyakorn Rongsawat[4], Samart Wanchana[2,4], Siwaret Arikit[3,4,*]

1. Center of Agricultural Biotechnology, Kasetsart University, Kamphaengsaen Campus, Nakhon Pathom 73140 Thailand
2. National Center for Genetic Engineering and Biotechnology (BIOTEC), 113 Thailand Science Park, Pahonyothin Road, Khlong Luang, Pathum Thani 12120, Thailand
3. Department of Agronomy, Faculty of Agriculture at Kamphaeng Saen, Kasetsart University, Kamphaeng Saen Campus, NaKhon Pathom, 73140, Thailand
4. Rice Science Center, Kasetsart University, Kamphaeng Saen, Nakhon Pathom 73140, Thailand

*e-mail: arikit@gmail.com

Abstract:

Rice (*Oryza sativa* L.) is a crucial source of carbohydrates and protein, essential for human nutrition. Seed storage proteins (SSPs) play a significant role in determining rice's nutritional and culinary attributes. Despite the importance of SSPs, the genetic basis for these traits remains unclear. This study aimed to identify SSP-related genes through the analysis of 2 seasons of indica rice varieties, including 2018 and 2019, using 189 and 210 accessions of indica rice varieties from the Thai rice germplasm, respectively. The SSPs were quantified using Bradford's method, and genotype-phenotype associations were examined via a Genome-Wide Association Study (GWAS) using GLM models. We identified 9 quantitative trait loci (QTLs) associated with SSPs across 7 chromosomes (2, 6, 7, 8, 9, 11, and 12). Interestingly, a QTL on chromosome 7 (*qSSP7*) was consistently identified in 2 seasons. Within a 400-kb window, linkage disequilibrium analysis (LD) revealed 27 genes, with 8 containing functional SNPs. Gene expression analysis (*RiceXpro* database) identified 5 candidate genes that are highly expressed in the rice endosperm. Based on Co-expression network analysis (*RiceFREND* database), our 4 identified candidate genes (*Os07g0213600*, *Os07g0213800*, *Os07g0214100*, and *Os07g0214300*) are involved in essential endosperm-specific regulation with seed storage protein regulatory genes such as *GLUD1* (Glutelin type-D 1) and prolamin-related genes. Therefore, these candidate genes are suggested to be involved in SSPs regulation. Our findings provide novel insights into the genetic mechanisms controlling protein synthesis and accumulation in rice, which may aid breeding programs focused on improving SSPs content.

Identification of Genetic Loci Associated with Stomatal Density in Rice (*Oryza sativa* L.) through Genome-Wide Association Studies

Watchara Phetluan[1,2], Samart Wanchana[3], Wanchana Aesomnuk[3], Julian Adams[4], Mutiara K. Pitaloka[5], Vinitchan Ruanjaichon[3], Apichart Vanavichit[5], Theerayut Toojinda[3], Julie E. Gray[4], Siwaret Arikit[5,6]*

[1] *Center for Agricultural Biotechnology, Kasetsart University, Kamphaeng Saen Campus, Nakhon Pathom 73140, Thailand*

[2] *Center of Excellence on Agricultural Biotechnology: (AG-BIO/MHESI), Bangkok 10900, Thailand*

[3] *National Center for Genetic Engineering and Biotechnology (BIOTEC), 113 Thailand Science Park, Pahonyothin Road, Khlong Nueng, Khlong Luang, Pathum Thani 12120, Thailand*

[4] *Plants, Photosynthesis and Soil, School of Biosciences, University of Sheffield, Sheffield S102TN, United Kingdom*

[5] *Rice Science Center, Kamphaeng Saen Campus, Kasetsart University, Nakhon Pathom 73140, Thailand*

[6] *Department of Agronomy, Faculty of Agriculture at Kamphaeng Saen, Kamphaeng Saen Campus, Kasetsart University, Nakhon Pathom 73140, Thailand*

**Corresponding author, e-mail: siwaret.a@ku.th*

Stomata play a pivotal role in controlling both photosynthetic activity and water loss. Although stomatal biology has been studied for centuries, the genetic determinants underlying stomatal development in crop species remain far less understood than in the model plant *Arabidopsis thaliana*. In our study, we observed more than a 2.5-fold variation in leaf stomatal density among 235 rice accessions. Genome-wide association analysis (GWAS) revealed five quantitative trait loci (QTLs) linked to stomatal density on chromosomes 2, 3, 9, and 12. Within the haplotype blocks of these QTLs, 42 genes were identified, nine of which exhibited haplotypes associated with distinct stomatal densities. These included a gene encoding trehalose-6-phosphate synthase, an enzyme previously implicated in stomatal density variation in Arabidopsis, as well as genes encoding a B-BOX zinc finger family protein, a leucine-rich repeat family protein, and the 40S ribosomal protein S3a, none of which have been previously associated with stomatal traits. Additional analysis demonstrated that a closely related B-BOX protein* influences stomatal development in Arabidopsis. Collectively, these findings provide new insights into the genetic basis of stomatal density in rice. The identified QTLs and candidate genes represent valuable targets for breeding programs aimed at manipulating stomatal density to enhance photosynthetic performance, water-use efficiency, and drought resilience.

Keywords: rice, stomatal density, GWAS, QTLs, gene

Identification of Root Responsive Genes Underlying Penetration Ability in Compacted Soil Using QTL-Seq in Rice (*Oryza sativa* L.)

Suparad Klinsawang[1], Wanchana aesomnuk[2], Samart Wanchana[3], Jonaliza L. Siangliw[2], and Siwaret Arikit[1,3,*]

[1] Department of Agronomy, Faculty of Agriculture at Kamphaeng Saen, Kasetsart University, Kamphaeng Saen, Nakhon Pathom 73140, Thailand

[2] National Center for Genetic Engineering and Biotechnology (BIOTEC), National Science and Technology Development Agency (NSTDA), Thailand Science Park, Phahonyothin, Khlong Nueng, Khlong Luang, Pathum Thani 12120, Thailand

[3] Rice Science Center, Kasetsart University, Kamphaeng Saen Campus, Nakhon Pathom 73140, Thailand

*Corresponding author, e-mail: siwaret.a@ku.th

Abstract:

Nowadays, many agricultural areas have been becoming modern agriculture, where heavy machinery and equipment have been intensively used. According to increasing crop intensity and reducing labor. Meanwhile, heavy machinery loads result in soil compaction, which has been affecting plant growth, which influence plant yield. The stunning root growth under compacted soil is directly contributed by restricted ethylene diffusion and the crosstalk between auxin, ABA, and ethylene. This study aims to screen and evaluate root-responsive characteristics under ethylene treatment and to identify genomic regions associated with root sensitivity to compaction by using three different systems. Firstly, the ethylene chamber system was used to evaluate the ethylene sensitivity in the root. Next, we developed a bi-parental population by crossing Dharia and PTT1 and used the F_2 progeny to perform QTL-seq for root penetrating ability (RPA) under a compacted gel-based system. As a result, significant QTLs on chromosome 3 were identified for RPA ($p<0.01$). Ten promising candidate genes for RPA were identified based on annotation, variant effect and literature mining. Notably, *LOC_Os03g18600* (*OsPYL/RCAR4*), an ABA receptor, *LOC_Os03g18910* (*OsBC1L1*), COBRA-Like (COBL) family protein and *LOC_Os03g19310* (*OsGT4*), a galactosyl transferase family protein, were identified as potential regulators of root responses under stress conditions. The polymorphism in all candidate genes can significantly group the phenotype based on the SNP allele and indels. In addition, we also evaluated the root response between control and soil compaction treatments among parents. The results in this study pave the way for further research into the genetic mechanism of root penetration ability in rice at the seedling stage and could be used as breeder-friendly markers in future breeding programs.

LOW-COST NITROGEN SOURCES FOR POLY-γ-GLUTAMIC ACID PRODUCTION FROM SUGARCANE BAGASSE

Panalee Watthana[1], Thanaporn Wichai[2], Panaya Kotchaplai[2,3,4]*
[1]Program in Biotechnology, Faculty of Science, Chulalongkorn University, Bangkok, Thailand
[2]Institute of Biotechnology and Genetic Engineering, Chulalongkorn University, Bangkok, Thailand
[3]Center of Excellence in Bioconversion and Bioseparation for Platform Chemical Production, Institute of Biotechnology and Genetic Engineering, Chulalongkorn University, Bangkok, Thailand
[4]Water Science and Technology for Sustainable Environment Research Unit, Chulalongkorn University, Bangkok, Thailand
*e-mail: panaya.k@chula.ac.th

Abstract:
Poly-γ-glutamic acid (γ-PGA) is a biodegradable anionic polymer produced by bacterial fermentation with potential as a plant growth promoter and fertilizer synergist. We previously isolated a γ-PGA-producing strain, *Bacillus subtilis* FSO3. Earlier studies identified yeast extract (YE) as a key factor influencing γ-PGA production. In this work, we investigated γ-PGA production using sugarcane bagasse as a solid substrate, and examined the effects of low-cost nitrogen sources, including soybean meal (SM) and fish meal (FM), at a 2:1 (w/w) ratio of bagasse to nitrogen source. After 7 days of fermentation with 5% (v/w) bacterial inoculum, the addition of YE increased γ-PGA yield by 2.4-fold (21.2 g/kg) compared to the control (9.0 g/kg), which contained only bagasse. In contrast, the addition of SM or FM, despite having comparable C/N ratios to YE, decreased γ-PGA yield to 3.0-4.4 g/kg. We further investigated alternative low-cost yeast sources, including feed-grade yeast (FY), and corn distiller's dried grains with soluble (DDGS). Interestingly, in the addition of YE, the γ-PGA yield after two days of fermentation was higher than that after 7 days, suggesting possible γ-PGA degradation over time. With FY, γ-PGA yields reached 1.2 and 9.7 g/kg after 2 and 7 days of fermentation, respectively. No γ-PGA was detected when DDGS was used as a nitrogen source. Overall, these results indicate that although YE remains the most effective nitrogen source for enhancing γ-PGA production from sugarcane bagasse, the performance of alternative low-cost nitrogen sources is limited. Future studies should therefore aim to optimize fermentation conditions and evaluate additional agro-industrial byproducts to enhance both the yield and economic viability of large-scale γ-PGA production.

MICROBIAL ISOLATED FROM RHIZOPHERE SOIL OF BANANA FOR CONTROLLING *Bipolaris maydis* OF LEAF BLIGHT IN CORN DISEASE

Orawan Piyaboon[1]*
[1]Mahidol Wittayanusorn School, Department of Biology and Health Science, Nakhon Pathom, Thailand, 73170
*e-mail: orawan.piy@mwit.ac.th

Abstract:

The rhizosphere, the soil surrounding plant roots, is a source for microbial activity. This research aims to examine the microorganisms isolated from the soil around banana roots for controlling *Bipolaris maydis*. This research aims to test the potential of beneficial microorganism isolated from the rhizosphere of banana plants in Nan Province, Thailand for controlling *B. maydis*. Thirteen bacterial and sixteen fungal isolates were collected and characterized. Their antagonistic activity was evaluated in *vitro* against *B. maydis* using a dual culture method on Potato Dextrose Agar (PDA). All thirteen bacterial isolates showed inhibitory effects, reducing the radial growth of the pathogen by 11.1% to 57.0%. Similarly, all sixteen fungal isolates demonstrated strong antagonistic action, with percent inhibition ranging from 42.2% to 100%. These findings indicate that microorganisms from the banana rhizosphere are promising candidates for developing effective biological controls to alleviate corn leaf blight in the field.

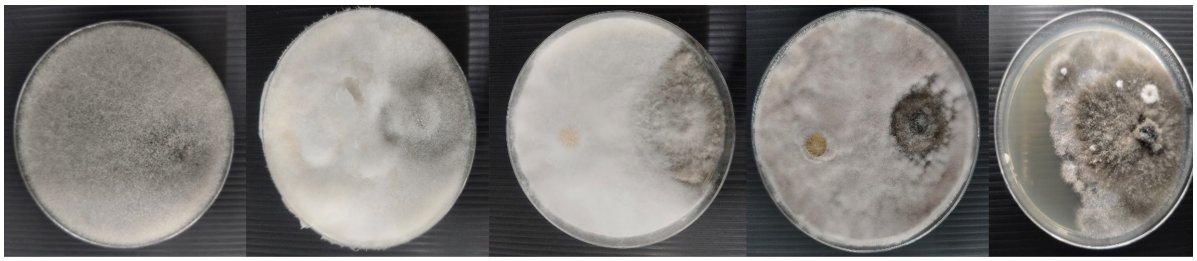

Figure 1.
Determination of antagonistic activity of fungal isolate against fugal pathogen: (A) fungal isolate 4.2, (B) fungal isolate 6.1, (C) fungal isolate 6.2, (D) fungal isolate 6.3, (E) control treatment (fungal pathogen only)

MICROBIOLOGICAL QUALITY EVALUATION OF ICE SAMPLES COLLECTED FROM FOREIGN AND THAI TOURIST ATTRACTION SITES IN BANGKOK, THAILAND

Nongsavajapon Suwansiyakul,[1] Tumnoon Charaslertrangsi[2,*]
[1]Undergraduate Program in Biological Sciences, Mahidol University International College, Salaya Phutthamonthon, Nakhon Pathom, Thailand
[2]Science Division, Mahidol University International College, Salaya Phutthamonthon, Nakhon Pathom, Thailand
*e-mail: tumnoon.cha@mahidol.ac.th

Abstract:
The Thai tourism sector welcomed approximately 35 million international tourists in 2024. At various tourist sites, Thai foods and drinks are served. Ice, a common beverage component, helps people cool off in Thailand's tropical climate and is a key part of the city's food and hospitality experience. However, ice remains a public health concern, as it can act as a carrier of harmful microorganisms, and travel advisories have advised caution against consuming it. To investigate ice safety, the use of indicator microorganisms such as *Escherichia coli* and coliforms suggests possible fecal contamination and the potential presence of other enteric pathogens. According to Thailand's Ministry of Public Health standards, ice must be free from *E. coli* and contain less than 2.2 MPN/100 mL of coliforms. This study evaluated the microbial quality of ice sold at ten tourist-related sites in Bangkok, Thailand, using the Most Probable Number (MPN) method. A total of 150 samples were collected from five major tourist attractions and five Thai local spots between September 2024 and February 2025. Results showed *E. coli* was not detected in any sample. Coliform bacteria were found only in some tourist areas, with Chinatown showing the highest mean value, followed by Chatuchak, Wat Arun, and Wat Phra Kaew at < 1 MPN/100 mL for all sites. All local sites showed no detection of coliforms and *E. coli* in 100 mL sample. Our findings suggest that Bangkok's ice complies with the microbiological requirements, but improved hygiene practices are recommended in busy tourist areas. This work provides additional empirical evidence reaffirming the safety of ice served at tourist sites. Regular inspections and vendor training are recommended to prevent potential health risks.

POLY-γ-GLUTAMIC ACID AS A GROWTH-PROMOTING AMENDMENT FOR WAXY CORN GROWTH UNDER NORMAL AND DROUGHT CONDITIONS

Thanaporn Wichai[1], Emmanuel O. Opadokun[2], Panaya Kotchaplai[1,3,4]*
[1]Institute of Biotechnology and Genetic Engineering, Chulalongkorn University, Bangkok, Thailand
[2]Program in Biotechnology, Faculty of Science, Chulalongkorn University, Bangkok, Thailand
[3]Center of Excellence in Bioconversion and Bioseparation for Platform Chemical Production, Institute of Biotechnology and Genetic Engineering, Chulalongkorn University, Bangkok, Thailand
[4]Water Science and Technology for Sustainable Environment Research Unit, Chulalongkorn University, Bangkok, Thailand
*e-mail: panaya.k@chula.ac.th

Abstract:

Poly-γ-glutamic acid or γ-PGA is a bacterial biopolymer of glutamic acid with applications in medicine, pharmaceuticals, and agricultural. In agriculture, its role in soil moisture retention and plant growth promotion has been of particular interest. This study investigated the effects γ-PGA and the γ-PGA-producing bacterium *Bacillus subtilis* FSO3 on the growth of waxy corn (Sweet Violet F1). Several forms of γ-PGA were tested including γ-PGA-rich fermentation medium, commercial γ-PGA, and γ-PGA hydrogel at a final concentration of 300 mg γ-PGA/kg soil. Under daily watering conditions, the addition of γ-PGA substantially enhanced germination rate, plant root and shoot length compared to controls. While the γ-PGA-rich fermentation medium showed positive effects on growth, adding the *B. subtilis* FSO3 inoculum alone did not significantly improve plant growth within the study period, possibly due to unfavorable soil conditions for the microorganism. In control group, sterile media containing glucose and yeast extract led to seed rot and low germination of only 11%. In contrast, treatments with γ-PGA-rich fermentation medium, commercial γ-PGA, or γ-PGA hydrogel increased germination rate to 89 -100%. Under simulated drought conditions (10 days without watering), all treatments maintained 100% germination. However, γ-PGA applications only substantially enhance shoot length but did not significantly increase root length or dry biomass, indicating their limited efficacy under tested extreme water stress. This study highlights the potential of γ-PGA to promote plant growth, however further investigation is required it develop its application for drought resilience.

POTENTIAL STRAINS OF *STREPTOMYCES* PROMOTE EUCALYPTUS SEEDLING GROWTH AND THEIR GENOME DATA MINING

Kawintip Kiakhunthod,[1] Onuma Kaewkla,[2]*

[1] Department of Biology, Faculty of Science, Mahasarakham University
[2] Isan Saline Soil Research Unit (ISSR), Faculty of Science, Mahasarakham University

*e-mail; onuma.k@msu.ac.th

Abstract:

This research aimed to study the ability of three *Streptomyces* strains, ECR3.8, EKS3.2, and ESR1.13 isolated from surface-sterilized eucalyptus tissues grown in saline soil, to promote the growth of eucalyptus seedlings. The surface-sterilized eucalyptus seeds were soaked with spore suspensions of strains ECR3.8, EKS3.2, and ESR1.13 with different spore concentrations, at 10^6, 10^7, 10^8, and 10^9 spores/mL. The results showed that the optimum spore concentration for strains EKS3.2 and ESR1.13 was 10^6 spores/mL, while 10^9 spores/mL was most effective for strain ECR3.8 to get the highest germination rate. The plant-growth promoting effects *in planta* of strains ECR3.8, EKS3.2, and ESR1.13 were studied. Treatments with strains ECR3.8, EKS3.2 resulted in the highest fresh weight and shoot length, respectively. Genome analysis of these three *Streptomyces* strains, revealed genes related to the biosynthetic substances, such as antibiotics that inhibit fungi and bacteria. The prediction of the genes of all three strains revealed genes related to promoting plant growth under salt stress and many enzymes that can be applied in various industries. In conclusion, *Streptomyces* strains ECR3.8 and ESR1.13 have the potential to be developed as inocula to promote the growth of eucalyptus in the future.

QTL-SEQ IDENTIFIES KEY GENES IMPORTANT FOR BACTERIAL LEAF STREAK (*Xanthomonas oryzae* pv. *oryzicola*) RESISTANCE IN RICE

Moe Moe Kyi Win[1,2], Wanchana Aesomnuk[2], Reajina Dumhai[2], Samart Wanchana[3] and Siwaret Arikit[2,4]*
[1]Program of Agricultural Sciences, Faculty of Agriculture at Kamphaeng Saen, Kamphaeng Saen Campus, Kasetsart University, Nakhon Pathom 73140, Thailand
[2]Rice Science Center, Kamphaeng Saen Campus, Kasetsart University, Nakhon Pathom 73140, Thailand
[3] National Center for Genetic Engineering and Biotechnology (BIOTEC), 113 Thailand Science Park, Pahonyothin Road, Khlong Nueng, Khlong Luang, Pathum Thani 12120, Thailand
[4]Department of Agronomy, Faculty of Agriculture at Kamphaeng Saen, Kamphaeng Saen Campus, Kasetsart University, Nakhon Pathom 73140, Thailand
*e-mail: siwaret.a@ku.th

Abstract:
Bacterial leaf streak (BLS), caused by *Xanthomonas oryzae* pv. *oryzicola* (*Xoc*), is an emerging threat to rice, a vital staple crop, and it can reduce yields by up to 32%. Despite the importance of host plant resistance, few genes conferring resistance against BLS have been identified. In this context, whole-genome resequencing and QTL-seq coupled with bulk-segregant analysis were used on a F2 population from a cross between the BLS-susceptible Thai variety Homcholasit (HCS) and the resistant variety Niaw Dam Chaw Mai Pai 49 (NDCMP49). Followed by inoculation with a Thai *Xoc* isolate (1NY2-2), a quantitative trait locus (QTL) on chromosome 2 was identified, covering 9,668 single nucleotide polymorphisms (SNPs). To pinpoint the most promising candidates, nonsynonymous SNPs and insertions/deletions (InDels) were selected, and the genes were annotated using the Rice Annotation Project Database. This process identified 22 candidate genes with known roles in pathogen response, including Os02g0597300 (NBS-LRR protein), Os02g0627100 (*OsPAL1*), and Os02g0650500 (*OsRLCK80*). RNA-seq analysis further revealed that Os02g0633066 (*OsWAK16*) was the most highly and significantly expressed gene among the candidates. Further validation using knockout lines showed that, upon inoculation, *oswak16* mutants led to longer bacterial lesions compared to the wild type, exhibiting the potential role of *OsWAK16* in BLS resistance. This research provides valuable genetic insights, offering promising candidate genes for breeding programs aimed at developing BLS-resistant rice varieties.

Keywords: Bacterial leaf streak (BLS), *Xanthomonas oryzae* pv. *oryzicola* (*Xoc*), rice, resistant genes, Quantitative trait loci (QTL).

Targeted aroma volatile compounds associated with consumer preferences in chilli

Papapin Prasertsil,[1] Pakavit Mathatheeranan,[2] Inthawoot Suppavorasatit,[2] Patcharaporn Tinchan,[3] and Chutchamas Kanchana-udomkan[1,*]

[1] Tropical Vegetable Research Center, Department of Horticulture, Faculty of Agriculture at Kamphaeng Saen, Kasetsart University Kamphaeng Saen Campus, Nakhon Pathom, 73140, Thailand

[2] Department of Food Technology, Faculty of Science, Chulalongkorn University, Bangkok, 10330, Thailand

[3] Faculty of Agriculture at Kamphaeng Saen, Kasetsart University Kamphaeng Saen Campus, Nakhon Pathom, 73140, Thailand

*e-mail: chutchamas.k@ku.th

Abstract:

Aroma is a key driver of consumer preference for chilli (*Capsicum* spp.), yet the volatile compounds underlying this response remain poorly defined. This study profiled three chilli cultivars—'Karen', 'Khee Noo Suan', and 'Jinda'—using Solid Phase Microextraction (SPME) and Direct Solvent Extraction (DSE) coupled with GC–MS and GC–O, combined with sensory evaluation by a nine-member trained panel and preference testing with 170 consumers. Fifty-seven volatile compounds were identified, with clear differences in acceptance across cultivars. 'Khee Noo Suan' achieved the highest liking score (52.9%), while 'Karen' and 'Jinda' received markedly lower ratings (31.8% and 15.3%, respectively). Multivariate analysis highlighted key volatiles associated with consumer responses: methyl 4-methylpentanoate, (E)-2-hexenal, 4-methyl-1-pentanol, 4-methylpentyl 2-methylpropanoate, 4-methylpentyl 8-methylnon-6-enoate, isohexyl isocaproate, fumaric acid, cis-hex-3-enyl pentyl ester, 2-decanol, hexyl hexanoate and methyl palmitate conferring floral notes, were consistently linked to higher liking, whereas (E)-3-hexen-1-ol, 1H-benzocycloheptene, (E)-ß-Ionone, nerolidol and hexanoic acid with musty attributes reduced acceptance. These findings identify specific aroma compounds that shape consumer preference, providing actionable targets for breeding and product development to align chilli varieties with market demand.

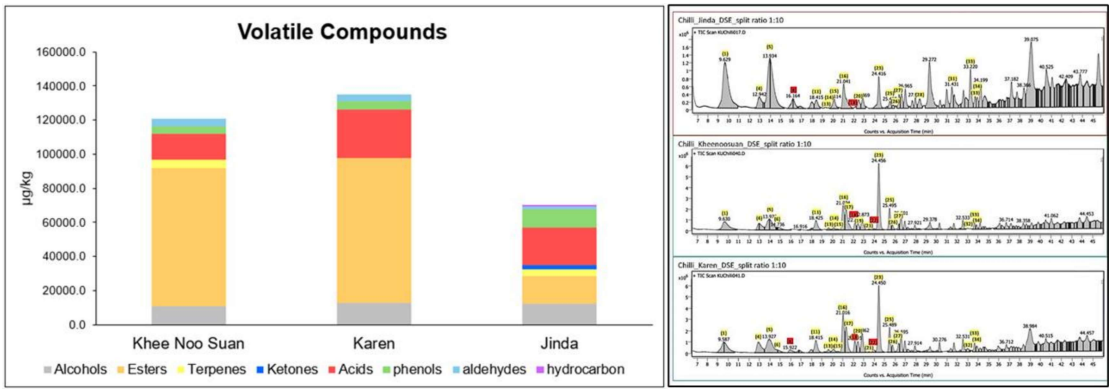

Figure 1.
Quantity of substance types of three chili cultivars (left). Chromatogram of volatile substances of three chili cultivars analyzed by GC-MS (right).

TASTING WITH ALGORITHMS: AI FOR MANGO FLAVOR IDENTIFICATION

Natthaphat Manasompong[1], Rajitha Phraephrewngarm[1], Aiyarin Arunthammasak[2]

[1]Bangkok International Preparatory and Secondary School (Thailand)

[2]St Andrews International School Bangkok (Thailand)

*email: manasompongmimi@gmail.com

Abstract:
As one of Thailand's most important agricultural exports, mangoes play a vital role in the economy. However, consumers often struggle to distinguish varieties by flavour. This study explores the use of a convolutional neural network (CNN), based on the Xception model to predict, by identification, mango flavor based on species and ripeness. The dataset of 236 images of mangoes includes eight common Thai varieties, all sampled at the unripe (green) stage. These were grouped into two flavour categories traditionally described as savoury (Falan, Kaew Khamin, Khiew Sawoey and Mun Salaya) and sour (Bao, Kaew, Nam Dok Mai and Ok Rong). The model was developed using Python on Google Colab and trained over 25 epochs, achieving a training accuracy of 98.26%, validation accuracy of 67.44%, and test accuracy of 88.89%. The most frequent error was confusing savoury for sour mangoes. By accurately detecting whether unripe mangoes are savoury or sour, this system provides a cost-effective tool to assist farmers with harvest timing, improve post-harvest sorting, ensure product consistency, and reinforce Thailand's global mango export competitiveness.

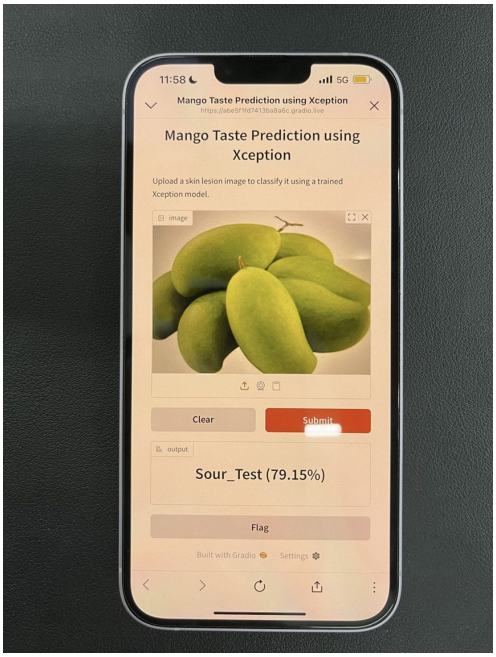

Figure 1.
showing the use of the program.

SP3: NEXGEN ENERGY: STORAGE AND CONVERSION FOR SUSTAINABILITY

A DUAL–FUNCTION LITHIUM BORATE GLASS CERAMICS–COPOLYMER COMPOSITE INTERLAYER FOR LITHIUM–SULFUR BATTERIES

Pakawan Sereerattanakorn,[1] Jintara Padchasri,[1] Pinit Kidkhunthod[1,*]
[1]Synchrotron Light Research Institute (Public Organization) (111 University Avenue, Muang District, Nakhon Ratchasima 30000, Thailand)
*e-mail: pinit@slri.or.th

Abstract:
Lithium–sulfur batteries (LSBs) are considered one of the most promising next-generation energy storage technologies due to their high theoretical specific energy (2600 Wh/kg), the natural abundance, and environmental compatibility of sulfur. Despite their advantages, LSBs are severely hindered by the polysulfide shuttle effect during cycling and the low migration efficiency of lithium-ion (Li^+). The dissolution and migration of lithium polysulfides (LiPS) during cycling cause active sulfur material loss, rapid capacity fading, and poor cycle stability. To overcome these challenges, a multifunctional polymer-based interlayer between the cathode and separator has been proposed to effectively confine and convert soluble LiPS. However, poly(vinylidene fluoride) (PVDF) displays a weak intermolecular force to intermediate LiPS. Herein, PVDF was fabricated via the phase inversion method with polyethylene glycol (PEG) and lithium borate glass ceramics (LBO) to construct a high-performance interlayer. The PEG was entrapped within the cross-linked PVDF framework, which facilitates Li^+ transport. At the same time, the uniformly dispersed LBO nanoparticles enhance electronic conductivity and introduce strong anchoring sites for soluble LiPS. It is suggested that the synergistic effect of copolymer and LBO (PVDF-PEG/LBO) results in an effective interlayer material, improving the efficiency and durability of LSBs.

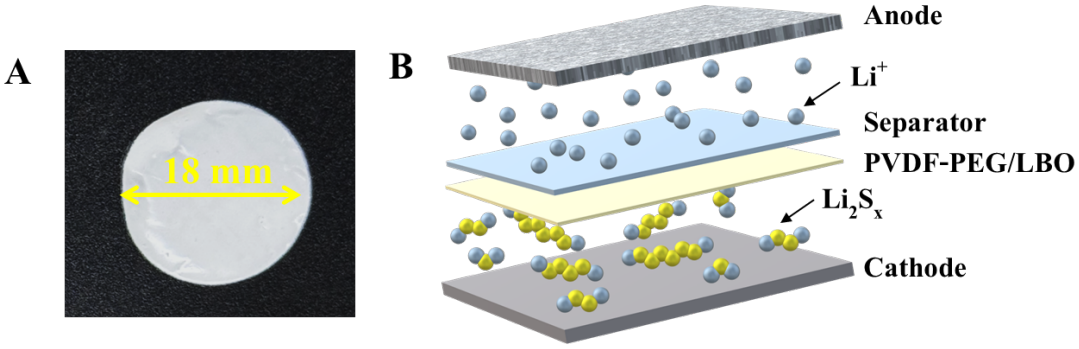

Figure 1.
The PVDF-PEG/LBO film (A) and the cell configuration of lithium–sulfur batteries (B).

An Experimental Investigation into the Effectiveness of Biomimetic Ship Hull Surface Materials from Three-Dimensional Simulations of the Shortfin Mako Shark *(Isurus oxyrinchus)* Scales for Drag Reduction in Turbulent Flow Toward Energy Conservation and Sustainable Emission Reduction

Ravisuda Sirinanthakate*, Chavisa Ketkuabratsuk, Nattamon Navapun
Satriwithaya School
*e-mail: ravisuda.sir@gmail.com

Abstract:
The shipping industry is growing commitment to carbon neutrality has made improving ship performance more important than ever, not just for reducing fuel consumption and emissions but also for enabling the smooth integration of new energy storage and conversion systems. One of the great technical challenges to meet this goal lies in reducing hydrodynamic drag, which has a direct impact on both how efficiently a ship moves through water and the energy required to power its systems. Passive drag reduction, or the reduction of resistance without the deployment of extra energy, has emerged as a critical solution. It is significant to the development of future marine technologies in that it facilitates ships to run on smaller engines, longer battery lifespan, and hybrid or renewable power sources that are more stable. This research explains how biomimetic surfaces inspired by the Shortfin Mako shark *(Isurus oxyrinchus)* special scales arrangement can make this possible. We specifically chose the Shortfin Mako shark because it is the speediest swimming shark, a product of millions of years of evolutionary streamlining for efficiency and speed. Its microscopic skin structure offers a window into passive separation control of turbulent flow. To examine this, we created 3D models using SOLIDWORKS that closely mimic the scales structure of the Shortfin Mako shark skin. The models were printed by Fused Deposition Modeling (FDM) 3D printer with two materials: rigid polylactic acid (PLA) and flexible thermoplastic polyurethane (TPU). By this material selection, the difference in the effect of surface stiffness versus flexibility on drag reduction was made clear. To model how water would flow over each surface in turbulent flow, Computational Fluid Dynamics (CFD) simulations were conducted using ANSYS 2024. After simulation, the 3D-printed surfaces were tested in a large scale controlled open-channel flume, where the behavior of the flow could be directly observed in real time. The results showed that both surface design and flexibility of the material had a significant contribution to drag reduction. Compliant surfaces made from thermoplastic polyurethane (TPU), which more accurately mimic the responsive feature of real shark skin, performed better than the rigid polylactic acid (PLA) surfaces. The findings promise exciting potential for future ship hull designs. By reducing drag, ships require less propulsion force to travel, lowering energy consumption and allowing for smaller, more efficient motors or storage systems. When combined with emerging energy systems, such as hybrid or renewable systems, passive drag reduction methods can have a profound effect on the overall efficiency of ships. This research suggests that by following the lead of nature templates like the Shortfin Mako shark skin, the world of shipping can navigate towards a new era of smarter, cleaner, and greener vessels that are better suited to meet the environmental and energy challenges of the modern world.

Phenazine-Conjugated Co^{II}-Phthalocyanine Polymer as a Robust Catalyst for Efficient Electrochemical CO_2 Conversion

Permsak Chairat[1], Jirapong Luangchaiyaporn[1], Supawadee Namuangruk[2], Yijiao Jiang[3], Patchanita Thamyongkit[1,*]

[1]*Department of Chemistry, Faculty of Science, Chulalongkorn University, Bangkok 10330, Thailand*

[2] *National Nanotechnology Center (NANOTEC), National Science and Technology Development Agency (NSTDA), Pathum Thani 12120, Thailand*

[3]*School of Engineering, Macquarie University, Sydney, NSW 2109, Australia*

*Corresponding Author E-mail: patchanita.v@chula.ac.th

ABSTRACT

Development of robust catalysts is a key requirement for practical electrochemical CO_2 reduction (ECO_2R). Here, we report the synthesis and electropolymerization of 4-aminophenoxy-substituted Co^{II}-phthalocyanine to construct a phenazine (PNZ)-conjugated Co^{II}-phthalocyanine polymer as a durable catalyst for heterogeneous ECO_2R on carbon fiber paper. Under 2 h of electrolysis, the polymer catalyst efficiently produced CO with a faradaic efficiency (FE_{CO}) of 94%, CO partial current density of 5.5 $mA \cdot cm^{-2}$, and turnover frequency of 1.1 s^{-1} at –1.19 V *vs.* normal hydrogen electrode (NHE). Moreover, this polymeric framework exhibited significantly greater stability than its monomeric counterpart by sustaining average FE_{CO} of 93%, current density of 7 $mA \cdot cm^{-2}$, and turnover number of 5.3×10^5 during 120-h electrolysis. Variable-frequency square-wave voltammetry revealed efficient electron transfer within the polymeric bulk through PNZ linkages, while in situ Raman spectroscopy confirmed a higher fraction of electrochemically active Co^{I} center in the polymer film over the monomer one. Furthermore, theoretical study ensured improvement of charge penetration in the covalently extended polymer network in comparison to that in the monomer stack. These findings provide fundamental insights into the rational design of robust Co^{II}-phthalocyanine-based catalysts and continue the development of efficient CO_2-to-CO conversion systems.

Keywords: $Cobalt^{II}$-phthalocyaine; Electrochemical CO_2 reduction; Electrocatalsyt; Phenazine

COMPARATIVE STUDY OF IONIC PUMPING AT MXENE AND CARBON-COATED MXENE INTERFACES FOR STABLE LITHIUM-ION BATTERIES AT LOW TEMPERATURES

Suparada Kamchompoo,[1] Yingying Lv,[2] and Siriporn Jungsuttiwong[1,*]
[1] Department of Chemistry and Center of Excellence for Innovation in Chemistry, Faculty of Science, Ubon Ratchathani University, Ubon Ratchathani 34190, Thailand
[2] Research Centre of Nanoscience and Nanotechnology, Department of Chemistry, Shanghai University, Shanghai 200444, China
*e-mail: siriporn.j@ubu.ac.t

Abstract:

Ion mobility at the interface plays a crucial role in determining the electrochemical efficiency of lithium-ion batteries, particularly under high-rate operations and low-temperature conditions. In this study, density functional theory (DFT) calculations were employed to investigate Li^+ adsorption and charge transfer at the interface of mesoporous carbon-coated Ti_3C_2OH MXene. Our findings demonstrate that carbon coating significantly enhances Li^+ interaction, as evidenced by a stronger adsorption energy (-2.20 eV compared to -1.05 eV for bare MXene) and more pronounced charge redistribution. These findings indicate the formation of an "ionic pump" at the interface, which facilitates ion accumulation and transport. Moreover, experimental validation supports theoretical predictions, with the mesoporous carbon-coated MXene exhibited excellent cycling stability (192.8 mAh/g after 9400 cycles) and outstanding low-temperature performance (205.3 mAh/g at -20 °C), attributed to enhanced ion kinetics and reduced charge-transfer resistance. These findings underscore the critical role of the mesoporous carbon interface in enabling efficient and robust Li^+ storage, particularly under demanding conditions.

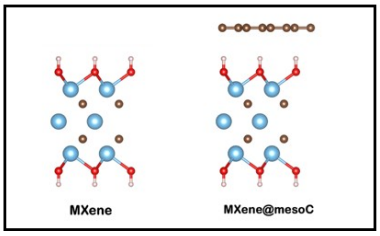

Figure 1.
Side view of MXene and MXene@mesoC structures

DEVELOPING SUPPORTER FOR MANGANESE-SODIUM CATALYSTS IN THE OXIDATIVE COUPLING OF METHANE TO HIGHER HYDROCARBONS

Tanat Srikhota,[1,*] Kritsapon Singcha,[1] Sarote Boonseng,[1] Anusorn Seubsai[2]
[1]Mahidol Wittayanusorn School, Salaya, Phutthamonthon, Nakhon Pathom, Thailand
[2]Department of Chemical Engineering, Faculty of Engineering, Kasetsart University, Bangkok, Thailand
*e-mail: tanat.sri_g33@mwit.ac.th

Abstract:
The greenhouse effect is a critical global challenge that must be urgently addressed in line with the Sustainable Development Goals (SDGs). One of the greenhouse gases which has a significant effect to the earth's atmosphere is methane. The methane, a potent greenhouse gas with low economic value, is often released into the atmosphere. The oxidative coupling of methane (OCM) offers a promising route to convert methane into higher-value hydrocarbons; however, current OCM catalysts, typically metal oxides with supports, remain suboptimal in performance and cost-effectiveness. This study investigates low-cost catalyst–support combinations prepared *via* the wet impregnation method using sodium sulfate and manganese sulfate at five Na:Mn ratios (2:5, 5:2, 1:1, 0:1, 1:0). Supports tested were silicon dioxide, silicon carbide, and aluminum oxide. Catalysts were evaluated in a quartz tube reactor at 800°C and 900°C, with reactant gases analyzed by thermal conductivity detection (TCD) and hydrocarbon products analyzed by flame ionization detection (FID) *via* gas chromatography. Methane conversion ranged from 30–45% at 900°C and 28–33% at 800°C, with the highest conversion (40.2%) observed for aluminum oxide (Na:Mn = 2:5) at 900°C. The maximum C_2 selectivity (22.5%) was achieved with silicon dioxide (Na:Mn = 0:1), while the highest C_2 yield (7.3%) was obtained with silicon dioxide (Na:Mn = 1:1) at 800°C. These results demonstrate that optimized, low-cost catalyst–support systems can improve OCM efficiency, offering a viable pathway for methane mitigation.

HIGHLY STABLE CATHODE DERIVED FROM MANGANESE-ALUMINIUM LAYERED DOUBLE HYDROXIDE FOR WET NONAQUEOUS ZINC-ION BATTERY

Wathanyu Kao-ian[1,*], Phonnapha Tangthuam[2], Pinit Kidkhunthod[3], Wanwisa Limphirat[3], Jintara Padchasri[3] Nicolas Aubert[4], Gianluca Ciatto[4], Soorathep Kheawhom[1]

[1]Department of Chemical Engineering, Faculty of Engineering, Chulalongkorn University, Bangkok 10330, Thailand
[2]Department of Chemical Technology, Faculty of Science, Chulalongkorn University, Bangkok 10330, Thailand
[3]Synchrotron Light Research Institute, 111 University Avenue, Muang District, Nakhon Ratchasima 30000, Thailand
[4]Synchrotron SOLEIL, L'Orme des Merisiers Départementale 128 91190 Saint-Aubin, France
*e-mail: Wathanyu.K@chula.ac.th

Abstract:
Zinc-ion batteries (ZIBs) with manganese dioxide (MnO_2) cathodes are promising for grid-scale energy storage owing to their safety and low cost. However, interfacial Mn dissolution and structural collapse cause severe long-term capacity fading. Here, we report a manganese-based cathode derived from the deprotonation reaction of manganese (Mn)/ aluminium (Al) layered double hydroxide (LDH), referred to as D-MnAl LDH. Characterization results i.e. transmission electron microscopy (TEM), energy-dispersive X-ray spectroscopy (EDS), X-ray diffraction (XRD) and Fourier-transform infrared spectroscopy (FT-IR) indicate the birnessite-like structure having both the characteristic of LDH and oxide, having residual Al in its structure. Electrochemical tests reveal that the D-MnAl LDH cathode delivers exceptional cycling stability, maintaining nearly unchanged specific capacity over 2,000 cycles. To probe behavior of Mn specie at cathode interface, in-situ grazing incidence X-ray absorption spectroscopy (GI-XAS) was employed, revealing that Mn dissolution is effectively suppressed in D-MnAl LDH compared to δ-MnO_2. Consequently, the D-MnAl LDH cathode exhibits markedly superior cycling durability which is much better than that of the regular MnO_2 cathode. These findings highlight a viable pathway toward the development of practical and long-lasting ZIBs.

SP7: COLOUR SCIENCE/TECHNOLOGY, LIGHT AND APPLICATIONS

INVESTIGATION OF SURROUND EFFECT ON SIMULTANEOUS COLOR CONTRAST UNDER VARIOUS DEVICES

Janejira Mepean,[1]* Chanprapha Phuangsuwan,[2] Mitsuo Ikeda[2], Miyoshi Ayama[3], Yoko Mizokami[4]
[1] Dept. Color Tech. and Design, Mass Communication Tech., Rajamangala Univ. Tech. Thanyaburi, Thailand
[2] Color Research Center, Rajamangala Univ. Tech. Thanyaburi, Thailand
[3] Professor emeritus Utsunomiya University, Japan
[4] Dept. of Imaging Sciences, Graduate School of Informatics, Chiba University, Japan
*e-mail: janejira_m@mail.rmutt.ac.th

Abstract:

Simultaneous color contrast (SCC) refers to changes in perceived color caused by surrounding colors. Understanding SCC is important for applications in color reproduction, display technologies, and lighting design. According to the Recognized Visual Space of Illumination (RVSI) theory, adaptation occurs primarily to the illumination of the space rather than to individual objects. Based on this theory, we hypothesize that the strength of SCC may vary depending on the device used to present the stimuli.

This study investigates surround effect using three devices: paper, electronic display, and the two-rooms technique under four color surrounds that were carefully controlled in chromaticity, luminance, chroma, and size. Observers performed achromatic adjustments by adjusting amount of R, G, and B values of a 4 × 4 cm^2 test patch on an electronic display which surrounded by a 21 × 31 cm^2 colored background until it appeared perceptually neutral gray. Six observers participated, and each color was repeated five times per device.

The results showed that the two-rooms method produced the strongest influence of surrounding colors, as seen in higher surround index (SI) values for all surround colors. Although, observer could detect a small chromaticness at surrounding. In contrast, the paper and electronic display, observer detected vivid surrounding color but SI showed weaker. This agrees with the RVSI theory predicted, it suggests the visual system pays more attention to the illumination rather than to color of objects. These findings suggest that SCC is possibly device dependent.

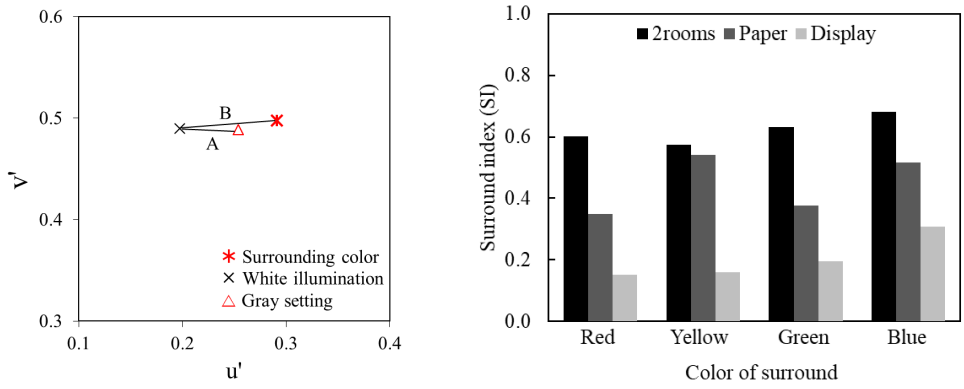

Figure 1.

On the left figure defined the surround index from the ratio of the distance from the gray setting to the white illumination (A) over the distance from the surrounding color to the white illumination (B), and the result among three devices are shown by bar graphs (right).

Simultaneous color contrast (SCC), refers to changes in perceived color caused by surrounding colors. Various devices and methods have been developed to measure SCC. According to the Recognized Visual Space of Illumination (RVSI) theory, adaptation occurs primarily to the illumination of the space rather than to individual objects, we assume that its strength may vary depending on the device used to present the stimuli.

ON THE DESIGN OF CIRCULAR SHAPE LIGHT GUIDE PLATE AS ARTIFICIAL LIGHTING FOR WOLFFIA ILLUMINATION TO INVESTIGATE THE EFFECT OF BLUE LIGHT AND RED LIGHT ON WOLFFIA BUDDING

Pakorn Prajuabwan*
Department of Physics, Faculty of Science and Technology, Kanchanaburi Rajabhat University, Kanchanaburi, 71190, Thailand
*e-mail: pakorn@kru.ac.th

Abstract:

Wolffia the fastest growing aquatic plant in the world, has no root system, and it reproduces by budding rather than by seeds. Wolffia typically measure only a few millimetres to less than a millimetre in size and grow as colonies of two individuals, one mother frond budding and giving rise to one or more daughter fronds within 24 hours with appropriate lighting. Circular shape Light Guide Plate (LGP) attached with Light Emitting Diode (LED) is proposed as the artificial lighting for Wolffia illumination instead of normal LED lighting panel. LGP is an acrylic panel typically made from pure Polymethyl methacrylate (PPMA) resin. LGP are normally used as backlight light in LCD screen backlight module, LED panel lighting for decoration and advertising display panel. The simple technique to scatter the light from the light source through LGP by making a matrix of drilling holes as a concave lens all over LGP panel is proposed. This technique with LGP can be used to mix red and blue LED light source with appropriate ratio between red and blue colour to be artificial lighting for Wolffia illumination. Surface mounted red color and blue color strip LEDs are attached at 120 cm. circumference of LGP. The appropriate 3 mm. diameter drilling holes and 5 mm. distance will scatter the mixed light out the front of the panel. In artificial LED lighting for plant illumination, The ratio between red and blue color is always fixed by the manufacturer of LED panel. The user cannot adjust the fixed red and blue ratio. With LGP technique, the user can design the ratio of red and blue color LED by selecting the number of red LED and blue LED to attach at circumference of circular LGP. Normally, the number of red LED is always higher than the number of blue LED, because the light intensity of red LED is lower than the light intensity of blue LED. In this experiment, The light intensity of various ratios of red color and blue color are measured with light spectrum instrument compared to the light intensity of unmixed red color and unmixed blue color at the center of circular LGP. Wolffia globosa was chosen for the experiment to investigate the effect of unmixed blue LED, unmixed red LED and various ratio of mixed blue and red LED on the budding of Wolffia. Experiments were carried out in 10 cm. circular glass container and microplate with liquid fish fertilizer mixed with water under LGP artificial lighting illumination. Unmixed blue lighting gives out higher budding rate than unmixed red lighting, mixed blue and red lighting with high proportion of blue ratio also causes higher budding rate than the case of high proportion of red ratio. On the other hand, mixed blue and red lighting with high proportion of red ratio will generate mor chlorophyll concentration (chlorophyll extraction through UV/VIS spectrophotometer) than the other cases. This investigation and proposed LGP lighting technique will encourage in using artificial lighting for vertical farming Wolffia illumination.

THE IMPACT OF SIMULATED LOW VISION ON THAI FONT LEGIBILITY: A STUDY OF FOVEA AND PARAFOVEA VISION

Phuttharaksa Lanoi[1], Pichayada Katemake*[1]
[1]Chulalongkorn University, Thailand
*e-mail: Phuttharaksa.ln@gmail.com, pichayada.k@chula.ac.th

Abstract:

This study focuses on evaluating the legibility of Thai font sets for individuals with simulated low vision, using three different Thai consonant font sets: FT Manifest UD, TH Sarabun New, and DB Ozone. The simulation of low vision was achieved using cloudy lens glasses that provided a visual acuity range of 20/100 to 20/400, which mimics conditions like cataracts and diabetic retinopathy. The experiment was conducted in a dark room, where 36 Thai consonants were displayed in the fovea and parafovea regions for display durations of 50 and 100 milliseconds. The accuracy and response time of 10 participants, aged between 19 and 25, consisting of 5 males and 5 females, with educational backgrounds ranging from undergraduate to master's level in fields such as education, psychology, arts, economics, letters, and science, were recorded. Each test was repeated three times. The experiment consisted of two parts: a Fovea vision and a Parafovea vision, utilizing the SuperLab program to present stimuli for durations of 100 ms and 50 ms. The tests were conducted in a dark room, and the display screen had a brightness of 26.8 cd/m². The results revealed that in the Fovea vision test at 100 ms and 50 ms display durations, the FT Manifest UD font set achieved the highest accuracy at 91.39% and 76.30% , respectively. In the Parafovea vision test, the FT Manifest UD font set still provided the highest accuracy of 71.11% (100 ms) and 48.61% (50 ms). The FT Manifest UD font also resulted in the shortest response times in both tests, with average times of 1624.70 ms (100 ms) and 1763.13 ms (50 ms), respectively. This study is expected to contribute to the development of Thai fonts that enhance reading efficiency for individuals with low vision. Additionally, it introduces the concept of designing fonts to improve legibility under blurred vision conditions, applicable to the Thai language, which has more complex writing characteristics compared to Roman scripts.

THE STUDY OF TANNIN QUANTITY ON FABRIC DYEING FOR THE DEVELOPMENT OF LOCAL TEXTILE DYEING QUALITY

Chiraphat Kongphet,[1] Kanokrat Singnui,[1*]

[1]Princess Chulabhorn Science High School Nakhon Si Thammarat, 120 M.1 Bangjak Sub district, Muang Nakhon Si Thammarat, Thailand

*e-mail: skanokrat208@gmail.com

Abstract:
This study investigates the influence of tannin concentration on the dyeing quality of local textiles. The objectives were to determine the optimal tannin concentration for fabric dyeing, compare the efficiency of different tannin levels in enhancing color fastness, and analyze the relationship between tannin content and dye adherence. Fabric color intensity was evaluated using RGB and HEX values through a Color Picker, and color differences were analyzed using Euclidean Distance.

The results indicated that tannin concentration significantly affected dye uptake. A solution containing 10 g of tannin per liter produced the darkest fabric color with a Euclidean Distance of 106.34. Lower concentrations of 0.5 g and 1.5 g yielded distances of 63.30 and 54.80, respectively. In terms of dyeing duration, fabrics dyed for 15, 30, 45, and 60 minutes showed progressive improvements in color adherence. The color difference was 25.07% at 15 minutes, approximately 52% at 30 and 45 minutes, and reached the maximum intensity of 97.31% at 60 minutes. The washing fastness test revealed that color stability was achieved from the third wash onwards, with an average color difference of 5.71% compared to the initial stage. These findings demonstrate the importance of optimizing tannin concentration and dyeing time to enhance both the quality and durability of local textile dyeing.

Keywords: tannin, textile dyeing, color fastness, natural dye, local fabric

WAVELENGTH-DEPENDENT DEGRADATION OF RED PIGMENTS UNDER NARROW-BAND LED ILLUMINATION

Duantemdoung Dethsuphar, Pichayada Katemake*
Department of Imaging and Printing Technology, Faculty of Science, Chulalongkorn University, Thailand
*e-mail: pichayada.k@chula.ac.th

Abstract:

The preservation of historical pigments under modern museum lighting remains a critical challenge, as light exposure inevitably induces color degradation. This study investigates the stability of red pigments when exposed to sixteen narrow-band LED wavelengths across the visible spectrum for 4,000 hours. A total of twenty-three pigment–binder specimens were prepared using traditional formulations and systematically evaluated for color change (ΔE_{ab}) using spectrophotometric measurements. The results reveal pronounced wavelength-dependent degradation, with the greatest instabilities occurring under violet–blue illumination (367–404 nm), where organic pigments such as Carmine Naccarat and Naphthol Scarlet exhibited ΔE_{ab} values exceeding 70. By contrast, inorganic reds including cadmium red and cinnabar demonstrated superior stability, typically maintaining ΔE_{ab} below 2 across most wavelengths. Mid-spectral excitation (471–599 nm) produced moderate fading in quinacridone and alizarin-based pigments, while long-wavelength illumination (628–740 nm) induced only minor shifts across all samples. These findings confirm that short-wavelength visible light constitutes the principal risk factor for red pigment deterioration, underscoring the necessity of spectral optimization in museum lighting design. The study advances the understanding of wavelength-specific vulnerability in historical pigments and provides actionable guidelines for developing LED-based lighting strategies that simultaneously safeguard cultural heritage and ensure high-quality visual presentation.

SP8: CULTURAL HERITAGE: TRADITIONAL/DIGITAL COLOR

SAFE REMOVAL OF AGED POLYVINYL ACETATE ADHESIVES FROM CANVAS USING NANOCELLULOSE AEROGEL: PRESERVING ORIGINAL COLOR OF ARTWORKS

Atikarn Kraichok,[1] Ochana Poonthongdeewatthana,[2] Watsachon Leksomboon,[1] Sasia Leelathaweewat,[1] Siriyakorn Khumsang,[1] Kamonwan Pacaphol,[1*]
[1]Department of Imaging and Printing Technology, Faculty of Science, Chulalongkorn University, Bangkok, 10330, Thailand
[2]Department of Art Theory, Faculty of Painting Sculpture and Graphic Arts, Silpakorn University, Bangkok, 10200, Thailand
*e-mail: kamonwan.p@chula.ac.th

Abstract:

The current problem of artwork remedial conservation is an inappropriate cleaning method on material surface, leading to an undesirable discoloration. The conventional method using cotton swabs raise concerns due to uncontrolled liquid release and the time-consuming process of repeated swabbing cycles. Therefore, delivery materials have been developed to provide controlled release while absorbing dissolved substances from the surface. This study focused on the removal of the aged adhesive from artworks using a highly porous aerogel derived from bacterial nanocellulose (BNC). BNC aerogel containing different concentrations of either acetic or citric acid solution, forming a hydrogel, was applied to aged polyvinyl acetate (PVAc)-coated linen canvas for different release times. Results showed that BNC aerogel with 10% w/v citric acid, left on the canvas for 80 min, was most effective in removing PVAc glue. Compared to the uncleaned canvas, the total color difference (ΔE) after cleaning was less than 2, indicating a change imperceptible to the naked eye. Microscopic images revealed separation of the PVAc-bonded fibers into individual fibers, and chemical analysis showed the greatest reduction of PVAc-related carbonyl groups at 1725 cm^{-1}. Moreover, the BNC hydrogel retained its mechanical properties after use, indicating its reusability. These results indicate that BNC aerogel has strong potential as a cleaning gel for canvas heritage conservation.

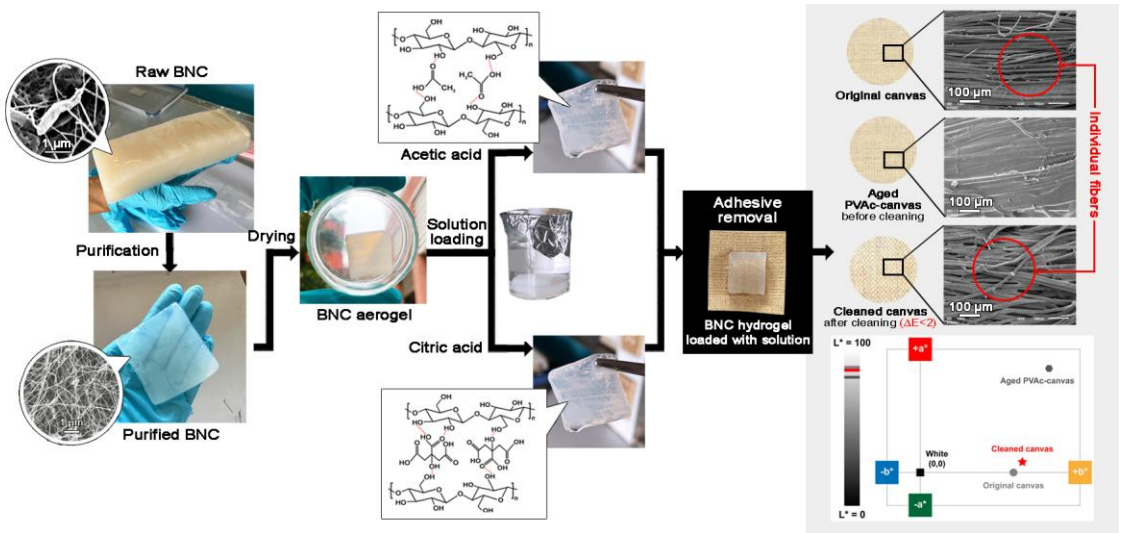

Graphical abstract

THERMAL AND LIGHT STABILITY OF PIGMENTS AND BINDERS USED IN PAINTING UNDER XENON AND MIXED WHITE LED ILLUMINATION

Krittin Assawaphom,[1] Pichayada Katemake,*[1]
[1] Department of Imaging and Printing Technology, Faculty of Science, Chulalongkorn University, Thailand
e-mail: Krittin.assawaphom@gmail.com, Pichayada.K@chula.ac.th

Abstract:
Pigments exhibit varying degrees of stability, and the museum environment—particularly exposure to light and heat can directly accelerate their deterioration in paintings. This study examined the stability of three organic and seven inorganic pigments mixed with three binders: gum arabic, egg yolk, and linseed oil. Linseed oil was applied to only five pigments, resulting in a total of 25 paint samples. The samples were coated onto paper with a thickness of 75 µm, cut into pieces measuring 1.5 × 3.0 cm, and mounted on white cardboard. Five sets of samples were prepared. The first set served as the control, stored in a black envelope inside a sealed plastic box. The second set was subjected to accelerated aging with xenon light simulating outdoor sunlight. The third set was exposed to a mixed white LED chamber. The fourth set was placed in a temperature-controlled chamber at 50 °C. The fifth set was exposed to xenon light simulating sunlight passing through window glass indoors. The CIELAB color measurements were conducted before exposure and at 24-hour intervals over a period of 240 hours. Multispectral imaging, XRF, and FTIR analyses were performed to examine pigment characteristics, elemental composition, and chemical components, respectively, at both the beginning and the end of the deterioration tests. Afterward, the third set was transferred to the 50 °C chamber, and the fourth set was placed in the mixed white LED chamber, with the same analyses repeated over another 240 hours. The results indicated that the second set exhibited the most significant overall color change (ΔE_{ab}) across all pigments. Among them, turmeric powder showed the highest color difference. Additionally, samples prepared with linseed oil displayed a noticeable yellowing compared with those prepared using gum arabic and egg yolk.

X-RAY FLUORESCENCE ANALYSIS OF PIGMENTS IN THE MURAL PAINTINGS AT WAT DON KRABUEANG, RATCHABURI, THAILAND

Nattawan Worawannotai* and Jirachaya Pummanee
Department of Chemistry, Faculty of Science, Silpakorn University, Thailand
*e-mail: worawannitai_n@su.ac.th

Abstract:
Wat Don Krabueang, located in Ratchaburi province, Thailand, is a Mon Raman temple established in 1815. The ordination hall houses mural paintings believed to date to the reign of King Rama V (1868-1910). To investigate both the traditional pigments and the materials introduced during later restoration work, *in situ* X-ray fluorescence (XRF) analysis and macro XRF (MA-XRF) mapping were conducted. Elemental analysis suggested the use of calcium carbonate in the ground layer. The original palette likely comprised vermilion/cinnabar, Prussian blue, emerald green, lead white, red ocher, and an organic yellow pigment, possibly gamboge, with gold leaf applied in gilded areas. In contrast, restored sections contained titanium white, Prussian blue, iron oxide, and possibly a green organic pigment. Macro XRF (MA-XRF) elemental mapping further provided spatial context and insights into the painting techniques. These results highlight the contrast between traditional pigments and modern restoration materials, providing insights into the interventions that have shaped the present appearance of the murals.

SP9: EXPLORING THE COSMOS: ADVANCES IN OBSERVATIONAL AND THEORETICAL ASTROPHYSICS

DISCOVERY OF SPIRAL BRIGHTEST CLUSTER GALAXIES AT Z = 0.1-1.2

Anas Yamalae,[1,*] Taweewat Somboonpanyakul,[2] Suraphong Yuma[1,]
[1]Department of Physics, Faculty of Science, Mahidol University, 272 Rama VI Road, Ratchathewi, Bangkok, 10400 Thailand
[2]Department of Physics, Faculty of Science, Chulalongkorn University, 254 Payathai Road, Pathumwan, Bangkok, 10330 Thailand
*e-mail: anas.yal@student.mahidol.edu

Abstract:
Brightest cluster galaxies (BCGs) are massive and luminous systems residing near the centers of galaxy clusters. They are generally believed to form through interactions with neighbors and hierarchical mergers, and their common morphology is elliptical, which has been studied up to z = 1.8. However, two spiral BCGs have been found unexpectedly. Such objects may provide more insight into the physical mechanisms of galaxy morphological evolution. We conducted a systematic search of spiral BCGs using the galaxy cluster catalog provided by the Hyper Suprime-Cam Subaru Strategic Program (HSC-SSP) PDR3, focusing on clusters with richness greater than 40 in the redshift range $0.1 < z < 1.2$. We identify 199 BCGs by analyzing publicly available HSC images and Sloan Digital Sky Survey (SDSS) spectra. Spiral BCG candidates were identified based on the Dn(4000) spectral index, which is generally lower than 1.55 for star-forming galaxies. Our current analysis focuses on a subset of 21 potential spiral candidates with their Dn(4000) values below the threshold. We assess whether they have similar properties to normal spiral galaxies using surface brightness profiles and morphological parameters. One possible explanation is that spiral features could arise from tidal interactions with massive satellites when the central galaxy is in a diffuse state. If so, spiral BCGs may represent a transitional phase before becoming elliptical galaxies.

SP10: X-RAY CRYSTALLOGRAPHY

CRYSTAL ENGINEERING OF ULTRAMICROPOROUS LANTHANIDE-BASED MOFs

Kanthida Kummoon,[1] Bunyarat Rungtaweevoranit,[2] Mongkol Sukwattanasintt,[3] Kittipong Chainok,[1,*]
[1]Thammasat University Research Unit in Multifunctional Crystalline Materials and Applications (TU-MCMA), Faculty of Science and Technology, Thammasat University, Pathum Thani 12121, Thailand
[2]National Nanotechnology Center (NANOTECH), National Science and Technology Development Agency (NSTDA), Pathum Thani 12120, Thailand
[3]Department of Chemistry, Faculty of Science, Chulalongkorn University, Bangkok 10330, Thailand
*e-mail: kc@tu.ac.th

Abstract:
Carbon capture and storage (CCS) can be enhanced by designing porous metal–organic frameworks (MOFs) with pore diameters matching the kinetic size of carbon dioxide (CO_2). In this work, we report two isostructural ultramicroporous MOFs (UM–MOFs), $[(CH_3)_2NH_2][Ln(HCOO)(C_2O_4)_{1.5}]\cdot 0.3H_2O$ (Ln = Yb, Lu), constructed from lanthanide ions with mixed formate ($HCOO^-$) and oxalate ($C_2O_4^{2-}$) linkers. Single–crystal X-ray diffraction reveals robust 3D anionic frameworks with square-pyramidal (*sqp*) topology, where Ln^{3+} centers are bridged by μ_2-bidentate formate and μ_2-tetradentate oxalate groups. The 1D ultramicropores (~5 Å) host lattice water molecules and charge–balancing $[(CH_3)_2NH_2]^+$ cations. The Yb– and Lu–MOFs exhibit high stability in water, organic solvents, and at elevated temperatures (up to 400 °C). High–pressure CO_2 adsorption experiments (0.1–50 bar) on activated samples reveal distinct S–shaped isotherms at low pressure and temperature, which transition to stable plateaus under higher conditions. DFT and in situ DRIFTS analyses indicate that these features arise from interactions between CO_2 and the guest $[(CH_3)_2NH_2]^+$ cations, leading to the formation of dimethyl carbamic acid. These findings highlight the potential of these MOFs as efficient CO_2 sorbents for practical use, offering energy–efficient method for large-scale capture via pressure or temperature swing adsorption (PSA/TSA).

CRYSTAL STRUCTURE AND FLOCCULATION BEHAVIOR OF CONGO RED INDUCED BY COMPLEX IONS OF THE HEXAAMINECOBALT(III) COMPLEX

Audchariyapon Chaowaprasit[1], Kittipong Chainok[2], Nanthawat Wannarit[1,2,*]
[1]Department of Chemistry, Faculty of Science and Technology, Thammasat University, Pathum Thani 12121, Thailand
[2]Thammasat University Research Unit in Multifunctional Crystalline Materials and Applications (TU-MCMA), Faculty of Science and Technology, Thammasat University, Pathum Thani 12121, Thailand
*e-mail: nwan0110@tu.ac.th

Abstract:
A new complex, $[Co(NH_3)_6][CdCl_3(H_2O)](NO_3)_2{\cdot}(H_2O)_{0.75}$ was successfully synthesized via the slow evaporation method at room temperature and characterized by various elemental analysis as infrared spectroscopy (IR), diffuse reflectance spectroscopy (DRS), powder X-ray diffraction (PXRD), scanning electron microscopy (SEM), energy-dispersive X-ray spectroscopy (EDX), and thermogravimetric analysis (TGA). Single-crystal X-ray diffraction revealed that the complex crystallizes in the orthorhombic system with space group $P2_12_12_1$ and refined unit cell parameters a = 7.7176(1) Å, b = 12.7524(2) Å, c = 16.6749(3) Å, V = 1641.11(5) Å^3, and Z = 1. The structure consists discrete $[Co(NH_3)_6]^{3+}$ cations and one-dimensional chain $\{[CdCl_3(H_2O)]^-\}_n$ anions. The crystal structure is stabilized by intermolecular hydrogen bonding interactions. Hirshfeld surface analysis and fingerprint indicate that hydrogen bonding is the dominant intermolecular interaction, accounting for 63.3% of the overall crystal packing. Furthermore, the Congo red dye's flocculation is observable flocs form within 30 minutes and the solution becomes clear within 12 hours.

CRYSTAL STRUCTURE AND IODINE ADSORPTION OF A NEW TWO-DIMENSIONAL CADMIUM(II) COORDINATION POLYMER BASED ON BENZIMIDAZOLE AND DICYANOARGENTATE(I) LIGANDS

Chompunuch Bunfrueang,[1] Kittipong Chainok,[2] and Nanthawat Wannarit[1,2]*
[1] Department of Chemistry, Faculty of Science and Technology, Thammasat University, Khlong Laung, Pathum Thani, 12121, Thailand
[2] Thammasat University Research Unit in Multifunctional Crystalline Materials and Applications (TU-MCMA), Faculty of Science and Technology, Thammasat University, Khlong Luang, Pathum Thani 12121, Thailand

*e-mail: nwan0110@tu.ac.th

Abstract:
A new two-dimensional cadmium(II) coordination polymer, $[Cd(bzIm)(Ag(CN)_2)_2]_n$ (where bzIm = benzimidazole), has been successfully synthesized and fully characterized by elemental analysis, FT-IR spectroscopy, thermogravimetric analysis (TGA) and powder X-ray diffraction (PXRD). The single-crystal X-ray diffraction study revealed that the compound crystallizes in a triclinic system with the *P*-1 space group. The asymmetric unit contains one Cd(II) atom, two dicyanoargentate(I) molecules and one benzimidazole (bzIm) molecule. The Cd(II) center adopts a distorted square pyramidal geometry (τ_5 = 0.14). The Cd(II) centers are linked by bridging dicyanoargentate(I) ligands along the crystallographic *b* and *c* axes, providing 2D square grid (4,4) network. Each 2D layer is further connected through strong intermolecular argentophilic interactions [$Ag^I \cdots Ag^I$, 3.3662(7) Å] between bridging dicyanoargentate(I) ligands, resulting in the formation of the 2D double-layer structure. The 3D supramolecular framework of this compound is stabilized by π–π interactions between the phenyl rings of bzIm ligands in neighboring layers. Interestingly, the iodine adsorption behavior of this compound was investigated. The results indicate that 2 mg of the compound exhibits excellent iodine adsorption from an aqueous solution (200 ppm) within 10 minutes. The interactions I_2 was further examined using FT-IR, PXRD, UV–visible spectroscopy and scanning electron microscopy (SEM).

Crystallization of α-L-rhamnosidase from *Pediococcus acidilactici*

Natcha Suparangkul[1,2], Pasunee Laohawutthichai[2], Thatcheewa Apichatayanon[2], Karan Wangpaiboon[2], Kuakarun Krusong[2]*

[1]Program in Biotechnology, Faculty of Science, Chulalongkorn University, Thailand

[2]Center of Excellence in Structural and Computational Biology, Department of Biochemistry, Faculty of Science, Chulalongkorn University, Thailand

Email: kuakarun.k@chula.ac.th

Abstract

α-L-Rhamnosidase (EC 3.2.1.40) catalyzes the hydrolysis of terminal α-L-rhamnose residues from natural rhamnoglycosides such as naringin, rutin, and hesperidin. The enzyme specifically cleaves α-1,2- or α-1,6-rhamnosidic linkages and plays an important role in food, beverage, and pharmaceutical industries by modifying flavonoid glycosides, which enhances product quality. In this study, a rhamnosidase from *Pediococcus acidilactici* (*Pa*Rham) was heterologously expressed in *Escherichia coli* BL21(DE3) and purified via Ni-NTA affinity chromatography.

Crystallization of *Pa*Rham with rhamnose or naringin was performed, and X-ray diffraction data were collected at beamline BL13B1 of the National Synchrotron Radiation Research Center (NSRRC, Taiwan). The *Pa*Rham crystals, comprising of 543 amino acid residues, belongs to space group $P6_{622}$, with unit cell parameters a = b = 164.564 Å, c = 90.036 Å, and α = β = 90°, γ = 120°. The crystal contains one molecule per asymmetric unit, with a Matthews coefficient of 2.88 Å³/Da and an estimated solvent content of 57.3% (P = 0.98). Phase determination by molecular replacement using the model from AlphaFold was on trial. Other phasing methods may be used to determine the crystal structure of *Pa*Rham.

STRUCTURAL FEATURES OF THREE ISOSTRUCTURAL Ca(II)/Cd(II) ANIONIC METAL–ORGANIC FRAMEWORKS

Kunlanit Chinchan,[1] Bunyarat Rungtaweevoranit,[2] Kittipong Chainok,[1,*]
[1]Thammasat University Research Unit in Multifunctional Crystalline Materials and Applications (TU-MCMA), Faculty of Science and Technology, Thammasat University, Pathum Thani, 12121, Thailand
[2]National Nanotechnology Center (NANOTECH), National Science and Technology Development Agency (NSTDA), Pathum Thani 12120, Thailand
*e-mail: kc@tu.ac.th

Abstract:
Three novel 3D bimetallic cadmium(II)/calcium(II) metal-organic frameworks (MOFs), $(C_3H_5N_2)[CaCd_2(btc)(Hbtc)_2]\cdot 2H_2O$ (**1**), $((CH_3)_2NH)((CH_3)_4N)[Ca_2Cd_4(btc)_2(Hbtc)_4]\cdot 8H_2O$ (**2**), and $((CH_3)_2NH)[CaCd_2(btc)(Hbtc)_2]\cdot 4H_2O$ (**3**) were synthesized under solvothermal conditions and structurally characterized by single-crystal X-ray diffraction. Compounds **1** and **3** crystallize in the monoclinic space group $P2_1/c$, whereas compound **2** crystallizes in $P2$. Their structures are composed of trimeric $\{CaCd_2(Hbtc)_3\}_n$ units linked by btc^{3-} ligands, creating three-dimensional anionic frameworks that are stabilized by guest cations via N–H···O, C–H···O hydrogen bonds, and π···π stacking interactions. All MOFs exhibit blue luminescence in the solid state at room temperature and function as multiresponsive sensors for Cu^{2+}, Fe^{2+}, and Fe^{3+} ions through fluorescence quenching. Additionally, the investigation into high-pressure CO_2 adsorption (up to 20 bar) for all MOFs demonstrates a significant uptake capacity, highlighting their potential as multifunctional materials for sensing and gas storage.

SUPRAMOLECULAR STRUCTURE OF SCHIFF BASE NICKEL(II) THIOCYANATE COMLEXE

Kulwadee Ponanunrirk,[1] Nongnaphat Buakhajorn,[1] Patimapon Suanprang,[1] Kittipong Chainok,[1,*]
[1]Thammasat University Research Unit in Multifunctional Crystalline Materials and Applications (TU-MCMA), Faculty of Science and Technology, Thammasat University, Pathum Thani, 12121, Thailand
*e-mail: kc@tu.ac.th

Abstract:
The reaction of the $[Ni(NCS)_2]$ precursor complex with four equivalents of (*E*)-4-fluoro-*N*-(pyridin-2-ylmethylene)aniline (*L*) ligand in a CH_3OH solution yielded green block-shaped crystals of a mononuclear nickel(II) complex $[Ni(NCS)_2(L)_2]\cdot 2H_2O$. The complex crystallizes in the trigonal system with space group *R*-3, containing two distinct molecules in the asymmetric unit. There are two crystallographically independent moieties. Each Ni(II) center has a distorted octahedral coordination geometry and is surrounded by two terminal *N*-bonded NCS anions and two neutral *L* ligands in a *cis* configuration. The crystal packing exhibits several intermolecular interactions, including C−H···F, C−H···S, C−H···π, and π···π interactions, which contribute to the creation of a porous supramolecular architecture. The cytotoxicity of the complex against selected cancer cell lines and its CO_2 adsorption is evaluated.

SYNTHESIS, STRUCTURE AND CO_2 ADSORPTION OF LANTHANIDE TETRABROMO-1,4-DICARBOXYLATE FRAMEWORKS

Suwadee Jiajaroen[a*], Kittipong Chainok[b]
[a]Department of Science and Mathematics, Faculty of Science and Technology, Rajamangala University of Technology Tawan-ok, Chon Buri 20110, Thailand
[b]Thammasat University Research Unit in Multifunctional Crystalline Materials and Applications (TU-McMa), Faculty of Science and Technology, Thammasat University, Pathum Thani 12121, Thailand
[*]e-mail: suwadee_ji@rmutto.ac.th

Abstract

Lanthanide metal–organic frameworks (Ln-MOFs) are significantly interest for structural design toward diverse applications. In this work, we report the synthesis and structural characterization of a new series of lanthanide tetrabromo-1,4-dicarboxylate frameworks, $[Ln(Br_4bdc)_{1.5}]\cdot 3H_2O$ (Ln = Er, Tm, Yb, Lu and Br_4bdc = tetrabromo-1,4-dicarboxylate). Single crystal X-ray diffraction revealed that each Ln^{3+} ion adopts a six-coordinated geometry with Br_4bdc ligands, forming a one-dimensional cavity. The porous structure accommodates the tubular hexameric water clusters. Furthermore, the CO_2 adsorption behavior of the activated Ln-MOF was investigated in detail.

THREE DINUCLEAR PADDLE WHEEL COPPER (II) COMPLEXES BEARING DIPHENYLACETATE LIGAND. SYNTHESIS, STRUCTURAL CHARACTERIZATION AND PHOTOLUMINESCENCE STUDIES

Chatphorn Theppitak,[1,*] Kittipong Chainok,[3] Somsak Ruchirawat,[2,4]
[1]Chulabhorn Research Institute, Bangkok 10210, Thailand
[2]Chulabhorn Graduate Institute, Bangkok 10210, Thailand
[3]Thammasat University Research Unit in Multifunctional Crystalline Materials and Applications (TU-McMa), Faculty of Science and Technology, Thammasat University, Pathum Thani 12121, Thailand
[4]Center of Excellence on Environmental Health and Toxicology, Office of the Permanent Secretary (OPS), Ministry of Higher Education, Science, Research, and Innovation (MHESI), Bangkok 10400, Thailand
*e-mail: chatphorn@cri.or.th

Abstract:
Three copper(II) complexes, $[Cu_2(dpn)_4(dmf)_2]$ (**1**), $[Cu_2(dpn)_4(def)_2]$ (**2**), and $[Cu_2(dpn)_4(acn)_2]\cdot 2acn$ (**3**) [dpn = diphenyl acetic acid, dmf = *N,N*-dimethylformamide, def = *N,N*-diethylformamide, acn = acetonitrile] were synthesized by solvothermal methods and their crystal structure were determined by single crystal X-ray diffraction analysis. Complexes **1-3** consists of bimetallic tetracarboxylate units that adopt the well-known paddle-wheel motif. All three complexes crystallize in the triclinic system with the centrosymmetric space group *P*-1. The intramolecular Cu···Cu distances were measured of 2.6382(5), 2.65284(4), and 2.6225(6) Å for **1-3**, respectively. In addition to the primary coordination environments, the crystal structures are stabilized by an extensive network of weak intermolecular interactions, including C–H···O hydrogen bonds and C–H···π interactions, which contribute to the overall supramolecular assembly. The solid-state pholuminescence properties of these complexes were investigated at room temperature. Upon excitation at 345 nm, complexes **1-3** exhibited blue emissions with maxima at 460, 470, and 450 nm, respectively. These variations in emission behavior reflect the influence of the coordinated solvent molecules on the electronic environment of the copper centers. The combined structural and optical studies emphasize the structure–property relationships of copper paddle-wheel complexes and suggest their potential for applications in luminescent materials and molecular design strategies.

X-RAY CRYSTALLOGRAPHIC STRUCTURE OF TWO LITHIUM(I) COORDINATION POLYMERS

Pacharapon Jearanaiwiwat,[1] Mongkol Sukwattanasinitt,[2] Kittipong Chainok,[1,*]
[1]Thammasat University Research Unit in Multifunctional Crystalline Materials and Applications (TU-MCMA), Faculty of science and Technology, Thammasat University, Pathum Thani, 12121, Thailand
[2]Department of Chemistry, Faculty of Science, Chulalongkorn University, Bangkok, 10330, Thailand
*e-mail: Kc@tu.ac.th

Abstract: Two lithium(I) coordination polymers were synthesized by reacting LiCl salts with the corresponding chloranilic acid (H_2CA) or squaric acid (H_2SA), a 1D chain $(NH_4)[Li(\mu_4\text{-}CA)_2(H_2O)]\cdot 0.25H_2O$ (LiCA) and a 3D network $[Li_{12}(\mu_8\text{-}SA)_6]\cdot 1.5H_2O$ (LiSA), were obtained. The $[Li(\mu_4\text{-}CA)_2]$ chains of LiCA are connected through O−H···hydrogen bonds and Cl···π interactions, forming a 3D supramolecular architecture. Whereas, LiSA has a 3D polymeric network composed of distorted tetrahedral Li^+ ions and $\mu_8\text{-}SA^{2-}$ anions. The N_2 and CO_2 adsorption isotherms for both compounds were investigated.

SP11: RADIOECOLOGY AND ENVIRONMENTAL RADIOACTIVITY

A Survey of Natural Radionuclides Contents in Beach Sand Samples Collected in the Vicinity of Coastal Seawalls Structure, Songkhla Province, Thailand

Komrit Wattanavatee,[1,] * Murnee Daoh,[2] Pacharakorn Petpradup,[3] Pathiphan Pinsook,[3] Nawee Noonanat,[4] Thawatchai Itthipoonthanakorn,[5] Prakrit Noppradit,[6]
[1,3,4]Division of Physical Science, Faculty of Science, Prince of Songkla University, Hat Yai, 90112, Thailand
[2]Department of Physics and General Science Program, Faculty of Science and Technology, Songkhla Rajabhat University, Mueang Songkhla, 90000, Thailand
[4]Division of Biological Science, Faculty of Science, Prince of Songkla University, Hat Yai, 90112, Thailand
[5]Office of Atoms for Peace, Bangkok, 10900, Thailand
[6]Climate Change Research Center, Faculty of Environmental Management, Prince of Songkla University, Hat Yai, 90110, Thailand
*e-mail: komrit.w@psu.ac.th

Abstract:

Seawall is a permanent structure that was constructed at a coastal area to protect against the waves and to reduce coastal erosion. The 'Riprap and Offshore' are two typical seawalls which are often found in Songkhla Province, and they were constructed from several rocks and almost especially granite. The aims of current study are determining the activity concentration of natural radionuclide (^{226}Ra, ^{232}Th and ^{40}K) and assessing the radiation hazard derived from beach sand and rock samples around the seawall.

The beach sand samples collected about 2-5 km away outside the seawall, and about while 9 beach sand samples and 6 rock samples were collected inside the seawall. After sample pretreatment, the gamma ray intensity of studied radionuclides was analyzed by using the 70% relative efficiency HPGe gamma spectrometer, and IAEA RGU1 was performed for determination of their activity concentration. It was found that the activity concentration of ^{226}Ra, ^{232}Th and ^{40}K in samples have high variability, however their average values in beach sand samples collected inside the seawall are significantly higher than outside the seawall. In addition, their average activity concentrations in rock samples are more than approximately 10 times compared to beach sand samples. Consequently, the calculated four radiation hazard indices Ra_{eq}, H_{ex}, D and AED derived from rock samples were more than 4 times above permissible values, in contrast, these indices were below for all beach sand samples.

COMPUTATIONAL FLUID DYNAMICS INVESTIGATION OF INDOOR RADON DISTRIBUTION AT HAT YAI HOT SPRING SPA IN RANONG PROVINCE, THAILAND

Dumrongsak Rodphothong,[1,*] Wipada Ngansom,[1] Thawatchai Itthipoonthanakorn,[2] Saroh Niyomdecha,[2] Monthon Yongprawat[3]
[1]Department of Physics, Faculty of Science, Ramkhamhaeng University, Bangkok, 10240, Thailand
[2]Regulatory Technical Support Divisions, Office of Atoms for Peace, Bangkok, 10900, Thailand
[3]Nuclear Technology Research and Development Center, Thailand Institute of Nuclear Technology, Nakhon Nayok, 26120, Thailand
*e-mail: dumrongsak.r@rumail.ru.ac.th

Abstract:
Hat Yai hot spring is situated in the Ranong geothermal field, located along the Ranong Fault Zone, characterized by radiogenic heat from the granitic basement. The hot spring water is used for health tourism and provides spa treatments. The present study investigates indoor radon distribution using three-dimensional fluid dynamics in the Hat Yai hot spring spa area. A model combines steady airflow with dynamic radon advection-diffusion and decay mechanisms. Radon release from the hot tub is modeled through Henry's law interfacial flux. Two scenarios are evaluated: a closed space and a ventilated environment with radon-free air for different durations. Simulations reveal a near-surface plume with elevated concentrations near the ceiling. In the closed space, the volume-averaged concentration rises steadily, indicating the effects of interfacial mass transfer and room volume. Ventilation markedly reduces concentrations, achieving a quasi-steady state where air exchange and decay are in equilibrium. This work serves as an effective evaluative instrument, enabling mitigation approaches like enhanced ventilation and surface agitation to reduce indoor radon levels.

INVESTIGATION OF ISOTOPIC DYNAMICS IN THE MEKONG RIVER BASIN

Chalermpong Polee* Monthon Yongprawat Nichtima Uapoonphol Kiattipong Kamdee Patchareeya Chanruang Chakrit Saengkorakot Niracha Sirisaen
Nuclear Technology Research and Development Center, Thailand Institute of Nuclear Technology, Nakhon Nayok, Thailand
*Email: chalermpong@tint.or.th

Abstract

Global warming, together with the construction of water infrastructure in the upstream reaches of the Mekong River over the past decade, has resulted in unseasonal fluctuations in the water level of the mainstream in Southeast Asia, leading to both flooding and droughts in many areas. To better understand the hydrological system and local flow interactions, it is necessary to establish a stable isotope database of precipitation and surface water within parts of the Mekong River Basin in Thailand.

The objective of this study is to analyze hydrodynamic variability and the relative contribution of local precipitation to the Mekong River using stable isotope analysis of water. Daily precipitation samples were collected from five stations along the Mekong River in Thailand: Chiang Rai, Nan, Nong Khai, Nakhon Phanom, and Ubon Ratchathani. Weekly surface water samples were also collected from three representative stations: Chiang Saen, Nong Khai, and Khong Chiam. In addition, supplementary samples were collected from six tributary stations (Sub-Mekong River). Altogether, approximately 1,500 water samples were collected and analyzed, including daily precipitation and weekly surface water from both the Mekong River and its tributaries.

The isotopic results show that the Mekong River entering Thailand at Chiang Saen is relatively depleted, primarily due to the latitude effect, as the river originates from snowmelt in the Tibetan Plateau before flowing into Thailand. However, isotopic values gradually become enriched downstream, with the values at Ubon Ratchathani approaching those of local precipitation and tributary rivers, especially during the rainy season. In contrast, tributary rivers display isotopic enrichment during the dry season and depletion during the monsoon season. These findings provide a basis for evaluating the mixing processes between the Mekong mainstream and its tributaries within Thailand.

INVESTIGATION OF RADON CONCENTRATION (RN-222) IN GEOTHERMAL SPRINGS, THE SOUTHERN PART OF THAILAND

Saroh Niyomdecha[1*], Wipada Ngansom[2], Dumrongsak Rodphothong[2], Monthon Yongprawat[3] and Thawatchai Itthipoonthanakorn[1]
[1]Regulatory Technical Support Division, Office of Atoms for Peace, Bangkok, 10900, Thailand
[2]Department of Physics, Faculty of Science, Ramkhamhaeng University, Bangkok, 10240, Thailand
[3]Nuclear Technology Research and Development Center (NTRDC), Thailand Institute of Nuclear Technology (TINT), Nakhon Nayok, 26120, Thailand
* Corresponding author: Saroh.n@oap.go.th

Abstract:
This research aims to study the activity of Radon (Rn-222) in the hot spring area, Southern Thailand. Fifteen hot spring water samples were collected from seven provinces located in southern Thailand, including Ranong province (RN1, RN3, and RN7), Surat Thani province (SR1, SR3, SR7, and SR9), Phang Nga province (PG1), Krabi province (KB2 and KB4), Trang province (TR1), Phatthalung province (PL1, PL3 and PL4) and Satun province (ST1). In those areas, ambient gamma dose rates were measured using a survey meter before collecting samples, and the radon concentrations in hot spring water samples were determined onsite using a RAD-7 electronic radon detector. Measured radon concentrations in hot spring water were ranged from 9 Bq/L (PG1) to 7,070 Bq/L (SR3) very consistent to the level of Ambient gamma dose rates, which were ranged between 0.246 - 14.83 μSv/h. It is concluded that Radon concentrations of hot spring water of three hot spring areas in Surat Thani province (SR3, SR7, SR9) and an area in Ranong province (RN7) exceed the alternative maximum concentration level (AMCL) in raw water suggested by the US.EPA (150 Bq/L) and perhaps needs appropriate management.

SP12: THE 2ND INTERNATIONAL SYMPOSIUM OF SCIENCE COMMUNICATION AND PUBLIC SCIENCE LITERACY

A JAPANESE HEALTH TV PROGRAM: EFFECTIVE COMMUNICATION OF MEDICAL SCIENCE FOR PROMOTING PUBLIC HEALTH

Kitipong Soontrapa,[1,*]

[1]Department of Pharmacology, Faculty of Medicine, Siriraj Hospital, Mahidol University, Thailand
*e-mail: kitipong.soo@mahidol.ac.th

Abstract:

Japan is widely recognized to be one of the healthiest countries owing to its low rates of lifestyle diseases and high life expectancy, mainly ascribed to a comprehensive universal healthcare system. As a consequence of effective health promotion, Japanese people are generally not only mindful but also knowledgeably aware of various medical information and healthy lifestyles. Television (TV) medium has long been a major mass media in Japan, and it serves as a dominant tool supporting health promotion by conveying health information to the public. Nevertheless, although, unlike entertainment, contents related to clinical and medical science knowledge are basically unattractive and non-popular, many Japanese media creators can remarkably overcome this challenge by producing both informative and entertaining health TV programs being able to be shown in prime time on numerous mainstream TV channels. One of the best examples is “Tameshite Gatten” or later renamed “Gatten”, a very notable and long running health TV program by NHK TV (1995-2022).Gatten took a scientific perspective at current topics related to medicine and healthy lifestyles by way of presenting cutting-edge research in fun, intuitive ways and offering valuable information that can be practical in real life. In closing, the style of making Japanese health TV programs like “Gatten” would rather be adoptable in other countries to help improve their public health.

A PROACTIVE APPROACH TO MISINFORMATION: LEVERAGING QFT TO CULTIVATE CRITICAL ANALYSIS AND EVALUATION SKILLS FOR THE AI ERA

Natdanai Nirutmeteekul,[1]* Sara Samiphak,[2]
[1] Kasem Phithaya School, Thailand
[2] Chulalongkorn University, Thailand
*e-mail: 6680048727@student.chula.ac.th

Abstract:
The objective of our study was to present QFT as an empirically proven pedagogical strategy that effectively develops the core critical thinking components (Analysis and Evaluation) necessary to safeguard public science literacy against the challenges of the Generative AI era. Participants were lower secondary students (N = 29), which were selected by purposive sampling approach. Research design was the pre-experiment one group pretest-posttest design. Participants were taught the fundamental content of the Chemical reactions and Materials in everyday life from Thailand's Core Standard Curriculum (revised edition 2017). Over 15 sessions (750 minutes), students engaged in QFT-based activities aimed at fostering critical thinking skills. Critical thinking skills was assessed using five components: Interpretation, Evaluation, Inference, Explanation, and Analysis.

The results revealed a statistically significant improvement in overall critical thinking skills ($p < .05$), with notable gains in Analysis and Evaluation, but no significant changes in Interpretation, Inference, and Explanation. To further promote critical thinking skills and make QFT more accessible beyond the classroom while strengthening the three skills that showed no significant improvement (Interpretation, Inference, and Explanation). A four-steps was proposed: 1) Interpret the Scientific Focus, 2) Pose Questions, 3) Analyze and Prioritize Questions, 4) Inquire, Explain, and Reflect on Reasoning.

BEYOND THE TEXTBOOK: DESIGNING FOR CURIOSITY AND DISCOVERY IN STEM

Namkang Sriwattanarothai[1,*]
[1] Institute for Innovative Learning, Mahidol University, Thailand
*e-mail: namkang.sri@mahidol.ac.th

Abstract:
In an era defined by rapid scientific and technological advancement, traditional pedagogical approaches often struggle to bridge the gap between complex frontier science and meaningful student engagement. The challenge for educators is no longer limited to transmitting information, but to designing learning experiences that cultivate curiosity, discovery, and lasting comprehension. This presentation examines how innovative tools and design strategies can make abstract STEM concepts accessible, tangible, and inspiring. Drawing on principles of cognitive psychology, design innovation, and communication theory, it traces the evolution of creative media—from physical models and analogies to animation, augmented reality, and game-based learning environments—that transform scientific ideas into participatory experiences. Each example highlights how conceptual clarity, learner-centered design, and technology-enhanced engagement can sustain motivation and deepen understanding. The presentation proposes a practical framework for designing STEM experiences that spark initial interest through storytelling, sustain exploration through interactivity, and reward curiosity through discovery. By emphasizing enjoyment as a gateway to understanding, these design approaches nurture curiosity-driven learners prepared to think critically and creatively about the scientific challenges of our time, ultimately advancing inclusive, frontier-ready STEM education aligned with the United Nations Sustainable Development Goals.

EFFECTIVENESS OF THAILAND SCIENCE CARAVAN: A CASE STUDY OF NST FAIR 2025 IN CHIANG MAI

Kuan-Chun Wang[1*]
[1]Department of Master Program of Science Communication and Education, National Pingtung University, Taiwan
*e-mail: sms1030120@gmail.com

Abstract:
The study guided by the Contextual Model of Learning (CML), examines the effectiveness of interactive exhibits in the Thailand Science Caravan at the NST Fair 2025 in Chiang Mai. A questionnaire was distributed to 213 visitors, focusing on three dimensions: Sociocultural context – exhibition design and planning, Physical context – usability of interactive exhibits, and Personal context – scientific knowledge and motivation for participation. Results indicate high visitor satisfaction across all dimensions, with usability and knowledge clarity receiving the strongest ratings. Nevertheless, crowding in the exhibition space was frequently reported as a barrier to engagement, and open-ended responses emphasized the importance of improved visitor flow and layout planning. These findings highlight both the strengths and limitations of mobile science outreach initiatives and provide a useful reference for comparative studies with science communication practices in Taiwan.

EMPOWERING NORTHERN YOUTH FOR ACTION ON THE SMOKE HAZE CRISIS THROUGH A HANDS-ON SCIENCE COMMUNICATION MODEL

Kreetha Kaewkhong[1], Pimjutha Winyarath[2], Orawee lawhana[2], Pichamon Sudecha[3], Sasipat Deemak[2], Sadanon Jaisaksern[4], Wan Wiriya[4,5,*]
[1] Department of Curriculum Teaching and Learning, Faculty of Education, Chiang Mai University 50200, Thailand
[2] Office of Strategy Management, Office of University, Chiang Mai University, 50200, Thailand
[3] Office of University, Chiang Mai University, 50200, Thailand
[4] Environmental Science Research Center, Faculty of Science, Chiang Mai University, 50200, Thailand
[5] Department of Chemistry, Faculty of Science, Chiang Mai University, 50200, Thailand
*e-mail: wan.w@cmu.ac.th

Abstract:
As a key initiative of the Academic Center for Air Pollution in Northern Thailand, this project addresses the region's recurring smoke haze crisis. This presentation introduces a hands-on science communication model designed to bridge the gap between awareness and action by empowering local youth as communicators. The model follows a structured production flow where students first engage in practical, based on activities—such as building low-cost air quality sensors and interpreting localized data—to ground their understanding. This enhanced awareness of particulate matter with diameter less than 2.5 micrometer (PM2.5), from its toxic composition to health impacts, is then translated into action. Students are guided to identify their target audiences and to transform complex data into simple, digestible messages using effective visual communication. To evaluate this process, focus groups are conducted with student and teacher leaders across nine northern provinces to gather qualitative insights for refinement. This approach not only enhances public science literacy but also builds the capacity of a new generation of science communicators by fostering a sense of agency and equipping them with the confidence to lead environmental action. This project serves as a replicable and evaluated framework for communicating frontier science in a challenging era.

ENHANCING PUBLIC UNDERSTANDING OF SYNCHROTRON TECHNOLOGY THROUGH TARGETED SCIENCE COMMUNICATION

Sarayut Tunmee,[1,*] Sasipun Tritan,[1] Kultida Pittayaporn,[1] Kallayanee Abking,[1]

[1]Synchrotron Light Research Institute (Public Organization), 111 University Avenue, Muang District, Nakhon Ratchasima 30000, Thailand
*e-mail: sarayut@slri.or.th

Abstract:

Effective communication of frontier science, particularly in synchrotron light technology, is crucial for maximizing research impact and fostering engagement across various sectors. This study presents a strategic framework developed by the Synchrotron Light Research Institute (SLRI) to cater to the diverse needs of four primary sectors: education (25%), private industry (35%), government (25%), and the public (15%). Key challenges include the complexity of scientific content, differing levels of science literacy, and varying expectations across sectors. To address these challenges, SLRI utilizes tailored communication methods such as interactive exhibitions, science camps, academic seminars, and industry-specific consultations. These activities, designed to translate advanced scientific concepts into accessible formats and promote meaningful dialogue, are a collaborative effort that supports engagement and practical applications. The findings emphasize the importance of adaptive, audience-centered strategies in enhancing public understanding and facilitating the societal integration of synchrotron-based innovations.

HERBAL INNOVATION AND MULTI-STAKEHOLDER INTEGRATION FOR SUSTAINABLE AREA-BASED DEVELOPMENT: POLICY RECOMMENDATIONS FROM THE MAEMOK HERBAL VALUE CHAIN, LAMPANG PROVINCE

Siraya Janasak[1,*], Suwannee Janta[1], Chadnaree Meesukho[1], Chiraprapa Khamrath[1], Ekasit Chaipin[1], Ratchadaporn Thongpaen[1], and Woraya Chatuphatrangsri[1]
[1] Lampang Rajabhat University 119 Moo9 Chompu, Mueang, Lampang, Thailand 52100
*e-mail: siraya.jana@gmail.com

Abstract:

The **Maemok Herbal Valley Project** demonstrates an area-based research model that integrates science, local wisdom, and participatory communication strategies to coordinate multi-stakeholder collaboration for poverty alleviation in Lampang Province, Thailand. The project was initiated in 2021 under the poverty alleviation program supported by the PMU-A. Using the 2019 TPMAP database, poor households were jointly screened by government, academia, civil society, and local communities. Data collection through standardized questionnaires was processed via PPP Connext and analyzed using the Sustainable Livelihood Framework (SLF) to classify households into four levels of deprivation. Those with potential were included in a poverty reduction model designed through community asset and identity analysis in collaboration with network partners.

The model positioned herbs as the key mechanism to transform cultural and indigenous knowledge into economic resources. Through cooperation among researchers, government agencies, the private sector, and the Maemok Herbal Agricultural Cooperative, 155 poor households were integrated into a pro-poor herbal value chain. Activities covered three stages: upstream (farmers adopted GAP and PGS standards through participatory workshops and visual training tools that translated complex technical standards into accessible practices), midstream (cooperative members learned processing and compound extraction techniques via step-by-step training kits and practical demonstrations), and downstream (in collaboration with LPRU and ICOS, the LANLA brand was established. Two prototypes—Aroma Massage Oil and Calming Herbal Cream—were developed from indigenous herbs (*Plantago major L.* and *Zingiber montanum*), with active compounds extracted and standardized under ASEAN Cosmetic GMP of ICOS. This brand strategically communicated both indigenous heritage and scientific validation, positioning local herbs as competitive, innovation-driven products for consumers).

The outcomes of the project confirm that communication was not a supplementary tool but the central enabler of success, achieved by speaking the language of farmers, simplifying science for cooperatives, narrating heritage to consumers, and presenting evidence to policymakers. This effort led to a provincial-level MOU among Lampang PAO, five universities, and three other organizations to institutionalize procurement of herbal products for 67 Subdistrict Health Promoting Hospitals (SHPHs), integrating them into the provincial public health and traditional medicine system as a model for poverty reduction, community empowerment, and sustainable development.

Asst. Prof. Dr. Siraya Janasak is a lecturer in the Logistics and International Business Program at Lampang Rajabhat University. She graduated with a Bachelor's degree followed by a Master's degree in Business Administration from Kasetsart University, and a doctorate in Business Administration from Ramkhamhaeng University. She began working on area-based research, focusing on poverty alleviation, from 2021 to the present, and has developed Thai herbal products under the brand name **"Lanla"**.

INNOVATIVE STEM CHALLENGE ACTIVITY THROUGH BIOMIMICRY-INSPIRED ENGINEERING: A STRATEGY FOR ENHANCING SCIENTIFIC COMPETENCIES IN SECONDARY STUDENTS FOR SUSTAINABLE COMMUNITY

Pranee Disrattakit*, Jatuporn Puntree, Thanatkrit Kaewtem, Weerawut Tiankao, Massuwan Pongpramoon, and Nitat Sripongpun
Affiliation
Mahidol Wittayanusorn School, Salaya, Phutthamonthon District, Nakhon Pathom, Thailand 73170
*e-mail:
pranee.dis@mwit.ac.th

Abstract:
The annual STEM Challenge, organized by Mahidol Wittayanusorn School, aims to enhance youth competencies in Science, Technology, Engineering, and Mathematics (STEM). It also fosters critical 21st-century skills, such as creative thinking, problem-solving, and collaboration. The 2024 Challenge focused on designing energy-efficient and safe structures using biomimicry principles. Examples include 'Designing Buildings to Reduce Temperature' and 'Designing Buildings to Reduce Wind Resistance.' This provided a strong context for integrating and measuring Science Communication as a foundational skill. Organizers restructured the competition to focus on the communication process needed to translate complex scientific knowledge into practical applications. A formal announcement included explicit problem statements and technical criteria, such as reductions in temperature and wind. A Science Communication metric was also formally added to the judging criteria. Besides technical performance, participants were evaluated on how clearly and practically they conveyed their scientific concepts, biomimicry inspiration, and design rationale to the judging panel. Temperature reduction was measured using the difference between the interior and exterior building temperatures in a simulated environment with an applied heat source. Wind resistance reduction was assessed by comparing the spring tension force exerted on the structure during wind simulation. This approach showed that hands-on STEM activities requiring explicit communication were highly effective. Student performance improved significantly in logical reasoning, problem-solving, and Science Communication. Specifically, 90.53% of participants (SD = 7.37) achieved targeted competencies—including communicating scientific designs—according to teacher evaluations. Students also reported high engagement and perceived skill gains, with an average satisfaction score of 4.54 (SD = 0.07) out of 5. This program demonstrates that embedding and assessing Science Communication in STEM challenges makes complex concepts, such as biomimicry, tangible and applicable. It provides a clear way for participants to turn understanding into practical skills, resulting in real impact for community and environmental sustainability.

SEED BANKING INITIATIVES IN NORTHERN THAILAND

Pimonrat Tiansawat[1,2,*], Nattanit Yiamthaisong[2], Pannachet Kijja[2], Dia Panitnard Shannon[1,2] Prasit Wangpakapattanawong[1,2], Khuanphirom Naruangsri[2], Supoj Aunkaew[2], Oeungarin saichan[2], Tharangkul phuntien[2], and Autain Fusri[2]

[1] Doi Suthep Nature Center, Faculty of Science, Chiang Mai University, Thailand 50200
[2] Forest Restoration Research Unit, Department of Biology, Faculty of Science, Chiang Mai University, Thailand 50200
*e-mail: pimonrat.t@cmu.ac.th

Abstract:
An *ex-situ* seed bank is a facility for storing and preserving plant genetic resources in the form of seeds. In the event of natural disasters or habitat changes that threaten plant survival, the stored seeds can be used for propagation and reintroduction into the wild. In addition, the seed bank provides seeds for seedling production used in ecosystem restoration efforts. The Seed Bank, Faculty of Science, Chiang Mai University, is located at the Doi Suthep Nature Center for Natural History, Huay Kaew Road, Suthep Subdistrict, Mueang District, Chiang Mai Province. It is the first officially established seed bank under the Faculty of Science. The establishment of this seed bank resulted from collaboration and support from several organizations, including the Office of Research Administration under the HRH Princess Maha Chakri Sirindhorn's Plant Genetic Conservation Project, Chiang Mai University, the Forest Restoration Research Unit, Department of Biology, Faculty of Science, and the Millennium Seed Bank, Royal Botanic Gardens, Kew, United Kingdom.

The seed bank began its establishment process in 2020 and has continued its operations to the present. Its activities include monthly field surveys and seed collection of local northern Thailand's tree species, seed-related research conducted by students of the Department of Biology, training workshops, and providing educational services to visitors. Currently, the Seed Bank preserves seeds from 70 species of native trees. Each year, it organized five training workshops and received more than 1,000 visitors.

TRAVEL LINK: CONNECTING DATA, DECISIONS, AND UNDERSTANDING

Unchalisa Taetragool[1]*

[1] Big Data Institute (Public Organization), Thailand
*e-mail: unchalisa.ta@bdi.or.th

Abstract:
Travel Link is a collaborative data initiative developed by the Big Data Institute to strengthen data-driven decision-making in Thailand's tourism sector. The project integrates tourism-related information from public agencies and business partners, creating a shared platform that supports evidence-based policy planning and business analysis. Designed as both an infrastructure and a learning space, Travel Link applies data science and AI to transform fragmented datasets into coherent, interpretable insights for the tourism ecosystem.

Beyond providing analytics, the initiative also engages with stakeholders through workshops and training to build capacity in data literacy and promote a culture of informed decision-making. This dual focus on technology and human understanding highlights how data can function not only as empirical evidence but also as a medium for communication and collaboration among government, researchers, and industry actors.

This presentation reflects on the opportunities and challenges of translating research into relevance, especially in communicating complex analytical results to diverse audiences. It discusses how trust, shared understanding, and institutional readiness influence the adoption of data-driven tools. By examining Travel Link as both a technical and social process, the talk offers insights into how scientific work can inform dialogue, support collective learning, and foster more effective connections between data, decisions, and the people who act upon them.

WHAT INSPIRES ME TO DEVELOP BOARD GAMES AS LEARNING TOOLS

Nutthapol Orpipath[1]*
[1]Board Game Designer, Thailand
*e-mail: Nutthapol.orp@gmail.com

Abstract:
This presentation explores the inspiration and design process behind developing board games for learning, drawing from the experience of a game designer with a background in science and engineering. The initial inspiration arose from the challenge of transforming complex academic content such as quantum physics into board games that are easy to understand, enjoyable, and thought-provoking. The development integrates key principles of Gamification, Experiential Learning, and Constructivism, resulting in a five-step framework known as MARCO, consisting of Motivation & Meaning, Analysis & Audience, Rule & Role Design, Creation & Component Design, and Observation & Optimization.

This study presents the design journey guided by the MARCO process, culminating in the creation of the board game Quantum Fighter. The result demonstrates that board games can serve as powerful learning media that foster engagement, systems thinking, and creative extension, aligning effectively with their role as efficient educational tools.

Keywords: board games, learning tools, gamification, experiential learning, constructivism

Figure 1.

Quantum Fighter fornt cover

WHERE SCIENCE MEETS ART: TRANSFORMING MEDICAL EDUCATION THROUGH CREATIVE MEDIA DESIGN

Kanchanaphan Poonudom[1]*
[1]Medical Education Technology Program, Faculty of Medicine, Siriraj Hospital, Mahidol University, Thailand
*e-mail: kanchanaphan.pon@mahidol.ac.th

Abstract:
Current medical education faces limitations in terms of time, resources, access to real patients, and traditional teaching methods, all of which affect the effectiveness of student learning. The integration of media, art, innovation, and technology has become a crucial mechanism for enhancing the quality of education and aligning it with the evolving healthcare system. Medical learning media, including illustrations, animations, 3D models, videos, infographics, and immersive technologies such as augmented and virtual reality, are essential for converting abstract or intricate information into understandable and memorable formats. Well-designed media make learning more engaging, help students remember what they've learned for a long time, and support active, competency-based learning by making complex information easier to understand while still being academically rigorous. Effective media design must therefore emphasize scientific accuracy, clear communication, relevance to target learners, and expert validation to ensure practical, safe, and effective application in real-world settings.

The creation of making high-quality medical and health education media is based on three core principles: accuracy, digestibility, and design. Accuracy ensures scientific reliability and applicability to real-world contexts via collaboration with medical professionals. Digestibility focuses on narrative structure and visual hierarchy, transforming complex systems into logical and learner-friendly narratives that facilitate comprehension without oversimplification. Design governs the aesthetic and cognitive structure, guiding attention and emotion and allowing learners to absorb information naturally. These principles work together to create a balanced framework that combines science and art and turns passive content into active learning experiences. This approach reflects the value of the Medical Education Technology Program, Faculty of Medicine, Siriraj Hospital, Mahidol University, presenting a multidisciplinary curriculum that blends medical science, art, and technology to produce high-quality educational media. By integrating scientific accuracy with creative design, it redefines the delivery of health education, transforming complex knowledge into accessible, engaging, and meaningful learning experiences that elevate the quality of healthcare education.

SP14: VALORIZATION OF BIOMASS-RELATED WASTES

ACID CATALYZED GLYCEROL ESTERIFICATION OF OLEIC ACID

Somya Lekcharoen[1], Narita Chanthon[1], Kanokwan Ngaosuwan[3,*], Worapon Kiatkittipong[4], Doonyapong Wongsawaeng[5], Weerinda Mens[6], Nopphon Weeranoppanant[2,7], Apinan Soottitantawat[2,8], Pongtorn Charoensuppanimit[2,8], and Suttichai Assabumrungrat[1,2]

[1]Center of Excellence on Catalysis and Catalytic Reaction Engineering, Department of Chemical Engineering, Faculty of Engineering, Chulalongkorn University, Bangkok, 10330, Thailand

[2]Bio-Circular-Green-economy Technology & Engineering Center (BCGeTEC), Faculty of Engineering, Chulalongkorn University, Bangkok, 10330, Thailand

[3]Chemical Engineering Division, Faculty of Engineering, Rajamangala University of Technology Krungthep, Bangkok, 10120, Thailand

[4]Department of Chemical Engineering, Faculty of Engineering and Industrial Technology, Silpakorn University, Nakhon Pathom, 73000, Thailand

[5]Department of Nuclear Engineering, Faculty of Engineering, Chulalongkorn University, Bangkok, 10330, Thailand

[6]Department of Chemical and Materials Engineering, Faculty of Engineering, Rajamangala University of Technology Thanyaburi, Pathumthani, 12110, Thailand

[7]Department of Chemical Engineering, Faculty of Engineering, Chulalongkorn University, Bangkok, 10330, Thailand

[8]Center of Excellence in Particle and Materials Processing Technology, Department of Chemical Engineering, Faculty of Engineering, Chulalongkorn University, Bangkok 10330, Thailand

*e-mail:
kanokwan.n@mail.rmutk.ac.th

Abstract:

Glycerol is an abundant by-product generated during biodiesel production. Numerous studies have explored the valorization of glycerol through its conversion into high-value chemicals. One promising pathway for glycerol utilization is the production of monoglycerides (MGs) and diglycerides (DGs), valuable emulsifiers extensively applied in food, cosmetic, and pharmaceutical industries. The esterification of glycerol with oleic acid (OA) was employed to produce MGs and DGs in the presence of an acid catalyst However, there are two types of acid catalysts, including Brønsted and Lewis acid catalysts. Therefore, this study proposed the utilization of proprane sultone ionic liquid (PEI-PS) as a Brønsted acid catalyst and manganese glycerolate (MnGly) as a Lewis acid catalyst for the production of MGs and DGs via glycerol esterification. As can be seen from Fig. 1, the PEI-PS catalyst demonstrated superior catalytic activity, affording 93.71% conversion in 4 h and producing 42.37% MGs and 45.89% DGs yields under the conditions of 130 °C, 2 wt.% catalyst loading, and a 3:1 glycerol to oleic acid molar ratio. In contrast, the MnGly catalyst exhibited reduced performance, achieving only 66.53% conversion, 26.82% MG yield, and 35.00% DG yield under the same conditions. The superior activity of the PEI-PS catalyst can be ascribed to the presence of sulfonate acid groups, which impart strong acidity and thereby accelerate the esterification rate relative to MnGly. However, the reusability of PEI-PS and MnGly was limited, as both catalysts dissolved into the reaction medium. This effect might be attributed to the high reaction temperature, which promotes solvation of the active sites and subsequent

detachment from the ligand. Therefore, immobilization on high surface area supports such as silica, mesoporous silica, activated carbon, g-C_3N_4, TiO_2, or alumina via wet impregnation could be a promising approach to enable practical industrial applications.

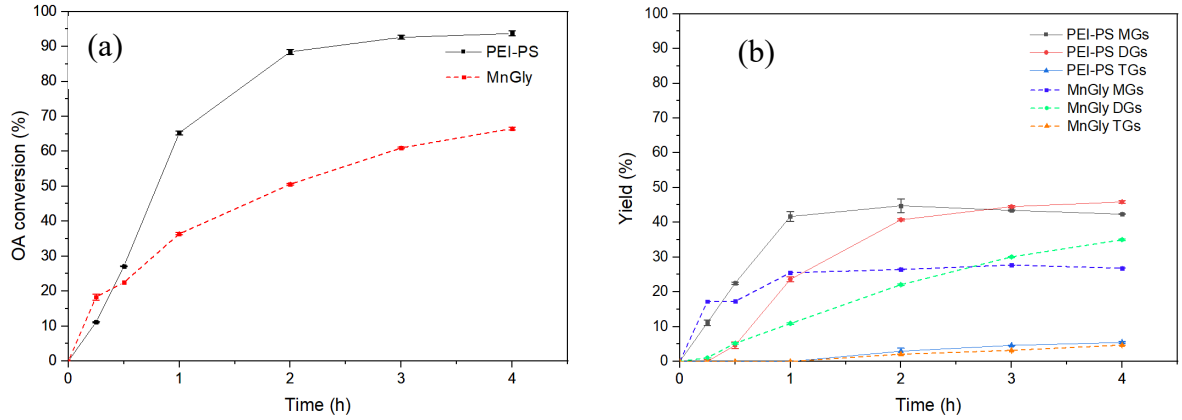

Figure 1.
Glycerol esterification of oleic acid using PEI-PS and MnGly catalysts (a) OA conversion and (b) MGs, DGs, and TGs yields.

DEGRADATION OF HESPERIDIN INTO HIGH-VALUE CHEMICALS BY CO_2-H_2O SYNERGY UNDER MICROWAVE IRRADIATION

Kota Nishimure[1], Armando T. Quitain [2,*], Tetsuya Kida[3]

[1]Graduate School of Science and Technology, Kumamoto University, Kumamoto 860-8555, Japan
[2]Graduate School of Social and Cultural Sciences, Kumamoto University, Kumamoto 860-8555, Japan
[3]Institute of Industrial Nanomaterials, Kumamoto University, Kumamoto 860-8555, Japan
*e-mail: quitain@kumamoto-u.ac.jp

Abstract:

Rutinose is a disaccharide of significant importance in pharmaceutical research, particularly in the structural analysis and functional studies of flavonoid glycosides. This sugar does not occur freely in nature and is usually obtained from glycosides such as hesperidin or rutin through enzymatic hydrolysis. However, these enzymes are difficult to obtain, and the reactions require extremely stringent conditions, making the production process complex and costly.

In this study, we propose a more practical and sustainable alternative: the use of a subcritical CO_2-H_2O reaction medium to produce rutinose from hesperidin. Excessive use of organic solvents in the pharmaceutical industry is a major source of environmental impact, and reducing their usage is a key challenge from the perspective of green chemistry. This method represents one of the sustainable hydrolysis techniques that have recently attracted attention as environmentally friendly process.

In the CO_2-H_2O system, dissolved CO_2 forms carbonic acid, which acts as a mild acid catalyst. Through this catalytic effect, hesperidin is hydrolyzed into the target product, rutinose, and its aglycone, hesperetin (Fig. 1). As a heating method, microwave irradiation was employed, which is expected to shorten heating time and improve energy efficiency. To enhance reaction efficiency, silicon carbide (SiC) was added as a microwave susceptor. SiC efficiently absorbs microwave energy and creates localized high-temperature regions, thereby promoting hydrolysis in the vicinity of the reaction sites.

In a representative experiment, 10 mg of hesperidin was dissolved in 3 mL of water and reacted at 130 °C and 1.5 MPa. Sugar analysis of the product by HPLC revealed a rutinose yield of 22.6% and a selectivity of 63.4%. Glucose and rhamnose, the constituent monosaccharides of rutinose, were also detected, suggesting that under the present conditions, part of the rutinose was further hydrolyzed into monosaccharides. Optimization of parameters such as reaction temperature, pressure, and SiC loading to improve the yield and selectivity of rutinose was also carried out.The yield of rutin hydrolyzed by conventional enzymatic methods was 74%. Therefore, further yield improvement is necessary.

This research is expected to contribute to the development of novel reaction systems involving the interaction between CO_2-H_2O system and microwave heating, leading to the practical implementation of environmentally friendly processes for the production of functional carbohydrates.

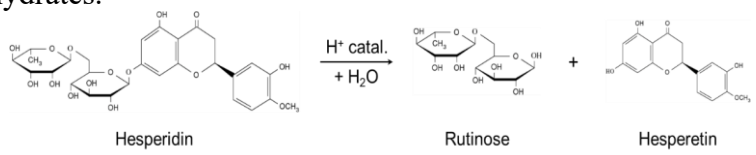

Figure 1. Acid-catalyzed hydrolysis of hesperidin into rutinose and hesperetin

Effect of Iron Oxide on Nanoporous Carbon from Pine Leaves via Hydrothermal Carbonization

Phannika Udomrak, Thanaphat poltirach, Khanatsanan Intaraprasert, Monthakarn Chanthip, Damrong Mingkhwankeeree, Narutchai Thongprasert, Apiluck *Eiad-Ua**
Department of Nanoscience and Nanotechnology, School of Integrated Innovative Technology, King Mongkut's Institute of Technology Ladkrabang.Bangkok, Thailand
Suratthani School, Mueang Suratthani,
Suratthani
**Corresponding author. E-mail: apiluck.ei@kmitl.ac.th*

This research aimed to develop nanoporous carbon from pine leaves using metal catalysts through a hydrothermal carbonization process, followed by carbonization under nitrogen atmosphere. The study systematically varied the mixing ratios of pine leaves and metal precursors (1:0, 1:5, 1:10, and 1:15), reaction times (4, 8, and 12 hours), and hydrothermal temperatures (200, 220, and 240°C), before subjecting the products to carbonization at 600–900°C. Structural and compositional characterization by FT-IR, Raman spectroscopy, and XRD revealed that the introduction of iron oxides significantly influenced the formation of nanoporous carbon. Specifically, FeO promoted pore development and enhanced conductivity, while Fe_3O_4 facilitated biomass decomposition and uniform nanostructure formation, leading to improved porosity and crystallinity. Higher carbonization temperatures further enhanced graphitic ordering and material stability. Under optimal conditions, nanoporous carbon with well-developed nanostructures and favorable physical properties was achieved. These findings demonstrate that the controlled use of FeO and Fe_3O_4 can effectively tailor the pore structure and performance of nanoporous carbon, highlighting its potential in energy environmental applications

Keywords: nanoporous carbon, Pine leaves, hydrothermal carbonization

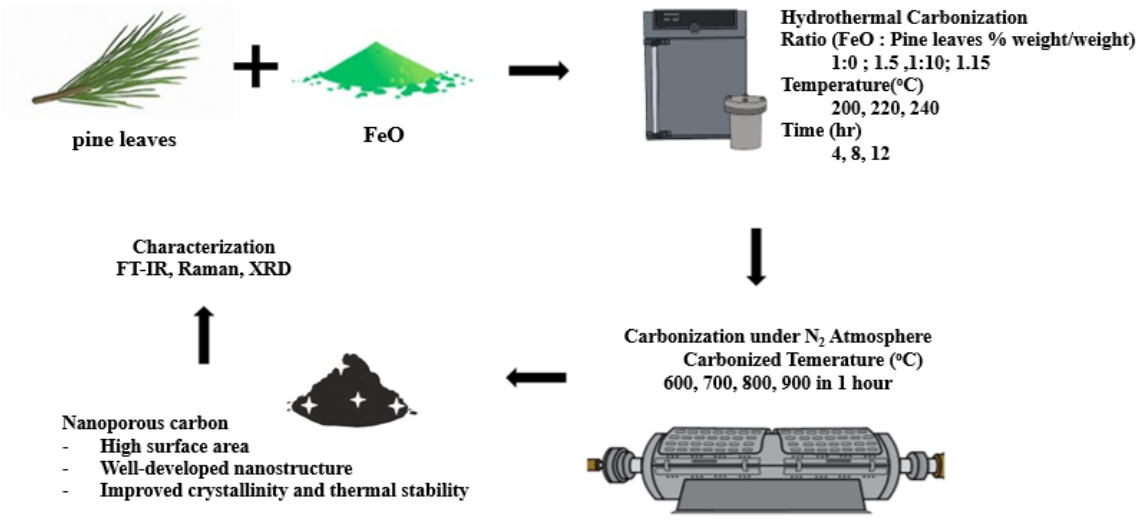

Figure 1. Process flow for syntheizing nanoporous carbon from pine leaves using

Environmentally Friendly Alcohol Oxidation Using Ni-Fe Spinel Catalysts With Tunable Redox Properties

Yota Tanari,[1] Yusuke Inomata,[2] Tetsuya Kida[3]
[1] Department of Materials and Technology, Kumamoto University, 860-8555, Japan
[2] Faculty of Advanced Science and Technology, Kumamoto University, 860-8555, Japan
[3] Institute of Industrial Nanomaterials, 860-8555, Japan,
*e-mail: tetsuya@kumamoto-u.ac.jp

Abstract:

The oxidation of alcohols to aldehydes or ketones is a fundamental and widely applied transformation in organic chemistry. However, conventional methods typically rely on toxic oxidants such as peracids or chromates, which generate large amounts of waste and offer poor catalyst reusability. To overcome these issues, the development of heterogeneous catalysts that allow easy separation, recyclability, and minimal environmental impact is highly desirable.

In this study, we focused on mixed metal oxides composed of iron and nickel, which are known as relatively inexpensive and earth-abundant metals. These elements can form spinel-type structures (e.x., $NiFe_2O_4$), which are expected to exhibit superior redox properties compared to single-metal oxides (Fig. 1). We synthesized a series of spinel oxides with varying Ni/Fe ratios and investigated their catalytic performance in the aerobic oxidation of benzyl alcohol using molecular oxygen as the oxidant.

A series of Ni–Fe spinel oxides with varying Ni/Fe ratios were synthesized via a citrate gel method using $Fe(NO_3)_3 \cdot 9H_2O$ and $Ni(NO_3)_2 \cdot 6H_2O$ as precursors. The resulting powders were calcined at 400 °C and characterized by X-ray diffraction (XRD) and nitrogen adsorption measurements to determine crystal phase and surface area.

Catalytic performance was evaluated in the aerobic oxidation of benzyl alcohol in xylene at 130 °C under open-air conditions. Reaction products were analyzed by GC-FID.

XRD confirmed the formation of spinel $NiFe_2O_4$ phases in all samples, and surface areas remained largely unaffected by the Ni/Fe ratio. Among the tested compositions, the highest benzaldehyde yield was achieved at 130 °C (Table 1.). Additionally, catalytic activity was examined under varying temperatures and atmospheric conditions. H_2-temperature programmed reduction (H_2-TPR) was performed to gain insight into the redox properties. Further investigation is underway to identify the active sites and clarify the reaction mechanism.

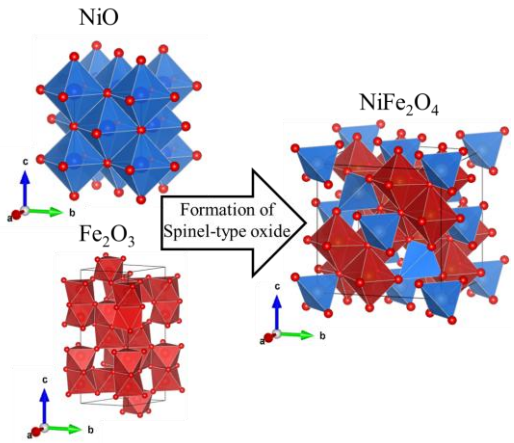

Fig 1. Structure of NiO, Fe_2O_3 and $NiFe_2O_4$

Table 1. Benzaldehyde yield and reaction temperature for each catalyst

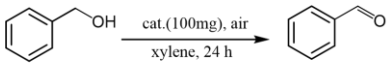

entry	cat.	temperature(°C)	yield(%)[a)]
1	NiO	130	55
2	Fe_2O_3	130	48
3	$NiFe_2O_4$	130	92
4	$NiFe_2O_4$	70	6
5	$NiFe_2O_4$	90	32
6	$NiFe_2O_4$	110	54

ESTERIFICATION OF CRUDE GLYCEROL TO ACETIN AS FUEL ADDITIVE

Arthit Jarungwongsathien[1,2], Kanokwan Ngaosuwan[3], Worapon Kiatkittipong[4], Doonyapong Wongsawaeng[5], Weerinda Mens[6], Santi Chuetor[7,8], Apiluck Eiad-Ua[9], Suttichai Assabumrungrat[1,2,*]

[1]Center of Excellence on Catalysis and Catalytic Reaction Engineering, Department of Chemical Engineering, Faculty of Engineering, Chulalongkorn University, Bangkok, 10330, Thailand

[2]Bio-Circular-Green-economy Technology & Engineering Center (BCGeTEC), Faculty of Engineering, Chulalongkorn University, Bangkok, 10330, Thailand

[3]Chemical Engineering Division, Faculty of Engineering, Rajamangala University of Technology Krungthep, Bangkok, 10120, Thailand

[4]Department of Chemical Engineering, Faculty of Engineering and Industrial Technology, Silpakorn University, Nakhon Pathom, 73000, Thailand

[5]Research Unit on Plasma Technology for High-Performance Materials Development, Department of Nuclear Engineering, Faculty of Engineering, Chulalongkorn University, Bangkok, 10330, Thailand

[6]Department of Chemical and Materials Engineering, Faculty of Engineering, Rajamangala University of Technology Thanyaburi, Pathumthani, 12110, Thailand

[7]Department of Chemical Engineering, Faculty of Engineering, King Mongkut's University of Technology North Bangkok, Bangkok, 10800, Thailand

[8]Center of Eco-Materials and Cleaner Technology, King Mongkut's University of Technology North Bangkok, Bangkok, 10800, Thailand

[9]College of Materials Innovation and Technology, King Mongkut's Institute of Technology Ladkrabang, Bangkok, 10520, Thailand

**e-mail: Suttichai.a@chula.ac.th

Abstract:

Owing to its abundant supply and low cost as a biodiesel by-product, glycerol has emerged as a pivotal resource for valorization, driving sustainable development through the circular economy and the BCG model. This study explores the utilization of pretreated crude glycerol (CG), a by-product of the biodiesel industry, as a feedstock for the esterification of acetic acid to produce acetin derivatives, which serve as valuable intermediates for diverse industrial applications. Different solid acid catalysts, including Indion 225H (a commercial ion-exchange resin) and graphene oxide (GO) synthesized via the Tour method, were used to catalyze this reaction. The crude glycerol was mainly composed of glycerol, moisture, salts, and other impurities, with contents of 83.6, 10.7, 4.8, and 0.9 wt.%, respectively. A simple pretreatment of crude glycerol by dehydration at 120 °C was implemented, and the pretreated glycerol was used to react with acetic acid for acetin production. After 2 h, the conversions of crude glycerol using Indion 225H and GO catalysts were 77.0% and 70.2%, respectively, under conditions of an acetic acid-to-glycerol molar ratio of 6:1, a catalyst loading of 5 wt.%, and a reaction temperature of 110 °C, as illustrated in Fig. 1. The highest monoacetin selectivity was achieved when using crude glycerol (CG) for both solid acid catalysts. In contrast, only 3.31% and 2.34% triacetin yields were observed at 2 h, whereas significantly higher triacetin yields were obtained in the esterification of commercial pure glycerol (PG) with acetic acid (95.3% and 99.6% using Indion 225H and GO catalysts, respectively). Catalytic activities were reduced by salts in pretreated crude glycerol, which blocks or poison acid catalyst sites. A techno-economic and environmental assessment is needed to balance

CG's low cost with pretreatment requirements for sustainable industrial use for acetin production.

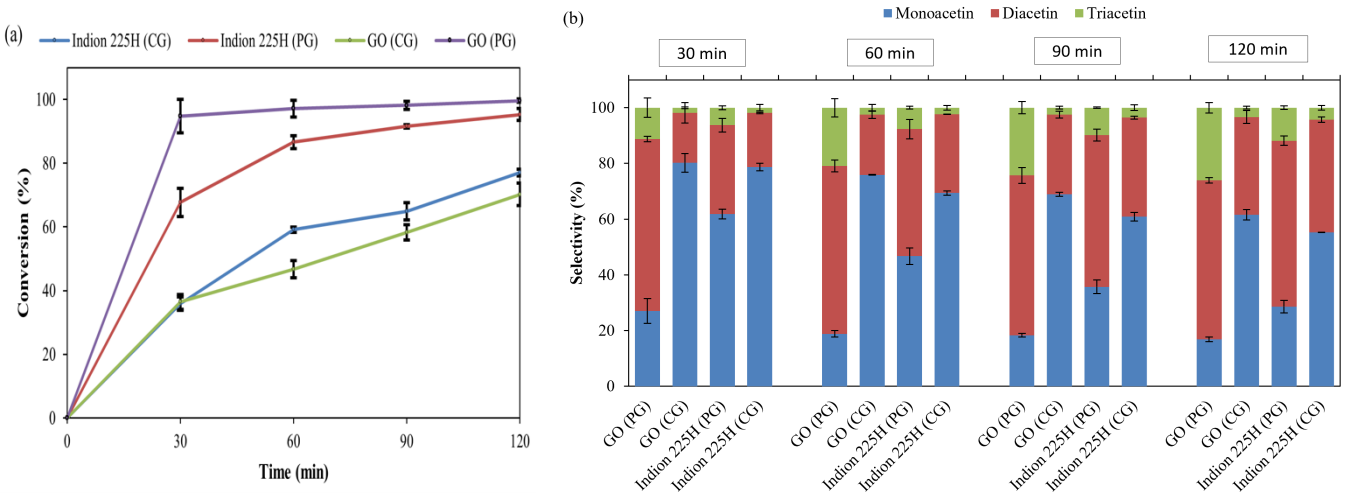

Figure 1.
(a) Glycerol conversion and (b) mono-, di-, and triactin selectivities from glycerol esterification with acetic acid (PG: Pure glycerol; CG: Crude glycerol).

GLYCEROLYSIS OF COCONUT OIL USING CALCIUM OXIDE CATALYST FROM EGGSHELL

Namfon Sirikul[1], Narita Chanthon[1], Kanokwan Ngaosuwan[2,*], Worapon Kiatkittipong[3], Doonyapong Wongsawaeng[4], Weerinda Mens[5], Nopphon Weeranoppanant[6,8], Apinan Soottitantawat[7,8], Pongton Charoensuppanitmit[7], and Suttichai Assabumrungrat[1,8]

[1]Center of Excellence on Catalysis and Catalytic Reaction Engineering, Department of Chemical Engineering, Faculty of Engineering, Chulalongkorn University, Bangkok 10330, Thailand
[2]Chemical Engineering Division, Faculty of Engineering, Rajamangala University of Technology Krungthep, Bangkok 10120, Thailand
[3]Department of Chemical Engineering, Faculty of Engineering and Industrial Technology, Silpakorn University, Nakhon Pathom 73000, Thailand
[4]Research Unit on Plasma Technology for High-Performance Materials Development, Department of Nuclear Engineering, Faculty of Engineering, Chulalongkorn University, Bangkok 10330, Thailand
[5]Departments of Chemical and Materials Engineering, Faculty of Engineering, Rajamangala University of Technology Thanyaburi, Pathum Thani 12120, Thailand
[6]Department of Chemical Engineering, Faculty of Engineering, Chulalongkorn University, Bangkok 10330, Thailand
[7]Center of Excellence in Particle and Materials Processing Technology, Department of Chemical Engineering, Faculty of Engineering, Biorefinery Cluster, Chulalongkorn University, Bangkok 10330, Thailand
[8]Bio-Circular-Green-economy Technology & Engineering Center (BCGeTEC), Department of Chemical Engineering, Faculty of Engineering, Chulalongkorn University, Bangkok 10330, Thailand
*e-mail: kanokwan.n@mail.rmutk.ac.th

Abstract:

Calcium oxide (CaO) can be derived from natural sources like limestone or animal shells containing calcium carbonate ($CaCO_3$), which can be converted to CaO by the calcination process. A high catalytic activity for CaO-catalyzed transesterification to produce biodiesel was already addressed because of its high basicity and high thermal stability. Therefore, the utilization of CaO derived from natural sources should be a promising heterogeneous catalyst for glycerolysis of coconut oil. This study aims to produce monoglycerides (MGs) and diglycerides (DGs) via the glycerolysis of coconut oil using a calcium oxide (CaO) catalyst derived from eggshells. Eggshells were calcined at 900 °C for 5 h. SEM analysis revealed that the CaO catalyst from eggshells exhibited an irregular, porous surface. The EDX result confirmed mainly Ca and O, indicating successful conversion of $CaCO_3$ to pure CaO after calcination. The synthesized CaO, with a surface area of 6.11 m^2/g and an average pore size of about 10.39 nm, could facilitate the diffusion of glycerol and coconut oil molecules to the active sites. Furthermore, the basic strength of this synthesized catalyst ranged from 7.2 to 9.8 with a basicity of 0.53 mmol/g. Using a coconut oil to glycerol molar ratio of 3:1, a reaction temperature of 180 °C, and 1.5 wt.% CaO with a reaction time of 240 min, a high coconut oil conversion of 86.46% was achieved, yielding 58.03% MGs and 23.31% DGs. This research demonstrates a promising pathway for producing valuable oleochemicals from renewable resources while promoting a circular economy.

HYDROCHAR PRODUCTION FROM POMELO PEELS AND PHYSICOCHEMICAL CHARACTERIZATIONS AS SOLID FUEL

Ahmad Danish[1]*, Umer Rashid[2], Balkis Hazmi[2], Azil Bahari Alias[3], Ramin Khezri[4] and Wan Azlina Wan Abdul Karim Ghani[1*]
[1]Sustainable Process Engineering Research Centre, Universiti Putra Malaysia, Serdang, Selangor, MALAYSIA
[2]Institute of Nanomaterials & Nanotechnology, Universiti Putra Malaysia, Serdang, Selangor, MALAYSIA
[3]Industrial Process Reliability & Sustainability (INPRES), Faculty of Chemical Engineering, Universiti Teknologi MARA, 40450 Shah Alam, Selangor, MALAYSIA
[4]Metallurgy and Materials Science Research Institute, Chulalongkorn University, Soi Chula 12, Phayathai Road, Patumwan, Bangkok 10330, THAILAND
*e-mail: wanazlina@upm.edu.my

Abstract:
The depletion of fossil fuels and increasing concerns over environmental impacts have accelerated the global transition toward renewable energy sources. Biomass, particularly fruit waste, represents a promising alternative due to its abundance and renewability. This study investigates the effectiveness of Hydrothermal Carbonization (HTC) in producing hydrochar from pomelo peels and compares its performance with conventional pyrolysis. Pomelo peels, selected for their thickness and availability, were treated under HTC conditions ranging from 160–200 °C for 10–20 h. Process optimization was conducted using Response Surface Methodology (RSM), and the resulting products were characterized using FTIR spectroscopy, thermogravimetric analysis (TGA), calorific value determination, and proximate and ultimate analyses. Pyrolysis achieved a maximum mass yield of 40.16 % at 400 °C for 30 min, while HTC produced a mass yield of 38.08 % at 180 °C for 15 h. Both hydrochar and biochar exhibited increased carbon content compared to the raw material (57.94 % and 67.48 %, respectively). Hydrochar demonstrated a higher calorific value (31.07 MJ/kg) due to elevated hydrogen content, lower ash and moisture levels, and improved thermal stability. Although HTC yields were relatively stable across the studied conditions, temperature and residence time significantly influenced pyrolysis output. This study demonstrated the potential of Hydrothermal Carbonization (HTC) to convert pomelo peel waste into energy-dense hydrochar under relatively mild operating conditions (160–200 °C, 10–20 h). Compared with pyrolysis, HTC produced a solid fuel with comparable mass yield and superior calorific value, attributed to its higher hydrogen content, lower ash and moisture levels, and enhanced thermal stability.

Keywords: Hydrochar, pomelo peels, solid fuel

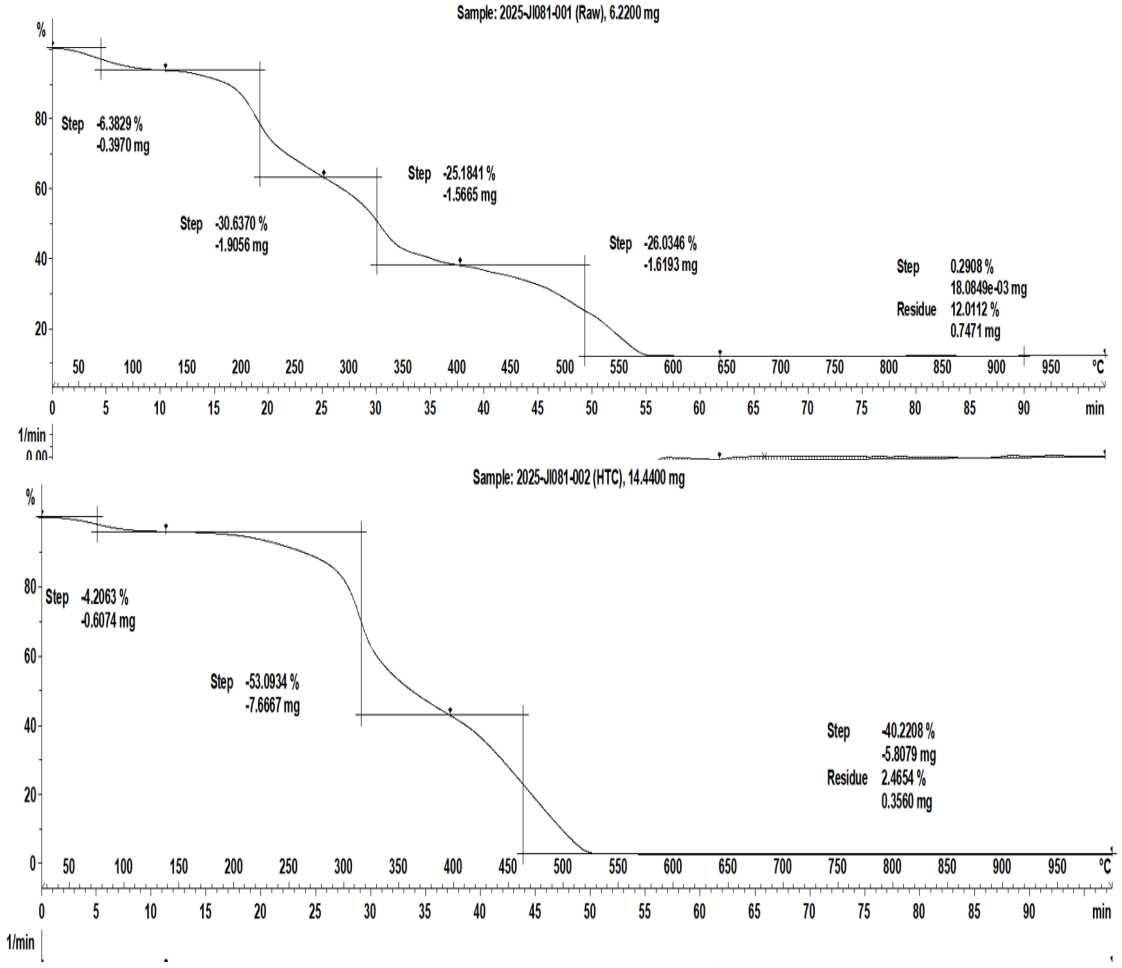

Figure 1. Thermogravimetric analyses (TGA) of raw and hydrochar

Table 1: Proximate and Ultimate analyses of Samples

Sample	Carbon (%)	Hydrogen (%)	Nitrogen (%)	Sulphur (%)	Oxygen (%)
Raw Pomelo Peels	38.44	6.70	0.88	0.08	53.9
Hydrochar	57.94	8.04	1.12	0.07	32.83
Biochar	67.48	4.10	1.99	0.08	26.35

METHANE GAS REMOVAL VIA PALM KERNEL SHELL-DERIVED XEROGEL ADSORBENTS

Nur Izzah Insyirah Hashim[1]*, Adam Haikal[2], Wan Azlina Wan Abdul Karim Ghani[2], Shiva Rezaei Motlagh[3] and Azil Bahari Alias[1]*

[1]Industrial Process Reliability & Sustainability (INPRES), Faculty of Chemical Engineering, Universiti Teknologi MARA, 40450 Shah Alam, Selangor, MALAYSIA

[2]Sustainable Process Engineering Research Centre, Universiti Putra Malaysia, Serdang, Selangor, MALAYSIA

[3]Research Unit on Sustainable Algal Cultivation and Applications, Faculty of Engineering, Chulalongkorn University, Bangkok, 10330, THAILAND

*e-mail: 2021899364@student.uitm.edu.my and azilbahari@uitm.edu.my

Abstract:

Methane emissions have become a significant environmental concern due to various anthropogenic activities, including agriculture and landfilling. Although less toxic than sulfur dioxide, methane is a far more potent greenhouse gas than carbon dioxide, contributing directly to global warming. Adsorption is a widely used technique for methane removal, with activating carbon being the predominant adsorbent. This study explores the potential of a novel xerogel adsorbent derived from palm kernel shell biomass (PKSBX) for methane (CH_4) capture. The PKSBX was synthesized via the sol–gel method and characterized using BET, FTIR, elemental analysis, TGA, and SEM. The xerogel exhibited a surface area of 29.45 m^2/g, pore volume of 0.0295 cm^3/g, and an average pore size of 4.62 nm, classifying it as a mesoporous material. Elemental analysis revealed 43.43% carbon, 3.60% hydrogen, and 50.92% oxygen, indicating abundant oxygenated functional groups favorable for gas adsorption. Response surface methodology (RSM) was applied to optimize process parameters prior to adsorption experiments. The effect of gas flow rate (23.0–42.9 L/h) and adsorbent dosage (1.14–13.9 g) on CH_4 adsorption performance was investigated. The results showed that lower flow rates (23.0 L/h) enhanced adsorption efficiency due to longer gas–solid contact time, while increasing adsorbent mass improved CH_4 uptake through greater surface area and active site availability. The breakthrough curves demonstrated that most adsorption equilibrium was reached within 3 minutes, indicating rapid CH_4 uptake kinetics. These findings confirm the feasibility of PKSBX as a sustainable, biomass-derived adsorbent for methane mitigation, offering a potential low-cost and eco-friendly alternative to commercial activated carbon for gas purification and biogas upgrading applications.

Keywords: Xerogel, Palm kernel shell (PKS), CH4 removal

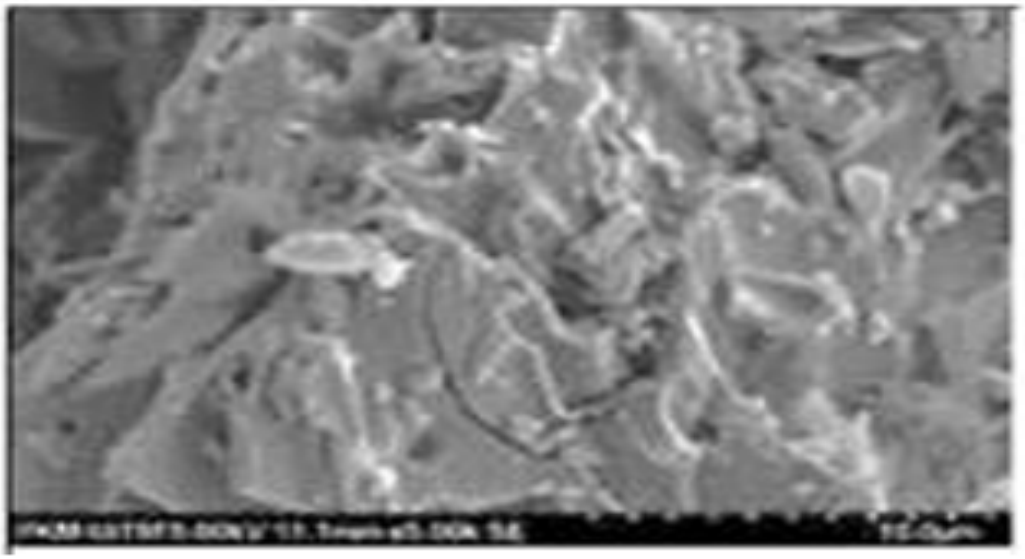

Figure 1. SEM image of PKSBX

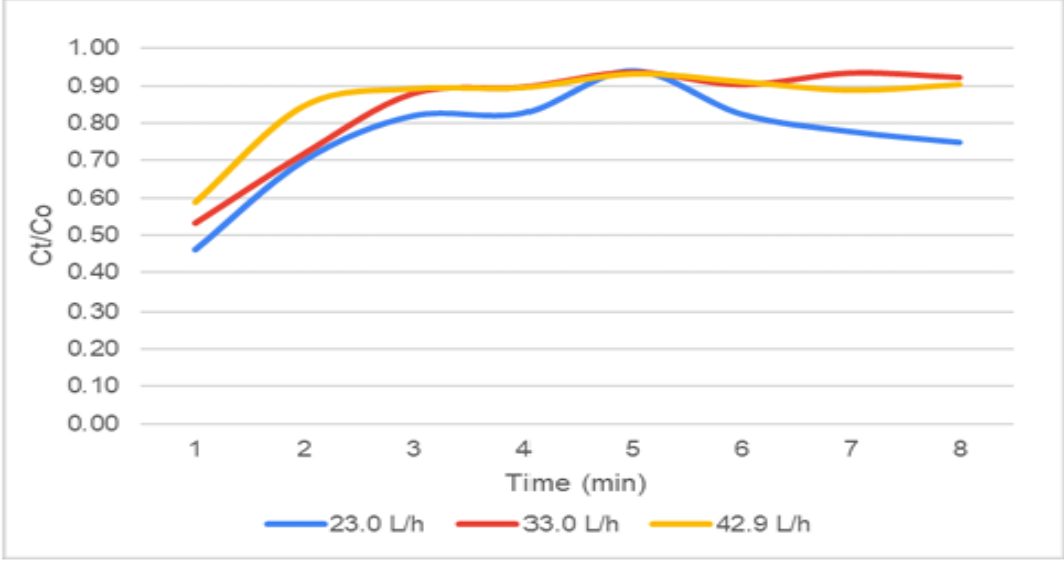

Figure 2. CH4 adsorption profile

MODIFIED SOLUBILITY MODELLING FOR PREDICTING BIOACTIVE COMPOUND EXTRACTION IN SUPERCRITICAL CARBON DIOXIDE SYSTEM WITH CO-SOLVENT

Nuttida Rosmontri,[1] Kokhao Chitniratna,[2] Dang Saebea[1*], Nopphon Weeranoppanat, [3, 4*]
[1] Department of Chemical Engineering, Faculty of Engineering, Burapha University, Chonburi 20131, Thailand
[2] School of Biomolecular Science and Engineering, Vidyasirimedhi Institute of Science and Technology (VISTEC), Wangchan Valley, Rayong, 21210, Thailand.
[3] Department of Chemical Engineering, Faculty of Engineering, Chulalongkorn University, Bangkok 10330 Thailand
[4] Bio-Circular-Green-economy Technology & Engineering Center (BCGeTEC), Department of Chemical Engineering, Faculty of Engineering, Chulalongkorn University, Bangkok, 10330 Thailand
*e-mail: dangs@eng.buu.ac.th, nopphon.w@chula.ac.th

Abstract:

The development of bioactive compound extraction typically begins with solvent screening, often relying on trial-and-error approaches. Recently, solubility models have been proposed to predict which solvents can dissolve specific molecules, offering potential guidance for solvent selection. Among these, Hansen solubility parameter (HSP) theory is one of the most widely used methods to predict solute–solvent interactions. However, conventional HSP applications are generally limited to single-solvent systems and conditions at atmospheric temperature and pressure. To enhance the capabilities of the Hansen Solubility Parameter (HSP) model, this study aims to further develop a modified HSP approach for describing solvent mixtures at elevated temperatures and pressures. Specifically, the modified HSP model was applied to screen co-solvent types and operating conditions for the supercritical carbon dioxide ($scCO_2$) extraction of *Centella asiatica* (L.) Urb. The focus was on four key bioactive compounds found in *Centella asiatica*—asiaticoside (AS), madecassoside (MS), asiatic acid (AA), and madecassic acid (MA)—due to their therapeutic applications, including wound healing, neuroprotection, and skin care. Physical property obtained from REFPROP database, and PR-BM (Peng-Robinson-Boston-Mathias) equation of state were incorporated into the model. Screening of co-solvents was performed by estimating relative energy difference (RED) values, where RED < 1 indicates a higher likelihood of dissolving the target bioactive compounds. Our analysis identified 1-butanol, 2-ethoxyethanol, 2-methoxy-ethanol, 3-methyl-1-butanol, 1-pentanol and 1-propanol as promising co-solvents for extracting the four bioactive compounds.

MONOLAURIN PRODUCTION VIA GLYCEROLYSIS USING CRUDE GLYCEROL FROM THE BIODIESEL INDUSTRY

Chan Myae Khin Hla Win[1], Namfon Sirikul[1], Narita Chanthon[1], Kanokwan Ngaosuwan[2*], Worapon Kiatkittipong[3], Doonyapong Wongsawaeng[4], Weerinda Mens[5], Nopphon Weeranoppanant[6,8], Apinan Soottitantawat[7,8], Pongton Charoensuppanitmit[7], and Suttichai Assabumrungrat[1,8]

[1]Center of Excellence on Catalysis and Catalytic Reaction Engineering, Department of Chemical Engineering, Faculty of Engineering, Chulalongkorn University, Bangkok 10330, Thailand
[2]Chemical Engineering Division, Faculty of Engineering, Rajamangala University of Technology Krungthep, Bangkok 10120, Thailand
[3]Department of Chemical Engineering, Faculty of Engineering and Industrial Technology, Silpakorn University, Nakhon Pathom 73000, Thailand
[4]Research Unit on Plasma Technology for High-Performance Materials Development, Department of Nuclear Engineering, Faculty of Engineering, Chulalongkorn University, Bangkok 10330, Thailand
[5]Departments of Chemical and Materials Engineering, Faculty of Engineering, Rajamangala University of Technology Thanyaburi, Pathum Thani 12120, Thailand
[6]Department of Chemical Engineering, Faculty of Engineering, Chulalongkorn University, Bangkok 10330, Thailand
[7]Center of Excellence in Particle and Materials Processing Technology, Department of Chemical Engineering, Faculty of Engineering, Chulalongkorn University, Bangkok 10330, Thailand
[8]Bio-Circular-Green-economy Technology & Engineering Center (BCGeTEC), Department of Chemical Engineering, Faculty of Engineering, Chulalongkorn University, Bangkok 10330, Thailand
*e-mail: kanokwan.n@mail.rmutk.ac.th

Abstract:

Crude glycerol, a major byproduct of the biodiesel industry, can be valorized into monolaurin, a high-value compound with antimicrobial and emulsifying properties. It is widely used in food, cosmetics, pharmaceuticals, and industrial applications. However, most studies have focused on commercial glycerol, while the direct use of crude glycerol remains underexplored due to its impurities. This knowledge gap limits the feasibility of monolaurin production at an industrial scale. This study evaluates methanesulfonic acid (MSA) catalyzed glycerolysis of biodiesel-derived crude glycerol compared with commercial glycerol. The obtained crude glycerol comprised glycerol (83.6%), moisture (10.7%), salts (4.8%), fatty acid methyl ester (0.025%), and other impurities (0.9%). Therefore, the simple pretreatment of this crude glycerol was applied by evaporation at 120 °C for 2 h. A significantly lower lauric acid conversion of only 48.6% was observed when using pretreated crude glycerol compared to commercial glycerol (99.5%) for glycerolysis using a glycerol to lauric acid molar ratio of 3:1, 1 wt.% of MSA, reaction temperature of 130 °C for 240 min, as depicted in Fig.1 (a). In contrast to the selectivity to monolaurin, dilaurin, and triaurin in Fig. 1 (b), a similar product distribution was achieved for the pretreated crude glycerol and commercial glycerol. This might be attributed to impurities, particularly NaCl, which can hinder the active sites through neutralization. Moreover, the effective salt removal method and process optimization of the pretreated crude glycerol are required to achieve a performance comparable to that of commercial glycerol.

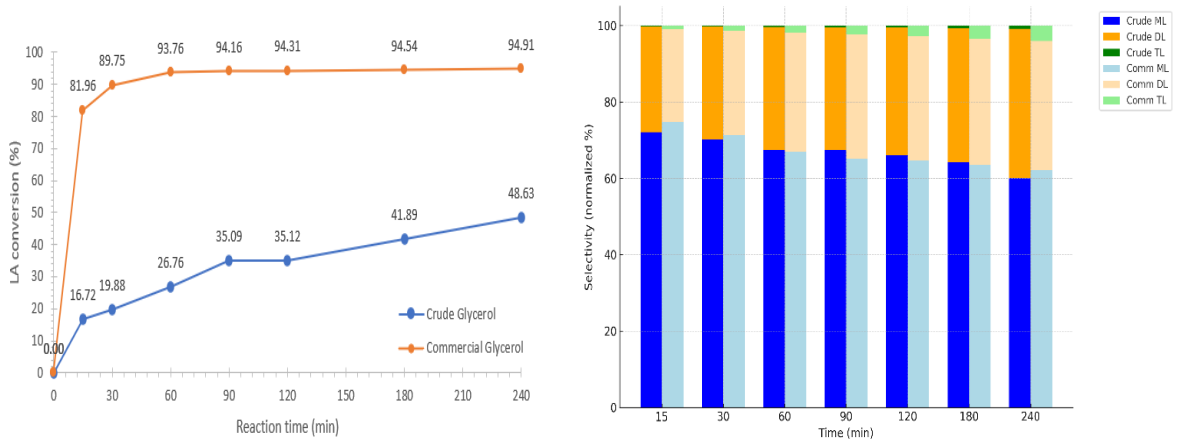

Figure 1. Glycerolysis of lauric acid with crude glycerol and commercial glycerol: (a) conversion of lauric and (b) selectivities of monolaurin, dilaurin, and trilaurin

Nanoporous Carbon from Tamarind Seeds via Hydrothermal-carbonization

Jarinya Srisakda, Khanatsanan Intaraprasert, Monthakarn Chanthip, Damrong Mingkhwankeeree, Narutchai Thongprasert, Apiluck Eiad-Ua*
Department of Nanoscience and Nanotechnology, School of Integrated Innovative Technology, King Mongkut's Institute of Technology Ladkrabang.Bangkok, Thailand
Suratthani School, Mueang Suratthani,Suratthani
*Corresponding author. E-mail: apiluck.ei@kmitl.ac.th

Abstract:
Nanoporous carbons (NPCs) were successfully synthesized from lignocellulosic tamarind seed biomass through a combination of pressurized air combustion pre-treatment at 300 °C for 2 h and subsequent carbonization under a nitrogen atmosphere at 600–900 °C for 1–2 h, followed by chemical activation using potassium hydroxide (KOH) solutions of varying concentrations. The process achieved a high carbon yield of approximately 35–40%, depending on the temperature and activation ratio. The air combustion pre-treatment effectively removed volatile components and enhanced the structural rigidity of the precursors, while the subsequent carbonization promoted carbon ordering and initial pore formation. KOH activation played a crucial role in further developing the pore network through redox reactions that released gases (H_2, CO, and CO_2) and intercalated potassium into the carbon matrix, producing highly interconnected micro- and mesopores. Characterization results confirmed these effects: Fourier-transform infrared spectroscopy (FTIR), Raman spectroscopy, and X-ray diffraction (XRD) indicated the transformation toward more ordered carbon structures, while scanning electron microscopy (SEM) and Brunauer–Emmett–Teller (BET) analyses revealed a well-developed porous morphology with a high specific surface area exceeding 1200 m^2/g. These results demonstrate that tamarind seeds are a sustainable and cost-effective precursor for producing high-performance nanoporous carbons, suitable for advanced environmental and energy storage applications.

Keywords: Tamarind seed, Air combustion, Carbonization, KOH activation, Yield, Nanoporous carbon

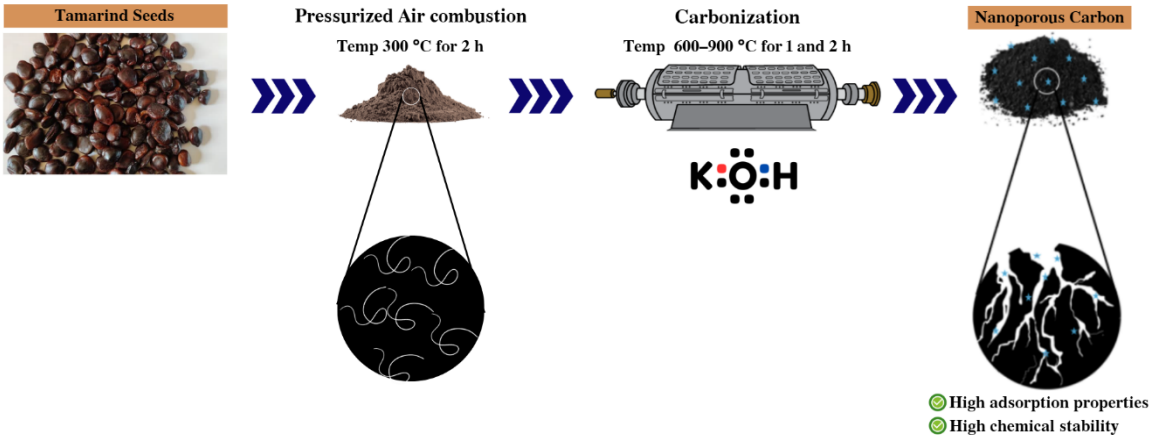

Figure 1. Scheme diagram of the research experiment

NOVEL GREEN SYNTHESIZED MAGNETIC-SILVER-CORN HUSK BIOCHAR AS ANTIMICROBIAL AGENT AND PHOTOCATALYST FOR METHYLENE BLUE DEGRADATION

Chetnipit Kunawong,[1] Kunlanard Langkaphin,[1] Supitchaya Piamchon[1], Chitawan Daolert[1], Chanyanut Thammasit,[2] Sakdinun Nuntang[2,*]

[1] Montfort College, Chiang Mai, 50000, Thailand
[2] Industrial Chemistry Innovation Program, Faculty of Science, Maejo University, Chiang Mai 50290, Thailand

*e-mail: Sakdinun.nt@gmail.com

Abstract:
Corn husk (CH) was used to create the multifunctional magnetic-silver/biochar material (M-Ag/CHB). A magnetic corn husk biochar containing colloidal Fe_2O_3 particles embedded inside a porous biochar matrix was synthesized by the thermal pyrolysis of $FeCl_3$-treated biomass. The manufacture of magnetic silver-biochar material utilizes $AgNO_3$ solution as the silver supply and polyphenol derived from green tea as the reducing agent. Their structure and morphology were analyzed using X-ray diffraction (XRD), Brunauer-Emmett-Teller (BET) specific surface area measurements (10-12.28 m^2/g), Fourier transform infrared spectroscopy (FTIR) and scanning electron microscopy (SEM). Testing the photocatalytic potential of M-Ag/CHB to remove methylene blue from wastewater demonstrated its high removal efficiency that reached 70 % due to its high efficiency of electron transfer confirmed via electrochemical impedance spectroscopy analysis. Their antibacterial efficacy against *Escherichia coli* (*E. coli*) was assessed using the tablet colony counting technique and the optical density (OD) method. The findings suggested that the magnetic-silver-biochar composites exhibited more efficacy and enhanced antibacterial performance compared to the original biochar, suggesting promising applications for these composites in the antibacterial domain.

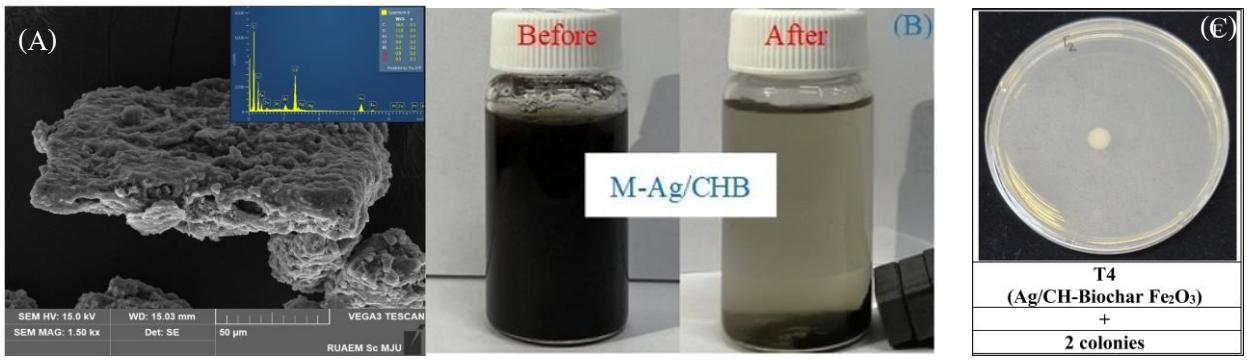

Figure 1.
(A) SEM-EDS images of M-Ag/CHB (B) magnetic separation of M-Ag/CHB
(C) antibacterial activity of M-Ag/CHB

PREPARATION OF AMINE-FUNCTIONALIZED RICE HUSK SILICA FOR UREA ADSORPTION

Thananan Wanitlertthnasarn,[1] Thatchatham Arrirak,[1] Warothkorn Luengvanish[1], Jedsadaporn Fakthong[1], Jinda Chuemue,[2] Sakdinun Nuntang[2,*]

[1] Montfort College, Chiang Mai, 50000, Thailand
[2] Industrial Chemistry Innovation Program, Faculty of Science, Maejo University, Chiang Mai 50290, Thailand

*e-mail: Sakdinun.nt@gmail.com

Abstract:
This study aims to prepare amine-functionalized rice husk silica (RHS-NH_2) as an adsorbent for urea removal from aqueous solution. The RHS–NH_2 were synthesized successfully via post grafting method using (3-Aminopropyl)-triethoxysilane (APTES), [3-(2 Aminoethylamino) propyl]-trimethoxysilane (AEA) and 3-[2-(2-Amino ethylamino)ethylamino] propyl-tri methoxysilane (AEEA) as amine group precursors. Surface and structural characteristics of RHS–NH_2 were examined using X-ray diffraction, N_2 adsorption–desorption analysis and Fourier transform infrared spectroscopy. In addition, the effects of type of RHS–NH_2 adsorbents, pH, adsorbent dose (M/V(g/L)), urea concentration, adsorption time, and shaking speed on the urea removal efficiency (%) of RHS–NH_2 were also analyzed. The optimal conditions for urea removal were as follows: M/V = 5 g/L; urea concentration = 38,000 µM; t = 80 min; pH = 8 and shaking speed = 120 rpm. Moreover, the maximum adsorption capacity of this RHS–NH_2 for urea was 220 mg/g. The results are promising as RHA–NH_2 could be used as adsorbent in artificial kidney applications.

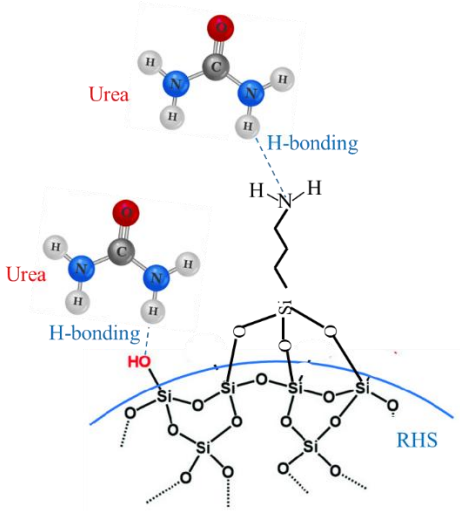

Figure 1.
Urea adsorption onto RHS-NH_2 surface

REMOVAL OF DEFERIPRONE FROM PHARMACEUTICAL WASTEWATER USING IRON-MODIFIED BIOCHAR

James Phil D. Flores,[1,2] Apichat Imyim[1,*]

[1]Department of Chemistry, Faculty of Science, Chulalongkorn University, Bangkok 10330, Thailand

[2]Davao del Sur State College, Brgy. Matti, Digos City, Davao del Sur 8002, Philippines
*e-mail: apichat.i@chula.ac.th

Abstract:
Pharmaceutical and personal care products (PPCPs) are emerging contaminants of concern due to their persistence, bioactivity and ecological and health risks even at trace levels. Conventional wastewater treatments often fail to remove PPCPs, necessitating sustainable alternatives. This study explores the removal of Deferiprone (DFP), a drug used in Thailand to treat iron overload, from pharmaceutical wastewater using iron-modified biochars derived from agricultural residues: sugarcane bagasse (FeSBB) and spent coffee grounds (FeCGB). SEM, XRD and FTIR analyses confirmed successful iron incorporation, enhancing surface reactivity. Batch adsorption experiments demonstrated near-complete DFP removal (~100%) at low concentrations under optimized conditions (50 mg adsorbent, 5 mg/L DFP, pH ~8, 1 h). Kinetic analysis fit a nonlinear pseudo-second-order model, indicating chemisorption via surface complexation, while adsorption isotherms followed the nonlinear Freundlich model, suggesting heterogeneous multilayer adsorption. Iron leaching was minimal (~7%) at high DFP concentrations and reduced by increasing adsorbent dosage, though its potential effect in real wastewater remains a consideration. Application to pharmaceutical effluents achieved appreciable DFP removal with FeSBB at 42.71% (q = 219.88 mg/g) and FeCGB at 39.70% (q = 202.94 mg/g), despite matrix interferences. These findings highlight the potential of agro-industrial waste-derived biochars as cost-effective, sustainable adsorbents for mitigating pharmaceutical pollutants.

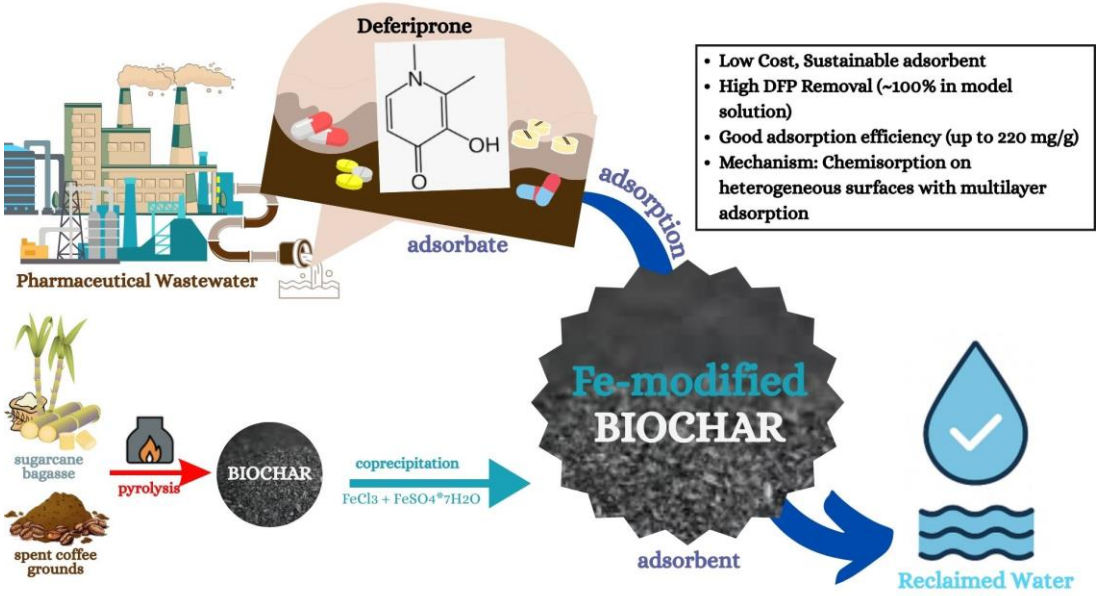

Figure 1. Removal of DFP from pharmaceutical wastewater using Fe-modified biochar derived from agricultural residues

SCALE-UP STRATEGY FOR HIGH-PRESSURE DYNAMIC-FLOW EXTRACTION OF TUMERIC

Athippracha Wattanawijit, [1] Waichaya Sirimongkhol, [1] Charoen Chinwanitcharoen [1*] and Nopphon Weeranoppanant [2,3*]

[1] Department of Chemical Engineering, Faculty of Engineering, Burapha University, Chonburi 20131, Thailand

[2] Department of Chemical Engineering, Faculty of Engineering, Chulalongkorn University, Bangkok 10330 Thailand

[3] Bio-Circular-Green-economy Technology & Engineering Center (BCGeTEC), Department of Chemical Engineering, Faculty of Engineering, Chulalongkorn University, Bangkok, 10330 Thailand

*e-mail: charoen@buu.ac.th, nopphon.w@chula.ac.th

Abstract:

Turmeric (*Curcuma longa* L.) is a traditional Thai herbal plant rich in curcuminoids, including curcumin, desmethoxycurcumin, and bis-desmethoxycurcumin. These compounds exhibit diverse bioactivities, such as antioxidant, anti-inflammatory, and anticancer properties. Conventionally, curcuminoids are recovered using steam distillation, Soxhlet extraction, or maceration. However, these techniques typically result in low yields and are time-consuming.

In this work, we explored the use of high pressure and high temperature to extract curcuminoids from turmeric, enabling higher yields in shorter extraction times. The process operates by flowing solvent through the turmeric matrix under heated and pressurized conditions. A key challenge in developing this dynamic-flow extraction method is scale-up. We demonstrated that by maintaining geometric and dynamic ratios, comparable performance can be achieved between laboratory (up to 5 g) and pilot (up to 200 g) scales. The dynamic ratio was defined as the ratio of flow rate to the mass of turmeric in the extraction chamber. As shown in Figure 1, although yield profiles over time differed between the two scales, the calculated mass transfer coefficients were highly similar. At the laboratory scale, yields of 5.492%, 1.797%, and 2.108% were obtained for curcumin, desmethoxycurcumin, and bis-desmethoxycurcumin, respectively. At the pilot scale, the yields increased to 8.071%, 2.379%, and 2.848% for the respective compounds. The validation enables us to verify the scale-up strategy, confirming its suitability for further expansion to production scale, typically ranging from 1 to 10 kg of extract.

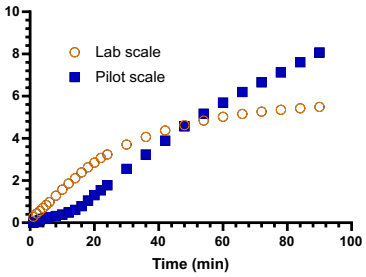

Figure 1.
Extraction yields of curcuminoids from turmeric over time at laboratory (5 g) and pilot (200 g) scales.

Synthesis of Alkoxy Alcohols via Ring-Opening Reactions of Epoxides Using Vanadium-Based Catalysts

Minami Murakami,[1] Yusuke Inomata,[2] Tetsuya Kida[3,*]
[1] Graduate School of Science and Technology, Kumamoto University, Japan
[2] Faculty of Advanced Science and Technology, Kumamoto University, Japan
[3] Institute of Industrial Nanomaterials, Kumamoto University, Japan
*e-mail: inomata@kumamoto-u.ac.jp

Abstract:

Epoxides are widely used as starting materials in the synthesis of pharmaceuticals and agrochemicals. Therefore, developing efficient and sustainable methods for epoxide conversion is of great importance. While homogeneous catalysts have been shown to promote epoxide ring-opening under mild conditions, heterogeneous catalysts are advantageous due to their ease of separation and reusability, making them more suitable for sustainable chemical processes. However, many heterogeneous systems require relatively high reaction temperatures, typically around 60 °C.

In this study, we focused on vanadium oxide as a solid acid catalyst for the ring-opening of epoxides. Using spherical silica (JRC-SIO-14) as a support, we prepared catalysts containing 5 wt% of vanadium, iron, or zinc by impregnating the metal salts in water, drying the mixture, and calcining at 450 °C for 4 hours. The catalytic performance was evaluated using the methanolysis of styrene oxide at room temperature. The reaction was carried out by stirring styrene oxide (1 mmol) with methanol (1 mL) and the catalyst (100 mg) for 24 hours. After adding anisole as an internal standard, the products were analyzed by GC-FID.

Among the tested catalysts, only the vanadium-supported silica showed high activity at room temperature, suggesting that solid acids are effective for this transformation. Varying the vanadium loading (1, 3, 5, 7, 10 wt%) revealed a clear effect on product selectivity. Low vanadium loadings resulted in high selectivity for the desired product, while higher loadings led to more byproduct formation. Raman spectroscopy indicated that the structure of vanadium species changes with loading: monomeric species were observed at low loadings, likely contributing to higher selectivity, whereas polymeric species formed at higher loadings, promoting side reactions.

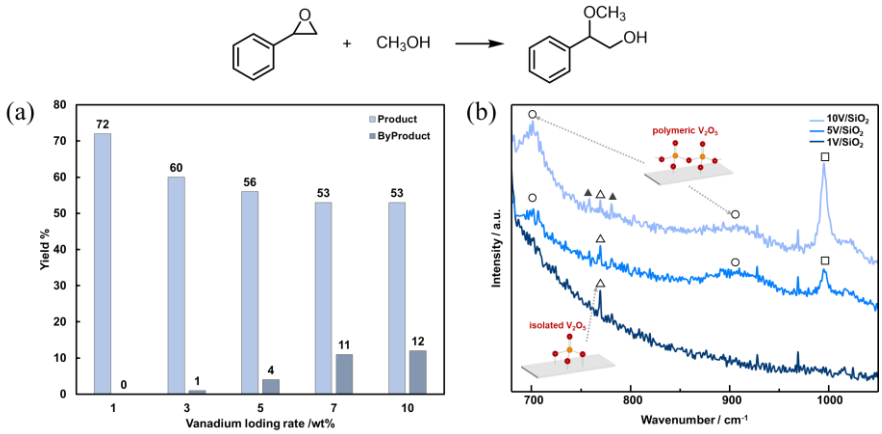

Figure 1. a) Yield for methanolysis of styrene oxide using V_2O_5-supported silica catalysts (1, 3, 5, 7, 10 wt%).b) Raman spectra of V_2O_5-supported silica catalysts (1, 5, 10 wt%).

SYNTHESIS OF GTBE BY CARBON-BASED CATALYTIC METHOD USING MICROWAVE IRRADIATION

Takata Nao[1], Armando T. Quitain[2], Yusuke Inomata[3], and Tetsuya Kida[4*]
[1]GSST, Kumamoto Univ, Japan [2] CIE, Kumamoto Univ, Japan
[3] FAST, Kumamoto Univ, Japan, [4]IINA, Kumamoto Univ, Japan
*e-mail: tetsuya@kumamoto-u.ac.jp

Abstract:
Biodiesel has garnered significant attention as a sustainable and renewable energy source. However, developing technology to convert glycerol, a byproduct of its production process, into high-value-added compounds is an urgent priority. In this study, glycerol tert-butyl ether (GTBE), a compound with high potential as a fuel additive, was synthesized using glycerol and tert-butyl alcohol (TBA) as raw materials. GTBE consists of three isomers: mono-tert-butyl glycerol (MTBG), di-tert-butyl glycerol (DTBG), and tri-tert-butyl glycerol (TTBG). Among these, DTBG and TTBG exhibit excellent performance as fuel additives, making them the primary target products. As a novel heating method, microwave irradiation was employed, enabling localized and rapid heating. In addition, graphene oxide (GO), which possesses a high specific surface area, abundant active sites, and excellent microwave absorption properties, was used as a catalyst. By utilizing the synergistic effect between the catalyst and the heating method, this study aimed to enhance the yield of the target product.
Catalyst properties were evaluated by FT-IR and XRD analysis. The reaction was conducted by sealing the raw materials, catalyst, and stirring rod in a pressurized container followed by microwave irradiation. After the reaction, the catalyst was removed by filtration, and the reaction solution was diluted with methanol. Glycerol conversion rate and the selectivity of each product were measured by GC-MS analysis. The conversion rates in the comparative experiment between conventional heating and microwave heating shown in Figure 1 were 68% for conventional heating and 86% for microwave heating. The yield of DTBG + TTBG showed a significant difference, being 13% for conventional heating and 46% for microwave heating. The reusability of catalysts will be further investigated to confirm the stability.

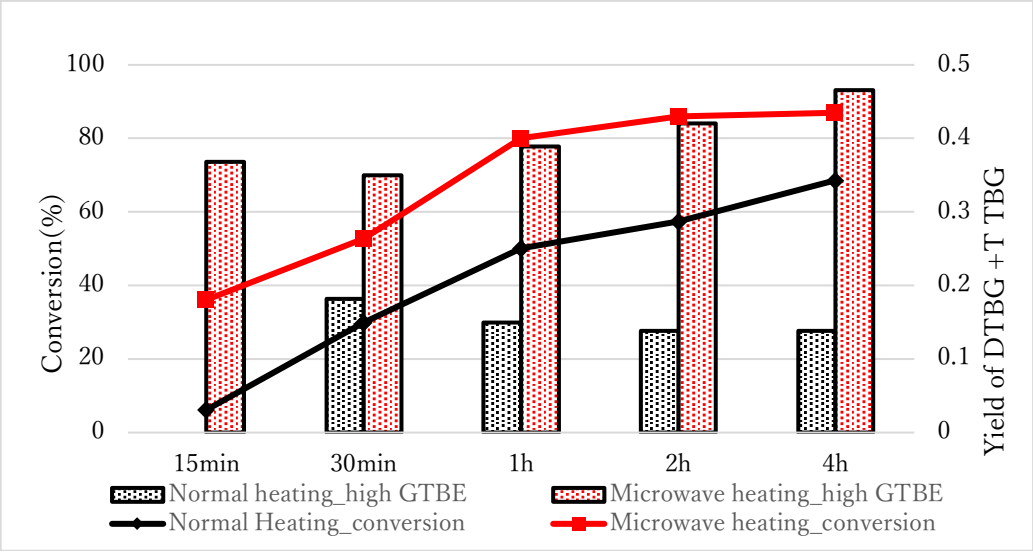

Figure 1. Yield and yield rate differences due to heating methods
(Gltycerol :1.46mL, Glycerol : TBA = 1:8, GO = 5wt%/Glycerol, T = 110°C, 300W)

SYNTHESIS OF Pd-LOADED GRAPHENE OXIDE CATALYSTS FOR ORGANIC TRANSFORMATIONS

Rio Sachi,[1] Muhammad Sohail Ahmad,[2] Yusuke Inomata,[3] Tetsuya Kida[2,*]
[1]Department of Materials Science and Applied Chemistry, Kumamoto University, Kumamoto, 860-8555, Japan
[2]Institute of Industrial Nanomaterials, Kumamoto University, Kumamoto 860-8555, Japan,
[3]Faculty of Advanced Science and Technology, Kumamoto University, Kumamoto, 860-8555, Japan
*tetsuya@kumamoto-u.ac.jp

Abstract:
Catalysts based on nanocarbon materials have attracted increasing attention due to their high surface area, tunable surface chemistry, and excellent stability. In this study, a palladium-containing carbon-based catalyst was developed using graphene oxide (GO) as the supporting matrix. GO was chosen for its excellent dispersibility in solution and its abundance of functional groups, which facilitate the incorporation of catalytically active species under mild conditions.
The catalyst material was fabricated into freestanding membranes by vacuum filtration and subsequently subjected to gentle thermal treatment (100–120 °C). To enhance the processability and surface exposure, the material was mechanically milled into fine powders suitable for catalytic applications.
Catalytic performance was evaluated using the Suzuki–Miyaura cross-coupling reaction (Scheme 1). The prepared material exhibited excellent activity under air at 50 °C, delivering high yields of biaryl products (up to 99%) as determined by GC and NMR analyses. The catalyst also demonstrated good recyclability with minimal loss in activity over multiple cycles, highlighting its potential for practical organic transformations.

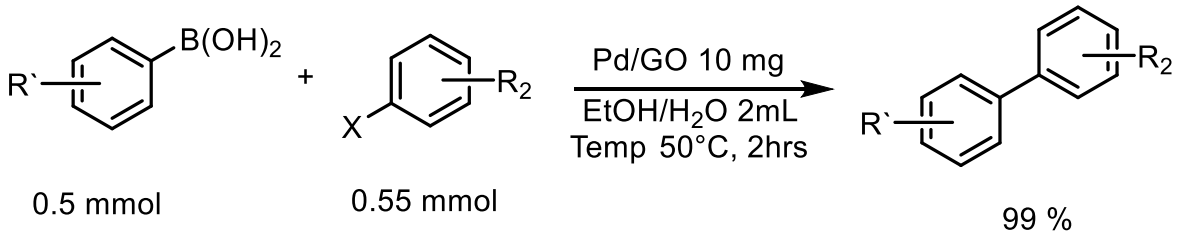

Scheme 1. Suzuki-Miyaura coupling reaction using Pd-GO catalyst

VALORIZATION OF METHYL PALMITATE TO NITROGEN- AND SULFUR-DOPED CARBON DOTS USING L-CYSTEINE

Thaenchet Soottitantawat,[1] Phuri Lohwacharin,[1] Kengkla Teerakoolpisut,[2] Chawanakorn Puangkaew,[3] Maythada Ruamjaithanakul,[3] Numpon Insin[3,*]

[1]Chulalongkorn University Demonstration Secondary School, Bangkok 10330, Thailand
[2]Triam Udom Suksa School, Bangkok, 10330, Thailand.
[3]Department of Chemistry, Faculty of Science, Chulalongkorn University, Bangkok, 10330, Thailand.
email: thaenchet.soottitantawat@gmail.com, *numpon.i@chula.ac.th,

Abstract:
This study introduces a sustainable method for synthesizing carbon dots (CDs) from methyl palmitate, a major component of palm biodiesel, via a solvothermal process using ethanol at 180 °C for 12 hours. Bandgap tuning was achieved through heteroatom doping with L-cysteine, serving as a nitrogen and sulfur source. The synthesized CDs were purified by centrifugation, followed by hexane and water extraction. The aqueous phase was vacuum-dried overnight and redispersed in water for further analysis. Structural and spectroscopic analyses (UV–Vis, photoluminescence (PL), Fourier-transform infrared spectroscopy (FTIR), and X-ray diffraction (XRD)) confirmed the formation of amorphous CDs bearing surface functional groups such as carboxyl, hydroxyl, amine, and thiol. Doping with L-cysteine significantly enhanced the photoluminescence, yielding excitation-dependent blue emission with tunable wavelengths ranging from 394 to 435 nm, as illustrated in Figure 1. The optimal CYS-CDs, synthesized with a cysteine-to-methyl palmitate molar ratio of 0.25:6, exhibited the highest quantum yield and emitted blue light at 396 nm when excited at 320 nm. However, excessive doping led to photoluminescence quenching due to increased non-radiative recombination. These findings demonstrate that methyl palmitate is a promising carbon source for eco-friendly CD synthesis and that dopant concentration plays a pivotal role in tuning their optical properties. This work offers a novel valorization route for biodiesel derivative and advances the development of functional nanomaterials for applications in bioimaging, sensing, and optoelectronics.

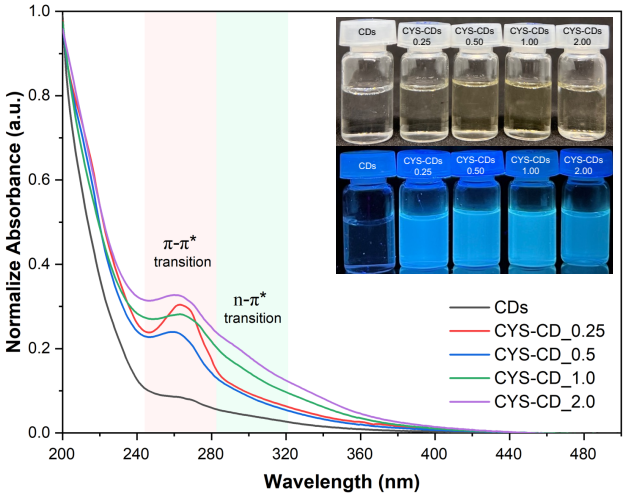

Figure 1. UV-vis absorption spectra of all prepared CDs. Inset: aqueous solutions of the prepared CDs under visible light (up) and UV light (down)

AUTHORS INDEX

Y